The biogeochemical fate of rare earth elements in aquatic ecosystems

A thesis submitted to the Committee on Graduate Studies

in partial fulfillment of the requirements for the degree of Master of Science

in the Faculty of Arts and Science

TRENT UNIVERSITY

Peterborough, Ontario, Canada

Environmental and Life Sciences M.Sc. Graduate Program

May 2025

Abstract

The biogeochemical fate of rare earth elements in aquatic ecosystems

Ashlyn Kernaghan

Rare earth elements (REEs) are in high demand globally for the green transition and high technologies. The growing demand leads to their release into aquatic ecosystems from various point and non-point sources, which creates urgency to investigate their fate and enrichment. This thesis further investigates the biogeochemical fate and REE uptake mechanisms throughout aquatic ecosystems. Rare earth element concentrations and fractionations were quantified to determine the natural uptake mechanism of three REE exposure pathways (dissolved, diet, and particulate) into aquatic organisms. Pelagic organisms accumulated heavy REEs, indicating they primarily uptake dissolved REEs. Benthic organisms were characterized by REE patterns specific for diet and particulate REEs. Furthermore, lanthanum (La) enrichment was investigated in a lake treated with La-based coagulants using La anomalies. Lanthanum enrichment in the water and organisms were directly related to La dispersion from sediments. This research provides information on preferential exposure pathways and REE enrichment in aquatic ecosystems.

Keywords**:** rare earth elements, fractionations, uptake mechanisms, bioaccumulation potential, lanthanum modified clay, lanthanum enrichment, metal organotropism

Preface

This thesis is written in a manuscript-based format and consists of two research chapters to be submitted for publication in suitable peer-reviewed journals. Acknowledgements and references from each manuscript are at the end of each chapter two and three sections. References used for the general introduction and conclusion are also compiled at the end of each chapter one and four sections. The methods used for sample preparation and chemical analysis are similar, but they were separated because the elements analyzed differ between the second and third chapters of this thesis. All research presented in this thesis was conducted with animal care protocols approved by the animal care committee of Trent University (Animal Use Protocol #26697), following the guidance set by the Canadian Council on Animal Care. We respectively acknowledge that the research work and learnings were completed on the traditional territory of the Anishinaabe peoples (Williams Treaty and Treaty 20). We offer gratitude to First Nations for their ongoing stewardship of this land.

Acknowledgements

I am honoured to have worked under the supervision of Dr. Huy Dang over the past 3.5 years as his undergraduate thesis student, research assistant, and graduate master's student. Dr. Huy Dang is an exceptional researcher in his field of environmental biogeochemistry, a charismatic colleague and friend, and an ambitious leader driven to make a positive difference in the world. As one of my role models, he has inspired me to build confidence in my scientific skills, to create trustworthy collaborations through respect and effective communication, to obtain self-awareness of my values, to reflect on my accomplishments and growth from overcoming challenges, to express gratitude and compassion to others and myself, and to surround myself with uplifting individuals. Thank you so much for the countless hours of support, guidance, patience, advice, and kindness you have shared throughout my scientific journey. Personal and professional growth has been abundant under his guidance. Thank you to my supervisory committee members Drs. Shaun Watmough and Claude Fortin for your encouragement, positivity, and generous insights on strengthening my conceptual and critical thinking. You provided me with reassurance and confidence since the beginning of my project.

I have also had the privilege of working alongside a diverse team of scientists and government collaborators who have helped me succeed in this project. Thank you to my partnership with the City of Markham, specifically Zahra Parhizgari and Robert Muir, who have allowed this project to become a reality. Thank you for your logistical support during the numerous sampling exhibitions and for sharing your invaluable knowledge on the physical and chemical characteristics of the sampling sites, as well as historical management practices at the sites. I greatly appreciate the substantial amount of time Dr. Wei Wang spent in the early stages of this project familiarizing me with sampling

collection and processing protocols, laboratory solution preparation, and providing guidance and advice through chemical analysis. Thank you to the Trent University Animal Care Facility staff, including the manager (Jason Allen) and technicians (Cynthia Grant & Andrea Rogers) for your tremendous care and support of the test subjects throughout the experiments. I also wanted to send a thank you to Spencer Grieve for his assistance during field sampling campaigns. Thank you to the research scientist, Dr. Karla Newman, and the manager, Dr. Hayla Evans of the Trent Water Quality Centre, for their technical and analytical support. My graduate studies were enriched by being a part of Dr. Huy Dang's EnIGMA research team. I would not have exceeded without the support and contributions of this outstanding team.

I would like to thank all my friends and colleagues at Trent University for making my graduate studies incredibly fulfilling through our connections, late-night conversations, and countless writing club/study group sessions. Specifically, to Minh Thao Nguyen Duong, Kaileigh Wright, Will Wood, Kelly Evans, Cerra Simmons, Mykhailo Rangaiev, David Boettcher, and Ruby Wetzl. My words cannot express how grateful I am to have had all of you as part of my community during my graduate studies. Of equal importance, are my friends, family, and partner who have shown endless love, positivity, engagement, and curiosity towards my research. To my best friend, Baptiste Lauzier, thank you for all your mental support, for believing in me since we met, and for seeing my strengths during my MSc journey. My parents, Leanne and Wayne Kernaghan, along with my brother, sister-in-law, and niece, Devan, Mikayla, and Ayla Kernaghan, for being my foundation. I greatly appreciate my Aunt Lisa, Uncle Tony, and the Lauzier/Gouchie family for your unconditional love, acceptance, and support. Lastly, I

am grateful for my beautiful friendships with Kaileigh Wright, Brittany Bell, Lauren Croucher, Minh Thao Nguyen Duong, Alex Bath, Cerra Simmons, Kelly Evans, Rebecca Pearce, and Emilie Bender, in which your endless checkups, words of encouragement, and support to help me accomplish this degree are immensely appreciated. Thank you to all my friends and family who have made countless journeys to visit me in Peterborough during my studies. Every one of you has entrusted me with the gifts and responsibilities of love, kindness, reciprocation, and my sense of belonging.

For the work presented here, I received funding from the Canadian Water Resource Association, the Trent University David and Joyce Woods Graduate Scholarship, the Ontario Graduate Scholarship (OGS), the National Sciences and Engineering Resource Council Masters Canada Graduate Scholarship (CGC-M), and from the Trent University Graduate Studies Entrance Award. Travel grants were provided by the International Institute for Environmental Studies (IIES). My project also received research fellowship funding from the Natural Sciences and Engineering Resource Council (NSERC) Alliance Grant (awarded by Dr. Huy Dang).

Dedication

This master's thesis is dedicated to my Grandma McLellan and Bella. Each of you has brought much light, laughter, and encouragement into my life during my educational and professional journey. I will carry your light with me and share it with others as memories of you.

Co-authorship

While this work is my own, I was fortunate to collaborate with my supportive supervisor, Dr. Huy Dang. Dr. Huy Dang has played a significant role in shaping and providing guidance during this works production. I have listed the manuscripts used as thesis chapters and the contributions of each co-author.

Chapter 2: Exposure pathways (diet, dissolved or particulate substrate) of rare earth elements to aquatic organisms

Kernaghan, A., Dang, D, H.

Published in *Ecotoxicity and Environmental Safety*.

Ashlyn Kernaghan: Writing – Original Draft, Writing – Review & Editing, Visualization, Validation, Project administration, Methodology, Investigation, Formal analysis, Data curation, Conceptualization. Duc Huy Dang: Writing – Review & Editing, Validation, Supervision, Methodology, Investigation, Conceptualization, Funding acquisition, Formal analysis, Conceptualization.

Chapter 3: Lanthanum enrichment throughout the ecosystem of Swan Lake (Canada) post-amendment to La-modified bentonite coagulant

Kernaghan, A., Dang, D, H.

Prepared for *Environmental Science and Technology*.

Ashlyn Kernaghan: Writing – Original Draft, Writing – Review & Editing, Visualization, Validation, Project administration, Methodology, Investigation, Formal analysis, Data curation, Conceptualization. Duc Huy Dang: Writing – Review & Editing, Validation, Supervision, Methodology, Investigation, Conceptualization, Funding acquisition, Formal analysis, Conceptualization.

Table of Contents

List of Figures

List of Tables

List of abbreviations:

ACC: Animal care committee

Ag: Silver

Al: Aluminum

AL: Acid-leachable

ANOVA: Analysis of Variance

As: Arsenic

Au: Gold

BAF: Bioaccumulation factor

BCF: Bioconcentration factor

Br: Bromine

C: Carbon

Ca: Calcium

Cd: Cadmium

Ce: Cerium

Ce/Ce*: Cerium anomaly

C_f: Contamination factor

Cl: Chorine

Co: Cobalt

Cr: Chromium

CRM: Certified reference material

Cs: Cesium

Cu: Copper

DAF: Diet accumulation factor

DOC: Dissolved organic carbon

Dy: Dysprosium

EDTA: ethylenediaminetetraacetic acid

EDXRF: Energy dispersive X-ray fluorescence

E_f: Enrichment factor

Er: Erbium

Er_{PAAS}: Erbium concentration normalized by erbium Post-Archean Australian shale value

Eu: Europium

Eu/Eu*: Europium anomaly

EUS: European shales

EV: Electric vehicle

Fe: Iron

Fla: Filterable lanthanum ion

Gd: Gadolinium

H_2O_2: hydrogen peroxide

Hg: Mercury

HNO_3: Nitric acid

H_o: Null hypothesis

HREE: Heavy rare earth element

HSD: Tukey's honestly significant difference test

IC: Inorganic carbon

ICP-MS: Inductively coupled plasma mass spectrometry

K: Potassium

K_{sp}: Solubility product constant

La: Lanthanum

La/La*: Lanthanum anomaly

La_{PAAS}: Lanthanum concentration normalized by lanthanum Post-Archean Australian shale value

LDPE: Low-density polyethylene bottles

LMB: Lanthanum-modified bentonite clay

LOI: Loss on ignition

LREE: Light rare earth element

Lu: Lutetium

MAM: Modified Acid Medium

Mg: Magnesium

Mn: Manganese

Mo: Molybdenum

MREE: Middle rare earth element

N: Nitrogen

Ni: Nickel

Na: Sodium

NaOH: Sodium hydroxide

NASC: North American shale composite

Nb: Niobium

Nd: Neodymium

O_2: Dioxygen

O: Oxygen

P: Phosphorous

PAAS: Post-Archean Australian shale

Pb: Lead

Pd: Palladium

Pr: Praseodymium

Pt: Platinum

Rb: Rubidium

REEs: Rare earth elements

S: Sulfur

Sc: Scandium

SEM-EDX: Scanning electron microscope with energy dispersive X-ray spectroscopy

Si: Silicon

Sm: Samarium

Sn: Tin

Sr: Strontium

SRM: Standard reference material

Tb: Terbium

Tb_{PAAS}: Terbium concentration normalized by terbium Post-Archean Australian shale value

Th: Thallium

Ti: Titanium

Tl: Thallium

TP: Total phosphorous

U: Uranium

UCC: Upper continental crust

V: Vanadium

Xe: Xenon

Y: Yttrium

Yb: Ytterbium

Zn: Zinc

Zr: Zirconium

Chapter 1. General Introduction

1.1 Definition, applications, and sources of rare earth elements

Rare earth elements (REEs) are a homogenous group of 17 elements of the lanthanide series ($_{57}$La to $_{71}$Lu) in the f-block of the periodic table (Rim, 2016), and non-lanthanides $_{21}$Sc and $_{39}$Y (Tyler, 2004). This group of elements contain consistent chemical and physical properties derived from uniform valence electron configurations ($5d^1$ & $6s^2$). They contain outer electron orbital shells such as $[Xe]4f^n5d^16s^2$, with a partially filled 4f orbital (Balaram, 1996; Garcia-Solsona and Jeandel, 2020). The 4f orbital is filled before the second $5d^1$ shell (Cicconi et al., 2021). Rare earth elements are magnetic, luminescent, hydrophilic, optical (Lundy et al., 2017), have similar ionic radii, and are characterized by a common valence of +III in environmental settings (Adeel et al., 2019; Dang et al., 2023b; Pastorino et al., 2020). Such chemical and physical homogeneity has enhanced their attractiveness to advance the efficiency, durability, and quality of essential modern-day technologies (Balaram, 2019), such as electric vehicles and wind turbines (Binnemans et al., 2013; Silvestri et al., 2021) in the low-carbon energy sectors (Moss et al., 2013). Rare earth elements are also implemented in high-end technologies such as electronics, national defence equipment, and medical equipment such as magnetic resonance imaging (MRI) scanning systems and X-ray machines (Bellin and Van Der Molen, 2008).

As the integration of REEs into the high-end technology sector increases, there are global efforts to intensify the extraction of REEs to meet the growing demand. This has led to exponential increases in global REE extraction outside of China (Gambogi, 2021; Paulick and Machacek, 2017). China holds the largest REE reserve in the world and held

the highest production of REEs (90%) in 2011 (Riesgo García et al., 2017). Following China, more than 96% of the remaining global REE reserves are in countries including Vietnam, Brazil, Russia, India, the USA, and Australia (Gambogi, 2021). The term rare earth elements is misleading as these lithophile elements can be found at higher abundances in major and minor geological constituents relative to other environmentally toxic metals (Kim et al., 2018) such as Cd, Hg, Pb, and U (Dang et al., 2021), precious metals such as Au, Pd, Pt, and other elements such as Sb and Se within the upper continental crust (UCC) (Rudnick and Gao, 2013). However, REEs are not found in pure form. They are found as minor constituents in more than 250 ore minerals of sedimentary or metamorphic rocks (Drobniak and Mastalerz, 2022) including bastnaesite (carbonate-fluoride), monazite (phosphate), ion-absorption clay deposits, carbonatites, monazite xenotime, silicates, loparites (oxides) and fergusonite (Balaram, 2019; Drobniak and Mastalerz, 2022). Though REEs are relatively abundant (total 9.2 mg kg^{-1}) in the earth's upper continental crust (Rudnick and Gao, 2013), REEs rarely form mineral deposits sizeable for extraction and economic interest (Gambogi, 2021). They are difficult to extract and separate due to their similar chemical properties and are commonly extracted in the form of oxides (Paulick and Machacek, 2017). The extraction of lanthanides involves the physical separation of REEs from sand or rock in the ores and sold as oxide compounds (Ling and Wang, 2015).

Rare earth elements can be further sub-categorized into three groups: Light rare earth elements (LREEs, $_{57}$La to $_{60}$Nd) are naturally more abundant than middle (MREE, $_{62}$Sm to $_{65}$Tb) and heavy rare earth elements (HREE, $_{66}$Dy to $_{71}$Lu) (Taylor and McLennan, 1995). Heavy REEs such as Dy and Tb are mined from mineral bastnaesite, monazite,

and xenotime deposits (Van Gosen et al., 2014) and are of high value ($323/kg and $1300/kg, respectively) (Cordier, 2024). Whereas LREEs and MREEs are preferentially incorporated in monazite and bastnaesite deposits and their value is lower at $80/kg for Nd, $27/kg for Eu, and $1/kg for La (Cordier, 2024; Ni and Hughes, 1995). Major end uses and applications of HREE and MREEs include auto catalysts, alloys, batteries of hybrid and electric vehicles, nuclear-reactor, polishing compounds, magnets, lasers, wind power, and flat panel displays (Gielen and Lyons, 2022; Humphries, 2013). The demand for clean energy technologies has increased the prices for the LREEs such as Pr, and Nd, and HREEs, such as Yb, and Dy which are essential for permanent magnet production in wind turbines and electric vehicles (Liu et al., 2023). Light REEs have been implemented in environmental remediation tools, in fertilizers to promote crop production, and feed additives (Tommasi et al., 2023). The unique chemical and physical properties of REEs that enhance their attractiveness to be used in modern-day technologies, also play an important role regarding REE environmental geochemistry.

1.2 Environmental geochemistry of rare earth elements (REEs)

Rare earth elements hold unique physical and chemical characteristics that differ from other elements and influence their geochemistry. For instance, the REE group is characterized by lanthanide contractions; their ionic radius progressively decreases (Dang et al., 2023b; Marginson et al., 2023; Yuan et al., 2017) with an increasing atomic number (Mayfield and Fairbrother, 2015), starting from La (1.03 Å, coordination number = 6) to Lu (0.86 Å, coordination number = 6) (Shannon, 1976). Additionally, all REEs hold the most thermodynamically stable trivalent form (+III) (Galhoum et al., 2015), except Eu and Ce. Europium and Ce can hold two oxidation states, where Eu^{+III} reduces

to Eu^{+II}, and Ce^{+III} oxidizes to Ce^{+IV} (Dahle and Arai, 2015). These distinct geochemical redox processes allow Eu and Ce to be enriched or depleted compared to their neighbouring REEs, making them important non-conservative geochemical tracers in the aquatic environment (Zheng et al., 2016). The depletion or enrichment of Ce and Eu from a system can be determined by the calculation of REE anomalies denoted by Ce/Ce* and Eu/Eu* (Dang et al., 2022b). A REE anomaly (REE/REE*) is calculated after the normalization of REE concentrations against natural geological standards, e.g. Post-Archean Australian Shale (PAAS). The ratio is between the normalized value of a specific REE (ex, Ce_{PAAS}) compared to the normalized values of its two neighbouring REEs (La_{PAAS} & Pr_{PAAS}). A REE/REE* value of 1 indicates no enrichment or depletion of a specific REE compared to its two neighbouring REEs. An anomaly > 1 indicates the element is enriched, whereas an anomaly < 1 indicates depletion. For instance, a common trend found in freshwater bodies around the world involves the depletion of Ce (Dang et al., 2022a; de Baar et al., 1988; Jiang et al., 2022a; Leybourne et al., 2000; Ling et al., 2013; Möller et al., 2003; Nozaki et al., 2000; Ratié et al., 2020; Sholkovitz, 1995; Sholkovitz and Schneider, 1991; Wang et al., 2021). Cerium anomalies < 1 suggests the oxidation transformation of Ce^{+III} into Ce^{+IV} (El-Akl et al., 2015; Jiang et al., 2022b; Sholkovitz, 1995). The oxidized Ce^{+IV} is less soluble, less mobile, and highly surface-reactive compared to Ce^{+III} (Byrne and Kim, 1990; Tostevin, 2021). Thus, Ce^{+IV} complexes and binds to organic ligands, carbonates (Yu and O'Keefe, 2006), colloidal fractions (El-Akl et al., 2015; Sholkovitz, 1992), precipitates as CeO_2, or combines with Fe-Mn hydroxides in the particulate phase (Bau and Koschinsky, 2009; Qian et al., 2022).

Consequently, Ce^{+IV} species are taken out of the dissolved fraction, inducing Ce anomalies < 1, i.e., depletion in the water (Bau et al., 1996; El-Akl et al., 2015).

Rare earth elements also follow the Oddo Harkins Rule, where with increasing atomic number from $_{57}$La to $_{71}$Lu, their natural abundances follow a zigzag pattern; elements with even atomic numbers are naturally more abundant than odd-numbered ones (Nikanorov, 2016). This standard pattern is created from the variable concentrations that the group of elements have due to the inconsistency in their atomic nuclei. Elements with even atomic numbers have more proton pairings in their chemical distribution, are more stable than their odd atomic numbered neighbours, and therefore have higher yields in the environment (Piper and Bau, 2013).

Further, the geochemical reactivity and environmental behaviours (Byrne and Li, 1995; Luo and Byrne, 2004) of REEs slightly differ in aquatic systems due to the gradual decrease in ionic radius (lanthanide contractions) and higher charge density. Light REEs hold a smaller charge density and are polarizable (Thomas et al., 2024). The larger proportion of dissolved LREEs existing as free ions then HREEs, results in in more susceptibility of LREEs to scavenge and bind to anions on the surfaces of minerals and particles. Heavy REEs have a higher charge density and are predominantly found in the dissolved form because of a higher affinity to weaker interactions with carbonate ions (Garcia-Solsona and Jeandel, 2020; Luo and Byrne, 2004; Sholkovitz, 1995), hydroxide complexes (de Baar et al., 1988), and other ligands (Byrne and Li, 1995; Merschel et al., 2017). Thus, HREEs are enriched in the dissolved and complexed form and have lower susceptibility to sorb onto particles (de Baar et al., 2018). The geochemical behaviours of LREEs and HREEs create a common pattern in natural waters known as “seawater-like”

patterns (Johannesson et al., 2006) following a linear and increasing trend displaying LREE depletion and HREE enrichment. The “seawater” patterns occur after the normalization of natural REE concentrations of water against natural geological standards of upper continental crust (UCC) (Taylor and McLennan, 1995) or post-Archean Australian shale (PAAS) (McLennan, 2001). Comparably, the middle REE group tend to be naturally enriched in aquatic systems by bonding with biogenic phosphates (Auer et al., 2017; Hannigan et al., 2001) or organic matter (Osborne et al., 2014). Quantitative MREE-enriched patterns are known as “hat-shaped” (Dang et al., 2023a; Hannigan et al., 2001; Pourret and Tuduri, 2017). Studies have confirmed the acid-leachable fractions of sediment from the water systems of the Yellow and East China Sea (Lim et al., 2014), the Mississippi (Adebayo et al., 2018), Amazon, Fly, and Sepik River systems (Hannigan et al., 2001) hold well developed MREE-enriched patterns. MREEs have a higher susceptibility to bind to organic ligands in solution than both lighter and heavier REEs (Marsac et al., 2013). Thus, natural terrestrial waters and sediment beds containing high molecular weight DOC or colloidal humic acid substances are dominated with REE speciation by MREE organic complexations (Tang and Johannesson, 2010).

Such differential environmental geochemical properties of REEs provide insights into the natural fates of each REE subgroup in different compartments of an aquatic ecosystem. The fractionations of REE subgroups are used to understand what group of REEs are more available in the sediment versus the water column for benthic or pelagic organisms to uptake, especially within aquatic ecosystems being added with higher REE levels from use of REE-based remediation tools or wastewater emissions of Gd from medical equipment (Bau and Dulski, 1996).

1.3 Rare earth elements as an ecological restoration tool

Eutrophication is defined as excessive phytoplankton growth within freshwater systems due to the increased availability of nutrients, carbon dioxide, sunlight, and temperature (Yang et al., 2008). Eutrophication leads to imbalanced biological production and is mitigated in standing lakes by controlling phosphorous (P) inflows from external sources and internal loading (Schindler et al., 2016). Eutrophication has promoted sediment capping technology to reduce or suppress sediment contribution to internal P loading. Conventional geoengineering techniques have used aluminum, iron, and calcium to chemically immobilize P to help control eutrophication (Lürling et al., 2016). However, the recent use of lanthanum (La) in sediment capping remediation tools for eutrophication restoration is due to the selectivity of La for P, i.e., La has a high affinity to bond with soluble reactive P (aka orthophosphate). Lanthanum and reactive P create the insoluble mineral rhabdophane ($LaPO_4 \cdot nH_2O$, Firsching and Bruñe, 1991). This stable rhabdophane mineral fall outs of water columns, immobilizes P, and becomes embedded in the sediments.

1.3.1 Phosphorus-related eutrophication in freshwater ecosystems

Anthropogenic activities have accelerated the rate and extent of eutrophication by excessive additions of limiting nutrients from external sources such as wastewater, storm runoff, fertilizer inputs, and deforestation (Khan and Ansari, 2005). Phosphorous has been considered as one of the most important factors controlling eutrophication (Schindler et al., 2016, 2008), as 80% of lake and reservoir eutrophication is restricted by P (Zhao, 2004). The total P nutrient levels within eutrophic waterbodies are 25 to 100 ug L^{-1}, and total nitrogen (N) is 600 to 1500 ug L^{-1} (Yang et al., 2008). The P nutrient levels

for hypereutrophic conditions are >100 ug L^{-1} and > 2000 ug L^{-1} for total N levels (Yang et al., 2008).

Enriched P nutrient levels create hypertrophic conditions (Conley et al., 2009), which have severe consequences for ecosystem function and services (Marsden, 1989; Paerl et al., 2020; Smith and Schindler, 2009). For instance, the presence of excessive algal blooms increases the turbidity of the water column and reduces light penetration to the bottom of water bodies. Reducing light penetration inhibits the growth of benthic macrophytes to produce oxygen in littoral zones, causing plants to die off and anoxic sediment to form (Smolders et al., 2006). Anoxic zones lack sufficient oxygen to support organisms, causing loss of macrophyte habitat, ecologically sensitive species, benthic communities (Desprez et al., 1992), biodiversity, and enhances the domination of blue-green algae (Boyd, 2020). Furthermore, carbon dioxide and pH fluctuate directly with the overproduction of phytoplankton in hypereutrophic waterbodies. As phytoplankton production increases during the day, the amount of free carbon dioxide (inorganic carbon) for photosynthesis becomes depleted, increasing the pH of water. The elevation of pH can impact organism survival by impairing their chemosensory abilities to protect themselves from prey (Turner and Chislock, 2010). Once algal blooms die off, microbial bacteria decomposers transform detritus into usable mineral forms, which depletes oxygen levels and creates larger anoxic dead zones (Ansari et al., 2011). Carbon dioxide levels then begin to rise from the decomposition of detritus and bacterial respiration, lowering the pH of the water (Ansari et al., 2011).

In shallow lakes, the whole water column is usually oxic, which establishes an oxidized microlayer at the sediment-water interface that inhibits the release of sediment P

(Penn et al., 2000). Oxygen serves as the primary oxidizing agent in the decay of organic matter by microbial processes (Smolders et al., 2006). However, large productions of detritus planktonic biomass induce bacteria to use up all available oxygen to break down detritus, leading to anoxic zones at the bottom of lakes, which causes sediment to become anoxic. Trapped P in the sediment can be released when the microlayer of sediment is reduced at the onset of anoxia (Søndergaard et al., 2003). Anoxia decreases the redox potentials in the bottom waters, which initiates both anaerobic decomposition and internal P loading (Smolders et al., 2006). Total phosphorous (TP) levels within water columns increase (Kemp et al., 2005) due to P recycling from anoxic sediment beds (Mortimer, 1941). More specifically, under anoxic conditions and within iron-rich sediments, iron phosphate or iron hydroxide compounds act as an electron acceptor and are reduced as bacteria break down detritus (Smolders et al., 2006). This leads to P having fewer sorption sites on the redox-sensitive Fe minerals within the sediment, thus an efflux of iron ions (Fe^{2+}) and phosphate ions (PO_4^{3-}) return to the water column (Søndergaard et al., 2003). Reducing conditions are also common at the sediment-water interface due to anoxia that develops in the hypolimnion when lakes thermally stratify in the summer (Kirol et al., 2024). The release of soluble reactive P from legacy sediment pools under anoxic conditions (Kirol et al., 2024; Wurtsbaugh et al., 2019), increases available nutrients which enhances algae bloom growth and the eutrophication positive feedback cycle (Ansari et al., 2011). Shallow lakes are very susceptible to internal loading and eutrophication because nutrients in their bottom sediments have a greater impact on water quality (Kowalczewska-Madura et al., 2022).

Controlling P inputs through the reduction of external loading has rapidly shifted the regimes of eutrophication back to a stable state in few lakes (Marsden, 1989; Sas, 1989). Remediation methods to reduce external loading include controlling inputs of anthropogenic pollutants, purifying waters of nutrients, and using biomanipulation to trap bioavailable nutrients (Sharma et al., 2011; Wang et al., 2009). However, mitigation efforts to reduce external loading are only effective in the short term, as eutrophication due to internal P loading persists (Jeppesen et al., 1991). Studies have found internal P loading persists for 30 years in shallow eutrophic lakes after reducing external loading (Søndergaard et al., 1999), and internal loading varies on a temporal scale. External and internal loading prevents a decrease in TP and prolongs impacts on eutrophic lakes (Kowalczewska-Madura et al., 2022). Wu et al., 2017 used the Bayesian hierarchical inference to compare if management initiatives for internal or external loading encourage more biochemical changes. The study concluded that managing internal P loading is most effective in decreasing eutrophication and rapidly reversing the severe ecological effects (Wu et al., 2017). Metal salts and modified clays control internal P by chemically immobilizing soluble P in water (George et al., 2019). However, these materials could pose harm to ecosystems during remediation efforts (George et al., 2019).

1.3.2 Lanthanum-modified bentonite clay (LMB) used for ecological remediation

Lanthanum, a LREE, is embedded in a lanthanum-modified bentonite clay (LMB) coagulant, commonly known as Phoslock, to help dephosphatize water columns (Robb et al., 2003). Phoslock® was created by Phoslock Europe GMbH and developed by the Commonwealth Scientific and Industrial Research Organization (CSIRO) of Australia (Douglas et al., 1999) to promote P uptake while reducing the release of P from the

sediment. Lanthanum-modified clays have been used in over 20 countries and applied in over 200 water bodies to remove excess phosphate ions and mitigate algal blooms (Copetti et al., 2015; Finsterle, 2014). The bentonite clay is made from aluminum-silicate minerals, which is compatible with aquatic sediment (Copetti et al., 2015). The bentonite clay minerals hold a high cation exchange, which creates a charge imbalance on the clay surfaces, but the charge is balanced by adsorbed cations (Ross et al., 2008). Lanthanum-modified bentonite (LMB) clay is formed by La ions exchanging places with Ca and Na ions in aqueous solutions, forming strongly bonded LMB matrixes (Finsterle, 2014). Lanthanum theoretically binds to soluble reactive phosphate in a 1:1 stoichiometric ratio (Finsterle, 2014; Haghseresht et al., 2009). Studies have found that 1 tonne of LMB can remove 34 kg of phosphates, thus, a recommended dosage is 100 kg of LMB to 1 kg of targeted P (Bishop and Richardson, 2018), based on releasable P in the upper 4 cm of the sediment plus water column P (Meis et al., 2013). This leads to the concentration of total La in water bodies during and one-month post-application reaching levels of 0.026 mg L^{-1} to 2.30 mg L^{-1} in the surface and bottom waters (Spears et al., 2013). Lanthanum-modified bentonite clay is applied to the entire surface area of water bodies in a slurry form, and the lanthanum cation within the bentonite clay binds with free phosphate anions (PO_4^{3-}) and forms a complexation (Ross et al., 2008). The lanthanum-phosphate rhabdophane complex is highly insoluble, with a K_{sp} in an aqueous solution of $10^{-26.16}$ (Firsching and Bruñe, 1991), and can form with low concentrations of reactants over a wide pH range (4 to 8.5) (Haghseresht et al., 2009). The complex precipitates and falls out of suspension, and its purpose is to cap the sediment-water interface to prevent anoxic release of bound P (Ross et al., 2008).

However, concerns are raised regarding the ineffectiveness of LMB causing the release of P and filtered lanthanum post-application under varying physiochemical conditions. Firstly, the bonding capacity of LMB lasts until the clay matrix has been saturated with soluble P (Finsterle, 2014), thus only having a 25-60% binding efficiency to soluble P (Pallí, 2015; Van Oosterhout and Lürling, 2013), causing soluble P concentrations post-treatment to return to pre-treatment levels (Lürling and Van Oosterhout, 2013; Moos et al., 2014). Specialists suggest a high dosage of LMB combined with controlling external inputs of P (Nürnberg, 2017), and dredging sediment will increase binding efficiency and decline P levels (Lürling and Faassen, 2012).

Furthermore, various chemical parameters impact LMB's efficacy in bonding to P. Under laboratory conditions, the adsorption capacity of phosphates by LMB was most effective between a pH of 5 and 7 (Ross et al., 2008). Effectiveness decreased when the pH of the water was increased to 9 (Haghseresht et al., 2009) and when algae was present. Phosphorous was not released under anoxic conditions (Ross et al., 2008), and additional evidence shows LMB is more effective at reducing reactive P levels and sediment phosphate fluxes under anoxia conditions compared to oxygenated conditions (Gibbs et al., 2011; Zeller and Alperin, 2021). The binding capacity for LMB can also be ineffective when La^{3+} complexes with humic substances or is interfered with oxyanions, such as CO_3^{2-}, under higher alkaline waters (Pourret et al., 2007; Tang and Johannesson, 2010). It was also found that filterable La^{3+} (FLa) concentrations were higher in lakes of very low alkalinity (soft waters) but lower in high alkaline lakes (hard waters) (Gibbs et al., 2011; Meis et al., 2013; Spears et al., 2013). Further, humic substances can interfere with the removal of filterable reactive P by LMB and cause increases in FLa

concentrations (Lürling et al., 2014; Pourret et al., 2007). The effect humic acid has on La dissolution is dependent on the conductivity and alkalinity of lake water. For instance, elevated FLa concentrations post-LMB treatment occurred in soft waters (low alkalinities) rich in DOC and humic acids (Reitzel et al., 2017). The higher FLa concentrations within soft waters could be due to the higher dispersion of LMB clays in low alkaline/conductive waters (Reitzel et al., 2013) or due to humic acid complexations of La retained in the LMB matrix. After the application of LMB in soft water with high humic acid content, La was mainly in the dissolved form, with FLa concentrations > 100 ug L^{-1}. Whereas in hard waters with high humic acid, La was associated with colloids, and FLa concentrations were below 10 ug L^{-1} (Reitzel et al., 2017). In hard waters, high concentrations of Ca^{2+} could create strong Van der Waal's forces leading to aggregation and preventing La from dissolution from the clay matrix, and carbonate-La complexes would strongly inhibit dissolved La and outcompete humic substances (Reitzel et al., 2017; Tang and Johannesson, 2003). In soft waters, humic acids have more opportunities to interact with La from the clay matrix and cause the dissolution of La. Thus, different size fractions and quantities of FLa and reactive P post-application of LMB within waterbodies are based on varying pH, alkalinity, and the presence of DOC.

Under field conditions, lanthanum-modified clay did not reduce P levels in Lake Het, Netherlands (Lürling and Van Oosterhout, 2013), the Guanda River of Brazil (Bacha et al., 2022), pore water in peaty soils (Geurts et al., 2011), Scanlon Reservoir (Moos et al., 2014), Cane Parkway stormwater management pond (Gibbs et al., 2011), and Swan lake of Canada (Nürnberg and LaZerte, 2016). It has been suggested that lanthanum-modified bentonite clay is not a long-term management solution in waterbodies with low

residence times, which are constantly being flushed and turned over with rapid inputs of water (Moos et al., 2014). Further, physical disturbances such as bioturbation (Meysman et al., 2006) and wind (Douglas and Rippey, 2000) can resuspend La back into the water column (Spears et al., 2013). The physical and chemical degradation of lanthanum-modified bentonite clay increases the release of legacy P and La into water bodies post-application (Nürnberg, 2017), causing the requirement of multiple treatments to maintain the water quality of small, eutrophic lakes (Meis et al., 2013; Nürnberg, 2017). The potential release of La into the ecosystem under varying physiochemical properties leads to a concerned notion regarding whether aquatic organisms are susceptible to uptaking and becoming enriched with La from the amended La-coagulants.

1.4 REE bioaccumulation, enrichment, and environmental risks to aquatic organisms

Lanthanum-modified bentonite clay has been applied globally to lakes that have several uses for biodiversity conservation, recreation, and human consumption (Paiva et al., 2009). Specifically, LMB has been applied to various lakes within Canada, including the Scanlon Reservoir, Cane Parkway Stormwater Pond, and Swan Lake in Ontario, Elk Lake in British Columbia, Henderson Lake in Alberta, and Lac Bromont in Quebec as remediation efforts to reduce eutrophication (Moos et al., 2014; Nürnberg, 2017). Although the application of LMB has been reported to control eutrophication in some Canadian lakes (Bacha et al., 2022; Nürnberg, 2017), there are concerns regarding the safety of LMB to the environment and raising the question of whether the dissolution of La from these clays can be bioavailable and bioaccumulate into biota.

The accumulation of REEs in all organisms depends on REEs bioavailability, their chemical speciation, and the affinity of REE ions toward the binding sites and transporters on cellular membranes (Valcheva-Traykova et al., 2014). There is increased evidence through laboratory exposure experiments regarding the adverse toxicity effects that solely dissolved lanthanum (La^{3+}) poses to aquatic organisms. For instance, dissolved La lowers the metabolism and energy reserves of benthic *Mytilus galloprovincialis*, and induces toxic effects on the gonads, gills, digestive glands, embryos and larvae (Freitas et al., 2020; Mestre et al., 2019; Pinto et al., 2019). Furthermore, various aquatic vertebrates exposed to dissolved La levels similarly found in lakes contaminated from mining activities suffered from adverse effects such as juvenile rainbow trout (*Oncorhynchus mykiss*) undergoing genotoxicity and oxidative stress in the liver and gills (Hanana et al., 2021), the neural and cardiovascular development was compromised in zebrafish (*Daniorerio*) (Zhao et al., 2021), and rare minnows (*Gobiocypris rarus*) underwent histopathological changes such as epithelial lifting, lamellar fusion, edema, and necrosis of gills (Hua et al., 2017). High-dose exposure to dissolved La has caused toxic effects and mortality on lower trophic state organisms including *Daphnia similis* and fungi (Bergsten-Torralba et al., 2020; Shu et al., 2023), *Chlorella* and *Phaeodactilum* (Sun et al., 2019), microalgae (Siciliano et al., 2021), and inhibition to bacteria growth (Wang et al., 2000). High doses of dissolved La in laboratory single organism exposure experiments caused adverse toxic effects.

There is an incomplete understanding of whether REEs in other exposure pathways, such as the diet (REE-laden prey) or REE particulates (REE-based coagulants), can cause similar adverse effects as dissolved REEs or can bioaccumulate and enrich within aquatic

organisms. Few laboratory studies, such as Cardon et al., (2020), found uptake efficiency of REEs through the dietary fraction was low (0.8-3%). Lürling and Tolman, (2010) found that exposure to lanthanum-modified bentonite clay indirectly decreased the growth rates of *Daphnia magna* due to insoluble mineral rhabdophane precipitating food algae from the system. During exposure to particulate LMB, marbled crayfish (*Procambarus fallax f. virginalis*) accumulated bioavailable La within tissues, but no toxic effects occurred (Van Oosterhout et al., 2014; Van Oosterhout and Lürling, 2013). Furthermore, survival and growth were not impacted after sediment-dwelling organisms *Hyalella Azteca*, *Hexagenia* spp., and *Chironumus dilutes* were exposed to a dilution series of Phoslock, but pelagic *Daphnia magna* and *Onchorykis mykiss* underwent mortality at Phoslock levels between 1.7 to 13.6 g/L (Watson-Leung, 2009). Under environmental lake conditions, the application of lanthanum-modified bentonite clay caused the reduction of macroinvertebrate biomass and bioaccumulation of La in pelagic fish livers and eels (Waajen et al., 2017). The application of LMB also caused the inhibition of fish growth due to decreases in food source (Han et al., 2021). In Lake Rauwbraken (Netherlands), La concentrations were 50 to 200 times higher post-application in sediment, macrophytes, and larvae compared to pre-application (Van Oosterhout et al., 2020). Most of the laboratory and field studies investigating adverse effects and enrichment of La^{3+} or lanthanum bentonite clay have been focusing on a single species and did not focus on the bioaccumulation or enrichment within multiple organisms from different phyla/trophic levels from one collective aquatic food web. Conversely, other studies investigating REE organotropism at the entire ecosystem level in natural aquatic food webs of rivers, lakes, and estuaries around the world not exposed

to high-level point sources have found a trophic dilution of REEs within ecosystems (Amyot et al., 2017; Rétif et al., 2024; Santos et al., 2023). Thus, investigating the interactions of lanthanum-modified bentonite clay at the entire ecosystem level under natural environmental conditions would give insights into whether ecosystems exposed to lanthanum-modified bentonite clay also follow natural trophic dilutions of REEs or if enrichment or bioaccumulation in organisms is occurring.

Bioaccumulation is the net accumulation of highly bioavailable elements within organisms after being exposed long-term to environmental contaminants from sources of air, water, and solids (Drexler et al., 2003). Through the aquatic food web, REEs can undergo bio-amplification or bio-dilution (Amyot et al., 2017; Dai et al., 2022; Santos et al., 2023; Souza et al., 2021); each would have contrasting needs for environmental regulation of these critical natural resources. Thus, bioaccumulation is quantified with bioaccumulation factors (BAF) and bioconcentration factors (BCF). Bioconcentration factors are calculated by comparing the proportion of dissolved elements available for uptake versus the quantity absorbed by organisms. The bioconcentration process often considers the assimilation of a chemical substance into organisms from its ambient environment only through respiratory and dermal surfaces (Arnot and Gobas, 2006), excluding their diet (Environment Canada, 2000). Ideally, BCF calculations are suitable for controlled laboratory conditions in which dietary intake of the chemical is deliberately not included (Arnot and Gobas, 2006). However, bioconcentration factors for metal exposure in laboratory experiments are questionable as it has been deemed not precise and accurate to use for hazard assessment or bioaccumulation (DeForest et al., 2007; Mcgeer et al., 2003). This is due to an inverse correlation between BCF and exposure

concentrations. Bioconcentration factor values for various metals were found to be the highest under natural exposure concentrations, whereas the lowest BCF values corresponded to the highest exposure concentrations (Mcgeer et al., 2003). These results are inconsistent with past toxicology literature, showing that organisms vary uptake and elimination within the spectrum of exposure regimes, leading to lower concentrations within the whole-body relative to high exposure concentrations (Mcgeer et al., 2003).

Comparably, the bioaccumulation factor is the ratio of the REE concentrations in an organism ($[REEs]_{organisms}$) to the REE concentration in unfiltered water, which is based on the uptake from all possible routes of exposure, such as the transfer of surrounding medium across respiratory surfaces and dietary absorption (DeForest et al., 2007; Environment Canada, 2000). The bioaccumulation processes consider the assimilation of a chemical substance into an organism by all routes of exposure as occurred in the natural environment, dietary, and ambient environmental sources (Arnot and Gobas, 2006). These bioaccumulation factors help quantify whether organisms are more susceptible to uptake and bioaccumulate REEs through dissolved, particulate or diet exposure pathways.

1.5 Hypothesis, objectives, and project goals

The objectives of this thesis are to investigate the natural uptake mechanisms and exposure pathways (diet, dissolved fraction, or particulate substrate) of REEs to organisms as well as determine the natural REE distribution, fate, and enrichment potential within freshwater ecosystems. For bioaccumulation to occur, rare earth elements must be bioavailable to aquatic organisms. Therefore, a lab-exposure experiment was conducted to determine the bioavailability and uptake mechanisms of three exposure

pathways (diet, dissolved, particulate substrate) to benthic (northern clearwater crayfish (*Faxonius propinquus*), chinese mystery snail (*Cipangopaludina chinensis*), and black sandshell mussel *(Ligumia recta*) and pelagic (striped shiner minnows (*Luxilus chrysocephalus*), the planktonic crustacean *Daphnia magna*, and the alga *Euglena gracilis*) organisms found at various levels of the food web. The objective is to determine whether REEs in different exposure pathways are bioavailable for organisms to take up and bioaccumulate in body tissues. Thus, the species most susceptible to uptake REEs in certain exposure pathways are species of interest for ecological monitoring.

Secondly, the uptake mechanism and bioaccumulation results from the laboratory experiments will be compared to the fate, distribution, and enrichment potential of La within the freshwater ecosystem of Swan Lake (Markham, Ontario), which was amended with Phoslock, a La-coagulant in 2013. Swan Lake is an urban pond within the Rouge River watershed (Wood Environment & Infrastructure Solutions, 2020). The Rouge River watershed spans 336 km^2 throughout Southern Ontario, and the land use in Rouge River is 40% rural, 35% urban, 24% natural cover, and 1% open water, which contains both natural rivers and ponds, as well as man-made storm management ponds (Barrett, 2007). Swan Lake is a highly eutrophic, urban stormwater pond and represents anthropogenic inputs of dissolved and particulate fractions of REEs into a freshwater ecosystem. The objective of this field study is to determine the natural fate, distribution, and concentrations of rare earth elements found in biotic and abiotic components and directly relate the enrichment of La and the potential transfer of La between the abiotic and biotic compartments. Enrichment and REE distribution trends within Swan Lake will be validated by the laboratory experiments. The comparison of mesocosm and real-world

ecosystems will give a better understanding of the natural uptake mechanism of REEs into organisms, and the distribution, accumulation, and enrichment of REEs in freshwater ecosystems.

Rare earth elements have similar ionic radius to major elements such as Ca^{2+} and Fe^{3+} ions (Cardon et al., 2020). This physical property allows rare earth elements to transfer into aquatic organisms through similar mechanisms or compete with these elements for bonding sites on cellular structures (Valcheva-Traykova et al., 2014). Therefore, it is hypothesized that REEs will be bioavailable and transfer into aquatic organisms, similar to trace elements. Moreover, MacMillan et al. (2017) suggest that the accumulation of REEs in marine organisms is species and tissue-specific. For instance, vertebrates and invertebrates had the highest REE concentrations after exposure to the ionic forms (MacMillan et al., 2019, 2017). However, vertebrates can metabolize and detoxify elements from their bodies, reducing accumulation in vertebrate tissues post-depuration compared to invertebrates (Nørregaard et al., 2019). Further, there is minimal understanding of the repartition or bioaccumulation of REEs within benthic organisms such as snails and mussels. Thus, studies on the distribution of non-REE elements in benthic organisms can guide our understanding of REE uptake mechanisms. Therefore, bioaccumulation and enrichment of REEs should occur in freshwater organisms but is consequential for species at certain trophic levels based on their ability to metabolize or excrete REEs from different exposure pathways and based on their length of exposure to the REE media.

Overall, this project will help understand REEs' biogeochemical fate, bioavailability, and enrichment within freshwater ecosystems. The knowledge gained

from this study is critical for understanding the fate and distribution of REEs in aquatic ecosystems. As the extraction and use of REEs in mining, restoration, and technologies in Canada increases, the exposure of these metals to the environment will increase (Liang et al., 2014). Therefore, it is essential to determine where REEs end up in aquatic ecosystems and if pelagic or benthic organisms to uptake, bioaccumulate, or enrich REEs from various pathways. Organisms susceptible to uptake and enrich REEs could be bioindicators of REE exposures and ensure the longevity of our freshwater ecosystems.

1.6 References

Adebayo, S.B., Cui, M., Hong, T., White, C.D., Martin, E.E., Johannesson, K.H., 2018. Rare earth elements geochemistry and Nd isotopes in the Mississippi River and Gulf of Mexico mixing zone. Front Mar Sci 5, 1–18. https://doi.org/10.3389/fmars.2018.00166

Adeel, M., Lee, J.Y., Zain, M., Rizwan, M., Nawab, A., Ahmad, M.A., Shafiq, M., Yi, H., Jilani, G., Javed, R., Horton, R., Rui, Y., Tsang, D., Xing, B., 2019. Cryptic footprints of rare earth elements on natural resources and living organisms. Environ Int 127, 785–800. https://doi.org/10.1016/j.envint.2019.03.022

Amyot, M., Clayden, M.G., MacMillan, G.A., Perron, T., Arscott-Gauvin, A., 2017. Fate and trophic transfer of rare earth elements in temperate lake food webs. Environ Sci Technol 51, 6009–6017. https://doi.org/10.1021/acs.est.7b00739

Ansari, A.A., Gill, S.S., Lanza, G.R., Rast, W., 2011. Eutrophication: cause, consequences and control. Springer 1–394. https://doi.org/10.1007/978-90-481-9625-8

Arnot, J.A., Gobas, F.A.P.C., 2006. A review of bioconcentration factor (BCF) and bioaccumulation factor (BAF) assessments for organic chemicals in aquatic organisms. Environ Rev. https://doi.org/10.1139/A06-005

Auer, G., Reuter, M., Hauzenberger, C.A., Piller, W.E., 2017. The impact of transport processes on rare earth element patterns in marine authigenic and biogenic phosphates. Geochim Cosmochim Acta 203, 140–156. https://doi.org/10.1016/j.gca.2017.01.001

Bacha, L., Ventura, R., Barrios, M., Seabra, J., Tschoeke, D., Garcia, G., Masi, B., Macedo, L., Godoy, J.M. de O., Cosenza, C., de Rezende, C.E., Lima, V., Ottoni, A.B., Thompson, C., Thompson, F., 2022. Risk of collapse in water quality in the Guandu River (Rio de Janeiro, Brazil). Microb Ecol 84, 314–324. https://doi.org/10.1007/s00248-021-01839-z

Balaram, V., 2019. Rare earth elements: A review of applications, occurrence, exploration, analysis, recycling, and environmental impact. Geosci Front 10, 1285–1303. https://doi.org/10.1016/j.gsf.2018.12.005

Balaram, V., 1996. Recent trends in the instrumental analysis of rare earth elements in geological and industrial materials. TRAC - Trend Anal Chem 15, 475–486. https://doi.org/10.1016/S0165-9936(96)00058-1

Barrett, S., 2007. Rouge River watershed plan: towards a healthy and sustainable future: report of the Rouge watershed task force. TRCA.

Bau, M., Dulski, P., 1996. EPSL Anthropogenic origin of positive gadolinium anomalies in river waters. Earth Planet Sci Lett 143, 245–255. https://doi.org/10.1016/0012-821X(96)00127-6

Bau, M., Koschinsky, A., 2009. Oxidative scavenging of cerium on hydrous Fe oxide: Evidence from the distribution of rare earth elements and yttrium between Fe oxides and Mn oxides in hydrogenetic ferromanganese crusts. Geochem J 43, 37–49. https://doi.org/https://doi.org/10.2343/geochemj.1.0005

Bau, M., Koschinsky, A., Dulski, P., Heinz, J.R., 1996. Comparison of the partitioning behaviours of yttrium, rare earth elements, and titanium between hydrogenetic marine ferromanganese crusts and seawater. Geochim Cosmochim Ac 60, 1709–1725. https://doi.org/https://doi.org/10.1016/0016-7037(96)00063-4

Bellin, M.F., Van Der Molen, A.J., 2008. Extracellular gadolinium-based contrast media: An overview. Eur J Radiol 66, 160–167. https://doi.org/10.1016/j.ejrad.2008.01.023

Bergsten-Torralba, L.R., Magalhães, D.P., Giese, E.C., Nascimento, C.R.S., Pinho, J.V.A., Buss, D.F., 2020. Toxicity of three rare earth elements, and their combinations to algae, microcrustaceans, and fungi. Ecotoxicol Environ Saf 201, 110795. https://doi.org/10.1016/j.ecoenv.2020.110795

Binnemans, K., Jones, P.T., Blanpain, B., Van Gerven, T., Yang, Y., Walton, A., Buchert, M., 2013. Recycling of rare earths: A critical review. J Clean Prod 51, 1–22. https://doi.org/10.1016/j.jclepro.2012.12.037

Bishop, W.M., Richardson, R.J., 2018. Influence of Phoslock® on legacy phosphorus, nutrient ratios, and algal assemblage composition in hypereutrophic water resources. Environ Sci Pollut R 25, 4544–4557. https://doi.org/10.1007/s11356-017-0832-2

Boyd, C.E., 2020. Water quality an introduction. Springer Nature 1–427. https://doi.org/10.1007/978-3-030-23335-8

Byrne, R.H., Kim, I.-H., 1990. Rare earth element scavenging in seawater. Geochim Cosmochim Acta 54, 2645–2656. https://doi.org/10.1016/0016-7037(90)90002-3

Byrne, R.H., Li, B., 1995. Comparative complexation behavior of the rare earths. Geochim Cosmochim Acta 59, 4575–4589. https://doi.org/10.1016/0016-7037(95)00303-7

Cardon, P.Y., Roques, O., Caron, A., Rosabal, M., Fortin, C., Amyot, M., 2020. Role of prey subcellular distribution on the bioaccumulation of yttrium (Y) in the rainbow trout. Environ Pollut 258, 113804. https://doi.org/10.1016/j.envpol.2019.113804

Cicconi, M.R., Le Losq, C., Henderson, G.S., Neuville, D.R., 2021. The redox behavior of rare earth elements, in: Magma Redox Geochem. Wiley Blackwell, pp. 381–398. https://doi.org/10.1002/9781119473206.ch19

Conley, D.J., Paerl, H.W., Howarth, R.W., Boesch, D.F., Seitzinger, S.P., Havens, K.E., Lancelot, C., Likens, G.E., 2009. Ecology - Controlling eutrophication: Nitrogen and phosphorus. Science (1979) 323, 1014–1015. https://doi.org/10.1126/science.1167755

Copetti, D., Finsterle, K., Marziali, L., Stefani, F., Tartari, G., Douglas, G., Reitzel, K., Spears, B.M., Winfield, I.J., Crosa, G., D'Haese, P., Yasseri, S., Lürling, M., 2015. Eutrophication management in surface waters using lanthanum modified bentonite: A review. Water Res 97, 162–174. https://doi.org/10.1016/j.watres.2015.11.056

Cordier, D., 2024. Rare Earths. USGS.

Dahle, J.T., Arai, Y., 2015. Environmental geochemistry of cerium: Applications and toxicology of cerium oxide nanoparticles. Int J Environ Res Public Health 12, 1253–1278. https://doi.org/10.3390/ijerph120201253

Dai, Y., Sun, S., Li, Y., Yang, J., Zhang, C., Cao, R., Zhang, H., Chen, J., Geng, N., 2022. Residual levels and health risk assessment of rare earth elements in Chinese resident diet: A market-based investigation. Sci Total Environ 828, 154119. https://doi.org/10.1016/j.scitotenv.2022.154119

Dang, D.H., Ha, Q.K., Némery, J., Strady, E., 2023a. The seasonal variations in the interactions between rare earth elements and organic matter in tropical rivers. Chem Geol 638, 121711. https://doi.org/10.1016/j.chemgeo.2023.121711

Dang, D.H., Ma, L., Ha, Q.K., Wang, W., 2022a. A multi-tracer approach to disentangle anthropogenic emissions from natural processes in the St. Lawrence river and estuary. Water Res 219, 118588. https://doi.org/10.1016/j.watres.2022.118588

Dang, D.H., Thompson, K.A., Ma, L., Nguyen, H.Q., Luu, S.T., Duong, M.T.N., Kernaghan, A., 2021. Toward the circular economy of rare earth elements: A review of abundance, extraction, applications, and environmental impacts. Arch Environ Contam Toxicol 81, 521–530. https://doi.org/10.1007/s00244-021-00867-7

Dang, D.H., Wang, W., Sikma, A., Chatzis, A., Mucci, A., 2022b. The contrasting estuarine geochemistry of rare earth elements between ice-covered and ice-free conditions. Geochim Cosmochim Acta 317, 488–506. https://doi.org/10.1016/j.gca.2021.10.025

Dang, D.H., Wang, W., Winkler, G., Chatzis, A., 2023b. Rare earth element uptake mechanisms in plankton in the Estuary and Gulf of St. Lawrence. Sci Total Environ 860, 160394. https://doi.org/10.1016/j.scitotenv.2022.160394

de Baar, H.J.W., Bruland, K.W., Schijf, J., van Heuven, S.M.A.C., Behrens, M.K., 2018. Low cerium among the dissolved rare earth elements in the central North Pacific Ocean. Geochim Cosmochim Acta 236, 5–40. https://doi.org/10.1016/j.gca.2018.03.003

de Baar, H.J.W., German, C.R., Elderfield, H., Van Gaans, P., 1988. Rare earth element distributions in anoxic waters of the Cariaco Trench*. Geochim Cosmochim Acta 52, 1203–1219. https://doi.org/10.1016/0016-7037(88)90275-X

DeForest, D.K., Brix, K. V., Adams, W.J., 2007. Assessing metal bioaccumulation in aquatic environments: The inverse relationship between bioaccumulation factors, trophic transfer factors and exposure concentration. Aquat Toxicol 84, 236–246. https://doi.org/10.1016/j.aquatox.2007.02.022

Desprez, M., Rybarczyk, H., Wilson, J., Ducrotoy, J., Sueur, F., Olivesi, R., Elkaim, B., 1992. Biological impact of eutrophication in the bay of somme and the induction and impact of anoxia. Neth J Sea Res 30, 149–159. https://doi.org/https://doi.org/10.1016/0077-7579(92)90054-I

Douglas, G., Adeney, J., Robb, M., 1999. A novel technique for reducing bioavailable phosphorus in water and sediments. CSIRO Land and Water.

Douglas, R.W., Rippey, B., 2000. The random redistribution of sediment by wind in a lake. Limnol Oceanogr 45, 686–694. https://doi.org/https://doi.org/10.4319/lo.2000.45.3.0686

Drexler, J., Fisher, N., Henningsen, G., Lanno, R., Mcgeer, J., Sappington, K., Beringer, M., 2003. Issue Paper on the Bioavailability of Metals, US EPA. Washington.

Drobniak, A., Mastalerz, M., 2022. Rare earth elements: A brief overview. Ind J Earth Sci 4, 1–7. https://doi.org/10.14434/ijes.v4i1.33628

El-Akl, P., Smith, S., Wilkinson, K.J., 2015. Linking the chemical speciation of cerium to its bioavailability in water for a freshwater alga. Environ Toxicol Chem 34, 1711–1719. https://doi.org/10.1002/etc.2991

Environment Canada, 2000. Persistence and bioaccumulation regulations [WWW Document]. Canada Gazette . URL https://laws-lois.justice.gc.ca/eng/regulations/SOR-2000-107/page-1.html#h-655345 (accessed 1.22.24).

Finsterle, K., 2014. Overview of Phoslock® Properties and its Use in the Aquatic Environment. Phoslock Europe GmbH 1–47.

Firsching, H.F., Bruñe, S.N., 1991. Solubility products of the trivalent rare-earth phosphates. J Chem Eng Data 36, 93–95. https://doi.org/https://doi.org/10.1021/je00001a028

Freitas, R., Costa, S., D Cardoso, C.E., Morais, T., Moleiro, P., Matias, A.C., Pereira, A.F., Machado, J., Correia, B., Pinheiro, D., Rodrigues, A., Colónia, J., Soares, A.M.V.M., Pereira, E., 2020. Toxicological effects of the rare earth element neodymium in Mytilus galloprovincialis. Chemosphere 244, 125457. https://doi.org/10.1016/j.chemosphere.2019.125457

Galhoum, A.A., Mahfouz, M.G., Abdel-Rehem, S.T., Gomaa, N.A., Atia, A.A., Vincent, T., Guibal, E., 2015. Diethylenetriamine-functionalized chitosan magnetic nano-based particles for the sorption of rare earth metal ions [Nd(III), Dy(III) and Yb(III)]. Cellulose 22, 2589–2605. https://doi.org/10.1007/s10570-015-0677-0

Gambogi, J., 2021. Rare earths. US Geological Survey, Mineral Commodity Summaries 1–2.

Garcia-Solsona, E., Jeandel, C., 2020. Balancing Rare Earth Element distributions in the Northwestern Mediterranean Sea. Chem Geol 532, 119372. https://doi.org/10.1016/j.chemgeo.2019.119372

George, K., Vargas, K., Qi, Z., 2019. P immonbilizing materials for lake internal loading control: A review towards future developments. Crit Rev Environ Sci Technol 29, 518–552. https://doi.org/https://doi.org/10.1080/10643389.2018.1551300

Geurts, J.J.M., van de Wouw, P.A.G., Smolders, A.J.P., Roelofs, J.G.M., Lamers, L.P.M., 2011. Ecological restoration on former agricultural soils: Feasibility of in situ phosphate fixation as an alternative to top soil removal. Ecol Eng 37, 1620–1629. https://doi.org/10.1016/j.ecoleng.2011.06.038

Gibbs, M.M., Hickey, C.W., Özkundakci, D., 2011. Sustainability assessment and comparison of efficacy of four P-inactivation agents for managing internal phosphorus loads in lakes: Sediment incubations. Hydrobiologia 658, 253–275. https://doi.org/10.1007/s10750-010-0477-3

Gielen, D., Lyons, M., 2022. Critical materials for the energy transition: Rare earth elements. IRENA 1–48.

Haghseresht, F., Wang, S., Do, D.D., 2009. A novel lanthanum-modified bentonite, Phoslock, for phosphate removal from wastewaters. Appl Clay Sci 46, 369–375. https://doi.org/10.1016/j.clay.2009.09.009

Han, Y., Li, Q., He, H., Gu, J., Wu, Z., Huang, X., Zou, X., Zhang, Y., Li, K., 2021. Effect of juvenile omni-benthivorous fish (Carassius carassius) disturbance on the efficiency of lanthanum-modified bentonite (LMB) for eutrophication control: a mesocosm study. Environ Sci Pollut Res 28, 21779–21788. https://doi.org/10.1007/s11356-020-12045-8

Hanana, H., Kleinert, C., Gagné, F., 2021. Toxicity of representative mixture of five rare earth elements in juvenile rainbow trout (Oncorhynchus mykiss) juveniles. Environ Sci Pollut R 28, 28263–28274. https://doi.org/10.1007/s11356-020-12218-5/Published

Hannigan, Robyn E, Sholkovitz, E.R., Hannigan, R E, 2001. The development of middle rare earth element enrichments in freshwaters: weathering of phosphate minerals. Chem Geol 175, 495–508. https://doi.org/10.1016/S0009-2541(00)00355-7

Hua, D., Wang, J., Yu, D., Liu, J., 2017. Lanthanum exerts acute toxicity and histopathological changes in gill and liver tissue of rare minnow (*Gobiocypris rarus*). Ecotoxicology 26, 1207–1215. https://doi.org/10.1007/s10646-017-1846-8

Humphries, M., 2013. Rare earth elements: The global supply chain. Congressional Research Service 1–27.

Jeppesen, E., Kristensen, P., Jensen, J., Sondergaard, M., Mortensen, E., Lauridsen, T., 1991. Recovery resilience following a reduction in external phosphorous loading of shallow, eutrophic Danish lakes: duration, regulating, factors and methods for overcoming resilience. Memorie dell'Istituto Italiano di Idrobiologia 48, 127–148.

Jiang, C., Li, Y., Li, C., Zheng, Lanlan, Zheng, Liugen, 2022a. Distribution, source and behavior of rare earth elements in surface water and sediments in a subtropical freshwater lake influenced by human activities. Environ Pollut 313, 120153. https://doi.org/10.1016/j.envpol.2022.120153

Jiang, C., Li, Y., Li, C., Zheng, Lanlan, Zheng, Liugen, 2022b. Distribution, source and behavior of rare earth elements in surface water and sediments in a subtropical freshwater lake influenced by human activities. Environ Pollut 313, 120153. https://doi.org/10.1016/j.envpol.2022.120153

Johannesson, K.H., Hawkins, D.L., Cortés, A., 2006. Do Archean chemical sediments record ancient seawater rare earth element patterns? Geochim Cosmochim Acta 70, 871–890. https://doi.org/10.1016/j.gca.2005.10.013

Kemp, W.M., Boynton, W.R., Adolf, J.E., Boesch, D.F., Boicourt, W.C., Brush, G., Cornwell, J.C., Fisher, T.R., Glibert, P.M., Hagy, J.D., Harding, L.W., Houde, E.D., Kimmel, D.G., Miller, W.D., Newell, R.I.E., Roman, M.R., Smith, E.M., Stevenson, J.C., 2005. Eutrophication of Chesapeake Bay: historical trends and ecological interactions. Mar Ecol Prog Ser 303, 1–29. https://doi.org/doi:10.3354/meps303001

Khan, F., Ansari, A., 2005. Eutrophication: An ecological vision. Bot Rev 71, 449–482. https://doi.org/https://doi.org/10.1663/0006-8101(2005)071[0449:EAEV]2.0.CO;2

Kim, P., Anderko, A., Navrotsky, A., Riman, R.E., 2018. Trends in structure and thermodynamic properties of normal rare earth carbonates and rare earth hydroxycarbonates. Minerals 8, 106. https://doi.org/10.3390/min8030106

Kirol, A.P., Morales-Williams, A.M., Braun, D.C., Marti, C.L., Pierson, O.E., Wagner, K.J., Schroth, A.W., 2024. Linking sediment and water column phosphorus dynamics to oxygen, temperature, and aeration in shallow eutrophic Lakes. Water Resour Res 60, 1–20. https://doi.org/10.1029/2023WR034813

Kowalczewska-Madura, K., Dondajewska-Pielka, R., Gołdyn, R., 2022. The assessment of external and internal nutrient loading as a basis for lake management. Water 14, 2844. https://doi.org/10.3390/w14182844

Leybourne, M.I., Goodfellow, W.D., Boyle, D.R., Hall, G.M., 2000. Rapid development of negative Ce anomalies in surface waters and contrasting REE patterns in groundwaters associated with Zn±Pb massive sulphide deposits. Appl Geochem 15, 695–723. https://doi.org/https://doi.org/10.1016/S0883-2927(99)00096-7

Lim, D., Jung, H.S., Choi, J.Y., 2014. REE partitioning in riverine sediments around the Yellow Sea and its importance in shelf sediment provenance. Mar Geol 357, 12–24. https://doi.org/10.1016/j.margeo.2014.07.002

Ling, H.F., Chen, X., Li, D., Wang, D., Shields-Zhou, G.A., Zhu, M., 2013. Cerium anomaly variations in Ediacaran-earliest Cambrian carbonates from the Yangtze Gorges area, South China: Implications for oxygenation of coeval shallow seawater. Precambrian Res 225, 110–127. https://doi.org/10.1016/j.precamres.2011.10.011

Ling, L., Wang, N.H.L., 2015. Ligand-assisted elution chromatography for separation of lanthanides. J Chromatogr A 1389, 28–38. https://doi.org/10.1016/j.chroma.2015.02.004

Liu, S.L., Fan, H.R., Liu, X., Meng, J., Butcher, A.R., Yann, L., Yang, K.F., Li, X.C., 2023. Global rare earth elements projects: New developments and supply chains. Ore Geol Rev 157, 105428. https://doi.org/10.1016/j.oregeorev.2023.105428

Lundy, R., Byrne, C., Bogan, J., Nolan, K., Collins, M.N., Dalton, E., Enright, R., 2017. Exploring the role of adsorption and surface state on the hydrophobicity of rare earth oxides. ACS Appl Mater Interfaces 9, 13751–13760. https://doi.org/10.1021/acsami.7b01515

Luo, Byrne, 2004. Carbonate complexation of yttrium and the rare earth elements in natural waters. Geochim Cosmochim Acta 68, 691–699. https://doi.org/10.1016/S0016-7037(03)00495-2

Lürling, M., Faassen, E.J., 2012. Controlling toxic cyanobacteria: Effects of dredging and phosphorus-binding clay on cyanobacteria and microcystins. Water Res 46, 1447–1459. https://doi.org/10.1016/j.watres.2011.11.008

Lürling, M., Mackay, E., Reitzel, K., Spears, B.M., 2016. Editorial – A critical perspective on geo-engineering for eutrophication management in lakes. Water Res 97, 1–10. https://doi.org/10.1016/j.watres.2016.03.035

Lürling, M., Tolman, Y., 2010. Effects of lanthanum and lanthanum-modified clay on growth, survival and reproduction of Daphnia magna. Water Res 44, 309–319. https://doi.org/10.1016/j.watres.2009.09.034

Lürling, M., Van Oosterhout, F., 2013. Case study on the efficacy of a lanthanum-enriched clay (Phoslock®) in controlling eutrophication in Lake Het Groene Eiland (The Netherlands). Hydrobiologia 710, 253–263. https://doi.org/10.1007/s10750-012-1141-x

Lürling, M., Waajen, G., Van Oosterhout, F., 2014. Humic substances interfere with phosphate removal by lanthanum modified clay in controlling eutrophication. Water Res 54, 78–88. https://doi.org/10.1016/j.watres.2014.01.059

MacMillan, G.A., Chételat, J., Heath, J., Mickpegak, R., Amyot, M., 2017. Rare earth elements (REE) in freshwater, marine, and terrestrial ecosystems in the eastern Canadian Arctic. Environ Sci-Proc Imp 10, 1336–1345. https://doi.org/10.1101/174870

MacMillan, G.A., Clayden, M.G., Chételat, J., Richardson, M.C., Ponton, D.E., Perron, T., Amyot, M., 2019. Environmental drivers of rare earth element bioaccumulation in freshwater zooplankton. Environ Sci Technol 53, 1650–1660. https://doi.org/10.1021/acs.est.8b05547

Marginson, H., MacMillan, G.A., Grant, E., Gérin-Lajoie, J., Amyot, M., 2023. Rare earth element bioaccumulation and cerium anomalies in biota from the Eastern Canadian subarctic (Nunavik). Sci Total Environ 879, 163024. https://doi.org/10.1016/j.scitotenv.2023.163024

Marsac, R., Davranche, M., Gruau, G., Dia, A., Pédrot, M., Le Coz-Bouhnik, M., Briant, N., 2013. Effects of Fe competition on REE binding to humic acid: Origin of REE pattern variability in organic waters. Chem Geol 342, 119–127. https://doi.org/10.1016/j.chemgeo.2013.01.020

Marsden, M., 1989. Lake restoration by reducing external phosphorus loading: the influence of sediment phosphorus release. Freshwater Biol 21, 139–162. https://doi.org/https://doi.org/10.1111/j.1365-2427.1989.tb01355.x

Mayfield, D.B., Fairbrother, A., 2015. Examination of rare earth element concentration patterns in freshwater fish tissues. Chemosphere 120, 68–74. https://doi.org/10.1016/j.chemosphere.2014.06.010

Mcgeer, J.C., Brix, K. V, Skeaff, J.M., Deforest, D.K., Brigham, S.I., Adams, W.J., Green, A., 2003. Inverse relationship between bioconcentration factor and exposure concentration for metals: implications for hazard assessment of metals in the aquatic environment. Environ Toxicol Chem 22, 1017–1037. https://doi.org/https://doi.org/10.1002/etc.5620220509

McLennan, S.M., 2001. Relationships between the trace element composition of sedimentary rocks and upper continental crust. Geochem Geophy Geosy 2, 1–24. https://doi.org/10.1029/2000GC000109

Meis, S., Spears, B.M., Maberly, S.C., Perkins, R.G., 2013. Assessing the mode of action of Phoslock® in the control of phosphorus release from the bed sediments in a shallow lake (Loch Flemington, UK). Water Res 47, 4460–4473. https://doi.org/10.1016/j.watres.2013.05.017

Merschel, G., Bau, M., Schmidt, K., Münker, C., Dantas, E.L., 2017. Hafnium and neodymium isotopes and REY distribution in the truly dissolved, nanoparticulate/colloidal and suspended loads of rivers in the Amazon Basin, Brazil. Geochim Cosmochim Acta 213, 383–399. https://doi.org/10.1016/j.gca.2017.07.006

Mestre, N.C., Sousa, V.S., Rocha, T.L., Bebianno, M.J., 2019. Ecotoxicity of rare earths in the marine mussel Mytilus galloprovincialis and a preliminary approach to assess environmental risk. Ecotoxicology 28, 294–301. https://doi.org/10.1007/s10646-019-02022-4

Meysman, F.J.R., Middelburg, J.J., Heip, C.H.R., 2006. Bioturbation: a fresh look at Darwin's last idea. Trends Ecol Evol 21, 688–695. https://doi.org/10.1016/j.tree.2006.08.002

Möller, P., Morteani, G., Dulski, P., 2003. Anomalous gadolinium, cerium, and yttrium contents in the Adige and Isarco River waters and in the water of their tributaries (Provinces Trento and Bolzano/Bozen, NE Italy). Acta Hydrochimica et Hydrobiologica 31, 225–239. https://doi.org/10.1002/aheh.200300492

Moos, M.T., Taffs, K.H., Longstaff, B.J., Ginn, B.K., 2014. Establishing ecological reference conditions and tracking post-application effectiveness of lanthanum-saturated bentonite clay (Phoslock®) for reducing phosphorus in aquatic systems: An applied paleolimnological approach. J Environ Manage 141, 77–85. https://doi.org/10.1016/j.jenvman.2014.02.038

Mortimer, C.H., 1941. The Exchange of Dissolved Substances Between Mud and Water in Lakes. J Ecol 29, 280–329. https://doi.org/https://doi.org/10.2307/2256395

Moss, R., Tzimas, E., Willis, P., Arendorf, J., Tercero Espinoza, L., Thompson, P., Chapman, A., Morley, N., Sims, E., Bryson, R., Pearson, J., 2013. Critical metals in the path towards the decarbonisation of the EU energy sector assessing rare metals as supply-chain bottlenecks in low-carbon energy technologies. EC 1–246. https://doi.org/10.2790/46338

Ni, Y., Hughes, J.M., 1995. Crystal chemistry of the monazite and xenotime structures. Am Mineral 80, 21–26. https://doi.org/https://doi.org/10.2138/am-1995-1-203

Nikanorov, A.M., 2016. Oddo–Harkins evenness rule as an indication of the abundances of chemical elements in the Earth's hydrosphere and estimations of the nature of cosmic bodies. Geochemistry International 54, 464–469. https://doi.org/10.1134/S0016702916050074

Nørregaard, R.D., Kaarsholm, H., Bach, L., Nowak, B., Geertz-Hansen, O., Søndergaard, J., Sonne, C., 2019. Bioaccumulation of rare earth elements in juvenile arctic char (Salvelinus alpinus) under field experimental conditions. Sci Total Environ 688, 529–535. https://doi.org/10.1016/j.scitotenv.2019.06.180

Nozaki, Y., Lerche, D., Alibo, D.S., Snidvongs, A., 2000. The estuarine geochemistry of rare earth elements and indium in the Chao Phraya River, Thailand. Geochim Cosmochim Acta 64, 3983–3994. https://doi.org/https://doi.org/10.1016/S0016-7037(00)00473-7

Nürnberg, G.K., 2017. Attempted management of cyanobacteria by Phoslock (lanthanum-modified clay) in Canadian lakes: water quality results and predictions. Lake Reserv Manag 33, 163–170. https://doi.org/10.1080/10402381.2016.1265618

Nürnberg, G.K., LaZerte, B.D., 2016. Trophic state decrease after lanthanum-modified bentonite (Phoslock) application to a hyper-eutrophic polymictic urban lake frequented by Canada geese (Branta canadensis). Lake Reserv Manag 32, 74–88. https://doi.org/10.1080/10402381.2015.1133739

Osborne, A.H., Haley, B.A., Hathorne, E.C., Plancherel, Y., Frank, M., 2014. Rare earth element distribution in Caribbean seawater: Continental inputs versus lateral transport of distinct REE compositions in subsurface water masses. Mar Chem 177, 172–183. https://doi.org/10.1016/j.marchem.2015.03.013

Paerl, H.W., Havens, K.E., Xu, H., Zhu, G., McCarthy, M.J., Newell, S.E., Scott, J.T., Hall, N.S., Otten, T.G., Qin, B., 2020. Mitigating eutrophication and toxic cyanobacterial blooms in large lakes: The evolution of a dual nutrient (N and P) reduction paradigm. Hydrobiologia 847, 4359–4375. https://doi.org/10.1007/s10750-019-04087-y

Paiva, A. V., De Oliveira, M.S., Yunes, S.N., De Oliveira, L.G., Cabral-Neto, J.B., De Almeida, C.E.B., 2009. Effects of lanthanum on human lymphocytes viability and DNA strand break. Bull Environ Contam Toxicol 82, 423–427. https://doi.org/10.1007/s00128-008-9596-1

Pallí, N.B., 2015. A comparison of two methods to reduce internal phosphorus cycling in lakes: Aluminium versus Phoslock (Master's thesis). Swedish University of Agricultural Sciences.

Pastorino, P., Brizio, P., Abete, M.C., Bertoli, M., Oss Noser, A.G., Piazza, G., Prearo, M., Elia, A.C., Pizzul, E., Squadrone, S., 2020. Macrobenthic invertebrates as tracers of rare earth elements in freshwater watercourses. Sc Total Environ 698, 134282. https://doi.org/10.1016/j.scitotenv.2019.134282

Paulick, H., Machacek, E., 2017. The global rare earth element exploration boom: An analysis of resources outside of China and discussion of development perspectives. Resour Policy 52, 134–153. https://doi.org/10.1016/j.resourpol.2017.02.002

Penn, M.R., Auer, M.T., Doerr, S.M., Driscoll, C.T., Brooks, C.M., Effler, S.W., 2000. Seasonality in phosphorus release rates from the sediments of a hypereutrophic lake under a matrix of pH and redox conditions. Can J Fish Aquat Sci 1033–1041. https://doi.org/https://doi.org/10.1139/f00-035

Pinto, J., Costa, M., Leite, C., Borges, C., Coppola, F., Henriques, B., Monteiro, R., Russo, T., Di Cosmo, A., Soares, A.M.V.M., Polese, G., Pereira, E., Freitas, R., 2019. Ecotoxicological effects of lanthanum in Mytilus galloprovincialis: Biochemical and histopathological impacts. Aquat Toxicol 211, 181–192. https://doi.org/10.1016/j.aquatox.2019.03.017

Piper, D.Z., Bau, M., 2013. Normalized rare earth elements in water, sediments, and wine: Identifying sources and environmental redox conditions. Am J Analyt Chem 04, 69–83. https://doi.org/10.4236/ajac.2013.410a1009

Pourret, O., Davranche, M., Gruau, G., Dia, A., 2007. Organic complexation of rare earth elements in natural waters: Evaluating model calculations from ultrafiltration data. Geochim Cosmochim Acta 71, 2718–2735. https://doi.org/10.1016/j.gca.2007.04.001

Pourret, O., Tuduri, J., 2017. Continental shelves as potential resource of rare earth elements. Sci Rep 7, 5857. https://doi.org/10.1038/s41598-017-06380-z

Qian, Y., Zheng, L., Jiang, C., Chen, X., Chen, Yongchun, Xu, Y., Chen, Yuanping, 2022. Environmental geochemical characteristics of rare-earth elements in surface waters in the Huainan coal mining area, Anhui Province, China. Environ Geochem Health 44, 3527–3539. https://doi.org/10.1007/s10653-021-01121-8

Ratié, G., Vantelon, D., Pédrot, M., Beauvois, A., Chaouchi, K., Fossé, C., Davranche, M., 2020. Cerium anomalies in riverbanks: Highlight into the role of ferric deposits. Sci Total Environ 713, 136544. https://doi.org/10.1016/j.scitotenv.2020.136544

Reitzel, K., Andersen, F.T., Egemose, S., Jensen, H.S., 2013. Phosphate adsorption by lanthanum modified bentonite clay in fresh and brackish water. Water Res 47, 2787–2796. https://doi.org/10.1016/j.watres.2013.02.051

Reitzel, K., Balslev, K.A., Jensen, H.S., 2017. The influence of lake water alkalinity and humic substances on particle dispersion and lanthanum desorption from a lanthanum modified bentonite. Water Res 125, 191–200. https://doi.org/10.1016/j.watres.2017.08.044

Rétif, J., Zalouk-Vergnoux, A., Briant, N., François, Y., Poirier, L., 2024. Trophic dilution of rare earth elements along the food chain of the Seine estuary (France). Mar Pollut Bull 206, 116671. https://doi.org/10.1016/j.marpolbul.2024.116671

Riesgo García, M.V., Krzemień, A., Manzanedo del Campo, M.Á., Menéndez Álvarez, M., Gent, M.R., 2017. Rare earth elements mining investment: It is not all about China. Resour Policy 53, 66–76. https://doi.org/10.1016/j.resourpol.2017.05.004

Rim, K.T., 2016. Effects of rare earth elements on the environment and human health: A literature review. Toxicol Environ Health Sci 8, 189–200. https://doi.org/10.1007/s13530-016-0276-y

Robb, M., Greenop, B., Goss, Z., Douglas, G., Adeney, J., 2003. Application of Phoslock TM , an innovative phosphorus binding clay, to two Western Australian waterways: preliminary findings. The interactions between sediments and water 169, 237–243. https://doi.org/10.1007/978-94-017-3366-3_32

Ross, G., Haghseresht, F., Cloete, T.E., 2008. The effect of pH and anoxia on the performance of Phoslock®, a phosphorus binding clay. Harmful Algae 7, 545–550. https://doi.org/10.1016/j.hal.2007.12.007

Rudnick, R.L., Gao, S., 2013. Composition of the Continental Crust, in: Treatise on Geochemistry: Second Edition. Elsevier Inc., Oxford, pp. 1–51. https://doi.org/10.1016/B978-0-08-095975-7.00301-6

Santos, A.C.S.S., Souza, L.A., Araujo, T.G., de Rezende, C.E., Hatje, V., 2023. Fate and trophic transfer of rare earth elements in a tropical estuarine food web. Environ Sci Technol 57, 2404–2414. https://doi.org/10.1021/acs.est.2c07726

Sas, H., 1989. Lake restoration by reduction of nutrient loading: Expectations, experiences, extrapolations. Chem Limnol 24, 247–251. https://doi.org/https://doi.org/10.1080/03680770.1989.11898731

Schindler, D.W., Carpenter, S.R., Chapra, S.C., Hecky, R.E., Orihel, D.M., 2016. Reducing phosphorus to curb lake eutrophication is a success. Environ Sci Technol 50, 8923–8929. https://doi.org/10.1021/acs.est.6b02204

Schindler, D.W., Hecky, R.E., Findlay, D.L., Stainton, M.P., Parker, B.R., Paterson, M.J., Beaty, K.G., Lyng, M., Kasian, S.E.M., 2008. Eutrophication of lakes cannot be controlled by reducing nitrogen input: Results of a 37-year whole-ecosystem experiment. Biol Sci 11254–11258. https://doi.org/https://doi.org/10.1073/pnas.080510810

Shannon, R.D., 1976. Revised effective ionic radii and systematic studies of interatomic distances in halides and chalcogenides. Acta Crystallographica Section A 32, 751–767. https://doi.org/10.1107/S0567739476001551

Sharma, C., Borgstrøm, R., Rosseland, B., 2011. Biomanipulation in Lake Årungen, Normay: A Tool for biological control, in: Ansari, A., Gill, S., Lanza, G., Rast, W. (Eds.), Eutrophication: Causes, Consequences and Control. Springer, pp. 295–323.

Sholkovitz, E.R., 1995. The aquatic chemistry of rare earth elements in rivers and estuaries. Aquat Geochem 1–34. https://doi.org/https://doi.org/10.1007/BF01025229

Sholkovitz, E.R., 1992. Chemical evolution of rare earth elements: fractionation between colloidal and solution phases of filtered river water. Earth Planet Sci Lett 114, 77–84. https://doi.org/https://doi.org/10.1016/0012-821X(92)90152-L

Sholkovitz, E.R., Schneider, D.L., 1991. Cerium redox cycles and rare earth elements in the Sargasso Sea. Geochimica ef Cosmochimica Acta 55, 2737–2743. https://doi.org/https://doi.org/10.1016/0016-7037(91)90440-G

Shu, J., Chen, W., Wang, Z., Jiang, D., Xiao, Y., Li, Z., 2023. Two-phase effects of environmentally relevant lanthanum on life-history traits of Daphnia magna and transgenerational bioenergetic profiles: Implications for nutritional and environmental consequences. Aquat Toxicol 255, 106380. https://doi.org/10.1016/j.aquatox.2022.106380

Siciliano, A., Guida, M., Serafini, S., Micillo, M., Galdiero, E., Carfagna, S., Salbitani, G., Tommasi, F., Lofrano, G., Padilla Suarez, E.G., Gjata, I., Brouziotis, A.A., Trifuoggi, M., Liguori, R., Race, M., Fabbricino, M., Libralato, G., 2021. Long-term multi-endpoint exposure of the microalga Raphidocelis subcapitata to lanthanum and cerium. Sci Total Environ 790, 148229. https://doi.org/10.1016/j.scitotenv.2021.148229

Silvestri, L., Forcina, A., Silvestri, C., Traverso, M., 2021. Circularity potential of rare earths for sustainable mobility: Recent developments, challenges and future prospects. J Clean Prod 292, 126089. https://doi.org/10.1016/j.jclepro.2021.126089

Smith, V.H., Schindler, D.W., 2009. Eutrophication science: where do we go from here? Trends Ecol Evol 24, 201–207. https://doi.org/10.1016/j.tree.2008.11.009

Smolders, A.J.P., Lamers, L.P.M., Lucassen, E.C.H.E.T., Van Der Velde, G., Roelofs, J.G.M., 2006. Internal eutrophication: How it works and what to do about it - A review. Chem Ecol 22, 93–111. https://doi.org/10.1080/02757540600579730

Søndergaard, M., Jensen, J.P., Jeppesen, E., 2003. Role of sediment and internal loading of phosphorus in shallow lakes. Hydrobiologia 506–509, 135–145. https://doi.org/https://doi.org/10.1023/B:HYDR.0000008611.12704.dd

Søndergaard, M., Jensen, J.P., Jeppesen, E., 1999. Internal phosphorus loading in shallow Danish lakes. Hydrobiologia 408/409, 145–152. https://doi.org/https://doi.org/10.1023/A:1017063431437

Souza, I.C., Morozesk, M., Azevedo, V.C., Mendes, V.A.S., Duarte, I.D., Rocha, L.D., Matsumoto, S.T., Elliott, M., Baroni, M. V., Wunderlin, D.A., Monferrán, M. V., Fernandes, M.N., 2021. Trophic transfer of emerging metallic contaminants in a neotropical mangrove ecosystem food web. J Hazard Mater 408, 124424. https://doi.org/10.1016/j.jhazmat.2020.124424

Spears, B.M., Lürling, M., Yasseri, S., Castro-Castellon, A.T., Gibbs, M., Meis, S., McDonald, C., McIntosh, J., Sleep, D., Van Oosterhout, F., 2013. Lake responses following lanthanum-modified bentonite clay (Phoslock®) application: An analysis of water column lanthanum data from 16 case study lakes. Water Res 47, 5930–5942. https://doi.org/10.1016/j.watres.2013.07.016

Sugiyama, N., 2020. Direct analysis of ultratrace rare earth elements in environmental waters by ICP-QQQ. ICP-QQQ Applications in Geochemistry, Mineral Analysis, and Nuclear Science 56–61.

Sun, D., He, N., Chen, Q., Duan, S., 2019. Effects of lanthanum on the photosystem ii energy fluxes and antioxidant system of chlorella vulgaris and phaeodactylum tricornutum. Int J Environ Res Public Health 16, 2242. https://doi.org/10.3390/ijerph16122242

Tang, J., Johannesson, K.H., 2010. Ligand extraction of rare earth elements from aquifer sediments: Implications for rare earth element complexation with organic matter in natural waters. Geochim Cosmochim Acta 74, 6690–6705. https://doi.org/10.1016/j.gca.2010.08.028

Tang, J., Johannesson, K.H., 2003. Speciation of rare earth elements in natural terrestrial waters: Assessing the role of dissolved organic matter from the modeling approach. Geochim Cosmochim Acta 67, 2321–2339. https://doi.org/10.1016/S0016-7037(02)01413-8

Taylor, S.R., McLennan, S.M., 1995. The geochemical evolution of the continental crust. Rev Geophys 33, 241–265. https://doi.org/10.1029/95RG00262

Thomas, B.S., Dimitriadis, P., Kundu, C., Vuppaladadiyam, S.S.V., Raman, R.K.S., Bhattacharya, S., 2024. Extraction and separation of rare earth elements from coal and coal fly ash: A review on fundamental understanding and on-going engineering advancements. J Environ Chem Eng. https://doi.org/10.1016/j.jece.2024.112769

Tommasi, F., Thomas, P.J., Lyons, D.M., Pagano, G., Oral, R., Siciliano, A., Toscanesi, M., Guida, M., Trifuoggi, M., 2023. Evaluation of rare earth element-associated hormetic effects in candidate fertilizers and livestock feed additives. Biol Trace Elem Res 201, 2573–2581. https://doi.org/10.1007/s12011-022-03331-2

Tostevin, R., 2021. Cerium anomalies and paleoredox. Cambridge University Press. https://doi.org/10.1017/9781108847223

Turner, A.M., Chislock, M.F., 2010. Blinded by the stink: Nutrient enrichment impairs the perception of predation risk by freshwater snails. Ecol Appl 20, 2089–2095. https://doi.org/10.1890/10-0208.1

Tyler, G., 2004. Rare earth elements in soil and plant systems-A review. Plant Soil 267, 191–206. https://doi.org/https://doi.org/10.1007/s11104-005-4888-2

Valcheva-Traykova, M., Saso, L., Kostova, I., 2014. Involvement of lanthanides in the free radicals homeostasis. Curr Top Med Chem 14, 1–12. https://doi.org/https://doi.org/10.2174/1568026614666141203123620

Van Gosen, B., Verplanck, P., Long, K., Gambogi, J., Seal, R., 2014. The rare-earth elements - Vital to modern technologies and lifestyles. USGS Mineral Resource Program 1–4. https://doi.org/10.3133/fs20143078

Van Oosterhout, F., Goitom, E., Roessink, I., Lürling, M., 2014. Lanthanum from a modified clay used in eutrophication control is bioavailable to the marbled crayfish (Procambarus fallax f. virginalis). PLoS One 9, 1–9. https://doi.org/10.1371/journal.pone.0102410

Van Oosterhout, F., Lürling, M., 2013. The effect of phosphorus binding clay (Phoslock®) in mitigating cyanobacterial nuisance: A laboratory study on the effects on water quality variables and plankton. Hydrobiologia 710, 265–277. https://doi.org/10.1007/s10750-012-1206-x

Van Oosterhout, F., Waajen, G., Yasseri, S., Manzi Marinho, M., Pessoa Noyma, N., Mucci, M., Douglas, G., Lürling, M., 2020. Lanthanum in water, sediment, macrophytes and chironomid larvae following application of lanthanum modified bentonite to lake Rauwbraken (The Netherlands). Sci Total Environ 706, 1–13. https://doi.org/10.1016/j.scitotenv.2019.135188

Waajen, G., van Oosterhout, F., Lürling, M., 2017. Bio-accumulation of lanthanum from lanthanum modified bentonite treatments in lake restoration. Environmental Pollution 230, 911–918. https://doi.org/10.1016/j.envpol.2017.07.046

Wang, G.X., Zhang, L.M., Chua, H., Li, X.D., Xia, M.F., Pu, P.M., 2009. A mosaic community of macrophytes for the ecological remediation of eutrophic shallow lakes. Ecol Eng 35, 582–590. https://doi.org/10.1016/j.ecoleng.2008.06.006

Wang, T., Wu, Q., Wang, Z., Dai, G., Jia, H., Gao, S., 2021. Anthropogenic gadolinium accumulation and rare earth element anomalies of river water from the middle reach of Yangtze River Basin, China. ACS Earth Space Chem 5, 3130–3139. https://doi.org/10.1021/acsearthspacechem.1c00238

Wang, Y., Zhang, M., Wang, X., 2000. Population growth responses of tetrahymena shanghaiensis in exposure to rare earth elements. Biol Trace Metal R 75, 265–275. https://doi.org/10.1385/BTER:75:1-3:265

Watson-Leung, T., 2009. PhoslockTM toxicity testing with three sediment dwelling organisms (Hyalella azteca, Hexagenia spp. and Chironomus dilutus) and two water column dwelling organisms (Rainbow Trout and Daphnia magna). MOE 1–55. https://doi.org/10.13140/RG.2.1.1833.1687

Wood Environment & Infrastructure Solutions, 2020. Toronto and region conservation authority rouge river floodplain mapping update phase 2 technical report. TRCA 1–97.

Wu, Z., Liu, Y., Liang, Z., Wu, S., Guo, H., 2017. Internal cycling, not external loading, decides the nutrient limitation in eutrophic lake: A dynamic model with temporal Bayesian hierarchical inference. Water Res 116, 231–240. https://doi.org/10.1016/j.watres.2017.03.039

Wurtsbaugh, W.A., Paerl, H.W., Dodds, W.K., 2019. Nutrients, eutrophication and harmful algal blooms along the freshwater to marine continuum. Wiley Interdisciplinary Reviews: Water 6, 1373. https://doi.org/10.1002/WAT2.1373

Yang, X.E., Wu, X., Hao, H.L., He, Z.L., 2008. Mechanisms and assessment of water eutrophication. J Zhejiang Univ Sci B 9, 197–209. https://doi.org/10.1631/jzus.B0710626

Yeghicheyan, D., Aubert, D., Bouhnik-Le Coz, M., Chmeleff, J., Delpoux, S., Djouraev, I., Granier, G., Lacan, F., Piro, J.L., Rousseau, T., Cloquet, C., Marquet, A., Menniti, C., Pradoux, C., Freydier, R., Vieira da Silva-Filho, E., Suchorski, K., 2019. A new interlaboratory characterisation of silicon, rare earth elements and twenty-two other trace element concentrations in the natural river water certified reference material SLRS-6 (NRC-CNRC). Geostand Geoanal Res 43, 475–496. https://doi.org/10.1111/ggr.12268

Yu, P., O'Keefe, T.J., 2006. The Phase Stability of Cerium Species in Aqueous Systems. J Electrochem Soc 153, C80–C85. https://doi.org/10.1149/1.2130574

Yuan, M., Guo, M.N., Liu, W.S., Liu, C., van der Ent, A., Morel, J.L., Huot, H., Zhao, W.Y., Wei, X.G., Qiu, R.L., Tang, Y.T., 2017. The accumulation and fractionation of Rare Earth Elements in hydroponically grown Phytolacca americana L. Plant Soil 421, 67–82. https://doi.org/10.1007/s11104-017-3426-3

Zeller, M.A., Alperin, M.J., 2021. The efficacy of Phoslock® in reducing internal phosphate loading varies with bottom water oxygenation. Water Res X 11, 100095. https://doi.org/10.1016/j.wroa.2021.10

Zhao, S., 2004. Mechanisms of lake eutrophication and technologies for controlling in China. Advance in Earth Sciences 19, 53–61.

Zhao, Y., Liang, J., Meng, H., Yin, Y., Zhen, H., Zheng, X., Shi, H., Wu, X., Zu, Y., Wang, B., Fan, L., Zhang, K., 2021. Rare earth elements lanthanum and praseodymium adversely affect neural and cardiovascular development in zebrafish (Danio rerio). Environ Sci Technol 55, 1155–1166. https://doi.org/10.1021/acs.est.0c06632

Zheng, X.Y., Plancherel, Y., Saito, M.A., Scott, P.M., Henderson, G.M., 2016. Rare earth elements (REEs) in the tropical South Atlantic and quantitative deconvolution of their non-conservative behavior. Geochim Cosmochim Acta 177, 217–237. https://doi.org/10.1016/j.gca.2016.01.018

Chapter 2. Exposure pathways (diet, dissolved or particulate substrate) of rare earth elements to aquatic organisms

2.1 Abstract

The global extraction and use of rare earth elements (REEs) continue to rise as they are implemented in technologies that improve human and environmental livelihoods. However, the general understanding of transfer processes and fates of REEs in aquatic systems remains limited. Here, we aim to determine the REEs' main exposure pathways, e.g., particulate fraction, diet, or dissolved (ionic) fractions, to three benthic and three pelagic organisms. They were maintained under laboratory conditions and exposed to natural river water, with or without a sand substrate and an adapted diet. The organisms include northern clearwater crayfish (*Faxonius propinquus*), chinese mystery snail (*Cipangopaludina chinensis*), black sandshell mussel *(Ligumia recta*), striped shiner minnows (*Luxilus chrysocephalus*), *Daphnia magna*, and *Euglena gracilis.* The combined results of REE concentrations, fractionations, and anomalies highlighted that pelagic organisms are characterized by heavy REEs enrichment indicating they mainly uptake REEs in the dissolved form with high bioaccumulation potential, i.e., bioconcentration (BCF) > 1 and diet accumulation factors (DAF) < 1. Pelagic organisms exhibited relatively low REE concentrations in their tissues ([La] ranging from 4.6 to 57.7 µg kg^{-1} in minnows, 18.4 µg kg^{-1} in whole body *D. magna, and 32.2* µg kg^{-1} in *E. gracilis*). On the other hand, snails and mussels were enriched in light REEs showing they mainly uptake REEs through their respective diets and particulate sand substrate. Relative to pelagic organisms, mussels and snails have higher DAFs (161.2 and 18.6, respectively) and REE levels in their soft tissues ([La] of 5,700 µg kg^{-1} and 650 µg kg^{-1},

respectively), but DAF for crayfish remains <1. In summary, under environmental-relevant conditions, the six aquatic organisms accumulate REEs through various uptake pathways. Nevertheless, our results confirming preferential uptake pathways of the six organisms can be used to select species to monitor REE exposure from various fractions: dissolved, particulate forms or in the food webs (i.e., diet).

Keywords: natural uptake mechanisms, REE fractionations, background conditions, bioaccumulation potential, freshwater organisms.

2.2 Introduction

Rare earth elements (REEs) form a homogenous group of elements, composed of 15 lanthanide ($_{57}$La to $_{71}$Lu) and two non-lanthanides: scandium ($_{21}$Sc) and yttrium ($_{39}$Y). Various jurisdictions have identified REEs as priority critical elements, e.g., Canada, USA, EU (Ellis, 2018; European Commission, 2020; Government of Canada, 2022), as their geochemical and physical properties allow for advancements in vital high-end technologies (Balaram, 1996; Dang et al., 2021; Labassa et al., 2023).

Rare earth elements can be subcategorized into light (LREEs: La to Nd), medium (MREEs: Sm to Tb), and heavy rare earth elements (HREEs: Dy to Lu) (Wang et al., 2022) due to their slightly progressive differing reactivities in aquatic environments (Dang et al., 2021; Garcia-Solsona and Jeandel, 2020; Mehmood, 2018). For instance, LREEs form strong inner sphere complexations (Lawrence & Kamber, 2006; Sholkovitz, 1995), whereas HREEs form weak outer sphere complexations via electrostatic forces (Byrne and Li, 1995). Consequently, LREEs have a higher susceptibility to scavenge (Labassa et al., 2023) and adsorb onto reactive surfaces of mineral and colloidal particles (Merschel et al., 2017), causing enrichment of LREEs in the particulate form (Dang et al., 2023; Luo et al., 2016). Heavy REEs are found more available in the dissolved form (Merschel et al., 2017), where they have a higher affinity to form complexations with inorganic dissolved carbonate (Luo and Byrne, 2004) and hydroxide complexes (Byrne and Li, 1995; de Baar et al., 2018; Goldstein and Jacobsen, 1988). The “hat-shaped” or MREE-enriched patterns are found to be associated with authigenic, diagenetic, and biogenic phosphate minerals (Hannigan et al., 2001; Pourret et al., 2007; Pourret and Tuduri, 2017). Middle REE enrichment is also associated with the organic carbon

fraction of sediments within lakes, rivers, estuaries, and ocean river systems (Freslon et al., 2014; Manoj et al., 2016; Morgan et al., 2012; Osborne et al., 2014; Zhang et al., 1998) due to the binding of REEs to the weak sites of solid-phase humic substances (Pourret et al., 2007; Tang and Johannesson, 2010).

Moreover, the Oddo-Harkins effect causes elemental abundances to be presented in a zigzag pattern (Ramos et al., 2016); REEs with even atomic numbers are more abundant than adjacent odd-atomic-numbered elements (Nikanorov, 2016; Piper and Bau, 2013). Normalization of REE patterns against a geological standard (e.g., Upper Continental Crust (UCC, Rudnick and Gao, 2013; Taylor and McLennan, 1995), Post-Archean Australian Shale (PAAS, McLennan, 2001, 1989), North American Shale Composite (NASC), or European Shales (EUS, Bau et al., 2018) helps eliminate the zig-zag REE patterns and create smooth trends for interpretation (Bau et al., 2018), e.g., geochemical processes, tracer of water masses, and anthropic releases (Arienzo et al., 2022). Normalized REE patterns are also used to recognize anomalous concentrations of an individual REE as either positive or negative anomalies (Pourret et al., 2022). Furthermore, all REEs have a stable oxidation state of +III (de Baar et al., 1988), except Eu and Ce. Europium holds the additional valance of +II under a strongly reducing environment, while Ce can be further oxidized to +IV (Dang et al., 2023; Tyler, 2004; Zheng et al., 2016). This distinct behaviour of Eu and Ce has made them important tracers of geochemical redox processes in the aquatic environment (Dang et al., 2022b; Floback and Moffett, 2021).

The emissions of REEs from various activities (e.g., ore extraction and refining processes, medical and residential wastewater effluent, agriculture, and REE-based

coagulants for ecological restoration) have led to progressive enrichments of REEs in the sediment and water column of aquatic systems (Amyot et al., 2017; Hatje et al., 2016). Aquatic organisms are susceptible to assimilating REEs into their bodies from surrounding abiotic environmental compartments (water column and sediments) and their diets, i.e., bioconcentration and bioaccumulation. There are a few reference points to consider; the global total mean concentrations of the lanthanides ($\sum[REE_{mean}]$) in the UCC is 146 mg kg^{-1} (Taylor et al., 1981), relative to 199 mg kg^{-1} in river sediment and 175 mg kg^{-1} in suspended particulate matters from rivers (Pereto et al., 2024). In freshwater systems, the global total median of all REEs ($\sum[REE_{med}]$) is 0.14 ± 0.17 μg L^{-1} based on a recent compilation (Pereto et al., 2024). Before REE levels continue to rise, investigations on the bioaccumulation potential of REEs will allow insights into whether organisms can depurate REEs through metabolizing or dilution processes (Amyot et al., 2017; Arnot and Gobas, 2006).

Currently, lab-based exposure experiments have investigated the impacts of solely dissolved REEs on freshwater organisms, including toxicity to mussels (Freitas et al., 2020; Pinto et al., 2019), Daphnia and fungi (Bergsten-Torralba et al., 2020; Lachaux et al., 2022), microalgae (Lachaux et al., 2022; Siciliano et al., 2021), and inhibition to planktivory bacteria growth (Wang et al., 2000). However, the impacts of particulate REE forms, e.g., REE-based coagulants, or the trophic transfers of contaminated food sources throughout the aquatic food web are less documented. Lanthanum from a REE-based coagulant has the potential to bioaccumulate into crayfish (*Procambarus sp.*) (Goitom, 2011). Nevertheless, the bioavailable forms of REEs to crayfish were not fully resolved, i.e., the particulate form, such as the coagulant that has been ingested, or the

dissolved La^{3+} released from the particles. There is also evidence of REE trophic transfers in rainbow trout, which slightly assimilated REEs from their prey, but no bioaccumulation occurred (Cardon et al., 2020). Despite these findings, there is no evidence on whether benthic and pelagic organisms are impacted by REE exposures or capable of uptaking and bioaccumulating dissolved, diet, or particulate forms of REEs.

Few studies have determined the uptake mechanisms of REEs in pelagic organisms. The bioaccumulation of REEs in zooplankton and in Arctic Char (*Salvelinus alpinus*) was strongly linked to uptaking free ionic dissolved forms (MacMillan et al., 2019; Nørregaard et al., 2019). Similarly, (Rétif et al., 2024) reported that both vertebrates and crustaceans held REE patterns similar to the dissolved phase. In marine diatoms, dissolved REEs quickly bind to cell surfaces and are assimilated (Bingler et al., 1989). The bioaccumulation and uptake mechanisms of REEs through the dissolved form have mainly been investigated on pelagic organisms of primary and secondary consumer trophic levels.

Here, we investigate the uptake mechanisms and exposure pathways (diet, dissolved fraction, or particulate substrate) of REEs to both pelagic and benthic organisms under environmental-relevant conditions using a lab-based approach. The objective is to determine whether aquatic organisms are susceptible to taking up and accumulating bioavailable REEs from the different exposure fractions. These results would provide insights on highly sensitive organisms to REE exposures under real-world ecosystems. Thus, organisms most susceptible to uptake REEs could be used to biomonitor REEs within aquatic ecosystems vulnerable to higher levels of REEs. It was hypothesized that the dominant uptake mechanisms of REEs for pelagic organisms was through the

dissolved form and dissolved LREEs from the Otonabee River will have higher susceptibility to complex to sand substrate, increasing benthic organism's exposure to REEs through the particulate forms.

2.3 Methods

2.3.1 Experimental design and organism collection

Test subjects were housed in a temperature-controlled (21°C) room with a 12h/12h light/dark cycle at the Trent University Animal Care Facilities for the duration of the study. Test subjects were placed in separate polypropylene plastic tanks filled with Otonabee River water that had been sand-filtered and ozonated. Bubblers and submersible active powerhead pumps (40 gallons per hour) were used for water circulation and aeration. Temperature was verified to be within a range of 19-21°C using a submersed thermometer. Other chemical parameters, i.e., pH, ammonia, nitrate, and nitrite concentrations, were measured every four days using a freshwater test kit (API) to determine whether water changes were needed. For the entire study, water changes were not required since water quality levels for each parameter did not exceed the danger thresholds for any organisms: constant pH at 7.6 ± 0.3, nitrite < 1 mg L^{-}, nitrate < 1 mg L^{-1}, and ammonia < 1.5 mg L^{-1}.

Tank water samples were collected at the beginning of the experiment and on the last day to determine changes in elemental composition over time; a volume of 50 mL of raw Otonabee River water was filtered at 0.45 µm using hydrophilic syringe filters (nylon, ChemScience TLG™). Unfiltered and filtered water was acidified with double-distilled trace metal grade HNO_3 (BDH Aristar Plus) to 0.2% v/v.

Organisms were collected from local natural habitats or purchased from local commercial stores and allowed a 21-day equilibration period to adapt to the diet and acclimate to housing conditions (Behets et al., 2020; Cardon et al., 2020). Benthic organisms, including crayfish (n=4), snails (n=6), and mussels (n=5), were collected from Jack Lake (Ontario). For benthic organisms, thoroughly rinsed and acclimated sand substrate (2-4 kg) was added to the tanks to provide refuge, protection, and habitat during the study period. Diet feed samples were purchased thoroughly dried from both local health and commercial stores. Crayfish were fed bottom-feeder shrimp pellets (API) at 2% of their body weight daily (Cardon et al., 2020) and housed in one 50 L polypropylene plastic tank. Freshwater snails and mussels were housed separately in two 30 L polypropylene plastic tanks and fed a daily 50 mL spirulina and chickpea powder (1:1 ratio) solution. Minnows (n=10) were purchased from Bridgenorth Sports & Marine (Bridgenorth, Ontario) and housed in one 200 L polypropylene plastic tank. They were fed spirulina flakes at 2% of their body weight daily (Cardon et al., 2020). *Daphnia magna* (n ~ 100) were cultured and housed in a 16 L polypropylene plastic container and fed a 50 mL spirulina and chickpea powder solution (1:2 ratio) daily. *Euglena gracilis* (six 50-mL culture flasks) was cultured in Otonabee River and amended with nutrients and trace elements following the formulations of the Modified Acid Medium (MAM) (Olaueson and Stokes, 1989); the composition is listed in **Table A1.1**. After the 21-day equilibration period, test subjects were housed in laboratory conditions for 64 days. The 64-day exposure period was chosen to assess short-term exposure for a duration corresponding to tripling the equilibration period. Benthic organisms were exposed to particulate REEs from the sand substrate, dissolved REEs from Otonabee River water,

and diet REEs while pelagic organisms were exposed to the dissolved and diet REEs. The survival rate of organisms was 100% during the experiment.

2.3.2 REE removal by the sand substrate

To assess the potential capacity of the sand substrate to scavenge dissolved REEs, 240 mL of the sand substrate and 760 mL of Otonabee River water were mixed into three 1-L HDPE bottles. The sand substrate was given an hour to settle, and the initial water samples were taken on day 1. On days 1, 5, 9, 12, 16, and 20, three water aliquots of 10 mL were collected and filtered through 0.45 µm using syringe filters and acidified. The sand substrates (before and after the experiments) were dried and analyzed using a scanning electron microscope (SEM, Hitachi FlexSEM1000 II) with energy-dispersive X-ray spectroscopy (EDX, Bruker Quantax Compact 30). The dried sand was sprinkled onto 12mm carbon conductive tabs (Pleco, Ted Pella Inc.) and placed in the SEM-EDX stage to collect images and elemental composition (Al, C, Ca, Fe, K, Mg, Na, O, and Si) using secondary electron, backscattered electron, and X-ray detectors.

2.3.3 Treatment of biological and feed samples

After exposure, organisms underwent a 72-hour depuration in ozonated and sand-filtered Otonabee River water without feed. A 72-hour depuration period was selected based on previous rare earth element exposure studies (Cardon et al., 2020; Fasola, 2010; Lachaux et al., 2023; Lam and Wang, 2006; Nørregaard et al., 2019). Minnows were housed in a separate clean 16 L propylene container, and snails, mussels, and crayfish were housed in a second 16 L propylene container to allow the depuration of feed and feces from bodies. *Daphnia magna* underwent depuration in separate 50 mL clean Falcon tubes to prevent sample loss due to predator consumption. After depuration, vertebrates

were humanely euthanized according to the Animal Use Protocol #26697, approved by the Trent University Animal Care Committee. Minnows were euthanized following the protocol "Use of MS-222". The test subjects were rinsed twice with high-purity water (18.2 MΩ cm) and ethylenediaminetetraacetic acid (EDTA, 1mM) solution to remove REE adsorbed on the organisms' body surfaces (Cardon et al., 2020). The fork length and whole-body wet weight of test subjects were recorded before dissection. The fish were dissected using a surgical razor blade, and individual tissues (soft tissue (n=10), swim bladder (n=10), gills (n=10), intestines (n=10), and liver (n=10)) were placed in Falcon tubes. Due to the low weight, we pooled tissue samples of five organisms in one composite sample, creating two replicates. Similarly, two replicate composite samples of ca. 50 *D. magna* individuals were collected by centrifugation at 4500 rpm for ten minutes. The pellets were separated from supernatant water and washed with high-purity water and EDTA. Crayfish were dissected into soft tissue (n=4), hard tissue (n=4), internal organs (n=4), and antennal glands (n=4), while mussels and snails were separated into soft (n=5 & n=6, respectively) and hard tissues (n=5 & n=6, respectively). Each crayfish, snail, and mussel subsample was treated individually as discrete samples, creating four replicates for four crayfish tissues (n=16), six replicates for both snail soft and hard tissues (n=12), and five replicates for both mussel soft and hard tissues (n=10). Additional information about the number of organisms, tissue dissection sub-samples, length, and feed sources are summarized in **Table A1.2**. After the dissection of all organisms, the samples were frozen at -20°C and further freeze-dried (Labconco).

Around 300-700 mg of dried biota and feed samples were weighed and digested using double-distilled trace-metal grade HNO_3 **(**15.6 M) and H_2O_2 (9.8 M) in a 1/0.2 (v/v)

ratio. Samples were left to digest overnight in the fume hood at 100°C until a clear solution was obtained. To test digestion recovery, the Standard Reference Materials (SRMs) NIST-1566a Oyster Tissue and NIST-1515 Apple Leaves (with information values of REE concentrations), underwent the same digestion procedure and analysis (Dang et al., 2023). The recovery of REEs in the two SRMs ranged from 81 to 100.6% (**Table A1.3**).

2.3.4 Chemical analysis

Elemental analysis was completed using Triple Quadrupole Inductively Coupled Plasma Mass Spectrometry (Agilent 8800) at the Trent University Water Quality Centre. Elements were analyzed under three gas modes following analytical procedures described by (Dang et al., 2022a). Major, minor, and trace elements (Cd, Co, Cs, Cu, Fe, Pb, Rb, Sc, Sr, Th, U, V, Zn) were analyzed in helium collision mode to eliminate polyatomic interferences. REEs were analyzed in an MS/MS mode with O_2 as the reaction cell gas (Dang et al., 2018). The quantification of Eu isotopes (^{151}Eu and ^{153}Eu) can be affected by isobaric overlap from various barium oxides and barium hydroxide interferences (Thompson et al., 2016), causing artificial positive Eu anomalies within samples. Due to their low abundance and potential polyatomic interferences, Eu isotopes were not assessed and Eu concentrations were not reported. The analytical procedure was verified using SRM NIST 1640a (Trace Elements in Natural Water) and the river water CRM SLRS-6 (National Research Council of Canada). A blank and water CRM were used to bracket every ten samples. The measured concentrations are compared against certified concentrations within solid and liquid CRMs (**Tables A1.3 & A1.4**).

2.3.5 Data analysis

2.3.5.1 REE patterns, normalization, and calculation of anomalies

Firstly, the organotropism of REEs in each organism was assessed by dissecting organisms into subsamples, including organs such as soft tissues, internal organs, gills, and shells. The REE concentrations within organs were analyzed and the distribution of REEs among different organs in organisms was ordered. Then, REE concentrations were normalized against Post-Archean Australian shale (PAAS, Bau and Dulski, 1996; McLennan, 2001; Taylor and McLennan, 1995); the PAAS-normalized concentrations are hereafter referred to as $REE_{PAAS.}$ This normalization also allowed for the calculation of Ce anomalies (Ce/Ce*) to characterize the behaviour of Ce relative to the abundance of their neighbouring REEs and trace biochemical redox transformations (Dang et al., 2023; Piper and Bau, 2013). Ce anomalies were calculated following Equation 1 (Dang et al., 2023; Och et al., 2014).

$$Ce/Ce^{*} = \frac{Ce_{PAAS}}{0.5 \times (La_{PAAS} + Pr_{PAAS})} \quad (Equation\ 1)$$

The PAAS-normalized REE patterns were used to quantify REE fractionation, i.e., the enrichment or depletion of three subgroups, including LREEs, MREEs, and HREEs. Lanthanum, Tb, and Er were used as representatives of the three LREE, MREE, and HREE subgroups, respectively. The particulate fraction is usually characterized by the enrichment in LREE, i.e., following a linear and decreasing trend displaying LREE enrichment and HREE depletion, and therefore reflects Tb_{PAAS}/La_{PAAS} and Er_{PAAS}/La_{PAAS} < 0.9 (Dang et al., 2023). The MREE enrichment is characterized by Er_{PAAS}/La_{PAAS} < 0.9 and Tb_{PAAS}/La_{PAAS} > 1.1, while the dissolved fraction (HREE enrichment) is characterized by Tb_{PAAS}/La_{PAAS} and Er_{PAAS}/La_{PAAS} > 1.1 (Dang et al., 2023).

2.3.5.2 Diet bioaccumulation factor and bioconcentration factor

The bioaccumulation potential of REEs in organisms can be empirically determined using the bioconcentration factor (BCF), which represents the ratio of REE concentration in an organism (typically the whole body, $[REEs]_{organisms}$ in mg kg^{-1}) to its dissolved concentration ($[REEs]_{water}$ in mg L^{-1}).

$$BCF = \frac{[REEs]_{organisms}}{[REEs]_{water}} \quad (Equation\ 2)$$

Comparably, the bioaccumulation factor (BAF) is typically calculated under field conditions as the ratio of the REE concentrations in an organism ($[REEs]_{organisms}$, mg kg^{-1}) to the total REE concentrations in the unfiltered water (mg L^{-1} or mg kg^{-1}) using the equation (Arnot and Gobas, 2006):

$$BAF = \frac{[REE]_{organisms}}{[REE]_{dissolved} + [REE]_{colloidal} + [REE]_{particulate} + [REE]_{diet}} \quad (Equation\ 3)$$

The BCF was calculated and BAFs were adapted into diet bioaccumulation factors (DAF) to assess the enrichment of two REE fractions (dissolved vs. diet) within organisms. Diet bioaccumulation factors were calculated to determine the extent of REE accumulation in aquatic organisms' tissue from the diet. The DAF is a ratio between the average concentration of the studied biota tissue (mg kg^{-1}) and that in their feed (mg kg^{-1}), following Equation 4.

$$DAF = \frac{[REE]_{Organisms' tissue}}{[REE]_{Feed}} \quad (Equation\ 4)$$

A DAF or BCF ratio > 1 indicates enrichment, whereas a ratio < 1 shows organisms did not bioaccumulate elements. Furthermore, bio-accumulative chemical

substances are identified using Canada's Persistence and Bio-accumulative Regulations; a DAF or BCF value over 5,000 indicates very bio-accumulative substances, whereas values between 2,000 and 5,000 indicate substances with high bioaccumulation potential (Arnot and Gobas, 2006; Government of Canada, 2023). For toxicity recommendations, BCF values should be mass-weighted based on the percentage a tissue constitutes of the total body weight (Mackay et al., 2018). For instance, the intestines constitute 5%, and muscle constitutes 50-80% of body weight, thus the highest metal burdens may be in muscles (Wood et al., 2012). Here, we chose to consider individual tissues rather than the mass-weighted approach to identify the specific enrichment of REEs. Furthermore, BCF and DAF were calculated for composite samples of minnow tissues and *Daphnia magna*, in addition to DAF values for discrete individual tissues of snails, mussels, and crayfish. Given the limited information on the uptake mechanism of REEs into aquatic organisms, we also related REE organotropisms and bioaccumulation patterns to other trace elements (such as Cd, Co, Cs, Cu, Fe, Pb, Rb, Th, U, V, Y, and Zn) with better documented biological roles.

2.3.5.3 Statistics

Non parametric Friedman's test for dependent samples was conducted using the Excel real statistics data analysis packages under ANOVA single factor. The Friedman test was performed to determine if La, Tb, and Er group mean concentrations within Otonabee River water on days 1, 5, 9, 12, 16, and 20 are significantly different. If the Friedman test reported a P value < 0.05, the null (H_o) hypothesis that there is no difference between La, Tb, or Er on days 1, 5, 9, 12, 16, and 20, was rejected. A Conover post-hoc annalysis test determined if there was a significant difference between group

means. If the difference between the two means is greater than the HSD calculated (diff > HSD), then the two means are considered significantly different.

2.4 Results and discussion

2.4.1 Scavenging potential of dissolved REEs on the sand substrate

The PAAS-normalized dissolved REE patterns were linear and showed an increasing trend from LREEs to HREEs (**Figure 2.1A**), that reflected the REE pattern commonly referred to as "seawater-like" (Alibo and Nozaki, 1999; Johannesson et al., 2006; Pourret and Tuduri, 2017). This behaviour is well documented in natural systems as LREEs have higher affinity to create strong inner-sphere complexes with the carbonates and oxides in the sand substrate (**Figure A1.1**), while HREEs tend to remain in solution as dissolved REE-carbonate complexes (Byrne and Li, 1995).

With increasing time after contact with the sand substrate, there is a depletion of light, medium, and heavy REEs from the Otonavee River water and the equilibrium was reached after two weeks (**Figure 2.1B**). For instance, La concentrations depleted in Otonabee River water from 29 ± 2 ng L^{-1} on day 1 to 5.6 ± 0.1 ng L^{-1} by day 20. The Tb and Er concentrations decreased from 1.0 ± 0.1 ng L^{-1} to 0.31 ± 0.02 ng L^{-1} and 4.5 ± 0.1 ng L^{-1} to 1.9 ± 0.2 ng L^{-1}, respectively. We observed a preferential removal of LREEs (80.2 ± 2.9 %, n =3) compared to MREE (67.4 ± 5.0%, n =3) and HREE (56.4 ± 5.5%, n=3) from the Otonabee River water (**Figure 2.1A**). The percent difference means from day 1 to day 20 for LREEs, MREEs, and HREEs were significantly different ($\rho = 0.04$ Friedman). Lanthanum held the highest average percent difference ($\rho < 0.05$ Conover) compared to Tb and Er. A description of the various minerals in the sand substrate and mechanisms responsible for scavenging dissolved REEs can be found in **A1**

supplementary text 1 and **Figure A1.1**. Similar observations were made studying the REE cycling and transportation from the Congo River into the sea by analyzing quartz samples (Garzanti et al., 2021). The silt and coarse sand had REE patterns with significant LREE enrichment. This experiment highlighted active scavenging of REEs onto the sand substrate, confirming that benthic organisms may be exposed to REEs through this additional particulate phase, which has a unique LREE enrichment pattern.

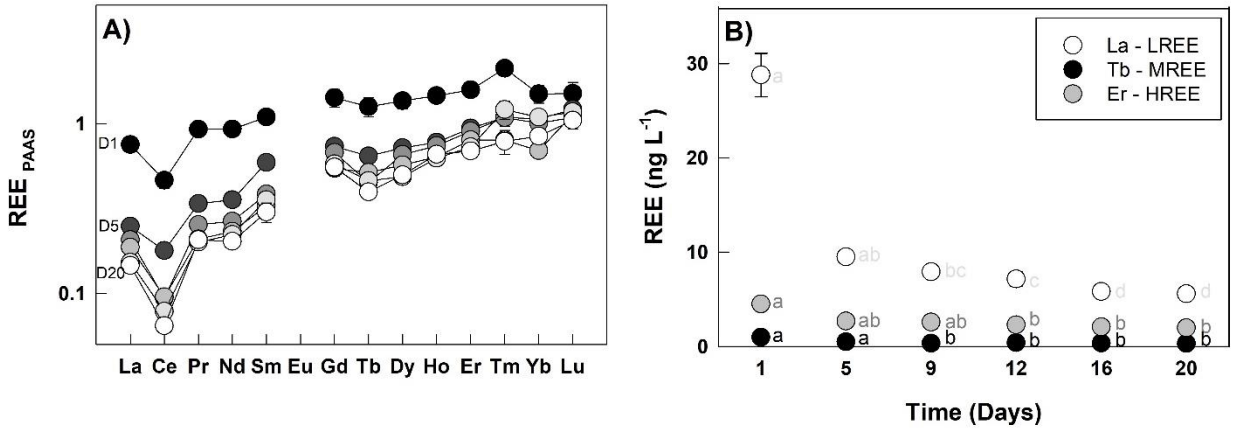

Figure 2.1 A) PAAS-normalized REE patterns of Otonabee River water over time after the contact with the sand substrate. The black-and-white gradient reflects the temporal sampling from day 1 (D1, black) to day 20 (D20, white). **B)** Variations of the average (n=3) concentrations of La (LREE), Tb (MREE), and Er (HREE) in Otonabee River water over time after the introduction of the sand substrate. The compact letters in B) display Conover post hoc test results for pairwise comparison among REE concentrations.

2.4.2 REE organotropism and REE fractionation in the organs relative to exposure pathways

2.4.2.1 Northern clearwater crayfish (Faxonius propinquus)

Using Ce as a representative REE, the REE organotropism in crayfish is as follows: antennal glands (1821 ± 549 µg kg $^{-1}$) > hard tissue (818 ± 196 µg kg $^{-1}$) > internal organs (212 ± 143 µg kg $^{-1}$) > soft tissue (59 ± 30 µg kg $^{-1}$) (**Figure 2.2 & A1.2F**, **Table A1.5**). The organotropism patterns for our crayfish were similarly found in marbled crayfish exposed to La-based coagulant (Goitom, 2011). Besides, the enrichment of Cd, Zn, and Cu in our crayfish samples followed the decreasing order of internal organs > antennal glands > soft tissue > hard tissue (**Table A1.6**), previously reported in multiple crayfish species (Guner, 2010). The correlation between La and Fe in crayfish tissues (**Figure 2.3**) is also noteworthy. Iron is an essential element used in crayfish for metabolism and in constituents of cytochrome proteins (Vuori, 1995). This strong relationship between Fe and La indicates similar uptake, storage, repartition, and elimination pathways or similar biochemical functions in crayfish. Further studies are required to investigate such relationships.

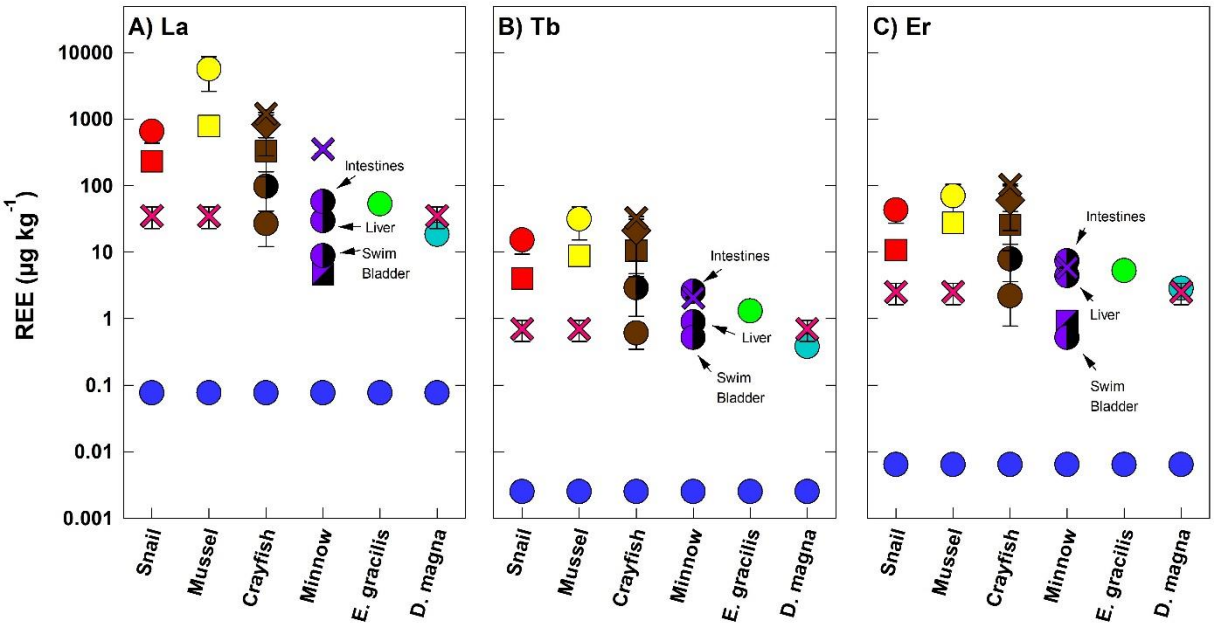

Figure 2.2 Average concentrations of La, Tb and Er in partitioned tissues within benthic (snail, mussel, crayfish) and pelagic (minnows, *D. magna*, and *E. gracilis*) organisms, compared to exposure sources. Tissue types are represented by various shapes: circle (soft tissue or whole body), square (hard tissue), half-filled circle (intestines/internal organs), half-filled square (gills), and diamond (antennal gland). The Otonabee River is represented by the dark blue circle and feed sources are represented by coloured cross symbols: shrimp pellet for crayfish (brown), spirulina flake for minnows (purple), and a combination of spirulina and chickpea powder for snail, mussel, and *D. magna* (pink).

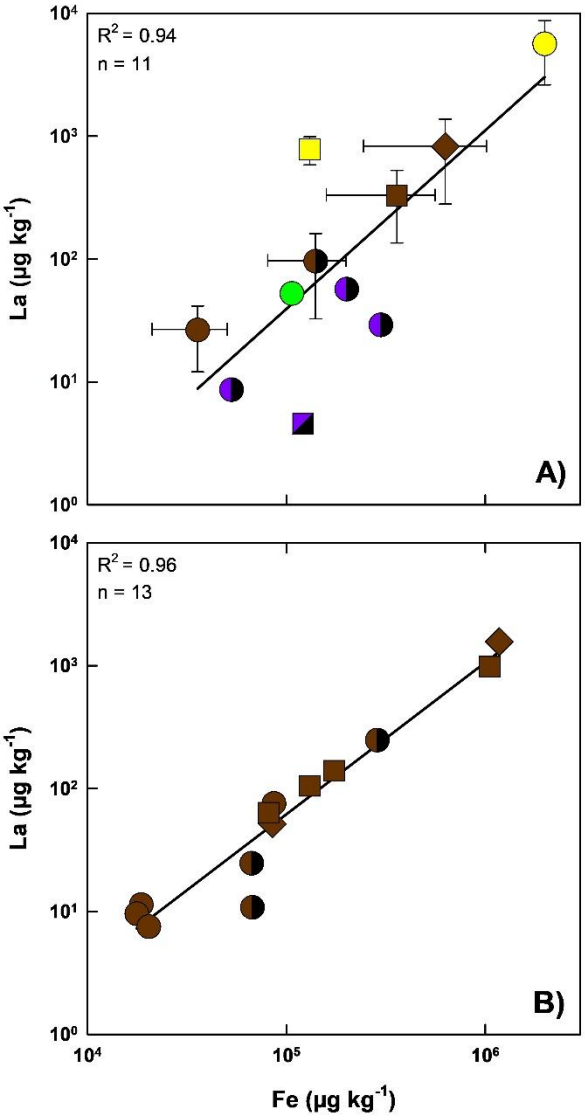

Figure 2.3 A) Correlation between the average concentrations of La and Fe in partitioned tissues of crayfish, mussels, *E. Gracilis*, and minnow. **B)** Correlation between La and Fe in all tissue samples of crayfish. Tissue types are represented by various shapes: circle (soft tissue or whole body), square (hard tissue), half-filled circle (intestines/internal organs), half-filled square (gills), and diamond (antennal gland). The colors represent different organisms: brown (crayfish), purple (minnows), yellow (mussel), green (*E. gracilis*), and light blue (*D. magna*).

The PAAS-normalized REE patterns for crayfish tissues show MREE enrichment, which also reflect their diet (**Figure A1.3F**). Nevertheless, the normalized REE concentrations in internal organs, hard and soft tissues were 1-2 orders of magnitude lower than the diet, whereas levels in antennal glands are in the same order of magnitude as their diet (**Figure A1.3F**). The fractionation signatures (Tb_{PAAS}/La_{PAAS} and Er_{PAAS}/La_{PAAS}) of crayfish hard tissue, internal organs, and soft tissues (brown symbols in **Figure 2.4**) overlap with the signatures of both the river water and their diet (blue circle and brown cross symbol in **Figure 2.4**). These overlapping signatures create difficulty in differentiating whether diet or dissolved fractions are the dominant pathway by which crayfish uptake REEs.

The REE organotropism order can be explained by crayfish physiology; crayfish passively absorb dissolved trace metals from their diet (Guner, 2010) or through the permeable ectodermal hard tissues (Rainbow and White, 1989). For instance, the antennal glands accumulated the highest concentrations of REEs, Fe, Pb, Sc, V, Th, and U (**Table A1.5 & A1.6**) because the glands acts as the excretory organ through pores at the base of the antenna (Riegel, 1966). The similar concentrations of REEs in the antennal glands and the diet suggest the regular transit of feed through this organ. Metals from the diet can be further transferred into other internal organs. However, the decreasing concentrations in internal organs and soft tissues (**Figure 2.2**) indicate a low transfer potential because of efficient excretion through the antennal glands or detoxification through the hepatopancreas (Guner, 2010).

On the other hand, the concentrations of REEs, Fe, V, Th, and U, were found to be second highest in the hard tissues, which are a composite of cheliped, carapace, and

pereiopods structured by a framework of α-chitin/protein microfibres and Ca carbonates (Sugawara et al., 2006). The lattice of these materials can retain dissolved metals by weak complexes (Chassard-Bouchard and Hallegot, 1984), explaining the accumulation of these trace elements in hard tissues from dissolved fractions.

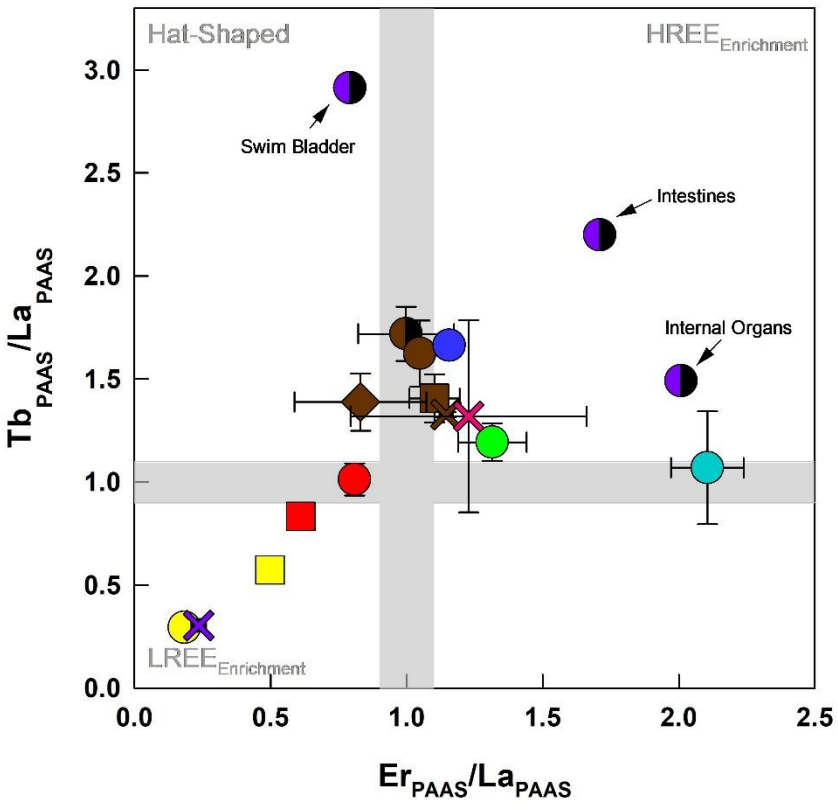

Figure 2.4 Biplot of Tb_{PAAS}/La_{PAAS} as the function of Er_{PAAS}/La_{PAAS} in benthic and pelagic organisms, Otonabee River, and feed sources. Refer to the caption of Figure 2.3 for symbol and colour legend. Note that Tb_{PAAS}/La_{PAAS} represents the ratios of MREE/LREE while Er_{PAAS}/La_{PAAS} represents the ratio of HREE/LREE. The gray texts, i.e. "Hat-shaped, $LREE_{Enrichment}$, $HREE_{Enrichment}$, identify the main REE pattern quadrants such as the dominance of MREEs, and the linear decrease with enrichment of LREEs in particles.

2.4.2.2 Black sandshell mussel (Ligumia recta)

Mussels have the potential to accumulate pollutants in their tissues at elevated levels related to pollutant availability in the diet or dissolved forms (Beyer et al., 2017). Within this study, the soft tissue samples of mussels are a composite of their gills, digestive gland, hemolymph, and rest of the soft tissues, which have higher REE concentrations ([Ce] of 3962 ± 2032 µg kg $^{-1}$) than hard tissue (1381 ± 357 µg kg $^{-1}$) (**Figure 2.2 & A1.2B, Table A1.5**). The soft tissue concentrations are also two to three orders of magnitude higher than that of their diet (**Figure A1.3B, Table A1.7**). The higher REE concentrations in our mussel soft tissues compared to hard tissue are similar to literature data for various mollusc species (Weltje et al., 2002). The REE organotropisms in the soft tissues of *Corbicula fluminea* clams after exposure to dissolved Nd, Gd, and Yb followed the decreasing order of gills > digestive glands > rest of soft tissues > hemolymph > mantle (Lachaux et al., 2023). Further, within freshwater mussel *Hyriopsis cumingii*, the mantle attached to the shell held the highest REE concentrations compared to the muscle, foot, and siphon (Xu et al., 2022). It has been suggested by Merschel and& Bau, (2015) that REEs are incorporated in the carbonate shells of mussels after uptake from ambient waters and food. Rare earth elements could pass through the mantle via extrapallial fluid and into the inorganic Ca concretions of carbonate shells (Marigómez et al., 2002; Merschel and Bau, 2015). Rare earth elements could be incorporated in the position of the Ca ion in the crystal lattice (Zhong and Mucci, 1995) during calcification and shell formation (Lachaux et al., 2023) due to the similarity of ionic radii (1.03 Å to 0.86 Å for La to Lu vs. 1.00 Å for Ca) (Merschel and Bau, 2015; Shannon, 1976).

The PAAS-normalized REE patterns for the soft and hard tissue of mussels show a distinctive enrichment of LREEs compared to MREEs and HREEs; both Tb_{PAAS}/La_{PAAS} and Er_{PAAS}/La_{PAAS} are < 1 (yellow symbols in **Figure 2.4**). This signature is different from that of the water (blue symbol) and the diet (pink cross symbol), suggesting a third end member that can be uniquely represented by the sand substrate that has been significantly enriched in LREEs (see section 2.4.1). Rare earth element patterns and fractionations in bivalve mussels have been previously studied to determine whether the accumulation of trace elements is associated with dissolved or particulate sources. For instance, the REE patterns in hard and soft tissue of bivalves from Tokyo Bay resembled patterns of resuspended particles, indicating REE accumulation was due from exposure to sediment (Akagi and Edanami, 2017). A similar confirmation was obtained for oysters from the Pearl River Estuary of China based on different REE anomalies in dissolved, particulate, and biological samples (Ma et al., 2019).

2.4.2.3 Chinese mystery snail (Cipangopaludina chinensis)

Snail soft tissue (combination of the viscera and foot, [Ce] ~ 1287 ± 493 µg kg^{-1}) contained higher concentrations of REEs and other trace elements (Zn, V, Co, Cu, Cd, Cs, Y, Rb, U, and Pb) than in their hard tissues ([Ce] ~ 404 ± 54 µg kg^{-1}) (**Table A1.5 & A1.6, Figure A1.2A**). Soft tissue of snails act as a more effective sink for metal accumulation than the hard tissue because of metal storage in subcellular fractions (Dallinger and Wieser, 1984; Gimbert et al., 2008). It should be noted that both soft and hard tissues of our snail samples have higher REE levels than their diet (**Figure A1.3A**). The fractionation patterns of snails (red symbols in **Figure 2.4**) also point toward the

LREE-enrichment quadrant, suggesting a potential contribution from sand substrate, which has been the case for mussels.

Among the trace elements we measured, there were correlations between REEs and V ($R^2 = 0.76$), as well as, REEs and Cs ($R^2 = 0.61$) (**Figure A1.4**). These elements have different ionic radii and charge numbers (Shannon, 1976), indicating non-selective uptake mechanisms (Aharchaou et al., 2020; Crémazy et al., 2019). Though limited studies have investigated uptake mechanisms of REEs into aquatic snails, we can compare our results to the uptake mechanisms of other trace elements. Littorinid snails exposed to dissolved Tl and Tl-amended green macroalgae (*Ulva lactuca*) in a 20:1 ratio, accumulated 2% of dissolved Tl vs. 15% from the diet (Turner and Pilsbury, 2013). Even though the relative contribution of metals through the aqueous form is higher, metals from the diet seem to accumulate in the soft tissues (Turner and Pilsbury, 2013).

2.4.2.4 Euglena gracilis

Rare earth element binding and uptake into phytoplankton cells due to their analogy with essential elements could be one of the most important processes explaining REE accumulation in *E. gracilis* (Valcheva-Traykova et al., 2014). The uptake of Nd^{3+} and Ce^{3+} in *E. gracilis* led to decreases in Zn, Ca, and Fe content, suggesting a competitive uptake through similar pathways (Shen et al., 2002). Furthermore, it has been suggested that Nd^{3+} can be transported into cellular compartments through Ca ion channels, with the largest quantity of Nd^{3+} residing in chloroplasts and replacing Mg in chlorophyll (Kang et al., 2000). The substitution of Mg^{2+} by REEs in chlorophyll suggests REEs accumulate in *E. gracilis* by replacing essential elements from the ion binding sites on proteins (Prokop et al., 2015).

The REE patterns for *E. gracilis* were similar to the Otonabee River water (**Figure A1.3C**). However, absorption process of REEs by phytoplankton and algae is complex and depends on REE availability and chemical speciation. It has been demonstrated that MREEs have slightly higher stability constants for biological uptake sites to outcompete for cellular binding spots on phytoplankton (Costa et al., 2020; Dang et al., 2023; Tan et al., 2017). Furthermore, when dissolved REEs were equally available, heavier REEs with smaller ionic radii were least preferentially uptaken by *Euglena gracilis* (Ishii et al., 2006), *Gracilaria gracilis* (Costa et al., 2020; Jacinto et al., 2018), and microalgae (Costa et al., 2020). Such fractionation processes might influence the change in REE patterns we observed for *Euglena gracilis* (**Figure 2.4**); the Tb_{PAAS}/La_{PAAS} decreased from the value of the river water (~ 1.7) to that of the algal cells (1.2 ± 0.1), highlighting a flatter pattern in biological tissues. Despite this slight fractionation between REEs, the overall signature of REEs in algae (green symbol) remains close to river water (blue symbol), in the HREE-enrichment quadrant (**Figure 2.4**).

2.4.2.5 Daphnia magna

D. magna accumulated low REE levels within the whole body (**Figure A1.3D**), ranging from Ce (30.7 ± 1.9 µg kg^{-1}) to Yb (1.9 ± 0.1 µg kg^{-1}) (**Table A1.5**). Rare earth element patterns for the whole body of *D. magna* were linear, following their Otonabee River water patterns and overlapping their diet (spirulina & chickpea powder) patterns (**Figure A1.3D**). Our *D. magna* samples were characterized by an enrichment of HREEs, holding a HREE fractionation (Er_{PAAS}/La_{PAAS} of 2.1± 0.1) that was higher than the

signature of the river water (blue circle in **Figure 2.4**) and had a MREE fractionation (Tb_{PAAS}/La_{PAAS} of 1.1 ± 0.1) similar to their diet (1.3 ± 0.3, pink cross in **Figure 2.4**).

Daphnia magna was used to determine the fractionation and distribution of particulate La vs. dissolved Gd (Revel et al., 2023). Ingested La precipitates accumulated in the intestines of *D. magna*, whereas ionic Gd^{3+} accumulated in tissues via metal-transporting proteins. The accumulation of REEs in intestines did not induce lethal effects since *D. magna* detoxified diet REEs, whereas ionic Gd taken up through the exoskeleton or gills, lowered mobility and induced oxidative stress (Di Toro et al., 2001; Revel et al., 2023).

This organism has various mechanisms for eliminating REEs; 75% of REEs absorbed through the gills and exoskeleton in *D. magna* are detoxified through sequestration in specific subcellular compartments, e.g., the NaOH-resistant fractions (Cardon et al., 2019). Further, 16 to 70% of diet trace metals are lost to offspring production, moulting, metal excretion, and fecal excretion (Barata et al., 2002; Tsui and Wang, 2007; Yu and Wang, 2002). These detoxification and elimination mechanisms might help *D. magna* minimize the uptake of REEs into their bodies, explaining the low REE levels compared to other organisms (**Figure 2.2**).

2.4.2.6 Striped shiner minnow (Luxilus chrysocephalus)

The lowest REE concentrations within minnows were found in the gills and swim bladder, and the highest in the intestines (**Figure 2.2 & A1.2E**). The REE organotropism for partitioned minnow tissues followed the decreasing order of intestines > liver > swim bladder ~ gills (**Figure 2.2**). The REE concentrations in soft tissues were below detection

limits and therefore not reported here. The REE organotropism for our minnows can be compared to wild-caught fish. Common sole (*Solea solea*) (Labassa et al., 2023), yellow eels (Lortholarie et al., 2021), arctic char (*Salvelinus alpinus*) (Nørregaard et al., 2019), rainbow trout (*Oncorhynchus mykiss*) (Cardon et al., 2020), and lumpfish *(Cyclopterus lumpus)* (Østerås, 2023) held the highest levels of REEs in gills (i.e., gills > kidneys > liver > soft tissue).

Despite the common organotropism in various fish species, differences in depuration and elimination response times exist. The ability to excrete metals during depuration is related to the response time of enzymatic activities surrounding the detoxification of non-essential elements (Regoli et al., 2011), such as the production of metallothionein (Si and Lang, 2018) which binds and sequesters metals from the intestines, liver, and gills (Deb and Fukushima, 1999). After three days of depuration, our minnows held the highest REE levels in the intestine and liver, the main sites for sequestration and detoxification of non-essential elements (Deb and Fukushima, 1999). Therefore, temporarily enhanced REE bioaccumulation in the liver and intestines of minnows could be due to a higher presence of metallothionein-bound metals and unregulated enzymatic response times (Deb and Fukushima, 1999). Furthermore, the assimilation efficiency of diet REEs was 0.8-3% in rainbow trout, highlighting low transfer of diet REEs into fish (Cardon et al., 2020). Overall, minimum REE levels within gills and swim bladder and maximum REE levels in excretory organs suggests minnows effectively eliminate diet and dissolved REEs post-exposure.

Most minnow tissues are characterized by an enrichment of HREEs, i.e., Tb_{PAAS}/La_{PAAS} and Er_{PAAS}/La_{PAAS} >1, which further accentuated the river water signature

(blue circle in **Figure 2.4**) and their diet (purple cross in **Figure 2.4**). The opposite direction between the diet and fish tissue would indicate minimal contributions from the diet and additional REE fractionation from the dissolved fractions. Minnows could uptake REEs similarly to Ca^{2+} past the cells of the branchial epithelium of gills via passive influx through divalent protein transporters located in the gills (Flik et al., 1995; Martin and Frederick, 1979). It is, however, uncertain whether such processes induce REE fractionations, i.e., the differential uptake of HREEs relative to LREEs.

In summary, the fractionation signatures highlight the dissolved fractions as the main exposure pathway to pelagic organisms. The effective digestive elimination decreases the possibility of REEs to be assimilated from the diet signatures. On the other hand, benthic organisms might have more complex exposure pathways. The REE signatures in crayfish overlap for the three sources of REEs, while the sand substrate seem to be the dominant source of REEs to snails and mussels as identified by the LREE-enrichment signatures. Overall, it is important to consider factors such as the physiochemical behaviour of REEs in organisms, REE availability, and binding capacities, impact whether REE accumulate into the organisms via the diet, dissolved, or particulate form.

2.4.3 Ce/Ce anomalies*

Cerium anomalies are used to reveal the enrichment ($Ce/Ce^* > 1.1$) or depletion ($Ce/Ce^* < 0.9$) behaviours of Ce caused by environmental processes decoupling Ce relative to neighbouring REEs (Barrat et al., 2023). The Otonabee River is characterized by a negative Ce anomaly ($Ce/Ce^* = 0.8$). However, spirulina flakes - the diet for minnows - contained positive anomalies (1.7 ± 0.05), while the diet for *D. magna*,

mussel, and snails had no Ce anomalies (1.0 ± 0.03) (**Table A1.8**). In the tissues, *D. magna* (0.6 ± 0.1), *E. gracilis* (0.5 ± 0.02), mussels (0.05 ± 0.01), snails (0.9 ± 0.04), and the soft tissues (0.5), gills (0.8), liver (0.8), swim bladder (0.5), and intestines (0.7) of minnows contain negative Ce anomalies that were lower than their respected diet and water exposures (**Figure 2.5**, **Table A1.8**).

The negative cerium anomaly in the Otonabee River water suggests depletion of Ce due too *in situ* oxidative transformation of Ce^{+III} into Ce^{+IV} (El-Akl et al., 2015; Jiang et al., 2022; Sholkovitz, 1995). Ce^{+IV} is less soluble, less mobile, and highly surface-reactive compared to Ce^{+III} (Byrne and Kim, 1990; Tostevin, 2021) and is, therefore, depleted from the aqueous environment. The negative Ce anomalies found in test subjects were consistent in arctic char, cod, whitefish, sculpin (MacMillan et al., 2017; Marginson et al., 2023), molluscs, crabs (Wang et al., 2019), and snails (Weltje et al., 2002). It has been suggested that Ce anomalies in aquatic organisms reflect Ce bio-availability (MacMillan et al., 2017); when there is less dissolved Ce available (more negative Ce/Ce*) in the aquatic environment, less Ce is uptaken.

In this study, various organisms, e.g., minnows, *D. magna*, and *E. gracilis* had lower Ce anomaly values than Otonabee River water and respective diet exposures (**Figure 2.5**, **Table A1.8**). Ce anomalies in minnow tissue are lower than the diet but align with river water (**Figure 2.5**), confirming dissolved REEs as the primary exposure pathway to minnow (section 2.4.2.6). The negative Ce anomalies in minnows, *D. magna*, and *E. gracilis* could be due to the further transformation of Ce^{+III} into Ce^{+IV} through biochemical oxidative pathways within the cells, as suggested in marine phytoplankton

(Dang et al., 2023). Marginson et al., (2023) also related Ce anomalies in the liver and bone of fish to their size, indicating metabolic, ecological, and environmental influence.

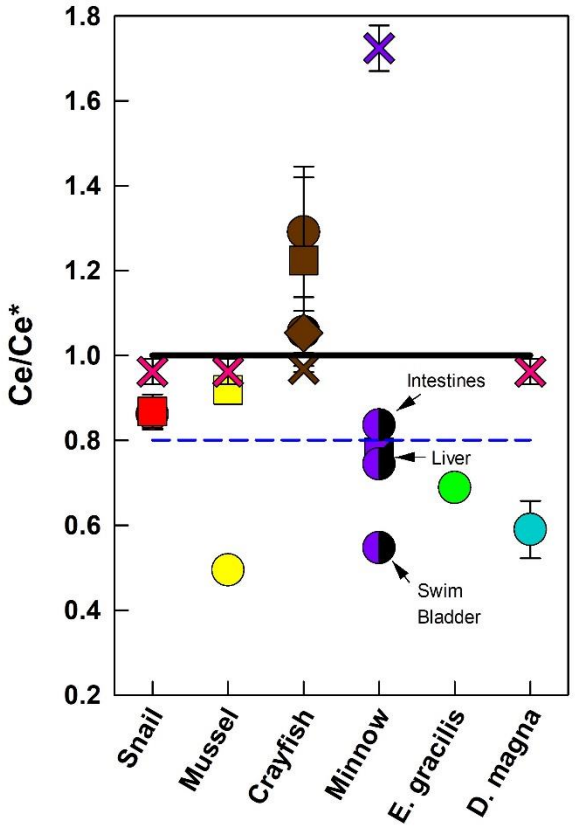

Figure 2.5 Ce anomalies of partitioned tissue parts within benthic and pelagic organisms, and their respected food and water exposures. The dashed blue line indicates Ce anomaly of Otonabee River (Ce/Ce* = 0.8), while the horizontal black line indicates the absence of Ce anomaly (Ce/Ce* = 1). See the caption of figure 2.3 for symbol and colour legend.

In contrast, crayfish tissues exhibit positive Ce anomalies (between 1 and 1.5), which is higher than their shrimp pellet diet (1.0 ± 0.01) and Otonabee River water (0.8) (**Figure 2.5**). Higher Ce anomalies were observed in hard tissues and the antennal gland with higher Ce concentrations (**Figure A1.5A**) but lower zinc (R^2 = 0.97, n=4, **Figure A1.5B**). These two tissues are directly in contact with environmental media; the hard tissue contacts with river water and sand substrate, while the antennal gland excretes ingested particles and feed. In the environment, the accumulation of Ce and high Ce anomalies might be related to the bioavailability to crayfish of the oxidized Ce^{+IV} on reactive surfaces (e.g., ferric deposit, Ratié et al., 2020) or by bio-mediated processes involving siderophores secreted by microbes (Kraemer and Bau, 2022). The crayfish feeding habit relies on vegetation, prey, decaying materials, and detrital biofilm (Ercoli et al., 2021) with their appendages. It is speculative at this stage, but our crayfish might uptake particles or the biofilm enriched in Ce^{+IV}, leading to pellicular positive Ce anomalies (**Figure A1.5A & B**). However, further studies will be required to investigate this hypothesis.

2.4.4 Bioconcentration factor (BCF) and diet bioaccumulation factor (DAF)

2.4.4.1 BCF & DAF for pelagic organisms

Relative to their diet, the REE concentrations in *D. magna* ([Ce] ~ 31 µg kg^{-1} ± 2) and minnows ([Ce] ~ 93 µg kg^{-1}) are lower than their respected spirulina/chickpea powder ([Ce] ~ 75 µg kg^{-1} ± 26) and spirulina flakes ([Ce] ~ 840 µg kg^{-1}) (**Figure 2.2**, **Table A1.5**). Therefore, the DAF values for REEs in pelagic organisms are < 1 (**Figure 2.6C & D**), reflecting the biodilution of diet REEs. The BCF values for REEs in pelagic organisms are >1 (**Figure 2.6C**, **Table A1.9**), reflecting enrichment near the

bioaccumulation potential threshold of 2000. Nevertheless, BCF values for REEs are one to three orders of magnitudes lower than those of other bioaccumulative trace elements, e.g., Zn, Cu, V, and Pb (**Figure A1.6**). This finding confirms that REEs behave distinctly from other divalent trace elements and might have limited bioaccumulation risks for these organisms, as previously suggested by lab and field studies (Amyot et al., 2017; Cardon et al., 2020; MacMillan et al., 2017).

The BCF values of REEs and other trace elements (Co, Cs, Pb, Rb, U, V, and Zn) for minnow tissues are 3-4 magnitudes higher than DAF (**Figure 2.6C & A1.6)**. These results relate to the fractionation signatures found in pelagic organisms and their exposure. The REE signatures in minnows were similar to water, indicating that minnows' primary uptake mechanisms would be dissolved REEs through the gills. These results align with those reported by Cardon et al. (2020) as the authors observed a strong correlation between dissolved Y and Y concentrations in the gills but minimal transfer of Y into internal organs (section 2.4.2.6). Our BCF values are similar to BCF values for various fish species collected in the field, e.g., reservoirs in Washington State (Mayfield and Fairbrother, 2015), the Po River (Pastorino et al., 2024), and 14 lakes in southern Quebec (Amyot et al., 2017). It is a common fact that BCF values reported in environmental studies are higher than BCF values reported in exposure laboratory studies, such as in carp (*Cyprinus carpio*) exposed to dissolved LREEs (Hao et al., 1996). However, our minnow BCF values were also higher than carp (*Cyprinus carpio*) BCF values. The accumulation of chemicals in aquatic organisms might differ based on the exposure levels. For example, interpreting BCF values in laboratory exposure experiments requires considering the inverse relationship for BCF vs. exposure

concentrations; BCF values were highest during low or natural exposure concentrations but lower when exposure concentrations increased because of differential accumulation rates (Mcgeer et al., 2003).

Additionally, DAF values gradually increased from LREEs to HREEs in minnow organs (**Figure 2.7A**). This fractionation indicates that LREEs might be less bioavailable than HREEs. This finding corroborates with the dissolved REE patterns highlighted by HREE enrichments because of reactivity with dissolved carbonates and ligands, ultimately pointing toward more contribution of the dissolved REE.

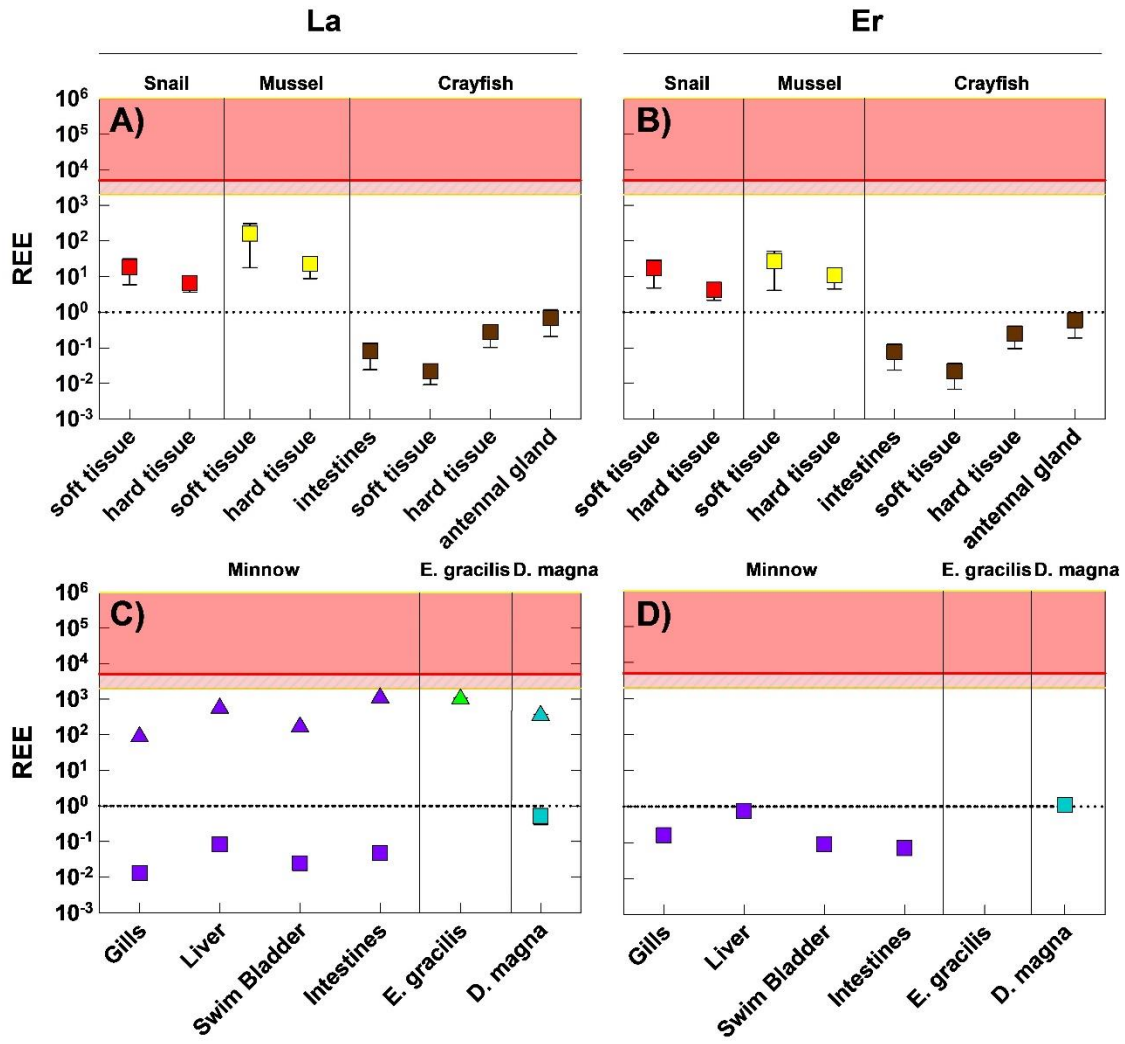

Figure 2.6 Diet bioaccumulation factors (DAF, square) and bioaccumulation concentration factors (BCF, triangle) for benthic **(A-B)** and pelagic **(C-D)** organisms. DAF and BCF ratios were calculated for representative light (La, left panels) and heavy (Er, right panels) REEs. Organisms are represented by various colours: red (snail), yellow (mussel), brown (crayfish), purple (minnow), green (*E. gracilis*), blue (*D. magna*). A BCF or DAF > 1 indicates enrichment of REEs into the tissues. Specifically, 2000 < BCF/BAF < 5000 and BCF/BAF > 5000 indicate bio-accumulative and very bio-accumulative potential, respectively. See text for more details.

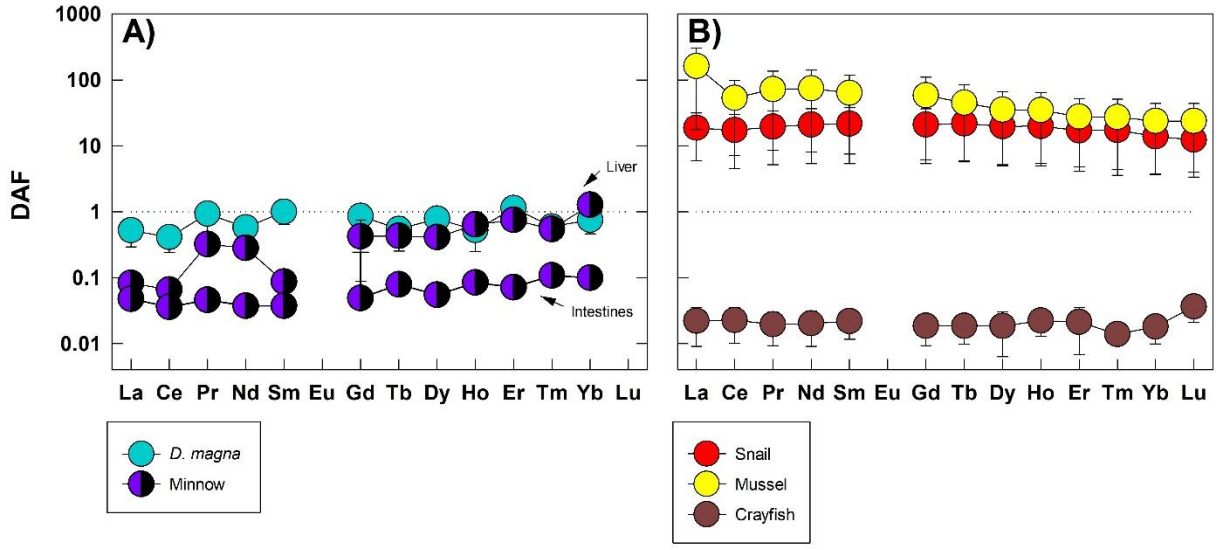

Figure 2.7 Comparison of diet accumulation factors (DAF) of REEs within the **A)** soft tissues of *D. magna* and internal organs of minnows and **B)** soft tissues of benthic organisms.

2.4.4.2 BCF & DAF for benthic organisms

The BCF values for benthic organisms were not reported because a large proportion of dissolved REEs scavenged onto the sand substrate (**Figure 2.1**). Instead, the primary exposure of REEs to benthic organisms was through the diet and particulate forms. The respective contribution of the sand substrate vs. the diet on the assimilated REE concentrations in the organisms cannot be determined. Therefore, DAF values based on the diet are reported only for comparison between organisms and individual REEs.

The REE concentrations within the soft and hard tissues of snails and mussels are 1-3 orders of magnitude higher than REE concentrations in their diets, i.e., spirulina and chickpea powder ([Ce] ~ 75 μg kg^{-1} ± 26) (**Figure 2.2, Table A1.5**). These results suggest that snails and mussels have the potential to bioaccumulate REEs from their feed or sand substrate. The DAF values for REEs (**Figure 2.6**, **Table A1.9 & A1.10**) and trace elements Cd, Co, Cs, and U (**Figure A1.7**) in mussel soft tissue are one order of magnitude higher than that of snail soft tissue. However, the DAF values for trace elements Pb, Rb, U, V, and Zn are within the same range for both snails and mussels (**Figure A1.7**). Further, DAF values of LREEs for snails and mussels are one order of magnitude higher than that of MREEs and HREEs (**Figure 2.7B**). Similarly to our mussel samples, oysters and mussels exposed to sediment on the eastern coast of China (Zhao et al., 2022) and unfiltered suspended particles in coastal systems of the Vigo Ria in Spain (Rodríguez-Velarte et al., 2022) showed preferential bioenrichment (> 1) of LREEs vs. MREEs and HREEs. These patterns are similar to that of the particulate fraction (sections 2.4.2.2 and 2.4.2.3), confirming the prevalence of particulate fractions in governing REE accumulation in benthic organisms (section 2.4.2).

On the other hand, REE concentrations in the antennal glands of crayfish are the same magnitude as their pellet feed (**Figure 2.2**), while the soft tissue, hard tissue, and internal organs of crayfish have REE concentrations lower than their shrimp pellet feed (**Figure 2.2**). These results suggest that crayfish organisms do not have the potential to bioaccumulate REEs from their feed, explaining the difficulty in assigning a primary exposure pathway for this organism (section 2.4.2.1). Among the REE subgroups, crayfish did not have preferential bioaccumulation as their DAF patterns were flat and remained at ca. 0.31 ± 0.05 (**Figure 2.7**, **Table A1.9 & A1.10**). Relative to snails and mussels, the DAF values for REEs (**Figure 2.6**) and other trace elements for crayfish are < 1 (**Figure A1.7**), indicating limited capacity to bioaccumulate trace elements. In environmental studies, crayfish hold a higher bioaccumulation potential of REEs when subjected to REE levels between 100 and 10000 mg/L but excreted REEs during depuration (Fasola, 2010).

The use of bioaccumulation factors needs to be carefully considered when looking at the bioaccumulation potential of metals in organisms through various exposure routes. The highest susceptibility of organisms to bioaccumulate metals depends on metals' uptake mechanisms through various exposure routes (dissolved, diet, and particulate). Bioaccumulation factors often consider the unfiltered fraction as bioavailable (Revel et al., 2023), and they represent accumulation from all exposure routes (dietary absorption, transport across respiratory surface) (Gobas and Morrison, 2000). However, the concentrations measured in whole organisms do not necessarily mean that contaminant–receptor interactions are occurring with the dissolved solution (Revel et al., 2023). For example, aquatic snails bioaccumulate metals in the intracellular granules or vesicles in

the digestive glands from exposure to the diet or sediment (Krupnova et al., 2018). Therefore, BAF values for snails should be based on diet and particulate exposures; the conventional approach, considering only the unfiltered dissolved solution, would neglect an important exposure pathway. Nevertheless, further studies are required to highlight the subcellular distributions of REE accumulation and whether the signatures of exposure (dissolved, diet, vs. particulate) are undergoing active metabolism and affecting the physiology of the organisms (Revel et al., 2023).

2.5 Conclusion

An in-depth understanding of REE bioavailability and exposure mechanisms to aquatic organisms is timely given the increasing demand and use for REE globally. This question can be addressed based on rare earth element fractionations, Ce anomalies, and bioaccumulation calculations (BCF and DAF). Our results highlighted that, under environmental conditions, the uptake mechanisms of REEs into pelagic organisms (minnows, *D. magna*, and *E. gracilis*) were mainly the dissolved form and benthic organisms (snails and mussels) uptake REEs mainly from the diet and particulate forms.

The bioaccumulative uptake of dissolved REEs into pelagic organisms remained high, based on BCF calculations, suggesting high transfer risks throughout the food web. The BCF values (72-1495, **Table A1.9**) for REEs in minnow organisms were in a similar range with BAF values (15-57,698) from various freshwater fish collected from a Washington reservoir (Mayfield and Fairbrother, 2015), from southern Quebec lakes (19.95) (Amyot et al., 2017), and BCF values of *Cyprinus carpio* (0.48-978) (Hao et al., 1996). It is important to note that we calculated BCF values using metal concentrations from water samples filtered at 0.45 µm, which might include some colloid fractions,

which does not represent total dissolved metal concentrations. While there is no evidence that colloidal REEs are bio-accumulative to organisms, further studies using different filtration cut-offs might be required to shed light on this environmental-relevant component. On the other hand, benthic organisms can bioaccumulate diet and sand substrate REEs in their soft tissue. The DAF values for snails (from 3.1 ± 1.5 to 21.8 ± 16.8) and mussels (from 8.3 ± 4.7 to 161.2 ± 143.7, **Table A1.9 & A1.10**) were in similar range to oysters (1.49) and mussels (1.10) collected from the Chinese coastline (Zhao et al., 2022) but 1-5 magnitudes lower then BAF values (3000-20000) for mussels from Vigo Ria (Rodríguez-Velarte et al., 2022). Within this study, mussels and snails are the most sensitive to bioaccumulate particulate REEs and minnows to bioaccumulate dissolved REEs. These organisms could be used to bio-monitor ecosystems vulnerable to rising REE levels.

2.6 Acknowledgements

The authors acknowledge the financial support from NSERC to D.H.D. (Discovery Grant) and A.K. (Undergraduate Student Research Awards). We thank the Trent University Animal Care Facility staff, including the manager (Jason Allen) and technicians (Cynthia Grant & Andrea Rogers). The authors also thanks Spencer Grieve for his assistance during field sampling campaigns and Dr. Wei Wang for his support relative to chemical analysis. The authors thank Dr. Karla Newman and Dr. Hayla Evans of the Trent Water Quality Centre, for their technical and analytical support.

2.7 References

Aharchaou, I., Beaubien, C., Campbell, P.G.C., Fortin, C., 2020. Lanthanum and cerium toxicity to the freshwater green alga Chlorella fusca: Applicability of the biotic ligand model. Environ Toxicol Chem 39, 996–1005. https://doi.org/10.1002/etc.4707

Akagi, T., Edanami, K., 2017. Sources of rare earth elements in shells and soft-tissues of bivalves from Tokyo Bay. Mar Chem 194, 55–62. https://doi.org/10.1016/j.marchem.2017.02.009

Alibo, D.S., Nozaki, Y., 1999. Rare earth elements in seawater: Particle association, shale-normalization, and Ce oxidation. Geochim Cosmochim Acta 63, 363–372. https://doi.org/10.1016/S0016-7037(98)00279-8

Amyot, M., Clayden, M.G., MacMillan, G.A., Perron, T., Arscott-Gauvin, A., 2017. Fate and trophic transfer of rare earth elements in temperate lake food webs. Environ Sci Technol 51, 6009–6017. https://doi.org/10.1021/acs.est.7b00739

Arienzo, M., Ferrara, L., Trifuoggi, M., Toscanesi, M., 2022. Advances in the fate of rare earth elements, REE, in transitional environments: Coasts and estuaries. Water (Basel) 14, 401. https://doi.org/10.3390/w14030401

Arnot, J.A., Gobas, F.A.P.C., 2006. A review of bioconcentration factor (BCF) and bioaccumulation factor (BAF) assessments for organic chemicals in aquatic organisms. Environ Rev. https://doi.org/10.1139/A06-005

Balaram, V., 1996. Recent trends in the instrumental analysis of rare earth elements in geological and industrial materials. TRAC - Trend Anal Chem 15, 475–486. https://doi.org/10.1016/S0165-9936(96)00058-1

Barata, C., Markich, S.J., Baird, D.J., Soares, A.M.V.M., 2002. The relative importance of water and food as cadmium sources to Daphnia magna Straus. Aquat Toxicol 61, 143–154. https://doi.org/10.1016/S0166-445X(02)00052-8

Barrat, J.A., Bayon, G., Lalonde, S., 2023. Calculation of cerium and lanthanum anomalies in geological and environmental samples. Chem Geol 615, 121202. https://doi.org/10.1016/j.chemgeo.2022.121202

Bau, M., Dulski, P., 1996. EPSL Anthropogenic origin of positive gadolinium anomalies in river waters. Earth Planet Sci Lett 143, 245–255. https://doi.org/10.1016/0012-821X(96)00127-6

Bau, M., Schmidt, K., Pack, A., Bendel, V., Kraemer, D., 2018. The European Shale: An improved data set for normalisation of rare earth element and yttrium concentrations in environmental and biological samples from Europe. Appl Geochem 90, 142–149. https://doi.org/10.1016/j.apgeochem.2018.01.008

Behets, G.J., Mubiana, K.V., Lamberts, L., Finsterle, K., Traill, N., Blust, R., D'Haese, P.C., 2020. Use of lanthanum for water treatment A matter of concern? Chemosphere 239, 124780. https://doi.org/10.1016/j.chemosphere.2019.124780

Bergsten-Torralba, L.R., Magalhães, D.P., Giese, E.C., Nascimento, C.R.S., Pinho, J.V.A., Buss, D.F., 2020. Toxicity of three rare earth elements, and their combinations to algae, microcrustaceans, and fungi. Ecotoxicol Environ Saf 201, 110795. https://doi.org/10.1016/j.ecoenv.2020.110795

Beyer, J., Green, N.W., Brooks, S., Allan, I.J., Ruus, A., Gomes, T., Bråte, I.L.N., Schøyen, M., 2017. Blue mussels (Mytilus edulis spp.) as sentinel organisms in coastal pollution monitoring: A review. Mar Environ Res 130, 338–365. https://doi.org/10.1016/j.marenvres.2017.07.024

Bingler, L.S., Byrne, R.H., Vargo, G.A., Tomas, C.R., 1989. Rare earth element uptake by the marine diatom. Chem Spec Bioavailab 1, 103–110. https://doi.org/10.1080/09542299.1989.11771986

Byrne, R.H., Kim, I.-H., 1990. Rare earth element scavenging in seawater. Geochim Cosmochim Acta 54, 2645–2656. https://doi.org/10.1016/0016-7037(90)90002-3

Byrne, R.H., Li, B., 1995. Comparative complexation behavior of the rare earths. Geochim Cosmochim Acta 59, 4575–4589. https://doi.org/10.1016/0016-7037(95)00303-7

Cardon, P.Y., Roques, O., Caron, A., Rosabal, M., Fortin, C., Amyot, M., 2020. Role of prey subcellular distribution on the bioaccumulation of yttrium (Y) in the rainbow trout. Environ Pollut 258, 113804. https://doi.org/10.1016/j.envpol.2019.113804

Cardon, P.Y., Triffault-Bouchet, G., Caron, A., Rosabal, M., Fortin, C., Amyot, M., 2019. Toxicity and subcellular fractionation of yttrium in three freshwater organisms: Daphnia magna, Chironomus riparius, and Oncorhynchus mykiss. ACS Omega 4, 13747–13755. https://doi.org/10.1021/acsomega.9b01238

Chassard-Bouchard, C., Hallegot, M., 1984. Thulium bioaccumulation by crab Carcinus maenas collected from the French Coasts of the channel: A structural, utrastructural and microanalytical study by secondary ion mass and x ray spectrometry. J Phys Colloq 45, 541–544. https://doi.org/10.1051/jphyscol:19842123

Costa, M., Henriques, B., Pinto, J., Fabre, E., Dias, M., Soares, J., Carvalho, L., Vale, C., Pinheiro-Torres, J., Pereira, E., 2020. Influence of toxic elements on the simultaneous uptake of rare earth elements from contaminated waters by estuarine macroalgae. Chemosphere 252, 126562. https://doi.org/10.1016/j.chemosphere.2020.126562

Crémazy, A., Brix, K. V., Wood, C.M., 2019. Using the biotic ligand model framework to investigate binary metal interactions on the uptake of Ag, Cd, Cu, Ni, Pb and Zn in the freshwater snail Lymnaea stagnalis. Sci Total Environ 647, 1611–1625. https://doi.org/10.1016/j.scitotenv.2018.07.455

Dallinger, L.R., Wieser, W., 1984. Patterns of accumulation, distribution and liberation of Zn, Cu, Cd and Pb in different organs of the land snail Helix pomatia L. J Physiol Biochem 79, 117–124. https://doi.org/10.1016/0742-8413(84)90173-7

Dang, D.H., Ma, L., Ha, Q.K., Wang, W., 2022a. A multi-tracer approach to disentangle anthropogenic emissions from natural processes in the St. Lawrence river and estuary. Water Res 219, 118588. https://doi.org/10.1016/j.watres.2022.118588

Dang, D.H., Thompson, K.A., Ma, L., Nguyen, H.Q., Luu, S.T., Duong, M.T.N., Kernaghan, A., 2021. Toward the circular economy of rare earth elements: A review of abundance, extraction, applications, and environmental impacts. Arch Environ Contam Toxicol 81, 521–530. https://doi.org/10.1007/s00244-021-00867-7

Dang, D.H., Wang, W., Pelletier, P., Poulain, A.J., Evans, R.D., 2018. Uranium dispersion from U tailings and mechanisms leading to U accumulation in sediments: Insights from biogeochemical and isotopic approaches. Sci Total Environ 610–611, 880–891. https://doi.org/10.1016/j.scitotenv.2017.08.156

Dang, D.H., Wang, W., Sikma, A., Chatzis, A., Mucci, A., 2022b. The contrasting estuarine geochemistry of rare earth elements between ice-covered and ice-free conditions. Geochim Cosmochim Acta 317, 488–506. https://doi.org/10.1016/j.gca.2021.10.025

Dang, D.H., Wang, W., Winkler, G., Chatzis, A., 2023. Rare earth element uptake mechanisms in plankton in the Estuary and Gulf of St. Lawrence. Sci Total Environ 860, 160394. https://doi.org/10.1016/j.scitotenv.2022.160394

de Baar, H.J.W., Bruland, K.W., Schijf, J., van Heuven, S.M.A.C., Behrens, M.K., 2018. Low cerium among the dissolved rare earth elements in the central North Pacific Ocean. Geochim Cosmochim Acta 236, 5–40. https://doi.org/10.1016/j.gca.2018.03.003

de Baar, H.J.W., German, C.R., Elderfield, H., Van Gaans, P., 1988. Rare earth element distributions in anoxic waters of the Cariaco Trench*. Geochim Cosmochim Acta 52, 1203–1219. https://doi.org/10.1016/0016-7037(88)90275-X

Deb, S.C., Fukushima, T., 1999. Metals in aquatic ecosystems: Mechanisms of uptake, accumulation and release-ecotoxicological perspectives. Int J Environ Stud 56, 385–417. https://doi.org/10.1080/00207239908711212

Di Toro, D.M., Allen, H.E., Bergman, J.S., Meyer, J.S., Paquin, P.R., Santore, R.C., 2001. Biotic ligand model of the acute toxicity of metals. 1. Technical basis. Environ Toxicol Chem 20, 2383–2396. https://doi.org/10.1002/etc.5620201034

El-Akl, P., Smith, S., Wilkinson, K.J., 2015. Linking the chemical speciation of cerium to its bioavailability in water for a freshwater alga. Environ Toxicol Chem 34, 1711–1719. https://doi.org/10.1002/etc.2991

Ellis, L., 2018. Final List of Critical Minerals 2018 83, 1–2.

Ercoli, F., Ghia, D., Gruppuso, L., Fea, G., Bo, T., Ruokonen, T.J., 2021. Diet and trophic niche of the invasive signal crayfish in the first invaded Italian stream ecosystem. Sci Rep 11, 8704. https://doi.org/10.1038/s41598-021-88073-2

European Commission, 2020. Critical raw materials resilience: Charting a path towards greater sustainability. Brussels. https://doi.org/https://eur-lex.europa.eu/legal-content/EN/TXT/?uri=CELEX:52020DC0474

Fasola, E., 2010. Phoslock ® Effects on benthic invertebrates: the example of crayfish (Procambarus Acutus) (Master in Risk Assessment and Risk Analysis). Wageningen University.

Flik, G., Verbost, P.M., Wendelaar Bonga, S.E., 1995. 12 Calcium Transport Processes in Fishes. Academic Press 14, 317–342. https://doi.org/10.1016/S1546-5098(08)60251-4

Floback, A.E., Moffett, J.W., 2021. Rare earth element distributions in the Arabian Sea reveal the influence of redox processes within the oxygen deficient zone. Chem Geol 577, 120214. https://doi.org/10.1016/j.chemgeo.2021.120214

Freitas, R., Costa, S., D Cardoso, C.E., Morais, T., Moleiro, P., Matias, A.C., Pereira, A.F., Machado, J., Correia, B., Pinheiro, D., Rodrigues, A., Colónia, J., Soares, A.M.V.M., Pereira, E., 2020. Toxicological effects of the rare earth element neodymium in Mytilus galloprovincialis. Chemosphere 244, 125457. https://doi.org/10.1016/j.chemosphere.2019.125457

Freslon, N., Bayon, G., Toucanne, S., Bermell, S., Bollinger, C., Chéron, S., Etoubleau, J., Germain, Y., Khripounoff, A., Ponzevera, E., Rouget, M.L., 2014. Rare earth elements and neodymium isotopes in sedimentary organic matter. Geochim Cosmochim Acta 140, 177–198. https://doi.org/10.1016/j.gca.2014.05.016

Garcia-Solsona, E., Jeandel, C., 2020. Balancing Rare Earth Element distributions in the Northwestern Mediterranean Sea. Chem Geol 532, 119372. https://doi.org/10.1016/j.chemgeo.2019.119372

Garzanti, E., Bayon, G., Dennielou, B., Barbarano, M., Limonta, M., Vezzoli, G., 2021. The Congo deep-sea fan: Mineralogical, REE, and ND-isotope variability in Quartzose passive-margin sand. J Sediment Res 91, 433–450. https://doi.org/10.2110/JSR.2020.100

Gimbert, F., Vijver, M.G., Coeurdassier, M., Scheifler, R., Peijnenburg, W.J.G.M., Badot, P.M., De Vaufleury, A., 2008. How subcellular partitioning can help to understand heavy metal accumulation and elimination kinetics in snails. Environ Toxicol Chem 27, 1284–1292. https://doi.org/10.1897/07-503.1

Gobas, F.A.P.C., Morrison, Heather.A., 2000. Bioconcentration and biomagnification in the aquatic environment, in: Property Estimation Methods for Chemicals Handbook of Environmental and Health Sciences. Lewis Publishers, pp. 189–233.

Goitom, E., 2011. Bioaccumulation of lanthanum in marbled crayfish (Procambarus sp.) (Master's thesis). Wageningen University.

Goldstein, S.J., Jacobsen, S.B., 1988. Rare earth elements in river waters. Earth Planet Sci Lett 89, 35–47. https://doi.org/10.1016/0012-821X(88)90031-3

Government of Canada, 2023. Persistence and bioaccumulation regulations SOR/2000-107 [WWW Document]. Minister of Justice. URL https://laws.justice.gc.ca/eng/regulations/SOR-2000-107/FullText.html Hoshino, M., Sanematsu. K., & Watanabe, Y. (2016). Chapter 279 – REE Minerology and (accessed 1.4.24).

Government of Canada, 2022. The Canadian critical minerals strategy, From exploration to recycling : Powering the Green and Digital Economy for Canada and the World.

Guner, U., 2010. Bioaccumulation of some heavy metals on freshwater crayfish, in: Impact, Monitoring, and Management of Environmental Pollution. Nova Science Publishers, pp. 1–19.

Hannigan, Robyn E, Sholkovitz, E.R., Hannigan, R E, 2001. The development of middle rare earth element enrichments in freshwaters: weathering of phosphate minerals. Chem Geol 175, 495–508. https://doi.org/10.1016/S0009-2541(00)00355-7

Hao, S., Xiaorong, W., Zhaozhe, H., Chonghua, W., Liansheng, W., Lemei, D., Zhong, L., Yijun, C., 1996. Bioconcentration and elimination of five light rare earth elements in carp (Cyprinus carpio L.). Chemosphere 33, 1475–1483. https://doi.org/10.1016/0045-6535(96)00286-X

Hatje, V., Bruland, K.W., Flegal, A.R., 2016. Increases in Anthropogenic Gadolinium Anomalies and Rare Earth Element Concentrations in San Francisco Bay over a 20 Year Record. Environ Sci Technol 50, 4159–4168. https://doi.org/10.1021/acs.est.5b04322

Ishii, N., Tagami, K., Uchida, S., 2006. Removal of rare earth elements by algal flagellate Euglena gracilis. J Alloy Compd 408–412, 417–420. https://doi.org/10.1016/j.jallcom.2004.12.105

Jacinto, J., Henriques, B., Duarte, A.C., Vale, C., Pereira, E., 2018. Removal and recovery of critical rare elements from contaminated waters by living Gracilaria gracilis. J Hazard Mater 344, 531–538. https://doi.org/10.1016/j.jhazmat.2017.10.054

Jiang, C., Li, Y., Li, C., Zheng, Lanlan, Zheng, Liugen, 2022. Distribution, source and behavior of rare earth elements in surface water and sediments in a subtropical freshwater lake influenced by human activities. Environ Pollut 313, 120153. https://doi.org/10.1016/j.envpol.2022.120153

Johannesson, K.H., Hawkins, D.L., Cortés, A., 2006. Do Archean chemical sediments record ancient seawater rare earth element patterns? Geochim Cosmochim Acta 70, 871–890. https://doi.org/10.1016/j.gca.2005.10.013

Kang, L., Shen, Z., Jin, C., 2000. Neodymium cations Nd3+ were transported to the interior of Euglena gracilis 277. Chinese Science Bulletin 45, 585–592. https://doi.org/10.1007/BF02886032

Kraemer, D., Bau, M., 2022. Siderophores and the formation of cerium anomalies in anoxic environments. Geochem Perspect Lett 22, 50–55. https://doi.org/10.7185/GEOCHEMLET.2227

Krupnova, T.G., Mashkova, I. V., Kostryukova, A.M., Schelkanova, E.E., Gavrilkina, S. V., 2018. Gastropods as potential biomonitors of contamination caused by heavy metals in South Ural lakes, Russia. Ecol Indic 95, 1001–1007. https://doi.org/10.1016/j.ecolind.2017.12.005

Labassa, M., Pereto, C., Schäfer, J., Hani, Y.M.I., Baudrimont, M., Bossy, C., Dassié, É.P., Mauffret, A., Deflandre, B., Grémare, A., Coynel, A., 2023. First assessment of rare earth element organotropism in Solea solea in a coastal area: The west Gironde Mud Patch (France). Mar Pollut Bull 197, 115730. https://doi.org/10.1016/j.marpolbul.2023.115730

Lachaux, N., Cossu-Leguille, C., Poirier, L., Gross, E.M., Giamberini, L., 2022. Integrated environmental risk assessment of rare earth elements mixture on aquatic ecosystems. Front Environ Sci 10, 1–18. https://doi.org/10.3389/fenvs.2022.974191

Lachaux, N., Otero-Fariña, A., Minguez, L., Sohm, B., Rétif, J., Châtel, A., Poirier, L., Devin, S., Pain-Devin, S., Gross, E.M., Giamberini, L., 2023. Fate, subcellular distribution and biological effects of rare earth elements in a freshwater bivalve under complex exposure. Sci Total Environ 905, 167302. https://doi.org/10.1016/j.scitotenv.2023.167302

Lam, I.K.S., Wang, W.X., 2006. Accumulation and elimination of aqueous and dietary silver in Daphnia magna. Chemosphere 64, 26–35. https://doi.org/10.1016/j.chemosphere.2005.12.023

Lawrence, M.G., Kamber, B.S., 2006. The behaviour of the rare earth elements during estuarine mixing-revisited. Mar Chem 100, 147–161. https://doi.org/10.1016/j.marchem.2005.11.007

Lortholarie, M., Poirier, L., Kamari, A., Herrenknecht, C., Zalouk-Vergnoux, A., 2021. Rare earth element organotropism in European eel (Anguilla anguilla). Sci Total Environ 766, 142513. https://doi.org/10.1016/j.scitotenv.2020.142513

Luo, Byrne, 2004. Carbonate complexation of yttrium and the rare earth elements in natural waters. Geochim Cosmochim Acta 68, 691–699. https://doi.org/10.1016/S0016-7037(03)00495-2

Luo, J., Huo, Y., Shen, Y., Hu, J., Ji, H., 2016. Effects of colloidal particle size on the geochemical characteristics of REE in the water in southern Jiangxi province, China. Environ Earth Sci 75, 1–17. https://doi.org/10.1007/s12665-015-4870-0

Ma, L., Dang, D.H., Wang, W., Evans, R.D., Wang, W.X., 2019. Rare earth elements in the Pearl River Delta of China: Potential impacts of the REE industry on water, suspended particles and oysters. Environ Pollut 244, 190–201. https://doi.org/10.1016/j.envpol.2018.10.015

Mackay, D., Celsie, A.K.D., Powell, D.E., Parnis, J.M., 2018. Bioconcentration, bioaccumulation, biomagnification and trophic magnification: A modelling perspective. Environ Sci Process Impacts 20, 72–85. https://doi.org/10.1039/c7em00485k

MacMillan, G.A., Chételat, J., Heath, J., Mickpegak, R., Amyot, M., 2017. Rare earth elements (REE) in freshwater, marine, and terrestrial ecosystems in the eastern Canadian Arctic. Environ Sci-Proc Imp 10, 1336–1345. https://doi.org/10.1101/174870

MacMillan, G.A., Clayden, M.G., Chételat, J., Richardson, M.C., Ponton, D.E., Perron, T., Amyot, M., 2019. Environmental drivers of rare earth element bioaccumulation in freshwater zooplankton. Environ Sci Technol 53, 1650–1660. https://doi.org/10.1021/acs.est.8b05547

Manoj, M.C., Thakur, B., Prasad, V., 2016. Rare earth element distribution in tropical coastal wetland sediments: a case study from Vembanad estuary, southwest India. Arab J Geosci 9, 1–11. https://doi.org/10.1007/s12517-015-2246-0

Marginson, H., MacMillan, G.A., Grant, E., Gérin-Lajoie, J., Amyot, M., 2023. Rare earth element bioaccumulation and cerium anomalies in biota from the Eastern Canadian subarctic (Nunavik). Sci Total Environ 879, 163024. https://doi.org/10.1016/j.scitotenv.2023.163024

Marigómez, I., Soto, M., Cajaraville, M.P., Angulo, E., Giamberini, L., 2002. Cellular and subcellular distribution of metals in molluscs. Microsc Res Tech 56, 358–392. https://doi.org/10.1002/jemt.10040

Martin, B.R., Frederick, R.S., 1979. Lanthanides as probes for calcium in biological systems. Q Rev Biophys 12, 181–209. https://doi.org/10.1017/S0033583500002754

Mayfield, D.B., Fairbrother, A., 2015. Examination of rare earth element concentration patterns in freshwater fish tissues. Chemosphere 120, 68–74. https://doi.org/10.1016/j.chemosphere.2014.06.010

Mcgeer, J.C., Brix, K. V, Skeaff, J.M., Deforest, D.K., Brigham, S.I., Adams, W.J., Green, A., 2003. Inverse relationship between bioconcentration factor and exposure concentration for metals: implications for hazard assessment of metals in the aquatic environment. Environ Toxicol Chem 22, 1017–1037. https://doi.org/https://doi.org/10.1002/etc.5620220509

McLennan, S.M., 2001. Relationships between the trace element composition of sedimentary rocks and upper continental crust. Geochem Geophy Geosy 2, 1–24. https://doi.org/10.1029/2000GC000109

McLennan, S.M., 1989. Rare earth elements in sedimentary rocks: Influence of provenance and sedimentary processes. Rev Mineral 169–200. https://doi.org/10.1515/9781501509032-010

Mehmood, M., 2018. Rare Earth Elements- A Review. J Ecol Nat Res 2, 1–6. https://doi.org/10.23880/jenr-16000128

Merschel, G., Bau, M., 2015. Rare earth elements in the aragonitic shell of freshwater mussel Corbicula fluminea and the bioavailability of anthropogenic lanthanum, samarium and gadolinium in river water. Sci Total Environ 533, 91–101. https://doi.org/10.1016/j.scitotenv.2015.06.042

Merschel, G., Bau, M., Schmidt, K., Münker, C., Dantas, E.L., 2017. Hafnium and neodymium isotopes and REY distribution in the truly dissolved, nanoparticulate/colloidal and suspended loads of rivers in the Amazon Basin, Brazil. Geochim Cosmochim Acta 213, 383–399. https://doi.org/10.1016/j.gca.2017.07.006

Morgan, B., Rate, A.W., Burton, E.D., Smirk, M.N., 2012. Enrichment and fractionation of rare earth elements in FeS- and organic-rich estuarine sediments receiving acid sulfate soil drainage. Chem Geol 308–309, 60–73. https://doi.org/10.1016/j.chemgeo.2012.03.012

Nikanorov, A.M., 2016. Oddo–Harkins evenness rule as an indication of the abundances of chemical elements in the Earth's hydrosphere and estimations of the nature of cosmic bodies. Geochem Int 54, 464–469. https://doi.org/10.1134/S0016702916050074

Nørregaard, R.D., Kaarsholm, H., Bach, L., Nowak, B., Geertz-Hansen, O., Søndergaard, J., Sonne, C., 2019. Bioaccumulation of rare earth elements in juvenile arctic char (Salvelinus alpinus) under field experimental conditions. Sci Total Environ 688, 529–535. https://doi.org/10.1016/j.scitotenv.2019.06.180

Och, L.M., Müller, B., Wichser, A., Ulrich, A., Vologina, E.G., Sturm, M., 2014. Rare earth elements in the sediments of Lake Baikal. Chem Geol 376, 61–75. https://doi.org/10.1016/j.chemgeo.2014.03.018

Olaueson, M.M., Stokes, P.M., 1989. Responses of the Acidophilic Alga Euglena Mutabilis (Euglenophyceae) to Carbon Enrcihment at h 3. J Phycol 25, 529–539. https://doi.org/10.1111/j.1529-8817.1989.tb00259.x

Osborne, A.H., Haley, B.A., Hathorne, E.C., Plancherel, Y., Frank, M., 2014. Rare earth element distribution in Caribbean seawater: Continental inputs versus lateral transport of distinct REE compositions in subsurface water masses. Mar Chem 177, 172–183. https://doi.org/10.1016/j.marchem.2015.03.013

Østerås, A., 2023. Accumulation of Gadolinium in lumpfish (Cyclopterus lumpus) (Master's thesis). Norwegian University of Science and Technology.

Pastorino, P., Squadrone, S., Berti, G., Esposito, G., Bondavalli, F., Renzi, M., Pizzul, E., Kazmi, S.S.U.H., Barceló, D., Abete, M.C., Prearo, M., 2024. Occurrence of rare earth elements in water, sediment, and freshwater fish of diverse trophic levels and feeding ecology: Insights from the Po river (northwest Italy). Environ Res 240, 117455. https://doi.org/10.1016/j.envres.2023.117455

Pereto, C., Baudrimont, M., Coynel, A., 2024. Global natural concentrations of rare earth elements in aquatic organisms: Progress and lessons from fifty years of studies. Sci Total Environ 922, 171241. https://doi.org/10.1016/j.scitotenv.2024.171241

Pinto, J., Costa, M., Leite, C., Borges, C., Coppola, F., Henriques, B., Monteiro, R., Russo, T., Di Cosmo, A., Soares, A.M.V.M., Polese, G., Pereira, E., Freitas, R., 2019. Ecotoxicological effects of lanthanum in Mytilus galloprovincialis: Biochemical and histopathological impacts. Aquat Toxicol 211, 181–192. https://doi.org/10.1016/j.aquatox.2019.03.017

Piper, D.Z., Bau, M., 2013. Normalized rare earth elements in water, sediments, and wine: Identifying sources and environmental redox conditions. Am J Analyt Chem 04, 69–83. https://doi.org/10.4236/ajac.2013.410a1009

Pourret, O., Davranche, M., Gruau, G., Dia, A., 2007. Rare earth elements complexation with humic acid. Chem Geol 243, 128–141. https://doi.org/10.1016/j.chemgeo.2007.05.018

Pourret, O., Tuduri, J., 2017. Continental shelves as potential resource of rare earth elements. Sci Rep 7, 5857. https://doi.org/10.1038/s41598-017-06380-z

Pourret, O., van der Ent, A., Hursthouse, A., Irawan, D.E., Liu, H., Wiche, O., 2022. The 'europium anomaly' in plants: facts and fiction. Plant Soil 476, 721–728. https://doi.org/10.1007/s11104-021-05210-6

Prokop, A., Bajpai, R., Zappi, M., 2015. Algal Biorefineries. Springer 2, 339–366.

Rainbow, P.S., White, S.L., 1989. Comparative strategies of heavy metal accumulation by crustaceans: zinc, copper and cadmium in a decapod, an amphipod and a barnacle. Hydrobiologia 174, 245–262. https://doi.org/https://doi.org/10.1007/BF00008164

Ramos, S.J., Dinali, G.S., Oliveira, C., Martins, G.C., Moreira, C.G., Siqueira, J.O., Guilherme, L.R.G., 2016. Rare earth elements in the soil environment. Curr Pollut Rep 2, 28–50. https://doi.org/10.1007/s40726-016-0026-4

Ratié, G., Vantelon, D., Pédrot, M., Beauvois, A., Chaouchi, K., Fossé, C., Davranche, M., 2020. Cerium anomalies in riverbanks: Highlight into the role of ferric deposits. Sci Total Environ 713, 136544. https://doi.org/10.1016/j.scitotenv.2020.136544

Regoli, F., Giuliani, M.E., Benedetti, M., Arukwe, A., 2011. Molecular and biochemical biomarkers in environmental monitoring: A comparison of biotransformation and antioxidant defense systems in multiple tissues. Aquat Toxicol 105, 56–66. https://doi.org/10.1016/j.aquatox.2011.06.014

Rétif, J., Zalouk-Vergnoux, A., Kamari, A., Briant, N., Poirier, L., 2024. Trophic transfer of rare earth elements in the food web of the Loire estuary (France). Sci Total Environ 914, 169652. https://doi.org/10.1016/j.scitotenv.2023.169652

Revel, M., Medjoubi, K., Rivard, C., Vantelon, D., Hursthouse, A., Heise, S., 2023. Determination of the distribution of rare earth elements La and Gd in Daphnia magna via micro and nano-SXRF imaging. Environ Sci Process Impacts 25, 1288–1297. https://doi.org/10.1039/d3em00133d

Riegel, J.A., 1966. Analysis of formed bodies in urine removed from the crayfish antennal gland by micropuncture. J. Exp. Biol 44, 387–395. https://doi.org/10.1242/jeb.44.2.387

Rodríguez-Velarte, P., Babarro, J.M.F., Cobelo-García, A., 2022. Bioaccumulation patterns of trace elements by native (M. galloprovincialis) and invasive (X. securis) mussels in coastal systems (Vigo Ria, NW Iberian Peninsula). Mar Pollut Bull 176, 113463. https://doi.org/10.1016/j.marpolbul.2022.113463

Rudnick, R.L., Gao, S., 2013. Composition of the Continental Crust, in: Treatise on Geochemistry: Second Edition. Elsevier Inc., Oxford, pp. 1–51. https://doi.org/10.1016/B978-0-08-095975-7.00301-6

Shannon, R.D., 1976. Revised effective ionic radii and systematic studies of interatomic distances in halides and chalcogenides. Acta Crystallographica Section A 32, 751–767. https://doi.org/10.1107/S0567739476001551

Shen, H., Ren, Q.G., Mi, Y., Shi, X.F., Yao, H.Y., Jin, C.Z., Huang, Y.Y., He, W., Zhang, J., Liu, B., 2002. Investigation of metal ion accumulation in Euglena gracilis by fluorescence methods. Nuc Instrum Methods 189, 506–610. https://doi.org/10.1016/S0168-583X(01)01132-6

Sholkovitz, Edward.R., 1995. The aquatic chemistry of rare earth elements in rivers and estuaries. Aquat Geochem 1, 1–34. https://doi.org/https://doi.org/10.1007/BF01025229

Si, M., Lang, J., 2018. The roles of metallothioneins in carcinogenesis. J Hematol Oncol 11, 1–20. https://doi.org/10.1186/s13045-018-0645-x

Siciliano, A., Guida, M., Serafini, S., Micillo, M., Galdiero, E., Carfagna, S., Salbitani, G., Tommasi, F., Lofrano, G., Padilla Suarez, E.G., Gjata, I., Brouziotis, A.A., Trifuoggi, M., Liguori, R., Race, M., Fabbricino, M., Libralato, G., 2021. Long-term multi-endpoint exposure of the microalga Raphidocelis subcapitata to lanthanum and cerium. Sci Total Environ 790, 148229. https://doi.org/10.1016/j.scitotenv.2021.148229

Sugawara, A., Nishimura, T., Yamamoto, Y., Inoue, H., Nagasawa, H., Kato, T., 2006. Self-organization of oriented calcium carbonate/polymer composites: Effects of a matrix peptide isolated from the exoskeleton of a crayfish. Angew Chem Int Edit 45, 2876–2879. https://doi.org/10.1002/anie.200503800

Tan, Q.G., Yang, G., Wilkinson, K.J., 2017. Biotic ligand model explains the effects of competition but not complexation for Sm biouptake by Chlamydomonas reinhardtii. Chemosphere 168, 426–434. https://doi.org/10.1016/j.chemosphere.2016.10.051

Tang, J., Johannesson, K.H., 2010. Ligand extraction of rare earth elements from aquifer sediments: Implications for rare earth element complexation with organic matter in natural waters. Geochim Cosmochim Acta 74, 6690–6705. https://doi.org/10.1016/j.gca.2010.08.028

Taylor, S.R., McLennan, S.M., 1995. The geochemical evolution of the continental crust. Rev Geophys 33, 241–265. https://doi.org/10.1029/95RG00262

Taylor, S.R., Mclennan, S.M., Armstrong, R.L., Tarney, J., 1981. The composition and evolution of the continental crust: rare earth element evidence from sedimentary rocks. Philos T R Soc S-A 301, 381–399. https://doi.org/https://doi.org/10.1098/rsta.1981.0119

Thompson, R.L., Bank, T., Roth, E., Granite, E., 2016. Resolution of rare earth element interferences in fossil energy by-product samples using sector-field ICP-MS. Fuel 185, 94–101. https://doi.org/10.1016/j.fuel.2016.07.093

Tostevin, R., 2021. Cerium anomalies and paleoredox. Cambridge University Press. https://doi.org/10.1017/9781108847223

Tsui, M.T.K., Wang, W.X., 2007. Biokinetics and tolerance development of toxic metals in Daphnia magna. Environ Toxicol Chem 26, 1023–1032. https://doi.org/10.1897/06-430R.1

Turner, A., Pilsbury, A., 2013. Accumulation of aqueous and dietary thallium by the marine snail, Littorina littorea. Estuar Coast Shelf Sci 129, 73–76. https://doi.org/10.1016/j.ecss.2013.05.030

Tyler, G., 2004. Rare earth elements in soil and plant systems-A review. Plant Soil 267, 191–206. https://doi.org/https://doi.org/10.1007/s11104-005-4888-2

Valcheva-Traykova, M., Saso, L., Kostova, I., 2014. Involvement of lanthanides in the free radicals homeostasis. Curr Top Med Chem 14, 1–12. https://doi.org/https://doi.org/10.2174/1568026614666141203123620

Vuori, K.-M., 1995. Direct and indirect effects of iron on river ecosystems. Ann Zool Fennici 32, 317–329.

Wang, Y., Zhang, M., Wang, X., 2000. Population growth responses of tetrahymena shanghaiensis in exposure to rare earth elements. Biol Trace Metal R 75, 265–275. https://doi.org/10.1385/BTER:75:1-3:265

Wang, Z., Yin, L., Xiang, H., Qin, X., Wang, S., 2019. Accumulation patterns and species-specific characteristics of yttrium and rare earth elements (YREEs) in biological matrices from Maluan Bay, China: Implications for biomonitoring. Environ Res 179, 108804. https://doi.org/10.1016/j.envres.2019.108804

Wang, Zaosheng, Shu, J., Wang, Zhaoru, Qin, X., Wang, S., 2022. Geochemical behavior and fractionation characteristics of rare earth elements (REEs) in riverine water profiles and sentinel Clam (Corbicula fluminea) across watershed scales: Insights for REEs monitoring. Sci Total Environ 803, 150090. https://doi.org/10.1016/j.scitotenv.2021.150090

Weltje, L., Heidenreich, H., Zhu, W., Wolterbeek, H.T., Korhammer, S., De Goeij, J.J.M., Markert, B., 2002. Lanthanide concentrations in freshwater plants and molluscs, related to those in surface water, pore water and sediment. A case study in The Netherlands. Sci Total Environ 286, 191–214. https://doi.org/10.1016/S0048-9697(01)00978-0

Wood, C., Farrell, A., Brauner, C., 2012. 11. Characterization of internal handling, in: Fish Physiology: Homeostasis and Toxicology of Essential Metals. pp. 27–38.

Xu, Pan, B., Shu, F., Chen, X., Xu, N., Ni, J., 2022. Bioaccumulation of 35 metal(loid)s in organs of a freshwater mussel (Hyriopsis cumingii) and environmental implications in Poyang Lake, China. Chemosphere 307, 136150. https://doi.org/10.1016/j.chemosphere.2022.136150

Yu, R.-Q., Wang, W.-X., 2002. Trace metal assimilation and release budget in Daphnia magna. Limnol. Oceanogr 47, 495–504. https://doi.org/10.4319/lo.2002.47.2.0495

Zhang, C., Wang, L., Zhang, S., Li, X., 1998. Geochemistry of rare earth elements in the mainstream of the Yangtze River, China. Appl Geochem 13, 451–462. https://doi.org/10.1016/S0883-2927(97)00079-6

Zhao, P., Bi, R., Sanganyado, E., Zeng, X., Li, W., Lyu, Z., Liu, J., Li, P., Du, H., Liu, W., Jia, Y., 2022. Rare earth elements in oysters and mussels collected from the Chinese coast: Bioaccumulation and human health risks. Mar Pollut Bull 184, 114127. https://doi.org/10.1016/j.marpolbul.2022.114127

Zheng, X.Y., Plancherel, Y., Saito, M.A., Scott, P.M., Henderson, G.M., 2016. Rare earth elements (REEs) in the tropical South Atlantic and quantitative deconvolution of their non-conservative behavior. Geochim Cosmochim Acta 177, 217–237. https://doi.org/10.1016/j.gca.2016.01.018

Zhong, S., Mucci, A., 1995. Partitioning of rare earth elements (REEs) between calcite and seawater solutions at 25°C and 1 atm, and high dissolved REE concentrations. Geochim Cosmochim Acta 59, 443–453. https://doi.org/10.1016/0016-7037(94)00381-U

Chapter 3. Lanthanum enrichment throughout the ecosystem of Swan Lake (Canada) post-amendment to lanthanum-modified bentonite coagulant

3.1 Abstract

Lanthanum-modified bentonite clay (LMB) is a remediation approach based on rare earth elements (REEs) to mitigate eutrophication in aquatic systems. This study assessed the distribution and enrichment of La and Pr throughout the food web of Swan Lake (Ontario), seven years post-application of LMB. Lanthanum concentrations in sediments ranged from 170 mg kg^{-1} to 1500 mg kg^{-1}. In the water column, the highest proportion of REEs were found in the acid-leachable particulate fraction in the intermediate (mid-depth: 80.0 ± 3.2%) and deep (above the sediments: 95.9 ± 2.5%) layers. Lanthanum levels in Swan Lake sediments, water, and biological organisms were one to three orders of magnitude higher than the reference site (Toogood Pond). The calculation of La anomalies indicated the extent of La enrichment. Benthic and pelagic organisms held positive La anomalies: macrophytes (5.8 ± 1.5), english bullhead internal organs (9.7 ± 2.3), and gills (5.8 ± 1.1), plankton (8.6 ± 0.5), and fathead minnow internal organs (8.2 ± 0.3), soft tissue (5.4 ± 0.5), gills (12.7 ± 3.7), and the brain (550 ± 240). Lanthanum accumulation in the brains of vertebrates needs further investigation to clarify the mechanisms and explore whether this is a standalone case for Swan Lake or if there could be a more prevalent risk associated with exposure to high REE concentrations.

Keywords: Lanthanum modified bentonite clay, distribution of rare earth elements, sediment risk assessment, elemental organotropism, lanthanum enrichment.

3.2 Introduction

Rare earth elements (REEs) include 17 chemically uniform metallic elements: 15 inner transition metals of group 3A, known as the lanthanide series ($_{57}$La to $_{71}$Lu) and two non-lanthanides ($_{21}$Sc and $_{39}$Y). Rare earth elements are integrated into various technologies and environmental applications such as renewable energies, electronics, health applications, and the defence industry (Migaszewski and Gałuszka, 2015). As the demand for REEs in technical products soar globally (Humphries, 2013; International Energy Agency, 2021), these elements have been identified as critical minerals of high priority by various jurisdictions (European Commission, 2020; Government of Canada, 2022; Lusty et al., 2021).

Besides major high-technological applications of REEs, La, a LREE can be used in a coagulant product to mitigate eutrophication (Zeller and Alperin, 2021). (Hyper)trophic conditions in water bodies are caused by surpluses of nitrogen and phosphorus in freshwater systems, leading to excessive algal growth (Khan and Ansari, 2005; Schindler, 2006). Naturally, eutrophication occurs from the gradual enrichment of water bodies due to inputs of eroding shorelines or decomposing organic matter (Thornton et al., 2013). However, anthropogenic inputs of non-point loadings (fertilizers from agroecosystems) or point discharges (wastewater effluent) have accelerated the rates and extent of eutrophication (Chislock et al., 2013). Over time, the decomposition of biomass detritus by bacteria leads to oxygen depletion in water systems and causes habitat loss for benthic organisms and vertebrate species (Keuskamp et al., 2015). The presence of anoxic zones also contributes to the release of phosphorous (P) from the sediment into the water column through internal loading processes (Søndergaard et al., 2003), which increases

biomass production and enhances the eutrophication positive feedback loop (Smith and Schindler, 2009). Internal P loading and eutrophication can be reduced through management techniques such as applying salts and modified clays that chemically immobilize soluble reactive P (George et al., 2019).

Lanthanum in REE-based coagulant products (Finsterle, 2014) has the potential to reduce internal P loading and eutrophication (Zeller and Alperin, 2021) by immobilizing soluble reactive P (Bishop and Richardson, 2018). Lanthanum based coagulants have been applied to lakes worldwide to enforce recovery processes (Epe et al., 2017; Lürling and Van Oosterhout, 2013; Meis et al., 2013; Nürnberg, 2017; Nürnberg and LaZerte, 2016). These coagulants are referred to as geo-engineered lanthanum-modified bentonite clays (LMB) and are produced through a cation exchange process which modifies natural bentonite clay by exchanging surface-adsorbed calcium and sodium ions with La ions (Finsterle, 2014). Lanthanum ions have a high affinity to bond with soluble reactive P (Firsching and Bruñe, 1991) to produce a poorly soluble lanthanum phosphate complex named rhabdophane, that precipitates. The LMB complex falls out of suspensions from the water column and forms a barrier on top of the sediments, intercepting the mobilized legacy P under anoxic conditions (Meis et al., 2013; Ross et al., 2008). The binding capacity of LMB lasts until saturated with soluble reactive P (Finsterle, 2014). Chemical parameters of water such as pH, low alkalinity, anaerobic waters, and high dissolved organic carbon content impact the efficiency of LMB (Dithmer et al., 2015; Finsterle, 2014; Meis et al., 2013; Spears et al., 2013). The effectiveness of LMB binding capacity is higher when applied to anoxic sediment and waters (Ross et al., 2008), but the binding capacity of LMB decreases when applied to aquatic systems with a pH of 9 (Haghseresht

et al., 2009), or when humic substance and CO_3^{2-} is present, complexes with LMB, and interfere with the removal of soluble reactive P (Pourret et al., 2007a). Further, physical disturbances such as bioturbation (Meysman et al., 2006) and wind (Douglas and Rippey, 2000) can also resuspend LMB back into the water column, which increases La exposure to aquatic organisms (Spears et al., 2013). The resuspension of LMB increases the release of legacy P post-application (Nürnberg, 2017); it might require multiple treatments of LMB to improve the water quality of eutrophic lakes (Meis et al., 2013; Nürnberg, 2017).

Lanthanum-modified bentonite clay has been applied to various lakes within Canada as remediation efforts to reduce algal blooms (Moos et al., 2014; Nürnberg, 2017). Despite increasing La concentrations within lakes to reduce eutrophication, there is an incomplete understanding of the impacts REE-based coagulants pose on freshwater systems. Post-application studies of LMB reported reduced photosynthesis (Van Oosterhout and Lürling, 2013) and inhibited fish growth due to a lack of available food (Han et al., 2021). Further, La concentrations within sediment and macrophytes reached 500 to 1000 folds higher than pre-exposure concentrations, respectively (Van Oosterhout et al., 2020). The effects of LMB on crayfish in a laboratory exposure setting found no short-term toxicity since crayfish can effectively eliminate REEs from their body by depuration processes (Fasola, 2010; Goitom, 2011). High La concentrations in biota reflect bioaccumulation and enrichment processes, which can induce transfer of La throughout the food web. The fate (Amyot et al., 2017; Arienzo et al., 2022; Santos et al., 2023), distribution (Lachaux et al., 2023; Moermond et al., 2001), and bioaccumulation potential of REEs in natural freshwater (Cardon et al., 2020; Goitom, 2011; Nørregaard et al., 2019) and oceanic food webs (Cardon et al., 2020; Marginson et al., 2023; Rétif et al.,

2024; Santos et al., 2023) have been extensively studied, highlighting the progressive enrichment of REEs within aquatic systems due to various sources, such as extraction and anthropogenic uses in industry (magnets, catalytic converters, lasers, batteries) (Adeel et al., 2019; Drobniak and Mastalerz, 2022; Jowitt et al., 2018; Long et al., 2010; Migaszewski and Gałuszka, 2015), agriculture such as REE-enriched fertilizers (Dang et al., 2024; Tommasi et al., 2023; Zhang and Shan, 2001) or medical sectors such as contrast agent for MRI (Damme et al., 2020; Rogosnitzky and Branch, 2016). However, few studies investigate aquatic ecosystems amended with REE-based remediation coagulants (Epe et al., 2017; Lürling and Van Oosterhout, 2013; Nürnberg, 2017; Nürnberg and LaZerte, 2016).

This study investigated the fate and REE concentrations in abiotic and biotic components in Swan Lake (Ontario), a highly eutrophic urban pond that received LMB treatments (Phoslock) in 2013, and a reference site (Toogood Pond, Ontario). The treatment of LMB improved water quality for two years, while hyper-eutrphic conditions reappeared in 2016 (Gertrud Nürnberg and LaZerte, 2020). This study aims to determine the distribution and enrichment potential of REEs within abiotic and biotic compartments throughout these ecosystems. Firstly, the abundance and distribution of REEs in the sediment and water (dissolved, colloids, and acid-leachable particulate fractions) were assessed. The distribution and fates of La in abiotic and biotic compartments were compared to praseodymium (Pr), the background representative of LREEs. Organotropism of REEs in the brain, gills, internal organs, and soft tissues of fathead minnows (*Pimephales promelas*), english brown bullhead fish (*Ameiurus nebulosus*), and round goby (*Neogobius melanostomus*) were also determined. Elemental concentrations

in vertebrates were compared to plankton and invertebrates to determine the potential for trophic transfer of REEs up the aquatic food web. Lanthanum anomalies for biotic and abiotic compartments were calculated to assess the potential enrichment of La throughout the ecosystems. It was hypothesized that particulate La from the sediment has the potential to transfer to benthic organism and disperse into the water column while the dispersion of La in the water increases exposure to pelagic organisms.

3.3 Methods

3.3.1 Treatment and reference sites

Environmental samples were collected in June and July of 2021 at Swan Lake (43° 54' N, 79°15' W) and Toogood Pond (3°52'N, 79° 19'W) within the City of Markham (Ontario). A detailed description of the lake, its water chemistry and P budget is provided in **A2 supplementary text 1**. Swan Lake was the first lake in Ontario treated with LMB in 2013 to address its hyper-eutrophic classification. The reference site Toogood Pond was also selected as a small urban pond in a municipal park-like area, with a wetland extending upstream in the northeast position (Prior et al., 2013) and a depth ranging from 0.3 to1.5 m.

3.3.2 Sample collection and treatment

Water samples were collected at ten locations in Swan Lake in July 2021, and at four locations in Toogood Pond in July 2021 (**Figure 3.1**)**.** Water samples were collected at three depths in Swan Lake using a Van Dorn sampler: surface water (S, 0.03m below the surface), intermediate water (I, 0.4 to 1.2 m, average of 0.7 ± 0.1 m), and deep waters (D, from 0.7 to 2.4 m, average of 1.4 ± 0.2 m). Water sampling depths in Toogood Pond were: surface water (S, 0.03m), intermediate water (I, 0.2 to 0.4 m, average of 0.31 ± 0.04

m), and deep waters (D, 0.38 to 0.79 m, average of 0.61 ± 0.08 m). The Van Dorn sampler was deployed off the side of the boat and conditioned by rinsing three times with lake water before lowered to discrete depths. Samples for surface water were first collected before intermediate waters. Within Swan Lake, deep-water samples were collected 30 cm above the lake bottom and within Toogood Pond, deep-water samples were collected 20 cm above the lake bottom to prevent the resuspension of particles. Water samples were transferred into pre-cleaned and pre-conditioned Low-Density Polyethylene bottles (LDPE); the bottles were cleaned with 10% v/v trace metal grade HNO_3 (BDH Aristar Plus), rinsed three times with high-purity water (18.2 MΩ cm), and three times with the sampled water before final refill, minimizing headspace. Water samples were stored in a cooler during transport to the laboratory (~2h) where aliquots (50 mL) of water samples were vacuum filtered through 1.2 µm and 0.2 µm hydrophilic membrane filter discs (polycarbonate, Millipore^{TM}) mounted on a 250 mL filtration holder (polycarbonate, Sartorius). The membrane filter discs and filtration holder were previously cleaned with a 1.5M HNO_3 acid solution, rinsed three times with high-purity water, and then conditioned with the filtered water sample. Unfiltered and filtered water samples were acidified with double-distilled trace metal grade HNO_3 (BDH Aristar Plus) to 0.2% v/v.

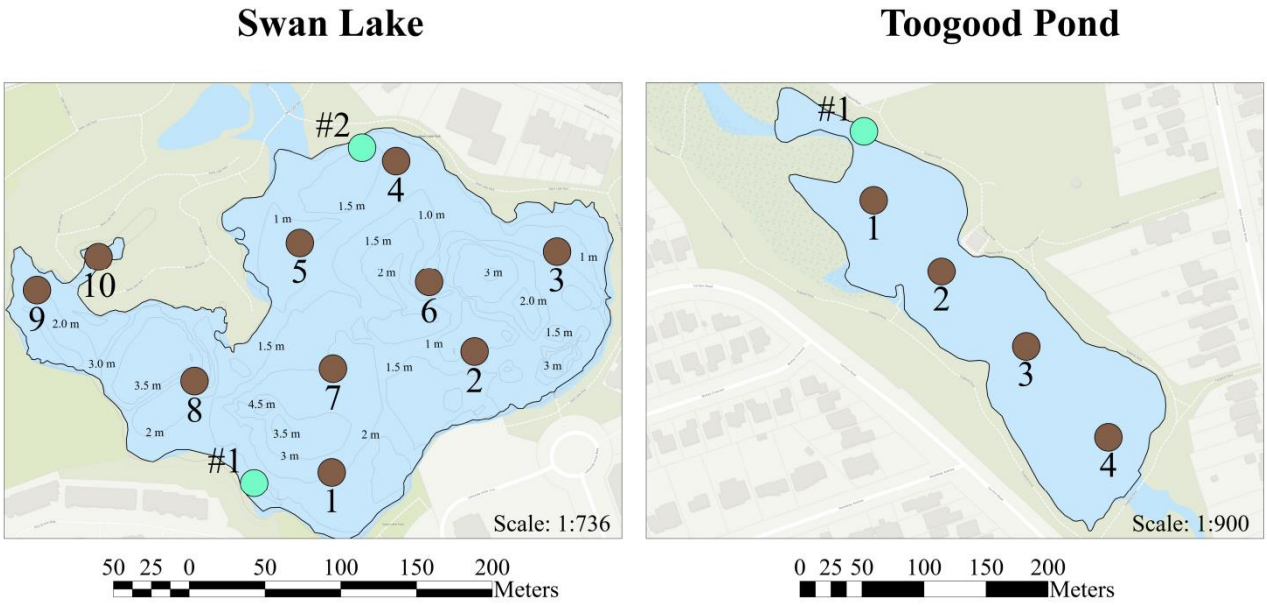

Figure 3.1 Sampling sites in Swan Lake (left) and Toogood Pond (right) in the City of Markham (Ontario). Light green circles represent sampling locations for fathead minnows within Swan Lake and for gobies within Toogood Pond. Brown circles represent sampling locations for water and sediment samples.

The concentrations of the elements measured in water filtered through 0.2 µm ($C_{<0.2\ \mu m}$), 1.2µm ($C_{<1.2\ \mu m}$), and unfiltered water ($C_{unfiltered}$) are used to determine the dissolved, colloidal, and acid-leachable (AL) particulate fractions (Equations 1-3). It is important to note that this categorization of the "dissolved", "colloidal", or "AL particulate" fractions is operationally defined for our conditions.

$$Dissolved\ fraction = [C_{<0.2\ \mu m}] \quad (Equation\ 1)$$

$$Colloidal\ fraction = [C_{<1.2\ \mu m}] - [C_{<0.2\ \mu m}] \quad (Equation\ 2)$$

$$AL\ Particulate\ fraction = \left[C_{unfiltered}\right] - [C_{<1.2\ \mu m}] \quad (Equation\ 3)$$

Sediment samples were collected from Swan Lake in June 2021, and Toogood Pond in July 2021 (**Figure 3.1**). Superficial (top 5 cm) lake sediment samples were collected using a gravity core sampler. Sediment aliquots were placed in clean, pre-weighed 50 mL Falcon tubes. The samples were immediately frozen at -20°C and freeze-dried (Labconco). Dried sediments were weighed and stored at room temperature for further processing.

Field sampling for biological samples took place from June to August 2021. Three bullheads (*Ameiurus melas*) were collected using bait-angling methods at treatment and reference sites. Fathead minnows (*Pimephales promelas*) were collected at the southeast and northwest sites of Swan Lake **(Figure 3.1**), and two round gobies (*Neogobius melanastomus*) at the northwest position of Toogood Pond **(Figure 3.1**), through minnow trapping methods. All vertebrates were euthanized humanely according to the Animal Use Protocol #26697 approved by the Trent University Animal Care Committee (ACC).

Vertebrates were euthanized following the protocol “Use of MS-222”. Vertebrates were weighed and measured for their fork length, then rinsed twice with high-purity water and 1mM of ethylenediaminetetraacetic acid (EDTA) solution to remove REEs adsorbed on the organisms’ body surfaces (Cardon et al., 2020). Fish were dissected using a surgical razor blade, and individual tissues were placed in falcon tubes to obtain the wet weight of gills, intestine, liver, muscle soft tissues, and brain. Due to their low weight, the five different tissues from 30 minnows were pooled into six composite samples (n=30). Tissues from each bullhead (n=12) and goby (n=6) were treated individually as discrete samples.

Plankton were collected towing an 80-µm phytoplankton net, 10-20 feet behind the boat. Plankton samples were transferred to the laboratory in 50 mL Falcon tubes. Plankton samples were then centrifuged at 4500 rpm for ten minutes. The pellets were separated from supernatant water and washed with high-purity water and 1mM of EDTA. Aquatic plants (macrophytes) were randomly collected along the shore. Species were identified and placed in plastic bags for transfer. Once in the laboratory, samples were rinsed three times with high-purity water and 1mM of EDTA. The wet weight was obtained for all plankton and macrophytes samples.

Invertebrates were collected at both sites through random sampling along the shorelines. Kick and sweep methods were used for 40 seconds to dislodge substrate and invertebrates into close-by D-nets. Bloodworms (*Chironomus plumosus*) were collected from Swan Lake. A trowel was used to dig up soil along the shorelines to extract earthworms (*Lumbricus terrestris*) and pillbugs (*Armadillidium vulgaris*). Invertebrates were rinsed with high-purity water, and 1mM of EDTA, and then wet weights were

recorded. After the dissection of all organisms, biological samples were frozen at -20°C and further freeze-dried (Labconco).

3.3.3 Sediment and biological sample preparation

Dried sediment samples were sieved to <2 mm; approximately 5 g of sieved sediment was used to determine sediment organic matter (SOM) and inorganic carbon (IC) by the loss of ignition (LOI) method at 550°C and 950°C (Heiri et al., 2001; Jensen et al., 2018). Another aliquot (5-10 g) of sieved sediment was pulverized using a planetary ball mill (PM 100, Retsch) at 500 rpm for 3 minutes with 30-second intervals, following the grinding procedures from Dang et al., (2024). Aliquots of 100 mg of pulverized sediments were digested using a microwave digestion lab station (Ethos Pro, Milestone) in *aqua regia* made from double-distilled trace-metal grade HNO_3 and HCl in a 1/3 v/v ratio. Blanks and certified reference material (CRM) MESS-4 from the National Research Council of Canada were included in each digestion batch; more details were previously provided (Dang et al., 2024). The acid mixture was briefly brought up to 200°C over 15 min, held at 200°C for 25 min, and cooled down over the following 25 min.

Between 11 mg to 7 g of freeze-dried biota samples were digested using double-distilled trace-metal grade HNO_3 (15.6 M) and H_2O_2 (9.8 M) in a 1/0.2 v/v ratio following the method described in previous studies (Dang et al., 2023). Briefly, samples were left to digest overnight in the fume hood at 100°C until a clear solution was obtained. Digestion blanks and two biological Standard Reference Materials (SRMs) NIST - 1566a Oyster Tissue and NIST - 1515 Apple Leaves underwent the same digestion procedure and analysis. Both SRMs contain information mass fraction values of

REE concentrations (Ma et al., 2019). Details on the recovery of biological standard reference materials are provided in **Table A2.1**.

3.3.4 Chemical analysis

Elemental analysis was completed using Triple Quadrupole Inductively Coupled Plasma Mass Spectrometry (8800 Agilent Technologies) at the Trent University Water Quality Centre. The workflow to analyze elements under three gas modes was described in previous studies (Dang et al., 2023, 2022a). Trace elements such as Ag, Cd, Co, Cs, Cu, Mo, Ni, Pb, Sn, Th, U, and V were analyzed in helium collision mode to remove polyatomic interferences. The lanthanides and Y were analyzed in an MS/MS mode with O_2 as the reaction cell gas (Dang et al., 2018). Indium (In) was added to all samples at a final concentration of 10 μg L^{-1} as an internal standard. The analytical procedure was verified using SRM NIST 1640a (Trace Elements in Natural Water) and river water CRM SLRS-6 (National Research Council of Canada). Two blanks and one water CRM were used to bracket every ten samples. The measured concentrations are compared against certified concentrations or compiled values (Yeghicheyan et al., 2019) of liquid and solid CRMs (**Table A2.1**, **A2.2**, and **A2.3**).

Sediment samples were also analyzed using EDXRF to quantify major constituents (Al_2O_3, CaO, Fe_2O_3 ,K_2O, MgO, MnO, Na_2O, P_2O_5, SiO_2, TiO_2,) and other elements such as As, Br, Cl, Cu, Mo, Nb, Rb, S, Sr, Zn, and Zr; some of these elements are either refractory to the *aqua regia* digestion method or difficult for ICP-MS analyses. A 2 g aliquot of pulverized sediment was mixed with a binding agent (X-ray Mix ®, SCP Science) at a 2/1 (w/w) ratio. The mixture was homogenized using a vortex for 5 minutes and pressed under 11 tons using a Carver hydraulic press and a die set (32 mm,

Chemplex). The pellets were analyzed by EDXRF (Quant'X, Thermo-Scientific) at the EnIGMA Lab (Trent University). A calibration curve was made using five soil and sediment CRMs: Till-2 and Till-3 from Natural Resources Canada and HISS-1, PACS-3, and MESS-4 from the National Research Council of Canada (NRCC). A copper standard was used to perform daily energy adjustments, and instrumental drifts were monitored using the CRM TILL-2 (**Table S4**).

3.3.5 Data analysis

3.3.5.1 REE patterns, normalization, and calculation of anomalies

To correct the Oddo-Harkins effects in REE natural abundances (Ramos et al., 2016), REE concentrations were normalized against Post-Archean Australian Shale (PAAS) (McLennan, 2001). The PAAS-normalized concentrations are hereafter referred to as REE_{PAAS}. This normalization allowed for the transformation of zigzag to smooth-like patterns that assist with interpretation (Bau et al., 2018) and assessing the presence of positive or negative REE anomalies (Pourret et al., 2022; Pourret and Tuduri, 2017). This normalization allows for the calculation of REE anomalies denoted as REE/REE* to characterize the behaviour of an REE of interest relative to its neighbouring REEs (Dang et al., 2022b). Lanthanum anomalies were calculated relative to Pr and Nd (Eq. 4).

$$\frac{La}{La^*} = \frac{La_{PAAS}}{\frac{(Pr_{PAAS})^3}{(Nd_{PAAS})^2}} \quad (Equation\ 4)$$

3.3.5.2 Contamination factor

The contamination factor (C_f) is used to quantify the contamination of an element in the sediment based on its concentrations relative to a background concentration (Haris et al., 2017). The C_f is calculated as follows:

$$C_f = \frac{C_{sample}}{C_{background}} \quad (Equation\ 5)$$

C_{sample} refers to the concentrations in the sediments of Swan Lake and $C_{background}$ is taken from the reference site Toogood Pond. Contamination factors lower than 1 indicate no contamination and can be compared to threshold values of 3 and 6 to determine low, moderate and high contamination (Bentum et al., 2011).

3.3.5.3 Element enrichment factor (E_f)

Enrichment factors are used as indices to evaluate the enrichment level of an element and identify the potential anthropogenic or natural influences (Godwyn-Paulson et al., 2022; Xu et al., 2022; Zhang et al., 2007). Enrichment factors allow geochemical normalization of concentration data by a conservative element (C_{ref}) such as Al or Ti to identify anomaly concentrations (Zhang et al., 2007).

$$E_f = \frac{\left(\frac{C_i}{C_{ref}}\right)_{samples}}{\left(\frac{C_i}{C_{ref}}\right)_{background}} \quad (Equation\ 6)$$

Where C_i is the content of the element of interest in Swan Lake sediments or Toogood Pond sediments as the background. C_{ref} represents reference elements (Al and Ti) in Swan Lake samples and the selected Toogood Pond background samples (Qingjie et al., 2008). An E_f value between 0.5 and 1.5 suggests that the trace metals may be entirely from crustal materials or natural weathering processes (Zhang and Liu, 2002). An E_f value > 1.5 suggests that trace metals are delivered from other point and non-point sources (Cao et al., 2018; Zhang and Liu, 2002).

3.3.5.4 Statistics analysis and data processing

Non parametric Friedman's test for dependent samples followed by Conover post-hoc test for pairwise comparison of REE concentrations within acid-leachable particulate water, colloidal water, and dissolved water between surface, intermediate, and deep-water samples using Excel (Ma et al., 2019). If the Friedman test reported a P value < 0.05, the null (H_o) hypothesis that there is no difference among REE level group means within AL particulate water, colloidal water, and dissolved water between surface, intermediate, and deep-water levels, was rejected. T-tests of two samples assuming unequal variances were conducted in Excel to determine if significant differences (p-value = 0.05) occurred between C_f and E_f for La and Pr, as well as to determine significant differences (p-value = 0.05) between elemental concentrations between Swan Lake and Toogood Pond sediment. Outlier tests such as box plots identify extreme values of REEs within samples (Walfish, 2006). Then, an extreme studentized deviation test determined if outliers can be removed from the observational data (Walfish, 2006). Concentration maps are created using ArcGIS Pro. Spatial interpolation of elements in Swan Lake was completed using ArcGIS Pro spline 3D analyst tool, and Toogood Pond interpolation was completed with inverse distance weighted analyst tool. Simple linear regression was conducted in Sigmaplot 15.0 to obtain the square of correction (R^2) and determine the relationship, correlation, and the association of La or Pr concentrations to the concentrations of Al, Ca, P, inorganic matter, and organic matter, in Swan Lake and Toogood Pond sediment.

3.4 Results & discussion

3.4.1 Major elements in the sediments of Swan Lake and Toogood Pond

The chemical composition in the sediments of Swan Lake and Toogood Pond reflects a mixture of SiO_2 (36.9 ± 1.2 % to 41.0 ± 1.9 %), CaO (19.7 ± 1.6 % to 21.0 ± 0.9%), Al_2O_3 (8.7 ± 0.3 % to 8.8 ± 0.3%), and Fe_2O_3 (3.4 ± 0.2 % to 4.1 ± 0.1%) (**Table 3.1**). This reflects the local lithology of the region, as discussed in **A2 supplementary text 2**. Besides, the sediments of Swan Lake contain 4.3 to 17.8% of organic matter and 3.6 to 12.9% of inorganic carbon and the sediments of Toogood Pond contain 6.5 to 8.7% of organic matter and 9.6 to 17.3% of inorganic carbon (**Table A2.5**). The organic matter content in Swan Lake sediment is a magnitude higher than the organic matter content in Toogood Pond sediment due to the continuous addition of detritus algae from algal blooms from historical eutrphic and hypereutrophic conditions in Swan Lake (Muir and Parhizgari, 2021).

Table 3.1 The average (AVG) and standard error (SE) of elemental percent composition (%) and concentrations (mg kg^{-1}) of sediment from Toogood Pond (N=4) and Swan Lake (N=10). An unpaired t-test was performed (p-value = 0.05) to determine significant differences between elemental composition within the sediment of reference vs. treatment sites. Values have been rounded to the most appropriate significant figures.

Analysis	Chemical composition	Units	Location				Unpaired t-test
			Toogood Pond		Swan Lake		
			AVG	SE	AVG	SE	P-value (0.05)
Depth		m	0.7	0.2	1.8	0.6	
Total analysis - EDXRF	Na_2O	%	0.7	0.1	1.3	0.1	0.001*
	MgO	%	1.8	0.1	1.8	0.04	0.4
	Al_2O_3	%	8.8	0.3	8.7	0.3	0.8
	SiO_2	%	41.0	1.9	36.9	1.2	0.1
	P_2O_5	mg kg^{-1}	0.18	0.01	0.29	0.01	0.0003**
	S	mg kg^{-1}	2600	150	5600	300	0.0001**
	Cl	mg kg^{-1}	520	32	6400	340	0.0001**
	K_2O	%	1.6	0.1	1.7	0.1	0.3
	CaO	%	21.0	0.9	20.0	1.6	0.7
	TiO_2	mg kg^{-1}	0.53	0.04	0.56	0.02	0.6
	Cr_2O_3	%	65	6	120	28	0.002*
	MnO	mg kg^{-1}	780	38	720	24	0.3
	Fe_2O_3	%	3.4	0.2	4.1	0.1	0.006*
	As	mg kg^{-1}	8.1	0.1	9.5	0.2	0.003*
	Br	mg kg^{-1}	10.7	0.5	16.3	0.7	0.0008**
	Cu	mg kg^{-1}	22.7	1.4	33.7	1.7	0.004*
	Nb	mg kg^{-1}	6.9	0.8	8.2	0.5	0.2
	Rb	mg kg^{-1}	57.0	1.8	70.0	2.0	0.002*
	Sr	mg kg^{-1}	370	28	430	39	0.4
	Zn	mg kg^{-1}	110.0	1.6	120.0	5.6	0.1
	Zr	mg kg^{-1}	220	30	280	12	0.07

3.4.2 Concentration and distribution of REEs in the sediment

In Swan Lake, the concentrations of Pr, considered as the background REE, were in a similar range (3.6 to 8.5 mg kg $^{-1}$) as upper continental crust levels (UCC: 7.1 mg kg $^{-1}$, (McLennan, 2001)) and Toogood Pond (4.4 to 5.5 mg kg^{-1}) (**Figure 3.2B & D**). However, La concentrations in Swan Lake sediments ranged from 169 mg kg^{-1} to 1,497 mg kg^{-1} (**Figure 3.2A**), which is 6 to 48 times higher than the UCC La levels (31 mg kg^{-1}) (McLennan, 2001) and reference site Toogood Pond (17.7 to 23.4 mg kg $^{-1}$) (**Figure 3.2C**). This La enrichment is reflected in the REE patterns (**Figure A2.1G**) with an average La/La* of 22.5 ± 3.0 (**Table A2.6**), while the PAAS-normalized patterns for Ce to Lu in Swan Lake sediment align well with that of Toogood Pond sediment. The latter confirms similar REE background levels between the two sites.

Lanthanum concentrations in Swan Lake sediments were slightly lower than other sites that received LMB treatment, e.g., Lake Rauwbraken (Netherlands) and Lake Lock Flemington (UK). In Lake Rauwbraken (Van Oosterhout et al., 2020), the La levels in surface sediments (0-2 cm) before the treatment was 0.5 mg kg^{-1} but increased to 6,702 mg kg^{-1} post-treatment, while [La] in deeper sediments (below 10 cm) remain close to 7 mg kg^{-1} (Van Oosterhout et al., 2020). Similarly, Lake Lock Flemington has pre-application La levels of 17.4 to 29.9 mg kg^{-1} in surface sediments (0 to 2 cm) and 19.5 to 20.9 mg kg^{-1} at deeper sediment layers (8 to 10 cm) (Meis et al., 2013). After the treatment, La concentrations in the surface sediment increased to 2,400-3,500 mg kg^{-1} (Meis et al., 2013).

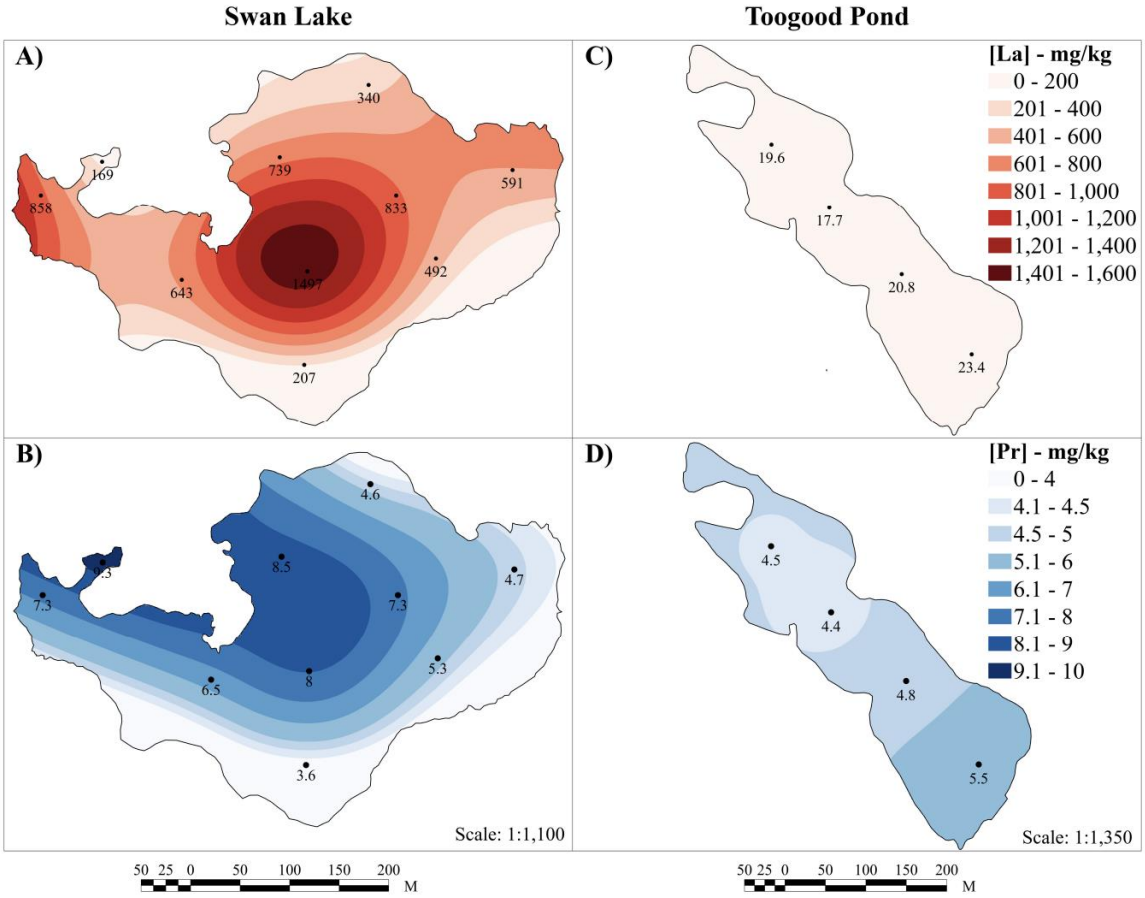

Figure 3.2 Spatial distribution and concentrations of La (mg kg^{-1}, upper panels) and Pr (mg kg^{-1}, lower panels) in the sediments of Swan Lake (**A & B**) and Toogood Pond (**C & D**). Spatial interpolation of REEs in Swan Lake was completed using ArcGIS spline 3D analyst tool and Toogood Pond interpolation with inverse distance weighted analyst tool.

The La concentrations reported in this study for sediments collected in 2021 were compared to those collected in June 2014, 1-year post-application of LMB in Swan Lake (Nürnberg and LaZerte, 2016). The range of La concentrations in the surface sediment in 2014 (0 to 10 cm, 93 to 300 mg kg^{-1}) is smaller compared to our study in 2021 (0 to 5 cm, 169 mg kg^{-1} to 1,497 mg kg^{-1}), but the spatial distribution of La within the lake can be reproduced; the highest La enrichment (Nürnberg and LaZerte, 2016) is observed at the deepest areas of Swan Lake (at 3.5 to 4.5 m, **Figure 1** (Nürnberg and LaZerte, 2016)) (**Figure 3.2**). Such enrichment of trace elements in the bottom and deep-water area of lakes has been well characterized and associated with the deposition of fine-grained particles as the results of wind-induced wave energy affect lake bottom dynamics and sediment characteristics (Hakanson, 1977). This phenomenon is commonly referred to as sediment focusing (Blais and Kalff, 1995; Edgington and Robbins, 1990; Hilton, 1985). Rare earth elements are also well known to have a high affinity to bind to the fine grain-size fraction (Herrmann et al., 2016; Zhang et al., 1998). The fact that La was directly associated with the bentonite as fine clay particles of the LMB and the correlations between La and other trace elements (Cr and Mo, **Figure A2.2B & C**) would further confirm that the enrichment of this elements at site 7 (**Figure 3.1**) is directly related to natural processes of fine particle movement and accumulation.

The accumulation of REEs in lake sediments can also be associated with removal processes from the water column by sorption and/or co-precipitation with suspended colloid particles in alkaline lakes (Jiang et al., 2022). Three main mechanisms for REE scavenging from the water column into the sediment have been reported: sorption or co-precipitation with calcium carbonate, organic matter, or reactive soluble P. First, ionic

REEs could rapidly settle in sediment beds of lakes of moderate to high alkalinity (> 40 mg L^{-1} $CaCO_3$) (Spears et al., 2013), as REEs can sorb onto calcium carbonate minerals and create insoluble REE-carbonates (Gabitov et al., 2017; Lakshtanov and Stipp, 2004). Given the high alkalinity of Swan Lake (118 mg L^{-1} as $CaCO_3$, (Nürnberg, 2017)), such mechanisms might appear to be possible (Spears et al., 2013). Nevertheless, a negative correlation was observed between the background REEs (Pr) vs. Ca concentrations (**Figure 3.3D**) and Pr vs. inorganic carbon (IC) (**Figure A2.3C**) in the sediment of both treatment and reference sites. The southern area of Swan Lake has relatively high Ca concentrations (**Figure A2.4A**), but little enrichment of REEs (**Figure 3.2**), which suggests that Ca-based minerals is not the main carrier phase for REEs in Swan Lake sediments.

Furthermore, REEs also have a high affinity to form complexes with organic matter fractions within the sediment (Chakraborty et al., 2011; Pourret et al., 2007b). The positive correlation (R^2 = 0.7) between Pr concentrations and organic matter (**Figure 3.3F**) points toward the formation of such complexes. There is also a weak positive correlation (R^2 = 0.39) between Pr and Al, indicating some interactions with clay materials of the sediment (**Figure A2.3D**). These positive correlations highlight the possible carrier phases and concentrations of background REEs in the sediment that are driven by natural complexation and sorption processes. However, there was no correlation between La and organic matter (**Figure 3.3C**) but rather a moderate correlation with P (R^2 = 0.49, **Figure 3.3B**), which was similarly reported in the sediments of Bow Lake in Ontario (Dang et al., 2021) and river sediment in Mongolia (Munemoto et al., 2020). Such behaviour can be related to the precipitation of dissolved

phosphate into lanthanum phosphate (Du et al., 2019; Liu and Byrne, 1997) or the sequestration in authigenic phosphate minerals (Auer et al., 2017).

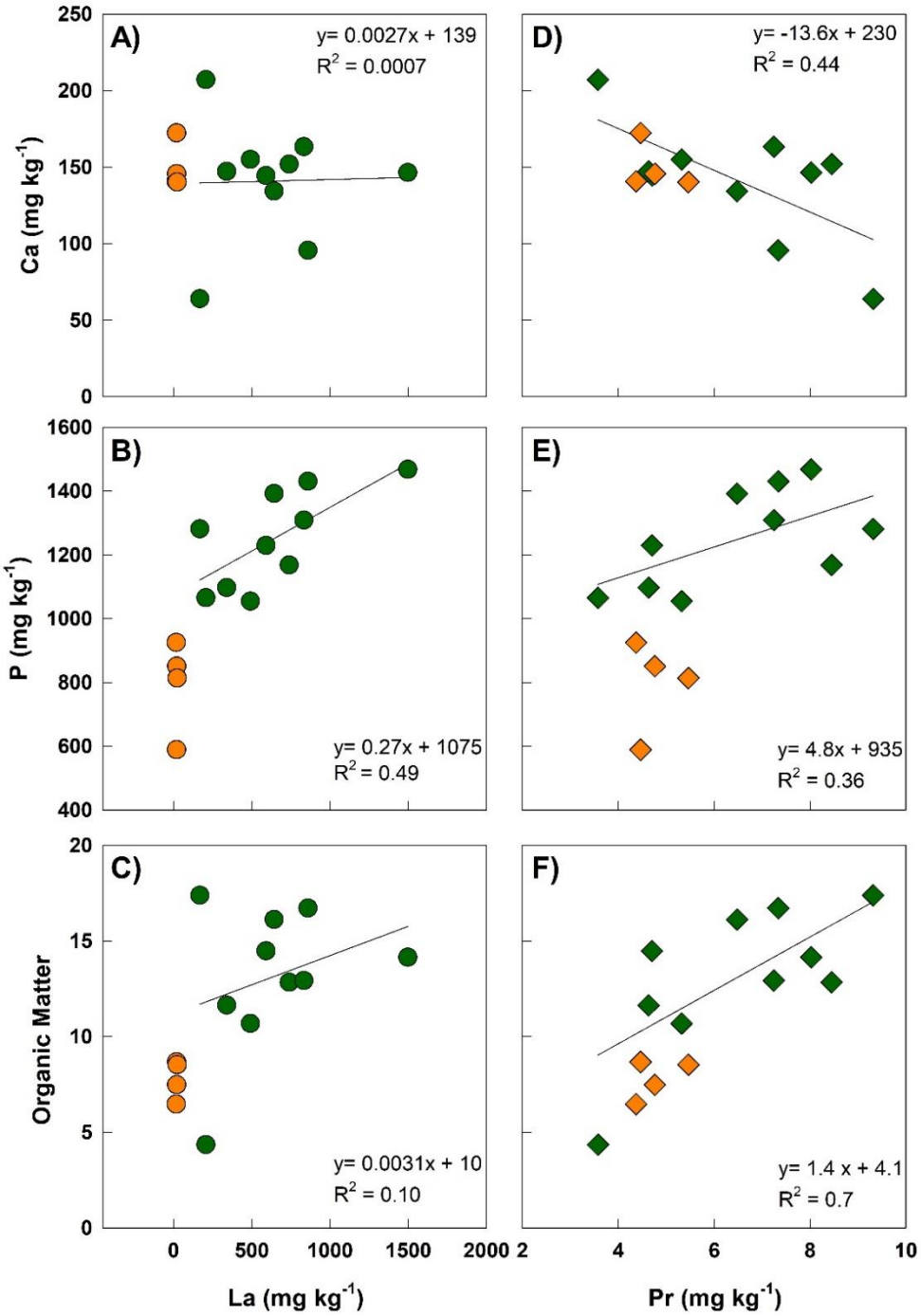

Figure 3.3 Biplots showing the relationship between the concentrations of La (A-C) and Pr (D-F) vs. Ca, P and organic matter in the sediments of both Toogood Pond (orange symbols) and Swan Lake (green symbols).

3.4.3 Sediment Risk Assessment

The concentrations of major and some trace elements (Al, Ca, K, Mg, Mn, Nb, Si, Sr, Ti, Zn, and Zr) within Swan Lake sediment are not significantly different from levels in Toogood Pond sediment (**Table 3.1, Table A2.7, Figure A2.5A & D**). However, the concentrations of P and S are two times higher in Swan Lake than in Toogood and Cl levels are 12 times higher in Swan Lake (**Table 3.1, Table A2.7, Figure A2.4B & D**). Similarly, the levels of As, Br, Cu, Fe, and Rb are all statistically higher in Swan Lake than in Toogood Pond (**Table 3.1**, **Table A2.7**, **Figure A2.5B & E**). Contamination factors for most of the major, minor and trace elements such as Ce to Lu, Ag, Al, As, Ca, Cd, Co, Cr, Fe, Mg, Mn, Na, Ni, P, Pb, S, Sn, Th, Ti, U, V, Y, and Zn (excluding La and Cl) in Swan Lake sediment were between 0.7 to 2.5 (**Table A2.8**), and enrichment factors normalized against conservative elements Al and Ti, were below 2.0 (**Table A2.9, A2.10, & A2.11**).

This assessment highlights limited contamination risks regarding these elements. Nevertheless, the enrichment factors for Cl were all above 1.5 (**Table A2.11).** Chloride concentrations within the Swan Lake water column were monitored in 2017 and 2018; the annual average levels were 500 mg L^{-1}, with spikes above 1,000 mg L^{-1} (Gertrud Nürnberg and LaZerte, 2020), exceeding the Canadian water quality guidelines of 120 mg L^{-1} (Sorichetti et al., 2022) and the Ontario provincial water quality aesthetic objective levels for chloride of 250 mg L^{-1} (Ontario Ministry of the Environment, 2003). This high contamination potential status of Cl in Swan Lake water and sediment compared to Toogood Pond suggests the contribution of urbanization development due to Cl usage in road salt for winter de-icing (Evans and Frick, 2001).

The C_f for La levels within Swan Lake sediments were between 8.3 to 40.9 (**Figure 3.4A, Table A2.8**), well above the threshold value of six for high contamination (Bentum et al., 2011), while C_f for Pr levels within Swan Lake sediment were between 1 to 3 (**Table A2.8**). Furthermore, the normalization against immobile elements (Al and Ti) in E_f calculations integrates better the lithogenic variability (Barbieri, 2016; Godwyn-Paulson et al., 2022; Liu et al., 2023). It is, however, important to note that Al can be used as a coagulant in water treatment and ecological restoration so the E_f calculation based on Al might be biased as the Al content is not strictly related to the lithogenic fractions but the anthropogenically amended Al from coagulants. However, there was no treatment with Al coagulant in Swan Lake before our sampling. Furthermore, similar La/Al vs. La/Ti and Pr/Al vs. Pr/Ti ratios (**Figure 3.4B**) would indicate a reliable normalization approach with both Al and Ti and that Al is still an appropriate tracer for fine and reactive particles for our dataset. The E_f values for La throughout Swan Lake are close to 80 and range between 0.6 to 2.0 for Pr (**Figure 3.4B**) and other REEs (**Table A2.9**). These calculations confirm natural levels for the background lanthanides, i.e., Ce to Lu, but significant La enrichment in the surface sediments of Swan Lake, which could indicate potential risks of dispersion in the water column, thus exposing the aquatic organisms to this element.

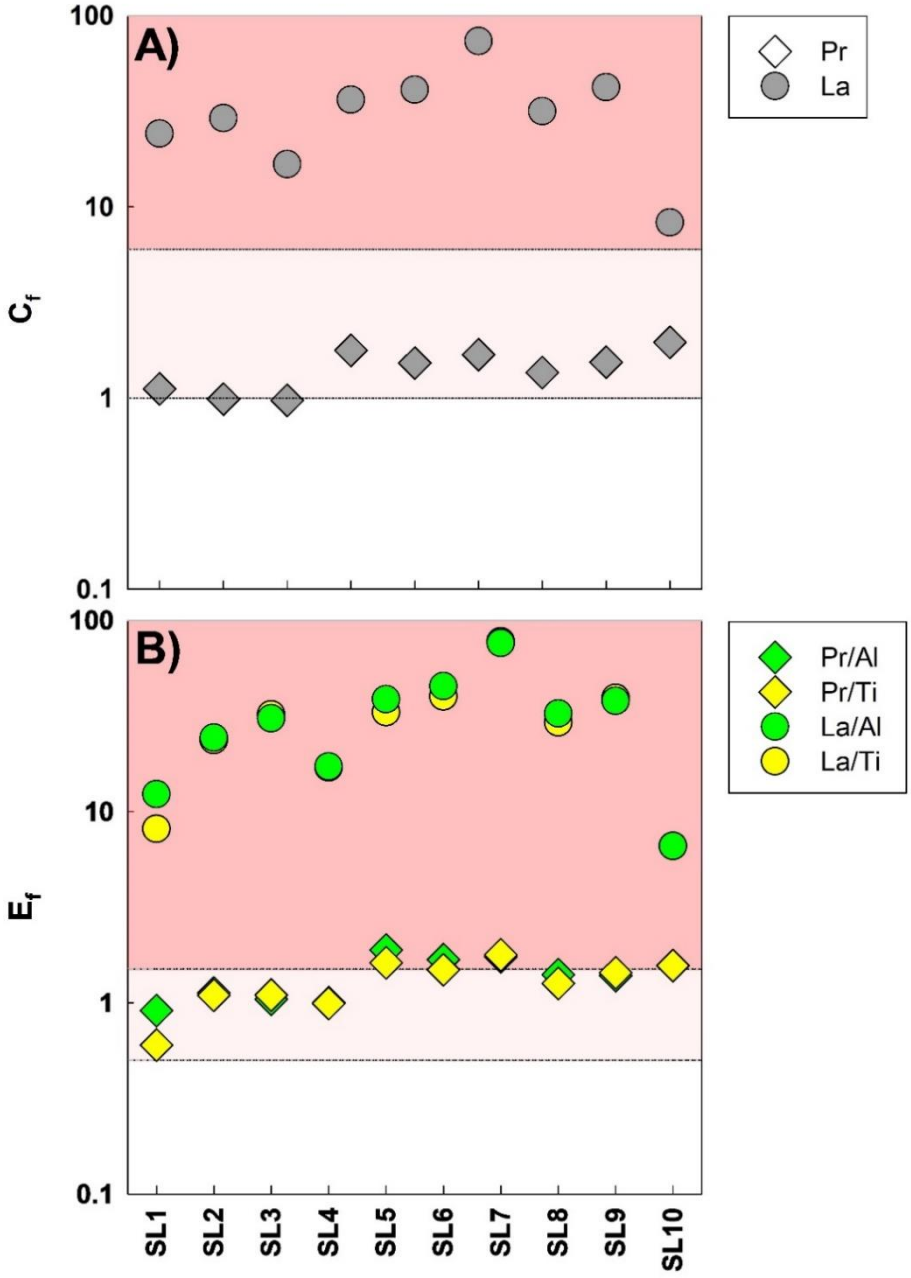

Figure 3.4 Contamination factor (C_f) and enrichment factor (E_f) of La (circles) and Pr (diamonds) within the sediment of Swan Lake, Canada. In (B), the normalization of REEs against both Al (green symbols) and Ti (yellow symbols) is shown.

3.4.4 REE concentrations in the water column

The distribution of REEs in the dissolved, colloidal, and acid-leachable (AL) particulate fractions in lake water points to a significant contribution of sedimentary particles in Swan Lake. The concentrations of La, Pr, and all other REEs in the AL particulate water of Swan Lake were significantly higher in the deep water than the surface and intermediate layers of all sampling sites (**Figure 3.5A & C, Table A2.12, Figure A2.6**). Close to the totality of these elements (La: 95.9 ± 2.5% and Pr: 92.2 ± 4.0%) was found in the AL particulate fraction in bottom water of Swan Lake close to the sediments (**Figure A2.7A & C**); La and Pr concentrations in the AL particulate fraction of bottom water ([La]: 59.5 ± 20.7 μg L^{-1}, [Pr]: 0.5 ± 0.2 μg L^{-1}) are 25 to 300 times higher than in the AL particulate fractions of surface waters ([La]: 0.15 ± 0.02 μg L^{-1}, [Pr]: 0.007 ± 0.001 μg L^{-1}) and intermediate waters ([La]: 1.7 ± 1.1 μg L^{-1}, [Pr]: 0.02 ± 0.01 μg L^{-1}) (**Figure 3.5A & C, Table A2.12**). The influence of acid-leachable particulate La can still be seen in the intermediate water of Swan Lake with 80.0% ± 3.2% of La, which decreases to 62.7% ± 2.78% of La in the surface water (**Figure A2.7A**). The La and Pr concentrations in the AL particulate fraction of deep waters of Toogood Pond are statistically different then levels in the surface and intermediate depths (**Figure 3.5 B & D**, **Table A2.13**). There were some larger variabilities in [La] and [Pr] in the AL particulate fractions of deep waters ([La]: 2.67 ± 0.96 μg L^{-1}, [Pr]: 0.5 ± 0.2 μg L^{-1}) compared to the concentrations in the particulate fractions of surface water ([La]: 0.65 ± 0.08 μg L^{-1}, [Pr]: 0.12 ± 0.02 μg L^{-1}, (**Figure 3.5B & D**). However, there is no significant difference for the percent composition of La and Pr in all three fractions between water depths within Toogood Pond (**Figure A2.7B & D, Table A2.13**).

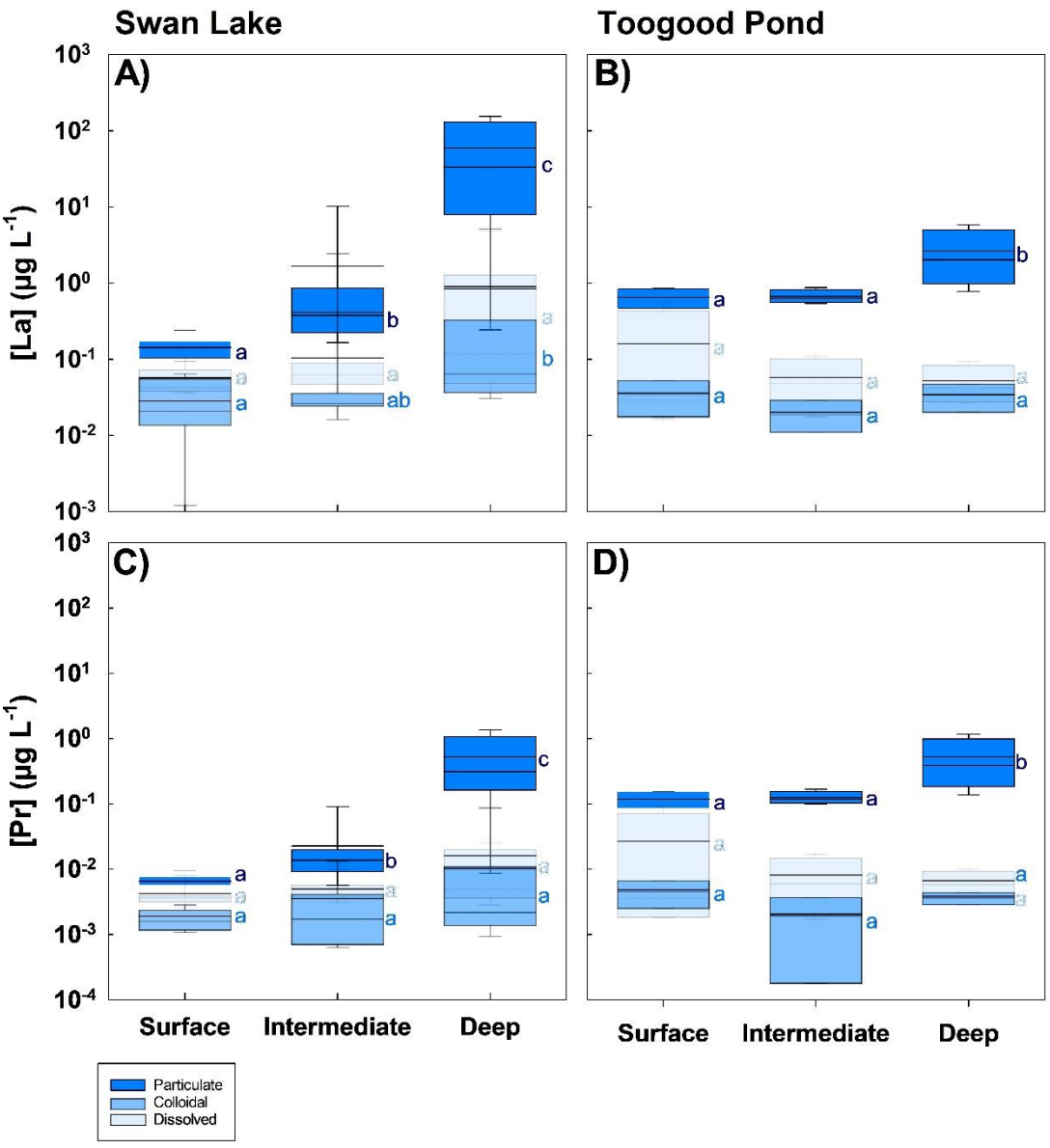

Figure 3.5 Boxplots of La and Pr concentrations (µg L^{-1}) in the acid-leachable particulate, colloidal, and dissolved fractions within surface, intermediate, and deep locations of Swan Lake (A & C, n=7 to 8) and Toogood Pond (B & D, n=2 to 4). The compact letter displays Conover post hoc results for pairwise comparison among particulate REE levels between surface, intermediate, and deep, colloidal REE levels between surface, intermediate, and deep, and comparison of dissolved REE levels within surface, intermediate, and deep.

The distribution of REEs in the acid-leachable particulate phases of Swan Lake deep water is also in general agreement with results from a case study analyzing 16 lakes ammended to LMB clay (Spears et al., 2013). Within these lakes, total unfiltered La concentrations one-month post-application ranged from 26 μg L^{-1} to 2,300 μg L^{-1} in the surface waters and 40 μg L^{-1} to 8,920 μg L^{-1} in deep waters (Spears et al., 2013). Lanthanum concentrations generally decrease with time as the LMB settle to the lake bottoms; six months post-application in Niedersachsen Lake, lower total unfiltered La concentrations were reported in surface waters (31 μg L^{-1}) and deep waters (68 μg L^{-1}) (Spears et al., 2013). The acid-leachable particulate La concentrations in surface water of Swan Lake in our study, eight years post application (0.15 ± 0.02 μg L^{-1}), are lower than surface [La] levels in Niedersachsen Lake (31 μg L^{-1}). But, AL particulate La concentrations in the deep waters of Swan Lake (59.5 ± 20.7 μg L^{-1}) are in similar ranges to total unfiltered La in the deep water of Niedersachsen Lake (68 μg L^{-1}) (Spears et al., 2013) (**Table A2.12**).

The La enrichment across environmental compartments of Swan Lake can also be presented by PAAS normalized patterns (**Figure A2.1H to J**). Lanthanum anomalies in Swan Lake sediment (22.5 ± 3.0) differ considerably from those of the reference sediment site which shows no La anomaly (1.00 ± 0.02) (**Table A2.14** and **A2.15, respectively**). The La anomalies calculation has a significant advantage compared to C_f and E_f as the latter are strictly relevant to the sediments while La/La* can be used to compare La enrichment between several environmental media, including the water. All Swan Lake water samples held high La anomalies that increased with water depth. For example, the variation ranges between different filtration cutoffs of La/La* increased

from the surface (5.5 ± 0.4 to 7.6 ± 1.0), intermediate (9.2 ± 1.1 to 9.9 ± 3.5), to deep (9.3 ± 1.5 to 19.9 ± 5.7) waters (**Table A2.14**). These La/La*values in Swan Lake water are 6 to 15 times higher than in Toogood Pond (1.4 ± 0.1 to 4.2 ± 1.1, **Table A2.15**). These results confirm the transfer of La from the sediment (La/La* of 22.5 ± 3.0) toward the water column of Swan Lake due to the resuspension of REE-enriched sediment through means of physically or biologically induced disturbances in shallow lakes (Lesven et al., 2009). Swan Lake is a polymictic lake (Bengtsson and Hellström, 1992; Nürnberg and LaZerte, 2016) thus the sediment at the bottom of the shallow water column (mean depth of 1.86 m) can readily be mixed thoroughly in the presence of wind (Bengtsson and Hellström, 1992), bioturbation (Chaffin and Kane, 2010), or inflows of water, which are all processes related to the disturbance of bed sediments.

3.4.5 REE concentrations in the aquatic organisms

Similarly to the water samples, all organisms in Swan Lake are enriched with La relative to neighbouring REEs (**Figure A2.1F**) as shown by the La anomalies (**Table A2.14**); La concentrations in all organisms from Swan Lake and Toogood Pond are indeed one to two magnitudes higher than those of Pr (**Figure 3.6**). There is also large variability within the organisms of Swan Lake with La concentrations ranging over six orders of magnitudes from 0.0009 ± 0.0002 mg kg^{-1} (soft tissue of bullhead) to 19.7 ± 4.9 mg kg^{-1} (intestine of minnow) (**Figure 3.6A**, **Table A2.16**). Benthic organisms (bloodworms, earthworms, common pillbug), plankton, and macrophytes showed the highest La and Pr concentrations in both lake systems (**Figure 3.6A & B**). This could be due to their direct accumulation of particulate La from sediments (Censi et al., 2004); note that the organisms have been rinsed with EDTA and, therefore, it is assumed the sorbed La on the surfaces have been removed.

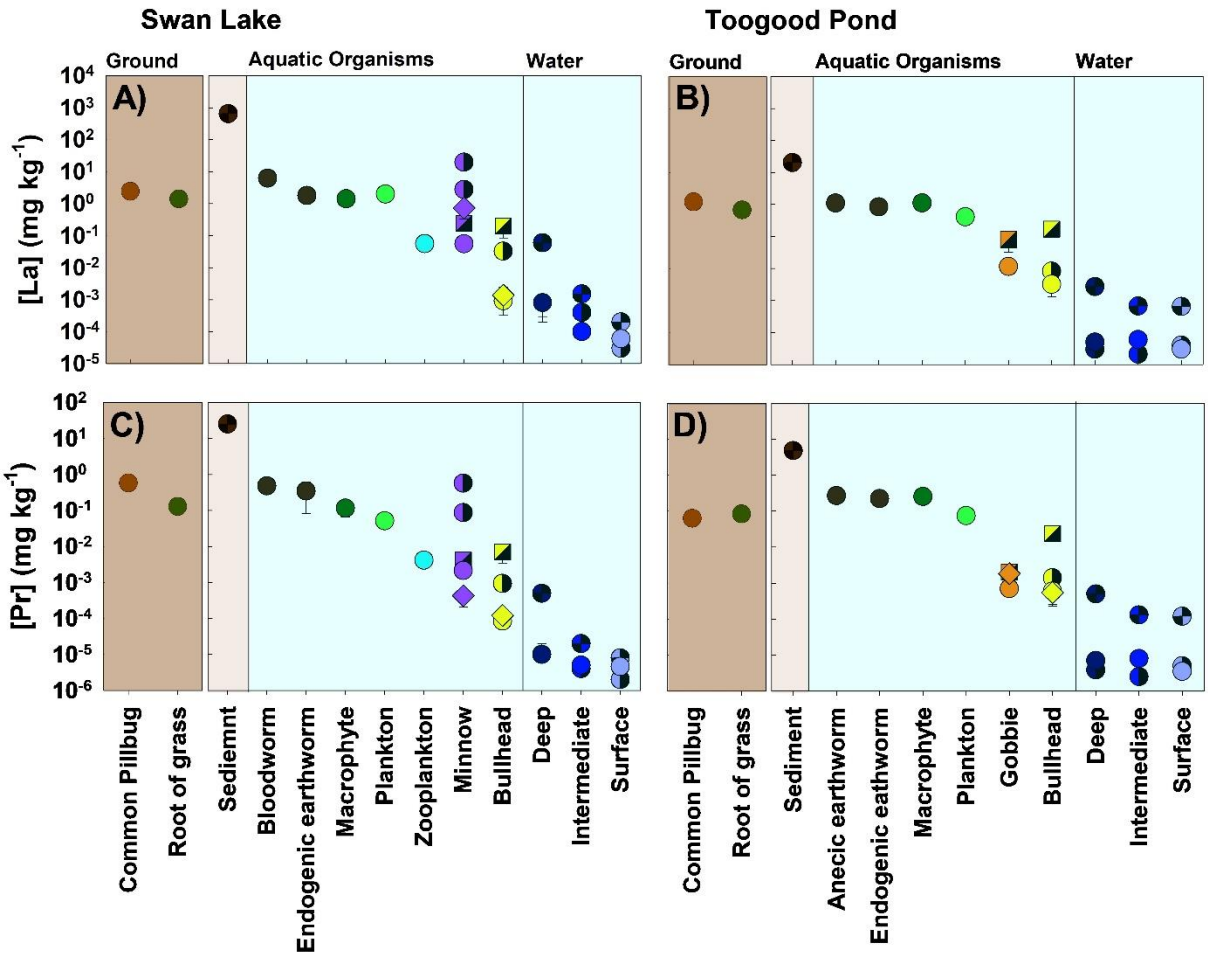

Figure 3.6 The concentrations of La and Pr in sediments, acid-leachable particulate (quartered circles), colloidal (half-filled circles), and dissolved (open circles) water fractions, and biological tissues collected from Swan Lake (A & C), and Toogood Pond (B & D). Tissue types are represented by various shapes: circles (soft tissue or whole body), squares (hard tissue), half-filled circles (intestines/internal organs), half-filled squares (gills), and diamonds (brain).

In Toogood Pond, La concentrations followed the decreasing order: common pillbug > earthworm > macrophyte > plankton > gobies > bullhead. The bio-dilution of REEs within Toogood Pond is reflected by the fact that macrophytes (1.1 ± 0.3mg kg^{-1}) and plankton (0.4 ± 0.2 mg kg^{-1}) contained La levels two magnitudes higher than the soft tissue of vertebrates such as gobies (0.012 ± 0.001 mg kg^{-1}) and bullhead (0.003 ± 0.002 mg kg^{-1}) (**Figure 3.6B**). This observation is similar to studies investigating the natural trophic transfer of REEs within natural temperate lakes and estuaries (Amyot et al., 2017; Rétif et al., 2024; Santos et al., 2023).

In Swan Lake, the minnows' intestines and internal organs are particularly enriched with La, with respective La concentrations of 19.7 ± 4.9 mg kg^{-1} and 2.8 ± 0.5 mg kg^{-1} **(Table A2.16)**. The benthic bloodworms collected from Swan Lake sediments held the second-highest La levels of 6.2 mg kg^{-1} (**Table A2.16**). Macrophytes and plankton from Swan Lake also have high concentrations of La (1.4 ± 0.4 mg kg^{-1} and 2.0 ± 0.5 mg kg^{-1}, respectively). The enrichment of La in plankton from Swan Lake is particularly intriguing as La levels in plankton (2.0 ± 0.5 mg kg^{-1}) are higher than benthic macrophytes (1.4 ± 0.4 mg kg^{-1}), earthworms from sediments (1.8 ± 0.2 mg kg^{-1}), and zooplankton (0.056 ± 0.009 mg kg^{-1}) (**Figure 3.6A**). In natural environments, the enrichment of La in phytoplankton is commonly observed, but the magnitude varies. For instance, La concentrations within phytoplankton collected from aquatic systems around the world range from 0.002 ± 0.001 mg kg^{-1} in the Mediterranean Sea (Strady et al., 2015), 0.01 ± 0.007 mg kg^{-1} in the Tyrrhenian Sea (del Buono et al., 2024), 4.3 mg kg^{-1} in the Ligurian Sea (Neira et al., 2022), 26.4 ± 4.8 mg kg^{-1} in the St. Lawrence Estuary (Dang et al., 2023) to 68.5 ± 1.3 mg kg^{-1} in the Subaé estuary (Santos et al., 2023).

The high enrichment of La in plankton and macrophytes in Swan Lake might explain the largest [La] within fathead minnows tissues out of all aquatic organisms, with decreasing order of intestines > liver > brain > gills > soft tissue. This organotropism for our minnow samples was similar to that reported for rainbow trout and carp: intestines > gills > liver > skeleton > muscles (Cardon et al., 2020; Hao et al., 1996). This trend suggests the dominant uptake pathway of La into minnows within Swan Lake is through their diet, as dissected minnow intestines contained a large proportion of green algae (**Figure A2.8**). The low La concentration in fish soft tissue is also in agreement with other field data suggesting the lowest bioaccumulation potential of REEs is in fish muscles (Amyot et al., 2017; Labassa et al., 2023; MacMillan et al., 2017; Marginson et al., 2023; Mayfield and Fairbrother, 2015; Nørregaard et al., 2019; Santos et al., 2023). However, it is striking that the brain of fathead minnows holds higher REE levels (0.7 ± 0.4 mg kg^{-1}) than gills (0.2 ± 0.1 mg kg^{-1}) and soft tissue (0.06 ± 0.01 mg kg^{-1}) (**Table A2.16**). The accumulation of REEs in the brains has been found in rats (Damme et al., 2020; Schmidt et al., 2019) after exposure to gadolinium MRI treatments, which can reduce neuron cell viability, induce endoplasmic reticulum stress, and cause in vitro neurotoxicity in rats (Xia et al., 2011). REEs can also cross the blood-brain barrier after MRI treatment and deposit in the brain of humans, inducing nerve damage (McDonald et al., 2017; Rogosnitzky and Branch, 2016; Vergauwen et al., 2018). Although there is no evidence from the literature on REE enrichment in wild aquatic organisms' brains under natural conditions, the evidence of REE crossing the blood-brain barrier in clinical results and the high La concentrations in minnow's brain in Swan Lake would support the hypothesis of the capacity for La to reach the brain tissues. Calcium plays a pivotal role

in the central nervous system and Ca homeostasis in the brain is tightly regulated by the electrogenic Ca-ATPase pumps on the choroid plexus membranes (Keep et al., 1999) of intracellular organelles such as the sarcoplasmic reticulum and mitochondria (Bkaily and Jacques, 2023). Given the similarity between the Ca and lanthanide ions in terms of ionic radius, coordination geometry and donor atom preference, the binding and even inhibition capacity of the lanthanides on Ca-ATPase is well established (Ogurusu et al., 1991). However, the exact mechanisms are not well elucidated (Henao et al., 1992).

The La and Pr levels in bullhead from Swan Lake are lower than primary producers and consumers, suggesting a lack of REE amplification in bullhead. The organotropism for english bullhead was gills > internal organs > brain > soft tissue (**Figure 3.6A & C**). The higher La levels within the gills suggest the dominant uptake form of REEs into bullhead is the dissolved trivalent REE^{3+} through the gills. This can be explained by fish gills being the main surfaces which transfer essential elements such as Ca^{2+} past passive and active protein channels (Kwong, 2024). Since REEs and Ca^{2+} hold similar ionic radii, (1.03 Å to 0.86 Å for La to Lu vs. 1.00 Å for Ca) (Shannon, 1976), REEs may replace Ca^{2+} during respiration via the gill epithelium (Labassa et al., 2023; Martin and Richardson, 2009).

3.4.6 Lanthanum anomalies in aquatic organisms

Lanthanum anomalies offer a unique alternative to La concentrations in the capacity of directly relating different environmental media, e.g., water, sediments and biota, to determine the extent of La enrichment and possible transfer of La from one medium to another. For a natural ecosystem like Toogood Pond, the absolute concentrations of La in biota might vary because of different exposure, uptake, and

elimination processes (**Figure 3.6**). However, La anomalies in benthic organisms from Toogood Pond such as anecic earthworms (0.95 ± 0.02), endogenic earthworms (0.9), and macroalgae (1.03 ± 0.02) hold La anomalies similar to sediment (1.00 ± 0.02) (**Figure 3.7B**). Nevertheless, pelagic organisms such as gobie soft tissue (2.6 ± 0.6), gobie gills (6.7 ± 3.0), plankton (1.4 ± 0.1), and english bullhead gills (1.9 ± 0.3), and liver (1.4 ± 0.2) contain La anomalies > 1, indicating potential enrichment of La. This range is very close to water fractions (1.35 ± 0.07 to 4.2 ± 1.07 for different filtration cutoffs), suggesting that pelagic organisms in Toogood Pond uptake mainly through the REE dissolved fraction.

Comparably, within Swan Lake, almost all organisms were enriched with La, shown by holding La anomalies higher than 1 (**Figure 3.7A**). The only organisms that did not reflect enrichment in Swan Lake were common pillbugs (La/La* = 1.0) and endogenic earthworms (1.09 ± 0.08), terrestrial organisms collected from the terrestrial land surrounding the lake. Benthic organisms and vegetation living in the sediment of Swan Lake have La anomalies 4 to 20 times lower than the sediments (22.5 ± 3.0), e.g., bloodworms (3.0) and macrophyte (5.8 ± 1.5) (**Figure 3.7A**, **Table A2.14**). Furthermore, even though the benthic bullhead in Swan Lake held the lowest REE concentrations within their tissues compared to all other organisms (**Figure 3.6A**), La anomalies in internal organs (9.7 ± 2.3), gills (5.8 ± 1.1), soft tissue (3.7 ± 1.5), and brain (4.3 ± 1.9) remain higher than some food sources such as plankton (8.6 ± 0.7) and macrophytes (5.8 ± 1.5), indicating some influence from the benthic particulate fractions from deep water (La/La* of 19.9 ± 5.7) or sediments (La/La* of 22.5 ± 3.0) (**Figure 3.7A**, **Table A2.14**).

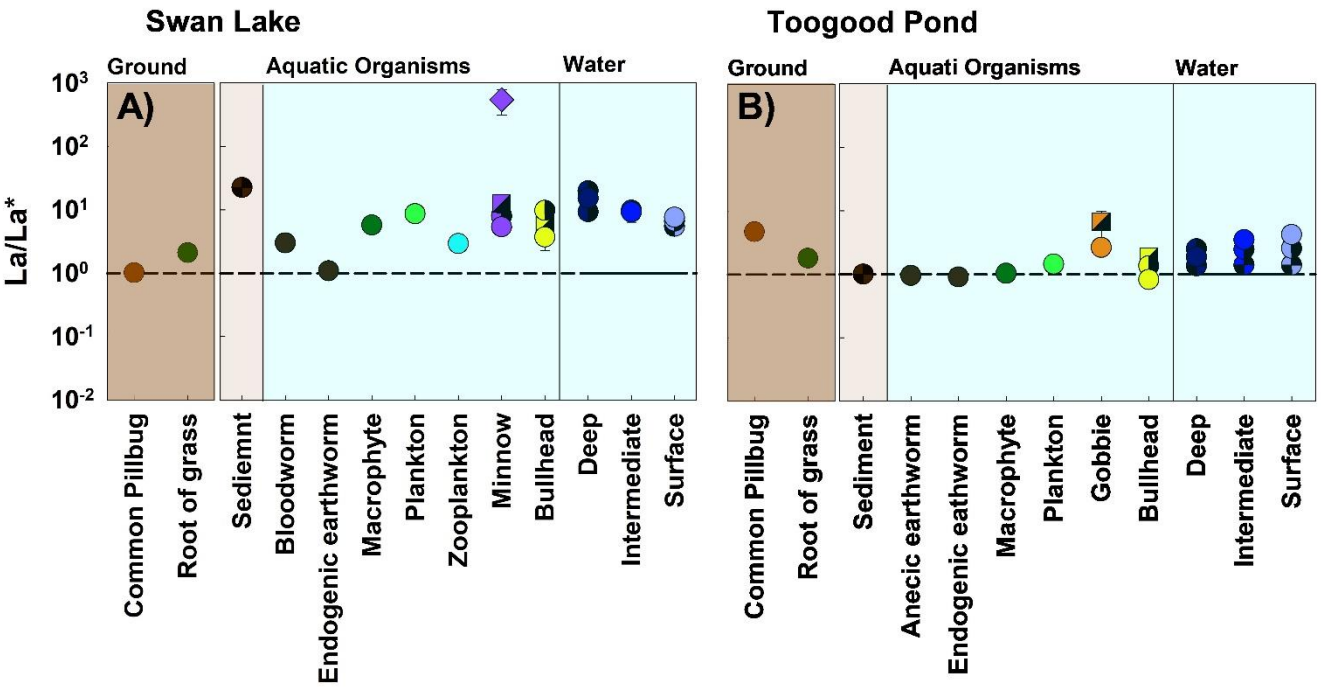

Figure 3.7 La anomalies in sediment, in acid-leachable (quartered circle), 1.2 µm (half-filled circle), and 0.2 µm (open circle) water fractions at three depths, and in organism tissues collected from Swan Lake and Toogood Pond. Tissue types are represented by various shapes: circles (soft tissue or whole body), squares (hard tissue), half-filled circles (intestines/internal organs), half-filled squares (gills), and diamonds (brain).

Lanthanum anomalies in minnows show the largest enrichment of La in the brain tissue (550 ± 240), compared to gills (12.7 ± 3.7) > internal organs (8.2 ± 0.3) > intestines (7.9 ± 1.0) > soft tissue (5.4 ± 0.5) (**Figure 3.7, Table A2.14**). The La anomalies in minnow tissue are higher than the potential food source of minnows, i.e., zooplankton (2.93±0.14) and macrophytes (5.8 ± 1.4)**.** These elevated La/La* in minnow tissues indicate accumulation and probably further enrichment of La within their tissues. Because minnows were instantly euthanized after capture in the field following ACC protocols, their intestines were found filled with green algae (**Figure A2.8**). The fact that minnows were directly consuming plankton caused REE levels and La anomalies in the minnow intestines (7.9 ± 1.0) and internal organs (8.2 ± 0.3) to be in similar magnitude as plankton (8.6 ± 0.5). Lanthanum might have been further translocated to other tissues, especially the brain to cause such a large La/La*. However, further studies are needed to highlight the exact mechanisms of transfer of La from the intestines through the bloodstream to reach their brains.

3.5 Conclusion

The aquatic ecosystem of Swan Lake post application to LMB revealed La enrichment in biotic and abiotic compartments. The transfer of La from the sediment reservoir to the water column, aquatic organisms, and vegetation was evidenced by La concentrations and La anomalies. Within Swan Lake the highest La concentrations were found in bloodworms, plankton, and minnows and the lowest concentrations were in the tissues of bullhead. However, La anomalies, as a specific means to track the extent of enrichment and transfer from the sediment reservoir, highlight that almost all organisms in Swan Lake enrich La relative to other REEs. Evidence about the highest enrichment of

La in the brain of pelagic fish, calls for further investigations on the potential transfer of these elements into the aquatic food web, despite recent findings on trophic biodilution in various natural ecosystems.

Ecosystems enriched in REEs might respond differently than pristine systems, especially because of different chemical speciation of REEs, a loss of biodiversity, disturbed trophic transfer mechanisms, and distinct inter-linkages between abiotic and biotic compartments. Although these results are reported from a local urban lake, there is a need to frame REE enrichment and transfer from abiotic to biotic compartments in the global context, especially as various jurisdictions' demands for these priority critical minerals continue to rise. The elevated concentrations of REEs in aquatic systems, as a result of increasing extraction, processing, and recycling across the globe, might lead to more enriched and impacted aquatic ecosystems. Further ecotoxicological studies are needed to shed light on the exact mechanisms of how REEs accumulate and translocate within living organisms.

3.6 Acknowledgments

The authors acknowledge the financial support from NSERC to D.H.D. (Discovery Grant) and A.K. (Undergraduate Student Research Awards). We are thankful to Spencer Grieve and Minh Duong for their assistance during field sampling campaigns and Dr. Wei Wang for his support relative to chemical analysis. The authors thank the research scientist, Dr. Karla Newman and manager, Hayla Evans of the Trent Water Quality Centre for technical and analytical support. Finally, the authors acknowledge and thank Zahra Parhizgari, Senior Environmental Engineer and Robert Muir, Stormwater Manager from the City of Markham for sampling time and logistical support.

3.7 References

Adeel, M., Lee, J.Y., Zain, M., Rizwan, M., Nawab, A., Ahmad, M.A., Shafiq, M., Yi, H., Jilani, G., Javed, R., Horton, R., Rui, Y., Tsang, D., Xing, B., 2019. Cryptic footprints of rare earth elements on natural resources and living organisms. Environ Int 127, 785–800. https://doi.org/10.1016/j.envint.2019.03.022

Amyot, M., Clayden, M.G., MacMillan, G.A., Perron, T., Arscott-Gauvin, A., 2017. Fate and trophic transfer of rare earth elements in temperate lake food webs. Environ Sci Technol 51, 6009–6017. https://doi.org/10.1021/acs.est.7b00739

Arienzo, M., Ferrara, L., Trifuoggi, M., Toscanesi, M., 2022. Advances in the fate of rare earth elements, REE, in transitional environments: Coasts and estuaries. Water (Basel) 14, 1–23. https://doi.org/10.3390/w14030401

Auer, G., Reuter, M., Hauzenberger, C.A., Piller, W.E., 2017. The impact of transport processes on rare earth element patterns in marine authigenic and biogenic phosphates. Geochim Cosmochim Acta 203, 140–156. https://doi.org/10.1016/j.gca.2017.01.001

Barbieri, M., 2016. The importance of enrichment factor (EF) and geoaccumulation index (Igeo) to evaluate the soil contamination. J Geo Geophys 5, 1–4. https://doi.org/10.4172/2381-8719.1000237

Bau, M., Schmidt, K., Pack, A., Bendel, V., Kraemer, D., 2018. The European Shale: An improved data set for normalisation of rare earth element and yttrium concentrations in environmental and biological samples from Europe. Appl Geochem 90, 142–149. https://doi.org/10.1016/j.apgeochem.2018.01.008

Bengtsson, L., Hellström, T., 1992. Wind-induced resuspension in a small shallow lake. Hydrobiologia 241, 163–172. https://doi.org/10.1007/BF00028639

Bentum, J.K., Anang, M., Boadu, K.O., Koranteng-Addo, E.J., Antwi, E.O., 2011. Assessment of heavy metals pollution of sediments from Fosu Lagoon in Ghana. Bull. Chem. Soc. Ethiop 25, 191–196. https://doi.org/10.4314/bcse.v25i2.65869

Bishop, W.M., Richardson, R.J., 2018. Influence of Phoslock® on legacy phosphorus, nutrient ratios, and algal assemblage composition in hypereutrophic water resources. Environ Sci Pollut R 25, 4544–4557. https://doi.org/10.1007/s11356-017-0832-2

Bkaily, G., Jacques, D., 2023. Calcium homeostasis, transporters, and blockers in health and diseases of the cardiovascular system. Int J Mol Sci 24, 8803. https://doi.org/10.3390/ijms24108803

Blais, J.M., Kalff, J., 1995. The influence of lake morphometry on sediment focusing. Limnol Oceanogr 40, 582–588. https://doi.org/10.4319/lo.1995.40.3.0582

Cao, Y., Lei, K., Zhang, X., Xu, L., Lin, C., Yang, Y., 2018. Contamination and ecological risks of toxic metals in the Hai River, China. Ecotoxicol Environ Saf 164, 210–218. https://doi.org/10.1016/j.ecoenv.2018.08.009

Cardon, P.Y., Roques, O., Caron, A., Rosabal, M., Fortin, C., Amyot, M., 2020. Role of prey subcellular distribution on the bioaccumulation of yttrium (Y) in the rainbow trout. Environ Pollut 258, 113804. https://doi.org/10.1016/j.envpol.2019.113804

Censi, P., Mazzola, S., Sprovieri, M., Bonanno, A., Patti, B., Punturo, R., Spoto, S.E., Saiano, F., Alonzo, G., 2004. Rare earth elements distribution in seawater and suspended particulate of the Central Mediterranean Sea. Chem Ecol 20, 323–343. https://doi.org/10.1080/02757540410001727954

Chaffin, J.D., Kane, D.D., 2010. Burrowing mayfly (Ephemeroptera: Ephemeridae: Hexagenia spp.) bioturbation and bioirrigation: A source of internal phosphorus loading in Lake Erie. J Great Lakes Res 36, 57–63. https://doi.org/10.1016/j.jglr.2009.09.003

Chakraborty, P., Raghunadh Babu, P. V., Sarma, V. V., 2011. A multi-method approach for the study of lanthanum speciation in coastal and estuarine sediments. J Geochem Explor 110, 225–231. https://doi.org/10.1016/j.gexplo.2011.05.013

Chislock, M.F., Doster, E., Zitomer, R.A., Wilson, A.E., 2013. Eutrophication: Causes, consequences, and controls in aquatic ecosystems. Nature Education Knowledge 4, 1–8.

Damme, N.M., Fernandez, D.P., Wang, L.M., Wu, Q., Kirk, R.A., Towner, R.A., McNally, J.S., Hoffman, J.M., Morton, K.A., 2020. Analysis of retention of gadolinium by brain, bone, and blood following linear gadolinium-based contrast agent administration in rats with experimental sepsis. Magn Reson Med 83, 1930–1939. https://doi.org/10.1002/mrm.28060

Dang, D.H., Kernaghan, A., Emery, R.J.N., Thompson, K.A., Kisiala, A., Wang, W., 2024. The mixed blessings of rare earth element supplements for tomatoes and ferns. Sci Total Environ 906, 1–10. https://doi.org/10.1016/j.scitotenv.2023.167822

Dang, D.H., Ma, L., Ha, Q.K., Wang, W., 2022a. A multi-tracer approach to disentangle anthropogenic emissions from natural processes in the St. Lawrence river and estuary. Water Res 219, 118588. https://doi.org/10.1016/j.watres.2022.118588

Dang, D.H., Wang, W., Evans, R.D., 2021. Rare earth element accumulation and fractionation in a lake ecosystem Impacted by past uranium mining. Arch Environ Contam Toxicol 81, 589–599. https://doi.org/10.1007/s00244-021-00866-8

Dang, D.H., Wang, W., Pelletier, P., Poulain, A.J., Evans, R.D., 2018. Uranium dispersion from U tailings and mechanisms leading to U accumulation in sediments: Insights from biogeochemical and isotopic approaches. Sci Total Environ 610–611, 880–891. https://doi.org/10.1016/j.scitotenv.2017.08.156

Dang, D.H., Wang, W., Sikma, A., Chatzis, A., Mucci, A., 2022b. The contrasting estuarine geochemistry of rare earth elements between ice-covered and ice-free conditions. Geochim Cosmochim Acta 317, 488–506. https://doi.org/10.1016/j.gca.2021.10.025

Dang, D.H., Wang, W., Winkler, G., Chatzis, A., 2023. Rare earth element uptake mechanisms in plankton in the Estuary and Gulf of St. Lawrence. Sci Total Environ 860, 160394. https://doi.org/10.1016/j.scitotenv.2022.160394

del Buono, E., Nurra, N., Sartor, R.M., Battuello, M., Favaro, L., Berti, G., Griglione, A., Trossi, A., Avolio, R., Abete, M.C., Squadrone, S., 2024. Trace and rare earth elements in phytoplankton from the Tyrrhenian Sea (Italy). Environ Monit Assess 196, 399. https://doi.org/10.1007/s10661-024-12552-y

Dithmer, L., Lipton, A.S., Reitzel, K., Warner, T.E., Lundberg, D., Nielsen, U.G., 2015. Characterization of phosphate sequestration by a lanthanum modified bentonite clay: A solid-state NMR, EXAFS, and PXRD study. Environ Sci Technol 49, 4559–4566. https://doi.org/10.1021/es506182s

Douglas, R.W., Rippey, B., 2000. The random redistribution of sediment by wind in a lake. Limnol Oceanogr 45, 686–694. https://doi.org/https://doi.org/10.4319/lo.2000.45.3.0686

Drobniak, A., Mastalerz, M., 2022. Rare earth elements: A brief overview. Ind J Earth Sci 4, 1–7. https://doi.org/10.14434/ijes.v4i1.33628

Du, Y., Zhang, Q., Liu, Z., He, H., Lürling, M., Chen, M., Zhang, Y., 2019. Composition of dissolved organic matter controls interactions with La and Al ions: Implications for phosphorus immobilization in eutrophic lakes. Environ Pollut 248, 36–47. https://doi.org/10.1016/j.envpol.2019.02.002

Edgington, D.N., Robbins, J.A., 1990. Time scales of sediment focusing in large lakes as revealed by measurement of fallout Cs-137, in: Springer S Contem Biosci. Springer Berlin Heidelberg, pp. 210–223. https://doi.org/https://doi.org/10.1007/978-3-642-84077-7_11

Epe, T.S., Finsterle, K., Yasseri, S., 2017. Nine years of phosphorus management with lanthanum modified bentonite (Phoslock) in a eutrophic, shallow swimming lake in Germany. Lake Reserv Manag 33, 119–129. https://doi.org/10.1080/10402381.2016.1263693

European Commission, 2020. Critical raw materials resilience: Charting a path towards greater sustainability. Brussels. https://doi.org/https://eur-lex.europa.eu/legal-content/EN/TXT/?uri=CELEX:52020DC0474

Evans, M., Frick, C., 2001. The effects of road salts on aquatic ecosystems [WWW Document]. Environment Canada. URL http://hdl.handle.net/11250/193946 (accessed 12.14.24).

Fasola, E., 2010. Phoslock ® Effects on benthic invertebrates: the example of crayfish (Procambarus Acutus) (Master in Risk Assessment and Risk Analysis). Wageningen University.

Finsterle, K., 2014. Overview of Phoslock® Properties and its Use in the Aquatic Environment. Phoslock Europe GmbH 1–47.

Firsching, H.F., Bruñe, S.N., 1991. Solubility products of the trivalent rare-earth phosphates. J Chem Eng Data 36, 93–95. https://doi.org/https://doi.org/10.1021/je00001a028

Gabitov, R.I., Sadekov, A., Migdisov, A., 2017. REE incorporation into calcite individual crystals as one time spike addition. Minerals 7, 1–11. https://doi.org/10.3390/min7110204

George, K., Vargas, K., Qi, Z., 2019. P immonbilizing materials for lake internal loading control: A review towards future developments. Crit Rev Environ Sci Technol 29, 518–552. https://doi.org/https://doi.org/10.1080/10643389.2018.1551300

Gertrud Nürnberg, P., LaZerte, B., 2020. Swan Lake Water Quality Management [WWW Document]. URL https://friendsofswanlakepark.ca/wp-content/uploads/2020/08/Freshwater-Research-Swan-Lake-Water-Quality_Final-Report_-2020-07-17-1.pdf (accessed 12.14.24).

Godwyn-Paulson, P., Jonathan, M.P., Rodríguez-Espinosa, P.F., Rodríguez-Figueroa, G.M., 2022. Rare earth element enrichments in beach sediments from Santa Rosalia mining region, Mexico: An index-based environmental approach. Mar Pollut Bull 174, 113271. https://doi.org/10.1016/j.marpolbul.2021.113271

Goitom, E., 2011. Bioaccumulation of lanthanum in marbled crayfish (Procambarus sp.) (Master's thesis). Wageningen University.

Government of Canada, 2022. The Canadian critical minerals strategy, from exploration to recycling: powering the green and digital economy for Canada and the world [WWW Document]. URL https://www.canada.ca/en/campaign/critical-minerals-in-canada/canadian-critical-minerals-strategy.html (accessed 1.2.25).

Haghseresht, F., Wang, S., Do, D.D., 2009. A novel lanthanum-modified bentonite, Phoslock, for phosphate removal from wastewaters. Appl Clay Sci 46, 369–375. https://doi.org/10.1016/j.clay.2009.09.009

Hakanson, L., 1977. The influence of wind, fetch, and water depth on the distribution of sediments in Lake Vanern, Sweden. Can J Earth Sci 14, 397–412. https://doi.org/10.1139/e77-040

Han, Y., Li, Q., He, H., Gu, J., Wu, Z., Huang, X., Zou, X., Zhang, Y., Li, K., 2021. Effect of juvenile omni-benthivorous fish (Carassius carassius) disturbance on the efficiency of lanthanum-modified bentonite (LMB) for eutrophication control: a mesocosm study. Environ Sci Pollut Res 28, 21779–21788. https://doi.org/10.1007/s11356-020-12045-8

Hao, S., Xiaorong, W., Zhaozhe, H., Chonghua, W., Liansheng, W., Lemei, D., Zhong, L., Yijun, C., 1996. Bioconcentration and elimination of five light rare earth elements in carp (Cyprinus carpio L.). Chemosphere 33, 1475–1483. https://doi.org/10.1016/0045-6535(96)00286-X

Haris, H., Looi, L.J., Aris, A.Z., Mokhtar, N.F., Ayob, N.A.A., Yusoff, F.M., Salleh, A.B., Praveena, S.M., 2017. Geo-accumulation index and contamination factors of heavy metals (Zn and Pb) in urban river sediment. Environ Geochem Health 39, 1259–1271. https://doi.org/10.1007/s10653-017-9971-0

Heiri, O., Lotter, A.F., Lemcke, G., 2001. Loss on ignition as a method for estimating organic and carbonate content in sediments: reproducibility and comparability of results. J Paleolimnol 25, 101–110. https://doi.org/https://doi.org/10.1023/A:1008119611481

Henao, F., Orlowski, S., Merah, Z., Champeil, P., 1992. The metal sites on sarcoplasmic reticulum membranes that bind lanthanide ions with the highest affinity are not the ATPase Ca2+ transport sites. J Biol Chem 267, 10302–10312. https://doi.org/10.1016/s0021-9258(19)50018-7

Herrmann, H., Nolde, J., Berger, S., Heise, S., 2016. Aquatic ecotoxicity of lanthanum - A review and an attempt to derive water and sediment quality criteria. Ecotoxicol Environ Saf 124, 213–238. https://doi.org/10.1016/j.ecoenv.2015.09.033

Hilton, J., 1985. A conceptual framework for predicting the occurrence of sediment focusing and sediment redistribution in small lakes. Limnol Oceanogr 30, 1131–1143. https://doi.org/10.4319/lo.1985.30.6.1131

Humphries, M., 2013. Rare earth elements: The global supply chain. Congressional Research Service 1–27.

International Energy Agency, 2021. The role of critical world energy in clean energy transitions [WWW Document]. URL https://www.iea.org/reports/the-role-of-critical-minerals-in-clean-energy-transitions (accessed 1.2.25).

Jensen, J.L., Christensen, B.T., Schjønning, P., Watts, C.W., Munkholm, L.J., 2018. Converting loss-on-ignition to organic carbon content in arable topsoil: pitfalls and proposed procedure. Eur J Soil Sci 69, 604–612. https://doi.org/10.1111/ejss.12558

Jiang, C., Li, Y., Li, C., Zheng, Lanlan, Zheng, Liugen, 2022. Distribution, source and behavior of rare earth elements in surface water and sediments in a subtropical freshwater lake influenced by human activities. Environ Pollut 313, 120153. https://doi.org/10.1016/j.envpol.2022.120153

Jowitt, S.M., Werner, T.T., Weng, Z., Mudd, G.M., 2018. Recycling of the rare earth elements. Curr Opin Green Sustain Chem 13, 1–7. https://doi.org/10.1016/j.cogsc.2018.02.008

Keep, R.F., Ii, L.J.U., Xiang, J., Ennis, S.R., Lorris Betz, A., 1999. Blood-brain barrier mechanisms involved in brain calcium and potassium homeostasis. Brain Res 815, 200–205. https://doi.org/https://doi.org/10.1016/S0006-8993(98)01155-X

Keuskamp, J.A., Hefting, M.M., Dingemans, B.J.J., Verhoeven, J.T.A., Feller, I.C., 2015. Effects of nutrient enrichment on mangrove leaf litter decomposition. Science of the Total Environment 508, 402–410. https://doi.org/10.1016/j.scitotenv.2014.11.092

Khan, F., Ansari, A., 2005. Eutrophication: An ecological vision. Bot Rev 71, 449–482. https://doi.org/https://doi.org/10.1663/0006-8101(2005)071[0449:EAEV]2.0.CO;2

Kwong, R.W.M., 2024. Trace metals in the teleost fish gill: biological roles, uptake regulation, and detoxification mechanisms. J Comp Physiol B 194, 749–763. https://doi.org/10.1007/s00360-024-01565-1

Labassa, M., Pereto, C., Schäfer, J., Hani, Y.M.I., Baudrimont, M., Bossy, C., Dassié, É.P., Mauffret, A., Deflandre, B., Grémare, A., Coynel, A., 2023. First assessment of rare earth element organotropism in Solea solea in a coastal area: The west Gironde Mud Patch (France). Mar Pollut Bull 197, 115730. https://doi.org/10.1016/j.marpolbul.2023.115730

Lachaux, N., Otero-Fariña, A., Minguez, L., Sohm, B., Rétif, J., Châtel, A., Poirier, L., Devin, S., Pain-Devin, S., Gross, E.M., Giamberini, L., 2023. Fate, subcellular distribution and biological effects of rare earth elements in a freshwater bivalve under complex exposure. Sci Total Environ 905, 167302. https://doi.org/10.1016/j.scitotenv.2023.167302

Lakshtanov, L.Z., Stipp, S.L.S., 2004. Experimental study of europium (III) coprecipitation with calcite. Geochim Cosmochim Acta 68, 819–827. https://doi.org/10.1016/j.gca.2003.07.010

Lesven, L., Lourino-Cabana, B., Billon, G., Proix, N., Recourt, P., Ouddane, B., Fischer, J.C., Boughriet, A., 2009. Water-quality diagnosis and metal distribution in a strongly polluted zone of Deûle River (Northern France). Water Air Soil Pollut 198, 31–44. https://doi.org/10.1007/s11270-008-9823-8

Liu, Gu, X., Lian, M., Wang, J., Xin, M., Wang, B., Ouyang, W., He, M., Liu, X., Lin, C., 2023. Occurrence, geochemical characteristics, enrichment, and ecological risks of rare earth elements in sediments of "the Yellow river−Estuary−bay" system. Environ Pollut 319, 121025. https://doi.org/10.1016/j.envpol.2023.121025

Liu, X., Byrne, R.H., 1997. Rare earth and yttrium phosphate solubilities in aqueous solution. Geochirnica et Cosmochimica Acta 61, 1625–1633. https://doi.org/https://doi.org/10.1016/S0016-7037(97)00037-9

Long, K., Van Gosen, B., Foley, N., Cordier, D., 2010. The principal rare earth elements deposits of the United States: A summary of domestic deposits and a global perspective, in: Non-Renewable Resource Issues. Springer, pp. 1–104. https://doi.org/https://doi.org/10.1007/978-90-481-8679-2_7

Lürling, M., Van Oosterhout, F., 2013. Case study on the efficacy of a lanthanum-enriched clay (Phoslock®) in controlling eutrophication in Lake Het Groene Eiland (The Netherlands). Hydrobiologia 710, 253–263. https://doi.org/10.1007/s10750-012-1141-x

Lusty, P.A.J., Shaw, R.A., Gunn, A.G., Idoine, N.E., 2021. UK criticality assessment of technology critical minerals and metals decarbonisation & resource management. British Geological Survey 1–76.

Ma, L., Dang, D.H., Wang, W., Evans, R.D., Wang, W.X., 2019. Rare earth elements in the Pearl River Delta of China: Potential impacts of the REE industry on water, suspended particles and oysters. Environ Pollut 244, 190–201. https://doi.org/10.1016/j.envpol.2018.10.015

MacMillan, G.A., Chételat, J., Heath, J., Mickpegak, R., Amyot, M., 2017. Rare earth elements (REE) in freshwater, marine, and terrestrial ecosystems in the eastern Canadian Arctic. Environ Sci-Proc Imp 10, 1336–1345. https://doi.org/10.1101/174870

Marginson, H., MacMillan, G.A., Grant, E., Gérin-Lajoie, J., Amyot, M., 2023. Rare earth element bioaccumulation and cerium anomalies in biota from the Eastern Canadian subarctic (Nunavik). Sci Total Environ 879, 163024. https://doi.org/10.1016/j.scitotenv.2023.163024

Martin, B., Richardson, F., 2009. Lanthanides as probes for calcium in biological systems. Q Rev Biophys 12, 181–209. https://doi.org/doi:10.1017/S0033583500002754

Mayfield, D.B., Fairbrother, A., 2015. Examination of rare earth element concentration patterns in freshwater fish tissues. Chemosphere 120, 68–74. https://doi.org/10.1016/j.chemosphere.2014.06.010

McDonald, R.J., McDonald, J.S., Kallmes, D.F., Jentoft, M.E., Paolini, M.A., Murray, D.L., Williamson, E.E., Eckel, L.J., 2017. Gadolinium deposition in human brain tissues after contrast-enhanced MR imaging in adult patients without intracranial abnormalities. Radiology 285, 546–554. https://doi.org/10.1148/radiol.2017161595

McLennan, S.M., 2001. Relationships between the trace element composition of sedimentary rocks and upper continental crust. Geochem Geophy Geosy 2, 1–24. https://doi.org/10.1029/2000GC000109

Meis, S., Spears, B.M., Maberly, S.C., Perkins, R.G., 2013. Assessing the mode of action of Phoslock® in the control of phosphorus release from the bed sediments in a shallow lake (Loch Flemington, UK). Water Res 47, 4460–4473. https://doi.org/10.1016/j.watres.2013.05.017

Meysman, F.J.R., Middelburg, J.J., Heip, C.H.R., 2006. Bioturbation: a fresh look at Darwin's last idea. Trends Ecol Evol 21, 688–695. https://doi.org/10.1016/j.tree.2006.08.002

Migaszewski, Z.M., Gałuszka, A., 2015. The characteristics, occurrence, and geochemical behavior of rare earth elements in the environment: A review. Crit Rev Environ Sci Technol 45, 429–471. https://doi.org/10.1080/10643389.2013.866622

Moermond, C.T.A., Tijink, J., Van Wezel, A.P., Koelmans, A.A., 2001. Distribution, speciation, and bioavailability of lanthanides in the Rhine-Meuse estuary, the Netherlands. Environ Toxicol Chem 20, 1916–1926. https://doi.org/10.1002/etc.5620200909

Moos, M.T., Taffs, K.H., Longstaff, B.J., Ginn, B.K., 2014. Establishing ecological reference conditions and tracking post-application effectiveness of lanthanum-saturated bentonite clay (Phoslock®) for reducing phosphorus in aquatic systems: An applied paleolimnological approach. J Environ Manage 141, 77–85. https://doi.org/10.1016/j.jenvman.2014.02.038

Muir, R., Parhizgari, Z., 2021. Swan Lake Long Term Management Plan Swan Lake Long Term Management Plan Environmental Services.

Munemoto, T., Solongo, T., Okuyama, A., Fukushi, K., Yunden, A., Batbold, T., Altansukh, O., Takahashi, Y., Iwai, H., Nagao, S., 2020. Rare earth element distributions in rivers and sediments from the Erdenet Cu–Mo mining area, Mongolia. Appl Geochem 123, 104800. https://doi.org/10.1016/j.apgeochem.2020.104800

Neira, P., Romero-Freire, A., Basallote, M.D., Qiu, H., Cobelo-García, A., Cánovas, C.R., 2022. Review of the concentration, bioaccumulation, and effects of lanthanides in marine systems. Front Mar Sci 9, 1–14. https://doi.org/10.3389/fmars.2022.920405

Nørregaard, R.D., Kaarsholm, H., Bach, L., Nowak, B., Geertz-Hansen, O., Søndergaard, J., Sonne, C., 2019. Bioaccumulation of rare earth elements in juvenile arctic char (Salvelinus alpinus) under field experimental conditions. Sci Total Environ 688, 529–535. https://doi.org/10.1016/j.scitotenv.2019.06.180

Nürnberg, G.K., 2017. Attempted management of cyanobacteria by Phoslock (lanthanum-modified clay) in Canadian lakes: water quality results and predictions. Lake Reserv Manag 33, 163–170. https://doi.org/10.1080/10402381.2016.1265618

Nürnberg, G.K., LaZerte, B.D., 2016. Trophic state decrease after lanthanum-modified bentonite (Phoslock) application to a hyper-eutrophic polymictic urban lake frequented by Canada geese (Branta canadensis). Lake Reserv Manag 32, 74–88. https://doi.org/10.1080/10402381.2015.1133739

Ogurusu, T., Wakaboyashi, S., Munekazu, S., 1991. Functional characterization of lanthanide binding sites in the sarcoplasmic reticulum Ca2+-ATPase: Do lanthanide ions bind to the calcium transport site? Biochemistry 30, 9966–9973. https://doi.org/10.1021/bi00105a022

Ontario Ministry of the Environment, 2003. Technical Support Document for Ontario Drinking Water Standards, Objectives and Guidelines 1–42.

Pourret, O., Davranche, M., Gruau, G., Dia, A., 2007a. Organic complexation of rare earth elements in natural waters: Evaluating model calculations from ultrafiltration data. Geochim Cosmochim Acta 71, 2718–2735. https://doi.org/10.1016/j.gca.2007.04.001

Pourret, O., Davranche, M., Gruau, G., Dia, A., 2007b. Rare earth elements complexation with humic acid. Chem Geol 243, 128–141. https://doi.org/10.1016/j.chemgeo.2007.05.018

Pourret, O., Tuduri, J., 2017. Continental shelves as potential resource of rare earth elements. Sci Rep 7, 5857. https://doi.org/10.1038/s41598-017-06380-z

Pourret, O., van der Ent, A., Hursthouse, A., Irawan, D.E., Liu, H., Wiche, O., 2022. The 'europium anomaly' in plants: facts and fiction. Plant Soil 476, 721–728. https://doi.org/10.1007/s11104-021-05210-6

Prior, P., Miller, G., Moleirinho, P., 2013. Toogood Pond Terrestrial Biological Inventory and Assessment. TRCA 1–58.

Qingjie, G., Deng, J., Yunchuan, X., Qingfei, W., Liqiang, Y., 2008. Calculating pollution indices by heavy metals in ecological geochemistry assessment and a case study in parks of Beijing. J China Univ Geosci 19, 230–241. https://doi.org/10.1016/S1002-0705(08)60042-4

Ramos, S.J., Dinali, G.S., Oliveira, C., Martins, G.C., Moreira, C.G., Siqueira, J.O., Guilherme, L.R.G., 2016. Rare earth elements in the soil environment. Curr Pollut Rep 2, 28–50. https://doi.org/10.1007/s40726-016-0026-4

Rétif, J., Zalouk-Vergnoux, A., Kamari, A., Briant, N., Poirier, L., 2024. Trophic transfer of rare earth elements in the food web of the Loire estuary (France). Sci Total Environ 914, 169652. https://doi.org/10.1016/j.scitotenv.2023.169652

Rogosnitzky, M., Branch, S., 2016. Gadolinium-based contrast agent toxicity: a review of known and proposed mechanisms. BioMetals 29, 365–376. https://doi.org/10.1007/s10534-016-9931-7

Ross, G., Haghseresht, F., Cloete, T.E., 2008. The effect of pH and anoxia on the performance of Phoslock®, a phosphorus binding clay. Harmful Algae 7, 545–550. https://doi.org/10.1016/j.hal.2007.12.007

Santos, A.C.S.S., Souza, L.A., Araujo, T.G., de Rezende, C.E., Hatje, V., 2023. Fate and trophic transfer of rare earth elements in a tropical estuarine food web. Environ Sci Technol 57, 2404–2414. https://doi.org/10.1021/acs.est.2c07726

Schindler, D.W., 2006. Recent advances in the understanding and management of eutrophication. Limnol Oceanogr 51, 356–363. https://doi.org/https://doi.org/10.4319/lo.2006.51.1_part_2.0356

Schmidt, K., Bau, M., Merschel, G., Tepe, N., 2019. Anthropogenic gadolinium in tap water and in tap water-based beverages from fast-food franchises in six major cities in Germany. Sci Total Environ 687, 1401–1408. https://doi.org/10.1016/j.scitotenv.2019.07.075

Shannon, R.D., 1976. Revised effective ionic radii and systematic studies of interatomic distances in halides and chalcogenides. Acta Crystallographica Section A 32, 751–767. https://doi.org/10.1107/S0567739476001551

Smith, V.H., Schindler, D.W., 2009. Eutrophication science: where do we go from here? Trends Ecol Evol 24, 201–207. https://doi.org/10.1016/j.tree.2008.11.009

Søndergaard, M., Jensen, J.P., Jeppesen, E., 2003. Role of sediment and internal loading of phosphorus in shallow lakes. Hydrobiologia 506–509, 135–145. https://doi.org/https://doi.org/10.1023/B:HYDR.0000008611.12704.dd

Sorichetti, R.J., Raby, M., Holeton, C., Benoit, N., Carson, L., DeSellas, A., Diep, N., Edwards, B.A., Howell, T., Kaltenecker, G., McConnell, C., Nelligan, C., Paterson, A.M., Rogojin, V., Tamanna, N., Yao, H., Young, J.D., 2022. Chloride trends in Ontario's surface and groundwaters. J Great Lakes Res 48, 512–525. https://doi.org/10.1016/j.jglr.2022.01.015

Spears, B.M., Lürling, M., Yasseri, S., Castro-Castellon, A.T., Gibbs, M., Meis, S., McDonald, C., McIntosh, J., Sleep, D., Van Oosterhout, F., 2013. Lake responses following lanthanum-modified bentonite clay (Phoslock®) application: An analysis of water column lanthanum data from 16 case study lakes. Water Res 47, 5930–5942. https://doi.org/10.1016/j.watres.2013.07.016

Strady, E., Kim, I., Radakovitch, O., Kim, G., 2015. Rare earth element distributions and fractionation in plankton from the northwestern Mediterranean Sea. Chemosphere 119, 72–82. https://doi.org/10.1016/j.chemosphere.2014.05.049

Thornton, J.A., Harding, W.R., Dent, M., Hart, R.C., Lin, H., Rast, C.L., Rast, W., Ryding, S.O., Slawski, T.M., 2013. Eutrophication as a "wicked" problem. Lakes Reserv 18, 298–316. https://doi.org/10.1111/lre.12044

Tommasi, F., Thomas, P.J., Lyons, D.M., Pagano, G., Oral, R., Siciliano, A., Toscanesi, M., Guida, M., Trifuoggi, M., 2023. Evaluation of rare earth element-associated hormetic effects in candidate fertilizers and livestock feed additives. Biol Trace Elem Res 201, 2573–2581. https://doi.org/10.1007/s12011-022-03331-2

Van Oosterhout, F., Lürling, M., 2013. The effect of phosphorus binding clay (Phoslock®) in mitigating cyanobacterial nuisance: A laboratory study on the effects on water quality variables and plankton. Hydrobiologia 710, 265–277. https://doi.org/10.1007/s10750-012-1206-x

Van Oosterhout, F., Waajen, G., Yasseri, S., Manzi Marinho, M., Pessoa Noyma, N., Mucci, M., Douglas, G., Lürling, M., 2020. Lanthanum in water, sediment, macrophytes and chironomid larvae following application of lanthanum modified bentonite to lake Rauwbraken (The Netherlands). Sci Total Environ 706, 1–13. https://doi.org/10.1016/j.scitotenv.2019.135188

Vergauwen, E., Vanbinst, A.M., Brussaard, C., Janssens, P., De Clerck, D., Van Lint, M., Houtman, A.C., Michel, O., Keymolen, K., Lefevere, B., Bohler, S., Michielsen, D., Jansen, A.C., Van Velthoven, V., Gläsker, S., 2018. Central nervous system gadolinium accumulation in patients undergoing periodical contrast mri screening for hereditary tumor syndromes. Hered Cancer Clin Pract 16, 1–9. https://doi.org/10.1186/s13053-017-0084-7

Walfish, S., 2006. A Review of Statistical Outlier Methods. Pharmaceutical Technology 1–5.

Xia, Q., Feng, X., Huang, H., Du, L., Yang, X., Wang, K., 2011. Gadolinium-induced oxidative stress triggers endoplasmic reticulum stress in rat cortical neurons. J Neurochem 117, 38–47. https://doi.org/10.1111/j.1471-4159.2010.07162.x

Xu, Pan, B., Shu, F., Chen, X., Xu, N., Ni, J., 2022. Bioaccumulation of 35 metal(loid)s in organs of a freshwater mussel (Hyriopsis cumingii) and environmental implications in Poyang Lake, China. Chemosphere 307, 136150. https://doi.org/10.1016/j.chemosphere.2022.136150

Yeghicheyan, D., Aubert, D., Bouhnik-Le Coz, M., Chmeleff, J., Delpoux, S., Djouraev, I., Granier, G., Lacan, F., Piro, J.L., Rousseau, T., Cloquet, C., Marquet, A., Menniti, C., Pradoux, C., Freydier, R., Vieira da Silva-Filho, E., Suchorski, K., 2019. A New Interlaboratory Characterisation of Silicon, Rare Earth Elements and Twenty-Two Other Trace Element Concentrations in the Natural River Water Certified Reference Material SLRS-6 (NRC-CNRC). Geostand Geoanal Res 43, 475–496. https://doi.org/10.1111/ggr.12268

Zeller, M.A., Alperin, M.J., 2021. The efficacy of Phoslock® in reducing internal phosphate loading varies with bottom water oxygenation. Water Res X 11, 100095. https://doi.org/10.1016/j.wroa.2021.10

Zhang, C., Wang, L., Zhang, S., Li, X., 1998. Geochemistry of rare earth elements in the mainstream of the Yangtze River, China. Appl Geochem 13, 451–462. https://doi.org/10.1016/S0883-2927(97)00079-6

Zhang, Liu, 2002. Riverine composition and estuarine geochemistry of particulate metals in China - Weathering features, anthropogenic impact and chemical fluxes. Estuar Coast Shelf Sci 54, 1051–1070. https://doi.org/10.1006/ecss.2001.0879

Zhang, S., Shan, X.-Q., 2001. Speciation of rare earth elements in soil and accumulation by wheat with rare earth fertilizer application. Environ Pollut 112, 395–405. https://doi.org/10.1016/S0269-7491(00)00143-3

Zhang, Ye, X., Feng, H., Jing, Y., Ouyang, T., Yu, X., Liang, R., Gao, C., Chen, W., 2007. Heavy metal contamination in western Xiamen Bay sediments and its vicinity, China. Mar Pollut Bull 54, 974–982. https://doi.org/10.1016/j.marpolbul.2007.02.010

Chapter 4. General Discussion

4.1 Synthesis

The overarching objective of this study was to determine the natural fate, distribution, uptake mechanisms, and potential bioaccumulation and enrichment of REEs within aquatic ecosystems. It was hypothesized that REEs would be bioavailable to aquatic organisms and that bioaccumulation and enrichment of REEs should occur but are species-specific. Chapters 2 and 3 explored REE exposure pathways, bioaccumulation, natural fate, and enrichment of REEs within aquatic organisms and ecosystems under environmental conditions. It was decided to complete the first section under naturally relevant and controlled mesocosm conditions, as scarce studies have investigated REE uptake mechanisms within both benthic and pelagic aquatic organisms through the dissolved, diet and particulate form (Cardon et al., 2020; Van Oosterhout and Lürling, 2013). The uptake mechanisms of dissolved REEs within pelagic organisms have been thoroughly studied (Cardon et al., 2019; Freitas et al., 2020; Hanana et al., 2021; Macmillan et al., 2019; Nørregaard et al., 2019; Pinto et al., 2019). Chapter 2 explored the exposure pathways (dissolved, diet, particulate) of REEs to six organisms from different trophic levels of the aquatic food web. Benthic organisms were characterized by light REEs indicating they mainly uptake REEs through their respective diets and particulate sand substrate with high bioaccumulation potential. Pelagic organisms were characterized by heavy REE enrichment indicating they primarily uptook and bioaccumulated dissolved REEs. The results from Chapter 2 were the first to identify benthic organisms such as mussels and snails and pelagic organisms such as minnows as potential monitoring species for the environmental risk assessment of REEs in natural systems, especially in selecting organisms depending on REE exposure pathways

(dissolved contamination, REE-rich sediment or contaminated food). However, limitations arise when using diet accumulation factors to access bioaccumulation for benthic organisms, since this factor does not consider the secondary particulate exposure route for benthic organisms. Since the sand substrate readily scavenged dissolved REEs, and benthic organisms were submerged in sand, it would be beneficial to compare biota sediment accumulation factors (BSAF) to diet accumulation factors, to determine which exposure pathway is the most dominant (Donaher et al., 2024; Geest and Watson-Leung, 2016). Chapter 3 showed La enrichment within benthic bloodworms and bottom waters were directly from the sediment reservoir. These results showed evidence that particulates influence benthic environments, thus, the biota sediment bioaccumulation factor is necessary to show the influence of sediment on biota. Further studies are required to shed light on REEs' uptake and elimination processes in these organisms to fully understand the biochemical mechanisms and ecotoxicology of REEs in aquatic species.

The REE uptake mechanism and bioaccumulation results for organisms from Chapter 2 were applied during the interpolation for chapter 3 of this study. The fate and distribution of REEs are understudied in environments exposed to La-coagulants (Bacha et al., 2022). For Chapter 3, field sampling was conducted within Swan Lake amended with La-coagulants to determine the fate, distribution, and enrichment of REEs throughout abiotic and biotic compartments. Previous research has explored the organotropisms, trophic transfer, dilution/bioaccumulation trends in natural aquatic ecosystems that represent background REE levels (Amyot et al., 2017; Arienzo et al., 2022; Labassa et al., 2023; Lortholarie et al., 2021; Marginson et al., 2023; Rétif et al., 2024; Santos et al., 2023). However, this research addresses some of the key components

missing regarding the REE enrichment, bioaccumulation, and distribution within ecosystems exposed to higher levels of REEs through point source means. The combinations of Chapter 2 results and La anomalies in Chapter 3 helped directly relate the extent of REE enrichment and transfer of REEs between abiotic and biotic compartments. The REE enrichment within benthic organisms was directly caused by exposure to the enriched REE particulates from the sediment reservoir. The REE enrichment within pelagic organisms was directly due exposure to REE-enriched dissolved and REE-laden diet.

Further, it is challenging to quantify REE levels within brain tissues of organisms collected from background conditions due to difficulties reaching analytical detection limits. However, the results from Chapter 3 quantified the enrichment of La in the brain of fathead minnows. Rare earth element concentrations within the brain of minnows were quantified because organisms were living within an environment amended to LMB and exposed to high enough REE levels within the diet and ambient environment to accumulate in the brain and meet analytical detection limits. There is currently no other evidence of REE enrichment in the brains of wild aquatic organisms. However, the evidence of REE crossing the blood-brain barrier in clinical trials (Damme et al., 2020; Eisele et al., 1980; McDonald et al., 2017; Vergauwen et al., 2018; Xia et al., 2011) and the high La concentrations within minnow's brain would support the hypothesis of the capacity for La to reach the brain tissues. These preliminary results are the first evidence that has discovered this REE organotropism brain trend. The uptake mechanisms, bioaccumulation, and enrichment results from Chapters 2 and 3 are important and open a novel direction in research on the biochemical processes of lanthanides causing

enrichment of REEs in the brain and the rest of the body of aquatic vertebrates. Specifically, Swan Lake could shed light on these new biochemical directions. The lake was applied with poly aluminum chloride in August 2021 post-sampling trips. Thus, all the phytoplankton enriched with REEs were removed from the water column and suspended in the sediment as organic mass. Thus, this could increase the exposure of REEs to benthic bullhead individuals compared to pelagic minnows, which contained high REE levels due to exposure to REE-contaminated phytoplankton and water post-application of LMB.

4.2 Future Work

This study highlighted REE organotropism, exposure pathways, and enrichment trends in aquatic organisms under environmentally relevant mesocosm conditions and in an ecosystem amended with La-coagulants. There is knowledge of REE organotropism under background levels within aquatic food webs throughout global water bodies (Amyot et al., 2017; Marginson et al., 2023; Rétif et al., 2024; Santos et al., 2023). However, this preliminary field study was the first to determine La enrichment throughout abiotic and biotic compartments within a lake amended with La coagulants. Specifically, evidence regarding the highest La enrichment within the brain of fathead minnow requires further investigations to determine whether this is a standalone trend or if there could be a prevalent risk within aquatic ecosystems exposed to higher REE levels. Thus, future sampling exhibitions within Swan Lake and other Canadian lakes amended with La-coagulants would be useful to validate the REE enrichment trends within aquatic organisms. There are universal knowledge gaps about the translocation mechanisms of REEs throughout aquatic organisms (Henao et al., 1992; Ogurusu et al., 1991).

Ecotoxicological studies are needed to understand the REE translocation processes throughout organisms and determine the certain target protein binding sites for REEs within cells. Knowing where REEs are most susceptible to accumulate in cells and the specific binding mechanisms causing enrichment is valuable information for how REEs accumulate in organisms.

Furthermore, even though the uptake mechanisms of three REE exposure pathways were studied, there is also less information on the trophic transfer and assimilation efficiency of REEs from prey to predator (Cardon et al., 2020). Evidence from Chapter 3 showed the potential trophic transfer of a REE-laden diet of phytoplankton to fathead minnows. Thus, it is essential to investigate the amount of REE-laden diet assimilated in aquatic organisms and track the translocation of REEs from prey throughout the body into cells. In addition, the exposure pathways experiment in Chapter 2 could be expanded to further investigate bioaccumulation mechanisms of REEs by designing a short or longer-term exposure bioaccumulation interval trial. A larger sample size of various organisms could be exposed to the three REE end members (diet, dissolved, and particulate) and regularly measure the concentration of REEs within their bodies over a set period, to observe if there is a build up of REEs over time, demonstrating the process of bioaccumulation. There could also be investigations to determine if in-situ sediment from where benthic organisms were collected also induce LREE enrichment through uptake of particulates. Furthermore, bioconcentration and diet bioaccumulation factors are specific calculations that subjectively targets the source end member to organisms, and it is assumed organisms are exposed to one source. However, in the natural aquatic system organisms are exposed to all members, thus it would be

essential to generate a bioaccumulation model that incorporates all exposure end members (diet, dissolved, and particulate) which consider the rate of uptake for each end members. Thorough experiments would be required to investigate the rate of uptake of each end member for various organisms found at different levels of aquatic food webs and under numerous environments with varying physiochemical parameters. Lastly, environmental context is important regarding the availability of REEs within different exposure pathways. Understanding REE organotropism and REE distribution in abiotic and biotic compartments of aquatic ecosystems under fluctuating pH, dissolved oxygen, alkalinity, temperature, dissolved inorganic carbon, and multiple seasons is necessary as these chemical parameters influence the susceptibility of REEs being available for uptake by aquatic organisms (Dithmer et al., 2015; Spears et al., 2013).

There are multiple knowledge gaps mentioned above that limit our understanding of REE mechanisms in aquatic ecosystems, however, further research should continue to help better understand these sections. Within the context of this present study, further exploration into trophic transfer assimilation, translocation mechanisms of REE within aquatic organism cells post-exposure to three pathways forms (dissolved, diet, particulate), and how seasonal changes impact the chemical availability of REEs within the particulate, dissolved, and diet forms to aquatic organisms in ecosystems would be useful. Incorporating both the translocation/binding mechanism of REEs within aquatic organisms and REE distribution throughout ecosystems under varying seasons will continue to improve the understanding of REE accumulation mechanisms and under what chemical parameters are certain aquatic organisms most susceptible to accumulating

REEs. This will narrow down which model species is used to monitor rising REE levels in water systems for resource protection.

4.3 References

Amyot, M., Clayden, M.G., Macmillan, G.A., Perron, T., Arscott-Gauvin, A., 2017. Fate and trophic transfer of rare earth elements in temperate lake food webs. Environ Sci Technol 51, 6009–6017. https://doi.org/10.1021/acs.est.7b00739

Arienzo, M., Ferrara, L., Trifuoggi, M., Toscanesi, M., 2022. Advances in the fate of rare earth elements, REE, in transitional environments: Coasts and estuaries. Water (Basel) 14, 401. https://doi.org/10.3390/w14030401

Bacha, L., Ventura, R., Barrios, M., Seabra, J., Tschoeke, D., Garcia, G., Masi, B., Macedo, L., Godoy, J.M. de O., Cosenza, C., de Rezende, C.E., Lima, V., Ottoni, A.B., Thompson, C., Thompson, F., 2022. Risk of collapse in water quality in the Guandu River (Rio de Janeiro, Brazil). Microb Ecol 84, 314–324. https://doi.org/10.1007/s00248-021-01839-z

Cardon, P.Y., Roques, O., Caron, A., Rosabal, M., Fortin, C., Amyot, M., 2020. Role of prey subcellular distribution on the bioaccumulation of yttrium (Y) in the rainbow trout. Environ Pollut 258, 113804. https://doi.org/10.1016/j.envpol.2019.113804

Cardon, P.Y., Triffault-Bouchet, G., Caron, A., Rosabal, M., Fortin, C., Amyot, M., 2019. Toxicity and subcellular fractionation of yttrium in three freshwater organisms: Daphnia magna, Chironomus riparius, and Oncorhynchus mykiss. ACS Omega 4, 13747–13755. https://doi.org/10.1021/acsomega.9b01238

Damme, N.M., Fernandez, D.P., Wang, L.M., Wu, Q., Kirk, R.A., Towner, R.A., McNally, J.S., Hoffman, J.M., Morton, K.A., 2020. Analysis of retention of gadolinium by brain, bone, and blood following linear gadolinium-based contrast agent administration in rats with experimental sepsis. Magn Reson Med 83, 1930–1939. https://doi.org/10.1002/mrm.28060

Dithmer, L., Lipton, A.S., Reitzel, K., Warner, T.E., Lundberg, D., Nielsen, U.G., 2015. Characterization of phosphate sequestration by a lanthanum modified bentonite clay: A solid-state NMR, EXAFS, and PXRD study. Environ Sci Technol 49, 4559–4566. https://doi.org/10.1021/es506182s

Donaher, S.E., Estes, S.L., Dunn, R.P., Gonzales, A.K., Powell, B.A., Martinez, N.E., 2024. Site- and species-specific metal concentrations, mobility, and bioavailability in sediment, flora, and fauna of a southeastern United States salt marsh. Sci Total Environ 922, 171262. https://doi.org/10.1016/j.scitotenv.2024.171262

Eisele, G.R., Mraz, F.R., Woody, M.C., 1980. Gastrointestinal uptake of 144Ce in the neonatal mouse, rat, and pig. Health Phys 39, 185–192. https://doi.org/10.1097/00004032-198008000-00004

Freitas, R., Costa, S., D Cardoso, C.E., Morais, T., Moleiro, P., Matias, A.C., Pereira, A.F., Machado, J., Correia, B., Pinheiro, D., Rodrigues, A., Colónia, J., Soares, A.M.V.M., Pereira, E., 2020. Toxicological effects of the rare earth element neodymium in Mytilus galloprovincialis. Chemosphere 244, 125457. https://doi.org/10.1016/j.chemosphere.2019.125457

Geest, J. Van, Watson-Leung, T., 2016. Bioaccumulation of sediment-associated contaminants in freshwater organisms. Ontario Ministry of the Environment and Climate Change 1–91.

Hanana, H., Kleinert, C., Gagné, F., 2021. Toxicity of representative mixture of five rare earth elements in juvenile rainbow trout (Oncorhynchus mykiss) juveniles. Environ Sci Pollut R 28, 28263–28274. https://doi.org/10.1007/s11356-020-12218-5/Published

Henao, F., Orlowski, S., Merah, Z., Champeil, P., 1992. The metal sites on sarcoplasmic reticulum membranes that bind lanthanide ions with the highest affinity are not the ATPase Ca2+ transport sites. J Biol Chem 267, 10302–10312. https://doi.org/10.1016/s0021-9258(19)50018-7

Labassa, M., Pereto, C., Schäfer, J., Hani, Y.M.I., Baudrimont, M., Bossy, C., Dassié, É.P., Mauffret, A., Deflandre, B., Grémare, A., Coynel, A., 2023. First assessment of rare earth element organotropism in Solea solea in a coastal area: The west Gironde Mud Patch (France). Mar Pollut Bull 197, 115730. https://doi.org/10.1016/j.marpolbul.2023.115730

Lortholarie, M., Poirier, L., Kamari, A., Herrenknecht, C., Zalouk-Vergnoux, A., 2021. Rare earth element organotropism in European eel (Anguilla anguilla). Sci Total Environ 766, 142513. https://doi.org/10.1016/j.scitotenv.2020.142513

Macmillan, G.A., Clayden, M.G., Chételat, J., Richardson, M.C., Ponton, D.E., Perron, T., Amyot, M., 2019. Environmental drivers of rare earth element bioaccumulation in freshwater zooplankton. Environ Sci Technol 53, 1650–1660. https://doi.org/10.1021/acs.est.8b05547

Marginson, H., MacMillan, G.A., Grant, E., Gérin-Lajoie, J., Amyot, M., 2023. Rare earth element bioaccumulation and cerium anomalies in biota from the Eastern Canadian subarctic (Nunavik). Sci Total Environ 879, 163024. https://doi.org/10.1016/j.scitotenv.2023.163024

McDonald, R.J., McDonald, J.S., Kallmes, D.F., Jentoft, M.E., Paolini, M.A., Murray, D.L., Williamson, E.E., Eckel, L.J., 2017. Gadolinium deposition in human brain tissues after contrast-enhanced MR imaging in adult patients without intracranial abnormalities. Radiology 285, 546–554. https://doi.org/10.1148/radiol.2017161595

Nørregaard, R.D., Kaarsholm, H., Bach, L., Nowak, B., Geertz-Hansen, O., Søndergaard, J., Sonne, C., 2019. Bioaccumulation of rare earth elements in juvenile arctic char (Salvelinus alpinus) under field experimental conditions. Sci Total Environ 688, 529–535. https://doi.org/10.1016/j.scitotenv.2019.06.180

Ogurusu, T., Wakaboyashi, S., Munekazu, S., 1991. Functional characterization of lanthanide binding sites in the sarcoplasmic reticulum Ca2+-ATPase: Do lanthanide ions bind to the calcium transport site? Biochemistry 30, 9966–9973. https://doi.org/10.1021/bi00105a022

Pinto, J., Costa, M., Leite, C., Borges, C., Coppola, F., Henriques, B., Monteiro, R., Russo, T., Di Cosmo, A., Soares, A.M.V.M., Polese, G., Pereira, E., Freitas, R., 2019. Ecotoxicological effects of lanthanum in Mytilus galloprovincialis: Biochemical and histopathological impacts. Aquat Toxicol 211, 181–192. https://doi.org/10.1016/j.aquatox.2019.03.017

Rétif, J., Zalouk-Vergnoux, A., Briant, N., François, Y., Poirier, L., 2024. Trophic dilution of rare earth elements along the food chain of the Seine estuary (France). Mar Pollut Bull 206, 116671. https://doi.org/10.1016/j.marpolbul.2024.116671

Santos, A.C.S.S., Souza, L.A., Araujo, T.G., de Rezende, C.E., Hatje, V., 2023. Fate and trophic transfer of rare earth elements in a tropical estuarine food web. Environ Sci Technol 57, 2404–2414. https://doi.org/10.1021/acs.est.2c07726

Spears, B.M., Lürling, M., Yasseri, S., Castro-Castellon, A.T., Gibbs, M., Meis, S., McDonald, C., McIntosh, J., Sleep, D., Van Oosterhout, F., 2013. Lake responses following lanthanum-modified bentonite clay (Phoslock®) application: An analysis of water column lanthanum data from 16 case study lakes. Water Res 47, 5930–5942. https://doi.org/10.1016/j.watres.2013.07.016

Van Oosterhout, F., Lürling, M., 2013. The effect of phosphorus binding clay (Phoslock®) in mitigating cyanobacterial nuisance: A laboratory study on the effects on water quality variables and plankton. Hydrobiologia 710, 265–277. https://doi.org/10.1007/s10750-012-1206-x

Vergauwen, E., Vanbinst, A.M., Brussaard, C., Janssens, P., De Clerck, D., Van Lint, M., Houtman, A.C., Michel, O., Keymolen, K., Lefevere, B., Bohler, S., Michielsen, D., Jansen, A.C., Van Velthoven, V., Gläsker, S., 2018. Central nervous system gadolinium accumulation in patients undergoing periodical contrast mri screening for hereditary tumor syndromes. Hered Cancer Clin Pract 16, 1–9. https://doi.org/10.1186/s13053-017-0084-7

Xia, Q., Feng, X., Huang, H., Du, L., Yang, X., Wang, K., 2011. Gadolinium-induced oxidative stress triggers endoplasmic reticulum stress in rat cortical neurons. J Neurochem 117, 38–47. https://doi.org/10.1111/j.1471-4159.2010.07162.x

Appendix A1: Chapter 2

Table A1.1 Composition of modified MAM (Modified Acid Medium) including Otonabee River used to culture *Euglena gracilis*. The recipe for MAM was formulated based on Olaveson & Stokes., (1989).

	Stock Concentration (g/L)	**Volume of Stock (mL) added to make Working Solution**	**Working Solution (g/L)**
KH_2PO_4	30	10	0.3
$(NH_4)_2SO_4$	50	10	0.5
$MnCl_2 * 4H_2O$	1.81	1	0.0081
$ZnNO_3 * 6H_2O$	0.23	1	0.00023
$Na_2MoO_4 * 2H_2O$	0.39	1	0.00039
$CuSO_4* 5H_2O$	0.079	1	0.000079
Biotin	1	1	0.001
Vitamin B12	0.1	1	0.0001
Otonabee River Water (four major ions: Ca^{2+}, Mg^{2+}, Na^{+}, Cl^{-})		978	

Olaveson, M., & Stokes, P. M. (1989). Responses of the acidophilic alga *Euglena mutabillis* (*Euglenophyceae*) to carbon enrichment at pH 3. Journal of Phycology. 25. 529-539.

Table A1.2 Sample size (n) and details regarding subsample tissue types of interest, and the type of feed exposed to test subjects during the entirety of the experiment.

Sample Group	Tissue Part	n	Length Range (cm)	Composite vs. Discrete	Food Source	Additional Information
Euglena gracilis	whole, soft	6	N/A	D	River Growing Medium	Grown in a 1:4 ratio of Euglena and River MAM
Daphnia magna	whole, soft	ca. 50	N/A	C	spirulina powder & chickpea powder	100 individuals divided into 2 composite samples (n =2)
Back sandshell mussel (*Ligumia recta*)	soft tissue	5	6 - 7.5	D	spirulina powder & chickpea powder	
	hard tissue	5		D		
Chinese mystery snail (*Cipangopaludina chinensis*)	soft tissue	6	2.2 – 3.5	D	spirulina powder & chickpea powder	
	hard tissue	6		D		
Northern clearwater crayfish (*Faxonius propinquus*)	soft tissue	4	5.5 - 8.5	D	shrimp pellets	
	hard tissue	4		D		
	internal organs	4		D		
	antennal glands	4		D		
	gills	10		C		
Striped shiner minnows (*Luxilus chrysocephalus)*	swim bladder	10	6.8 - 9.7	C	spirulina flakes	10 individuals divided into 2 composite samples (n=5 minnow tissues in one composite sample)
	liver	10		C		
	intestines	10		C		
	soft tissue	10		C		

Table A1.3 Measured, certified, and informational (represented by *) concentrations (mg kg^{-1}) of 33 trace elements in CRMs NIST-1515 and NIST-1566a.

Elements	NIST 1515 (mg kg^{-1})			NIST 1566a (mg kg^{-1})		
	Measured Concentrations (n=1)	**Certified Concentrations**	**S.D.**	**Measured Concentrations (n=1)**	**Certified Concentrations**	**S.D.**
B	24.4	27.6	2.8	4.7		
Ba	42.9	48.8	2.3	1.24		
Cd	0.02	0.01	0.002	3.33	4.15	0.38
Ce	2.69	3.00*		0.18	0.40*	
Co	0.67	0.09*		0.21	0.57	0.11
Cs	0.004			0.01	0.02*	
Cu	4.71	5.69	0.13	48.61	66.30	4.30
Dy	1.54			0.04		
Er	0.48			0.02		
Eu	0.22	0.20*		0.01	0.01*	
Fe	68.2	82.7	2.6	526.2	539.0	15.0
Gd	2.7	3.0*		0.04		
Ho	0.27			0.01		
La	18.9	20.0*		0.15	0.30*	
Lu	0.02			0.01		
Mn	49.3	54.1	1.1	8.68	12.3	1.5
Nb	1.17			0.48		
Nd	14.5	17.0*		0.15		
Pb	0.32	0.47	0.02	0.27	0.37	0.01
Pr	3.72			0.03		
Rb	8.41	10.20	1.60	2.37	3.00*	
Sc	0.02	0.03*		0.03	0.06*	
Se	1.01			0.95	2.21	0.24
Sm	2.52	3.00*		0.04	0.06*	
Sr	22.0	25.1	1.1	7.9	11.1	1.0
Tb	0.31	0.40*		0.01	0.01*	
Th	0.08	0.03*		0.03	0.04*	
Tm	0.04			0.002		
U	0.003	0.006*		0.09	0.13	0.01
V	0.08	0.25	0.03	3.03	4.68	0.15
Y	8.34			0.23		
Yb	0.17	0.30*		0.03		
Zn	10.87	12.45	0.43	747.01	830.00	57.00

Table A1.4 Measured, certified, and literature concentrations (μg L^{-1}) of 49 trace elements in liquid CRM SLRS-6 and NIST 1640a. Symbol (*) demarks concentrations reported by Yeghicheyan et al., (2019) and (**) represents concentrations from Sugiyama, (2020).

	SLRS – 6 (μg L^{-1})				NIST 1640a (μg L^{-1})			
Elements	**Measured Concentrations (n=50)**	**S.D.**	**Certified Concentrations (n=9)**	**S.D.**	**Measured Concentrations (n=57)**	**S.D.**	**Certified Concentrations (n=9)**	**S.D.**
Al	38.7	1.6	33.8	2.2	61.0	2.2	53.0	1.8
As	0.7	0.1	0.6	0.1	8.1	0.9	8.1	0.1
B	10.9	1.9	7.4*	1.2	306.0	130.5	303.1	3.1
Ba	18.4	1.1	14.3	0.5	191.2	9.8	151.8	0.8
Be	0.008	0.004	0.007	0.002	3.35	0.59	3.00	0.03
Cd	0.012	0.002	0.006	0.001	4.17	0.06	3.99	0.07
Ce	0.31	0.01	0.29*	0.02	0.004	0.001		
Co	0.05	0.00	0.05	0.01	20.59	0.21	20.24	0.24
Cr	0.33	0.01	0.25*	0.01	43.03	0.62	40.50	0.30
Cs	0.009	0.004	0.005*	0.001	0.031	0.006		
Cu	31.0	0.3	24.0	1.8	103.8	1.2	85.8	0.5
Dy	0.025	0.002	0.022*	0.001	0.013	0.016		
Er	0.013	0.002	0.012*	0.001	0.012	0.006		
Eu	0.010	0.001	0.007*	0.0004	0.021	0.002		
Fe	98.6	1.4	84.5	3.6	44.5	0.7	36.8	1.8
Gd	0.032	0.003	0.032*	0.003	0.004	0.001		
Ge	0.02	0.01	0.01*	0.01	0.008	0.005		
Hf	0.034	0.029	0.010*	0.0004	0.071	0.099		
Ho	0.0049	0.0003	0.0043*	0.0003	0.011	0.022		
K	779	21	652	54	712	22	580	2
La	0.29	0.01	0.25*	0.01	0.011	0.001		
Li	0.59	0.07	0.53*	0.03	0.47	0.07	0.41	0.01
Lu	0.002	0.0005	0.002*	0.0002	0.005	0.001		
Mg	2348	85	2137	58	1170	51	1057	41
Mn	2.5	0.0	2.1	0.1	46.0	0.6	40.4	0.4
Mo	0.4	0.1	0.2	0.02	45.8	1.8	45.6	0.6
Na	3534.1	140.6	2770.0	220.0	4056.0	153.5	4137.0	31.0
Nd	0.23	0.01	0.23*	0.01	0.01	0.004		
Ni	0.67	0.04	0.62*	0.02	26.49	0.33	25.32	0.14
Pb	0.18	0.01	0.17	0.03	12.15	0.40	12.10	0.05
Pr	0.064	0.002	0.059*	0.002	0.004	0.000		
Rb	1.49	0.04	1.41*	0.05	1.25	0.05		
Re	0.017	0.003	0.014*	0.0002	0.005	0.008		
Rh	0.004	0.0	0.001*	0.0002	0.004	0.004		
Sb	0.36	0.04	0.34	0.01	4.95	0.26	5.10	0.05
Sc	0.02	0.00	0.02**	0.0	0.04	0.02		
Sm	0.041	0.002	0.040*	0.002	0.009	0.002		
Sn	0.02	0.04	0.01*	0.01	0.10	0.09		
Sr	42.1	0.5	40.7	0.3	129.2	2.1	126.0	0.9
Tb	0.004	0.000	0.004*	0.0003	0.001	0.0002		
Th	0.013	0.004	0.016*	0.007	0.016	0.025		
Ti	0.09	0.18	0.53*	0.01	1.92	0.63	1.62	0.02
Tm	0.002	0.001	0.002*	0.0002	0.002	0.0005		
U	0.07	0.003	0.07	0.003	25.59	0.86	25.40	0.27
V	0.36	0.02	0.35	0.01	14.88	0.86	15.00	0.25
Y	0.13	0.004	0.13*	0.01	0.08	0.01		
Yb	0.012	0.001	0.011*	0.001	0.02	0.002		
Zn	2.4	0.0	1.8	0.1	69.0	0.5	55.6	0.4
Zr	0.09	0.03	0.06	0.01	0.07	0.09		

Table A1.5 Average concentrations (AVG) and standard error (SE) of REEs in the test organisms (μg kg^{-1}). The concentrations have been rounded to the most appropriate significant figures.

Organisms	Tissues	La		Ce		Pr		Nd		Sm		Gd	
		AVG	SE	AVG	SE	AVG	SE	AVG	SE	AVG	SE	AVG	SE
Snail	soft tissue	650	220	1300	490	160	59	610	240	120	48	110	43
	hard tissue	233	21	404	54	48	5.3	180	21	33	4.5	29	4.3
Mussel	soft tissue	5700	3000	4000	2000	570	300	2200	1200	350	190	310	170
	hard tissue	790	200	1400	360	150	42	560	150	85	23	68	16
Crayfish	internal organs	97	64	210	140	25	18	110	77	24	15	21	14
	soft tissue	27	15	59	30	6.2	3.0	25	13	5.5	2.4	4.7	2.2
	hard tissue	330	200	820	430	90	51	350	210	68	42	66	38
	antennal glands	830	550	1800	600	230	150	890	580	170	120	160	110
Minnow	gills	4.6		8.7		1.4		2.5		0.7		1.7	
	liver	30		55		7.9		25		1.5		8.7	
	swim bladder	8.8		9.1		1.7		3.6		1.0		1.0	
	intestines	58		93		15		47		9.4		11	
E. gracilis	whole body	53	4.2	80	6.7	14	1.1	49	3.1	10	0.8	8.1	1.0
D. magna	whole body	18	1.5	31	1.9	7.4	1.0	17	0.5	5.6	0.01	4.6	0.1

Organisms	Tissues	Tb		Dy		Ho		Er		Tm		Yb		Lu	
		AVG	SE	AVG	SE	AVG	SE	AVG	SE	AVG	SE	AVG	SE	AVG	SE
Snail	soft tissue	15	5.9	80	31	16	6.1	43	16	7.0	2.8	35	13	5.6	2.1
	hard tissue	4.0	0.6	21	3.2	4.2	0.6	11	1.5	1.9	0.3	8.8	1.3	1.4	0.2
Mussel	soft tissue	31	16	140	72	29	14	70	35	11	5.6	61	30	11	5.2
	hard tissue	8.8	2.1	45	11	9.6	2.0	28	6.6	4.4	0.8	24	5.2	3.8	0.8
Crayfish	internal organs	2.9	1.8	15	11	3.4	2.2	7.9	5.2	0.7	0.6	5.7	4.7	1.0	0.6
	soft tissue	0.6	0.3	3.6	2.2	0.8	0.3	2.2	1.4			0.7	0.5	0.2	0.1
	hard tissue	11	6.2	48	29	11	6.3	26	15	3.4	2.2	24	14	4.1	2.2
	antennal glands	21	14	130	81	24	15	61	39	7.6	5.4	47	31	7.2	4.4
Minnow	gills			1.6		1.0		0.9				0.4		0.6	
	liver	0.9		4.6		1.3		4.4		0.4		5.9		0.9	
	swim bladder	0.5		2.4		0.3		0.5						0.4	
	intestines	2.6		11		3.0		7.4		1.3		7.2		2.0	
E. gracilis	whole body	1.3	0.2	8.2	0.8	1.5	0.2	5.3	0.7	0.2		2.8	1.3	0.8	0.1
D. magna	whole body	0.4	0.1	3.2	0.5	0.4	0.1	2.9	0.1	0.2	0.01	1.9	0.1		

Table A1.6 Average concentrations (AVG) and standard error (SE) of trace elements in the test subjects (μg kg^{-1}). The concentrations have been rounded to the most appropriate significant figures.

Sample Group	Tissue Part	Fe		Sc		Zn		V		Co		Cu		Cd	
		AVG	SE	AVG	SE	AVG	SE	AVG	SE	AVG	SE	AVG	SE	AVG	SE
Snail	soft tissue			410	99	260	20	640	170	410	59	140	14	430	28
	hard tissue			130	22	5.6	1.0	190	20	120	13	3.8	1.0	11	1.6
Mussel	soft tissue	2000		730	190	96	26	120	18	580	260	5.3	0.7	2100	1100
	hard tissue	130		280	90	2.9	0.1	460	180	270	35	4.7	1.4	18	3.8
Crayfish	internal organs	140	60	18	12	91	20	300	120	2000	840	88	3.6	660	200
	soft tissue	36	15			100	6.6	43	16	99	15	65	18	28	4.9
	hard tissue	360	200	60	34	15	5.1	520	290	490	100	15	5.2	17	2.9
	antennal glands	630	380	98	61	48	14	970	560	1200	310	33	7.5	99	18
	gills	120				160		130		17		3.5		4.7	
Minnow	liver	300		3.6		56		160		47		36		30	
	swim bladder	53				76		54		18		6.4		11	
	intestines	200		6.2		73		87		49		21		200	
E. gracilis	whole body	110	7.4	6.8	0.6	190	12	100	8.9	9000	580	55	3.3	100	5.6
D. magna	whole body			2.7	0.7	260	2.7	43	8.0	68	15	30	5.0	380	41

Sample Group	Tissue Part	Cs		Sr		Y		Rb		U		Pb		Th	
		AVG	SE	AVG	SE	AVG	SE	AVG	SE	AVG	SE	AVG	SE	AVG	SE
Snail	soft tissue	23	5.9			630	220	2900	120	86	7.3	560	140	59	25
	hard tissue	7.1	1.0			160	21	120	21	15	0.7	230	18	20	2.9
Mussel	soft tissue	36	5.2	90000		1700	950	2900	350	130	43	230	76	39	16
	hard tissue	2.6	0.6	190000		410	100	57	14	21	4.7	85	18	15	4.5
Crayfish	internal organs	27	4.7	9700	1200	80	56	7100	810	23	8.4	180	71	31	16
	soft tissue	67	15	9000	1300	19	9.6	11700	1400	1.9	0.7	75	15	12	5.3
	hard tissue	24	7.6	420000	15600	250	150	2200	510	18	9.5	590	210	60	31
	antennal glands	32	14	66000	2500	640	420	3200	120	51	29	780	440	93	55
	gills	5.9		33000		6.8		5300		10		96		2.6	
Minnow	liver	9.0		1400		22		4600		8.7		550		6.3	
	swim bladder	5.6		1400		7.5		2900		2.8		120			
	intestines	9.5		1300		41		4800		8.1		940		7.1	
E. gracilis	whole body	4.7	1.1	1900	75	43	4.1	100	10	300	27	140	11	14	3.0
D. magna	whole body			54300	7100	19	0.4	900	13	55	13	560	8.9	2.2	0.3

Table A1.7 Average concentrations (AVG) and standard error (SE) of REEs in the exposure feed (µg kg^{-1}), and Otonabee River water (µg L^{-1}). The concentrations have been rounded to the most appropriate significant figures.

Organisms	Exposure Type	La		Ce		Pr		Nd		Sm		Gd	
		AVG	SE	AVG	SE	AVG	SE	AVG	SE	AVG	SE	AVG	SE
Crayfish	shrimp pellets	1200	47	2600	98	310	14	1300	50	250	9.9	230	9.4
Minnow	spirulina flakes	360	48	840	120	25	1.2	88	2.4	17	0.5	21	1.0
D.magna, mussel, snail	spirulina & chickpea powder	35	12	75	26	8.0	2.8	29	10	5.6	2.0	5.3	1.9
	Otonabee river	0.07		0.1		0.02		0.05		0.01		0.01	

Organisms	Exposure Type	Tb		Dy		Ho		Er		Tm		Yb		Lu	
		AVG	SE	AVG	SE	AVG	SE	AVG	SE	AVG	SE	AVG	SE	AVG	SE
Crayfish	shrimp pellets	33	1.4	200	7.7	35	1.3	100	3.1	12	0.1	72	1.1	9.9	0.2
Minnow	spirulina flakes	2.1	0.1	11	0.3	2.0	0.1	5.9	0.1	0.7	0.04	4.7	0.2	0.7	0.02
D.magna, mussel, snail	spirulina & chickpea powder	0.7	0.3	4.1	1.4	0.8	0.3	2.5	0.9	0.4	0.1	2.5	0.9	0.5	0.2
	Otonabee river	0.003		0.01		0.004		0.01		0.001		0.01		0.01	

Table A1.8 Average concentrations (AVG) and standard error (SE) of REE fractionations (Tb_{MREE}/La_{LREE} & Er_{HREE}/La_{LREE}) and Ce/Ce* anomalies for test subjects, exposure diet, and Otonabee river.

Organisms	Tissues	Number	Tb_{PAAS}/La_{PAAS}		Er_{PAAS}/La_{PAAS}		Ce/Ce*	
			AVG	SE	AVG	SE	AVG	SE
Snail	soft tissue	6	1.0	0.1	0.8	0.04	0.9	0.04
	hard tissue	6	0.8	0.1	0.6	0.04	0.9	0.04
Mussel	soft tissue	6	0.3	0.008	0.2	0.02	0.5	0.01
	hard tissue	6	0.6	0.04	0.5	0.1	0.9	0.03
Crayfish	internal organs	4	1.7	0.1	1.0	0.2	1.1	0.05
	soft tissue	4	1.4	0.1	0.8	0.2	1.1	0.004
	hard tissue	4	1.6	0.2	1.0	0.03	1.3	0.2
	antennal glands	4	1.4	0.1	1.1	0.1	1.2	0.2
Minnow	gills	10			2.7		0.8	
	liver	10	1.5		2.0		0.8	
	swim bladder	10	2.9		0.8		0.5	
	intestines	10	2.2		1.7		0.7	
E. gracilis	whole body	6 containers	1.2	0.1	1.3	0.1	0.7	0.02
D. magna	whole body	100	1.1	0.1	2.1	0.1	0.6	0.1

Organisms	Exposure Type	Number	Tb_{PAAS}/La_{PAAS}		Er_{PAAS}/La_{PAAS}		Ce/Ce*	
			AVG	SE	AVG	SE	AVG	SE
Crayfish	shrimp pellets	4	1.3	0.01	1.1	0.02	1.0	0.01
Minnow	spirulina flakes	4	0.3	0.03	0.2	0.03	1.7	0.05
D.magna, mussel, snail	spirulina & chickpea powder	4	1.3	0.3	1.2	0.3	1.0	0.03
All Organisms	Otonabee river	1	1.7		1.2		0.8	

Table A1.9 Diet bioaccumulation factors (DAF) and bioconcentration factors (BCF) for LREEs (La to Nd). The DAF and BCF values have been rounded to the most appropriate significant figures.

Organisms	Tissue	Food Type	La				Ce				Pr				Nd			
			DAF		BCF		DAF		BCF		DAF		BCF		DAF		BCF	
			AVG	SE	AVG	SE	AVG	SE	AVG	SE	AVG	SE	AVG	SE	AVG	SE	AVG	SE
Snail	soft tissue	chickpea & spirulina powder	19*	13	N/A		17*	13	N/A		20*	14	N/A		21*	16	N/A	
	hard tissue		6.6*	2.9	N/A		5.4*	2.6	N/A		6.0*	2.8	N/A		6.0*	2.9	N/A	
Mussel	soft tissue	chickpea & spirulina powder	160*	140	N/A		53*	46	N/A		72*	64	N/A		74*	66	N/A	
	hard tissue		22*	14	N/A		19*	11	N/A		19*	12	N/A		19*	12	N/A	
Crayfish	internal organs	shrimp pellets	0.10	0.06	N/A		0.08	0.06	N/A		0.10	0.06	N/A		0.10	0.06	N/A	
	soft tissue		0.02	0.01	N/A		0.02	0.01	N/A		0.05	0.01	N/A		0.02	0.01	N/A	
	hard tissue		0.3	0.2	N/A		0.32	0.2	N/A		0.3	0.2	N/A		0.3	0.2	N/A	
	antennal glands		0.7	0.4	N/A		0.70	0.5	N/A		0.7	0.5	N/A		0.7	0.4	N/A	
Minnow	gills	spirulina flakes	0.01	0.002	87*		0.01	0.002	95*		0.1	0.003	150*		0.03	0.001	49*	
	liver		0.1	0.01	560*		0.07	0.01	600*		0.3	0.02	810*		0.3	0.01	490*	
	swim bladder		0.02	0.003	170*		0.01	0.002	99*		0.1	0.003	170*		0.04	0.001	72*	
	intestines		0.05	0.01	1100*		0.04	0.01	1000*		0.05	0.002	1500*		0.04	0.001	930*	
D.magna	whole body	chickpea & spirulina powder	0.5	0.2	350*	29	0.4	0.2	340*	21	0.9	0.5	770*	99	0.6	0.2	340*	10
E.gracilis	whole body	Otonabee river	N/A		1000*	79	N/A		900*	73	N/A		1400*	114	N/A		970*	61

Table A1.10 Diet bioaccumulation factors (DAF) for MREEs (Sm to Tb) and HREEs (Dy to Lu). DAF values > 1 (symbol *) represent bio enrichment, whereas DAF values < 1 represent elimination. The DAF values have been rounded to the most appropriate significant figures.

Organisms	Tissue	Food Type	Sm		Gb		Tb		Dy		Ho		Er		Tm		Yb		Lu	
			DAF		DAF		DAF		DAF		DAF		DAF		DAF		DAF		DAF	
			AVG	SE	AVG	SE	AVG	SE	AVG	SE	AVG	SE	AVG	SE	AVG	SE	AVG	SE	AVG	SE
Snail	soft tissue	chickpea & spirulina powder	22*	16	21*	16	22*	16	20*	15	20*	15	17*	12	17*	13	14*	10	12*	8.9
	hard tissue		5.8*	2.9	5.5*	2.8	5.8*	3.0	5.2*	2.6	5.1*	2.5	4.3*	2.1	4.7*	2.4	3.5*	1.7	3.1*	1.5
Mussel	soft tissue	chickpea & spirulina powder	63*	56	58*	52	45*	39	35*	30	35*	30	28*	24	27*	24	24*	20	24*	20
	hard tissue		15*	9.4	13*	7.4	13*	7.5	11*	6.7	12*	6.6	11*	6.5	11*	5.9	9.4*	5.3	8.3*	4.7
Crayfish	internal organs	shrimp pellets	0.1	0.06	0.1	1.6	0.08	0.06	0.1	0.06	0.1	0.07	0.1	0.05	0.1	0.05	0.1	0.07	0.1	0.07
	soft tissue		0.02	0.01	0.02	1.3	0.02	0.01	0.02	0.01	0.02	0.01	0.02	0.01	0.003	0.00	0.01	0.01	0.02	0.01
	hard tissue		0.3	0.2	0.3	0.9	0.32	0.2	0.2	0.2	0.3	0.2	0.2	0.2	0.3	0.19	0.3	0.20	0.4	0.2
	antennal glands		0.7	0.5	0.7	0.4	0.70	0.5	0.6	0.4	0.7	0.5	0.6	0.40	0.7	0.47	0.7	0.5	0.7	0.5
Minnow	gills	spirulina flakes	0.04	0.001	0.1	0.01	0.01		0.1	0.004	0.5	0.01	0.2	0.004	0.0		0.1	0.00	0.9	0.02
	liver		0.1	0.00	0.4	0.3	0.07	0.01	0.4	0.01	0.6	0.02	0.8	0.02	0.5	0.03	1.3	0.05	1.2	0.03
	swim bladder		0.1	0.002	0.05	0.4	0.01	0.01	0.2	0.01	0.2	0.005	0.1	0.002	0.0		0.00		0.6	0.01
	intestines		0.04	0.00	0.05	0.2	0.04	0.002	0.1	0.00	0.1	0.003	0.1	0.002	0.1	0.01	0.1	0.004	0.2	0.005
D.magna	whole body	chickpea & spirulina powder	1.0	0.4	0.9	0.3	0.5	0.3	0.8	0.4	0.5	0.3	1.1	0.4	0.6	0.2	0.8	0.3		

Supplementary Text: Scavenging of rare earth elements on sand substrate

Various minerals in the sand substrate are responsible for scavenging dissolved REEs. SEM-EDX analyses (**Figure A1.1**) highlighted the dominance of Si and Al (silica and/or clay) and the presence of iron oxides and carbonates (Fe, Ca, and Mg concentrations). The removal of REEs by these minerals has been well documented in the literature. For example, REEs in groundwater of the Darling Hills granite terrain of southwestern South Africa are retained by clay, iron-oxides, and carbonates (Compton et al., 2003). Another experiment looking at the adsorption of REEs onto quartz sand at neutral pH values (6.8) and lower REE concentrations (10^{-7} M) highlighted between 90-100% sorption of all REEs onto strong surface sites like hydrous ferric oxides or hematite minerals (Iqbal et al., 2023). However, the authors observed more efficient removal of MREEs and HREEs by the sand than LREEs; it is important to note that the experiments were conducted with 5mM NaCl solution to shed light on the mechanistic surface complexation processes. This condition does not represent the natural conditions as other water chemistry parameters can impact REE sorption, especially the complexation with organic matter (Pourret et al., 2007), carbonates and phosphates (Censi et al., 2004; Deng et al., 2017).

Supplementary References:

Censi, P., Mazzola, S., Sprovieri, M., Bonanno, A., Patti, B., Punturo, R., Spoto, S. E., Saiano, F., & Alonzo, G. (2004). Rare earth elements distribution in seawater and suspended particulate of the Central Mediterranean Sea. *Chem Ecol*, *20*(5), 323–343. https://doi.org/10.1080/02757540410001727954

Compton, J. S., White, R. A., & Smith, M. (2003). Rare earth element behavior in soils and salt pan sediments of a semi-arid granitic terrain in the Western Cape, South Africa. *Chem Geol*, *201*(3–4), 239–255. https://doi.org/10.1016/S0009-2541(03)00239-0

Deng, Y., Ren, J., Guo, Q., Cao, J., Wang, H., & Liu, C. (2017). Rare earth element geochemistry characteristics of seawater and porewater from deep sea in western Pacific. *Sci Rep*, *7*(1), 16539. https://doi.org/10.1038/s41598-017-16379-1

Iqbal, M., Marsac, R., Davranche, M., Dia, A., & Hanna, K. (2023). A mechanistic surface complexation approach for the prediction of rare earth element reactive transport in quartz porous media. *Chem Geol*, *634*, 121601. https://doi.org/10.1016/j.chemgeo.2023.121601

Pourret, O., Davranche, M., Gruau, G., & Dia, A. (2007). Rare earth elements complexation with humic acid. *Chem Geol*, *243*(1–2), 128–141. https://doi.org/10.1016/j.chemgeo.2007.05.018

Sugiyama, N. (2020). Direct analysis of ultratrace rare earth elements in environmental waters by ICP-QQQ. *ICP-QQQ Applications in Geochemistry, Mineral Analysis, and Nuclear Science*, 56–61. https://www.agilent.com/cs/library/applications/application_ultratrace_ree_icp-qqq-5994-1785en_us_agilent.pdf

Yeghicheyan, D., Aubert, D., Bouhnik-Le Coz, M., Chmeleff, J., Delpoux, S., Djouraev, I., Granier, G., Lacan, F., Piro, J. L., Rousseau, T., Cloquet, C., Marquet, A., Menniti, C., Pradoux, C., Freydier, R., Vieira da Silva-Filho, E., & Suchorski, K. (2019). A new interlaboratory characterisation of silicon, rare earth elements and twenty-two other trace element concentrations in the natural river water certified reference material SLRS-6 (NRC-CNRC). *Geostand Geoanal Res*, *43*(3), 475–496. https://doi.org/10.1111/ggr.12268

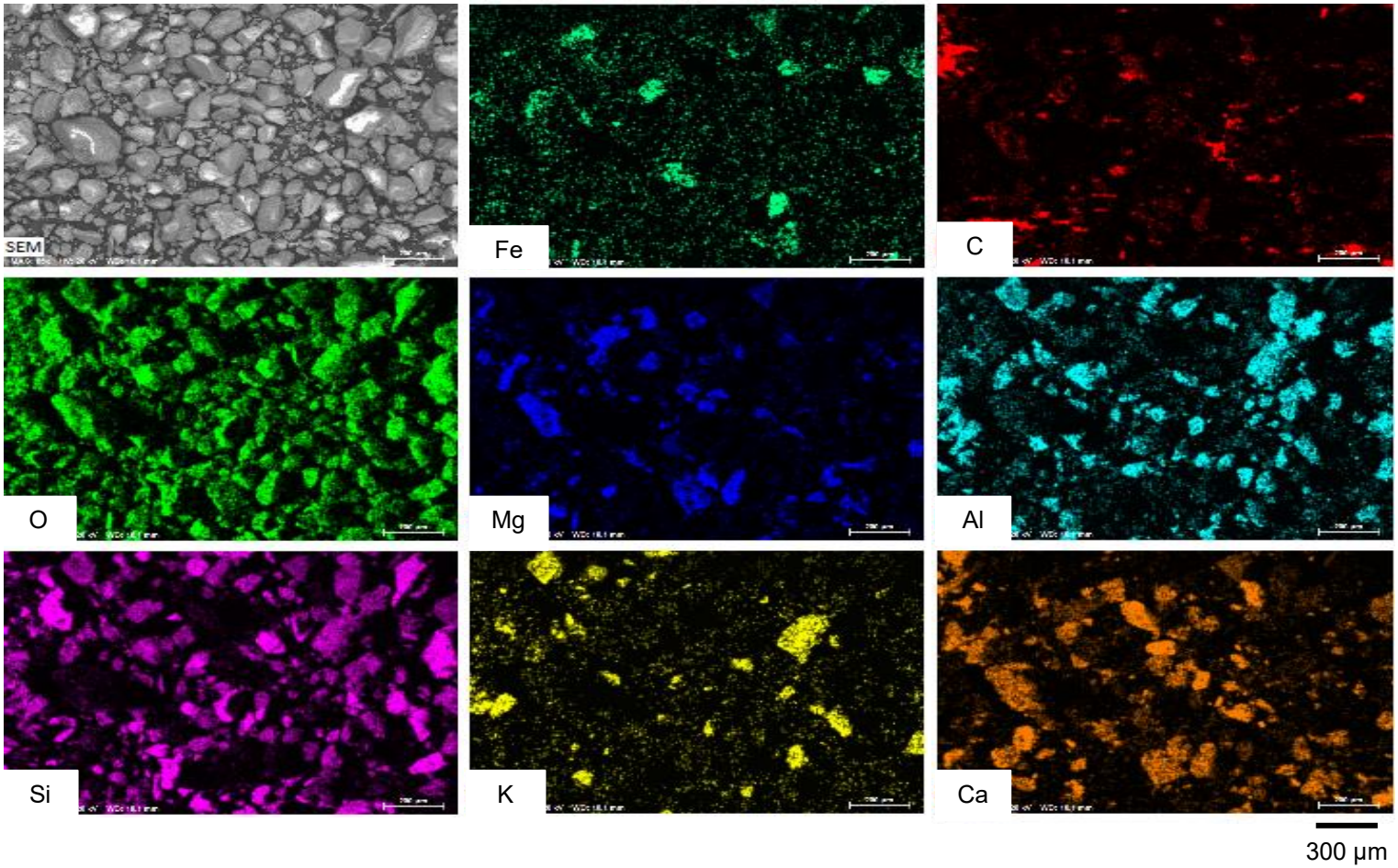

Figure A1.1 SEM-EDX images of the sand substrate and its elemental composition (C, O, Mg, Al, Si, K, Ca and Fe) before adding to Otonabee River water.

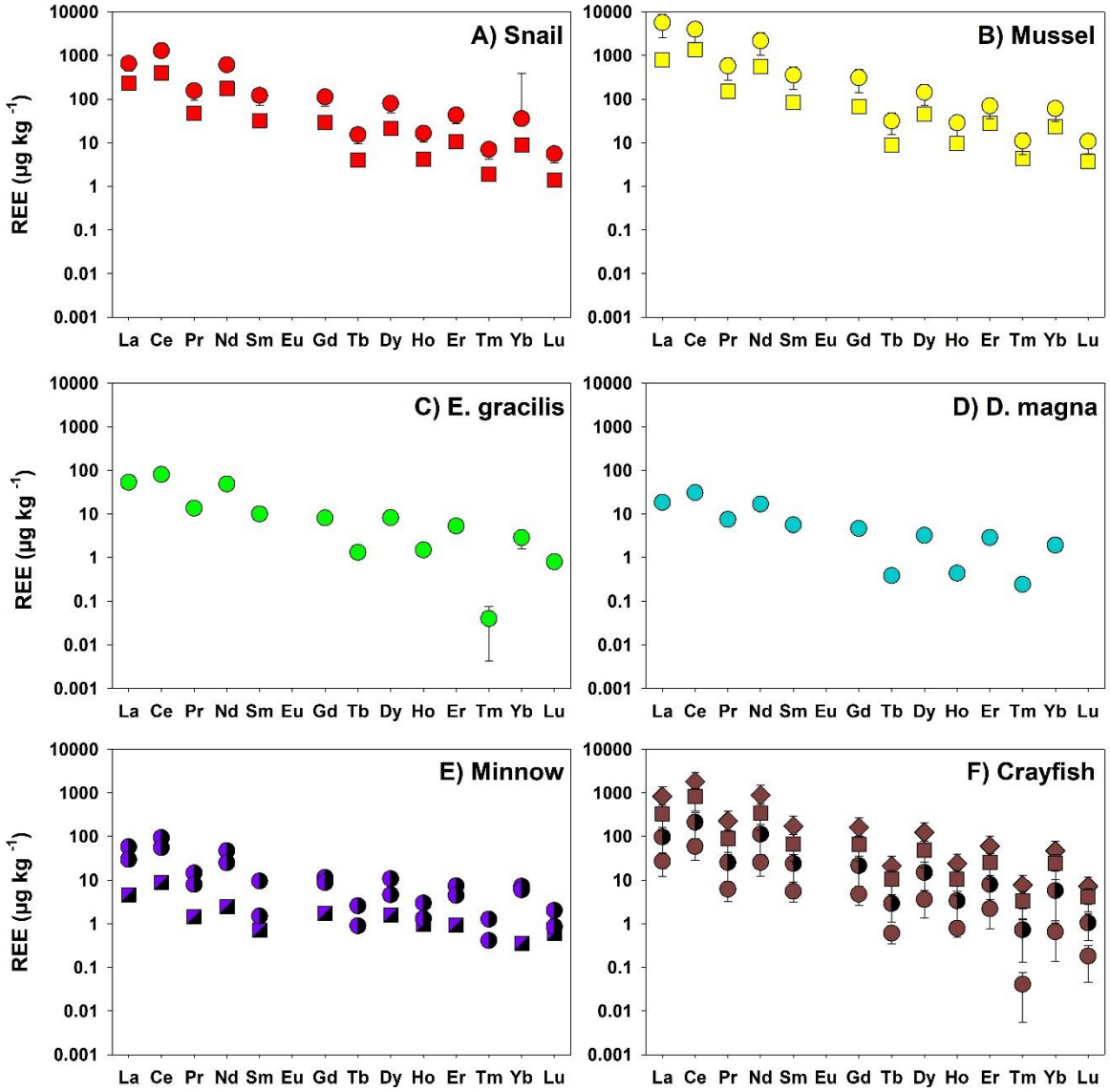

Figure A1.2 Average concentrations (µg kg $^{-1}$) of REEs in the tissues of benthic (snail, mussel, crayfish) and pelagic (minnows, *D. magna*, and *E. gracilis*) organisms. Tissue types are represented by various shapes: circle (soft tissue or whole body), square (hard tissue), half-filled circle (intestines/internal organs), half-filled square (gills), and diamond (antennal gland).

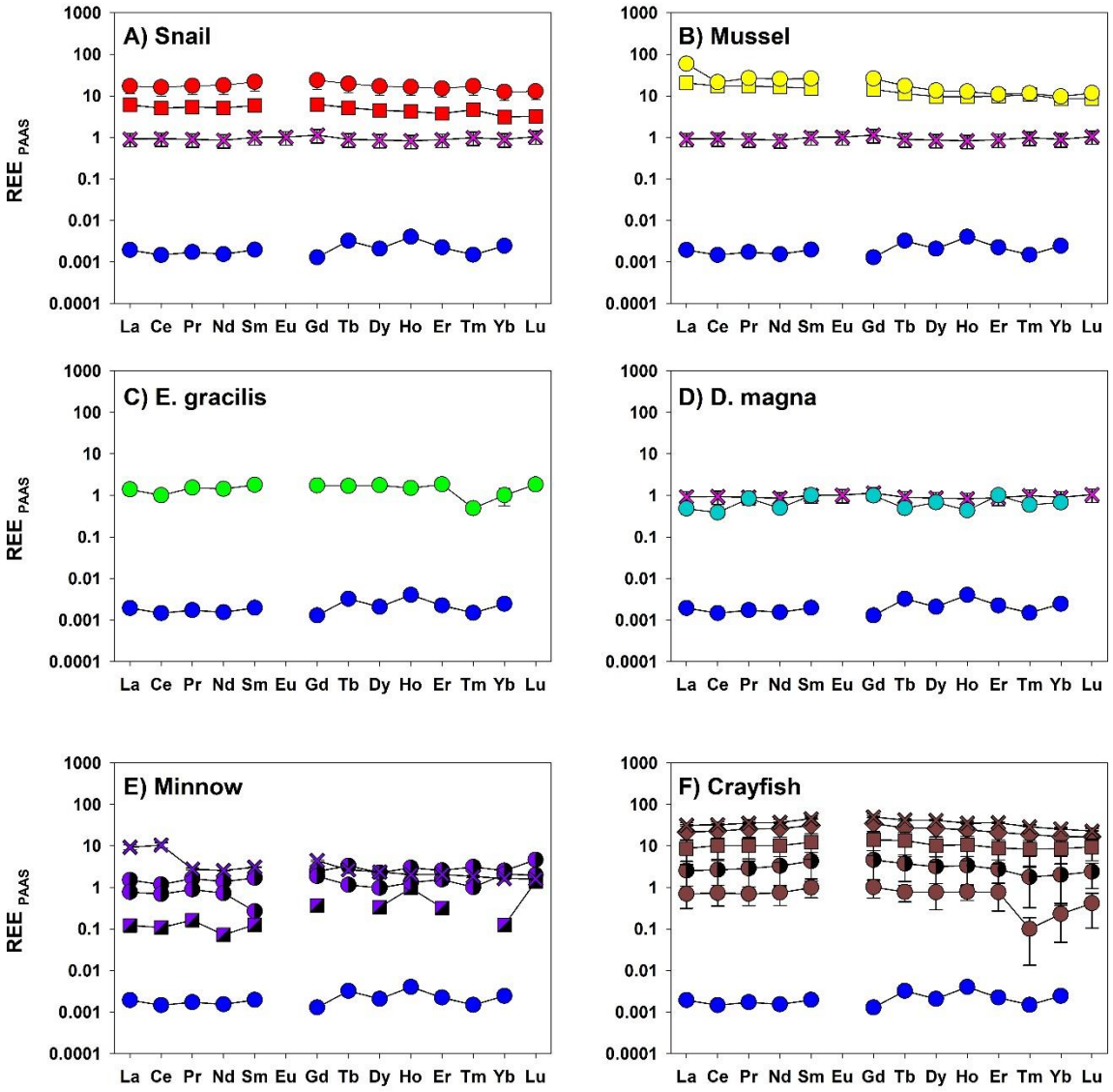

Figure A1.3 [REEs] normalized against Post-Archean Australian shale (PAAS) to characterize REE patterns in partitioned tissues within benthic (snail, mussel, crayfish) and pelagic (minnows, *D. magna*, and *E. gracilis*), feed sources (coloured X's) and Otonabee River (dark blue circles). Tissue types are represented by various shapes: circle (soft tissue or whole body), square (hard tissue), half-filled circle (intestines/internal organs), half-filled square (gills), and diamond (antennal gland). Feed sources are represented by coloured X's: crayfish shrimp pellets (brown cross symbol) minnow spirulina flakes (purple cross symbol), *D. magna*, snail, and mussel feed is a combination of spirulina and chickpea powder (pink cross symbol).

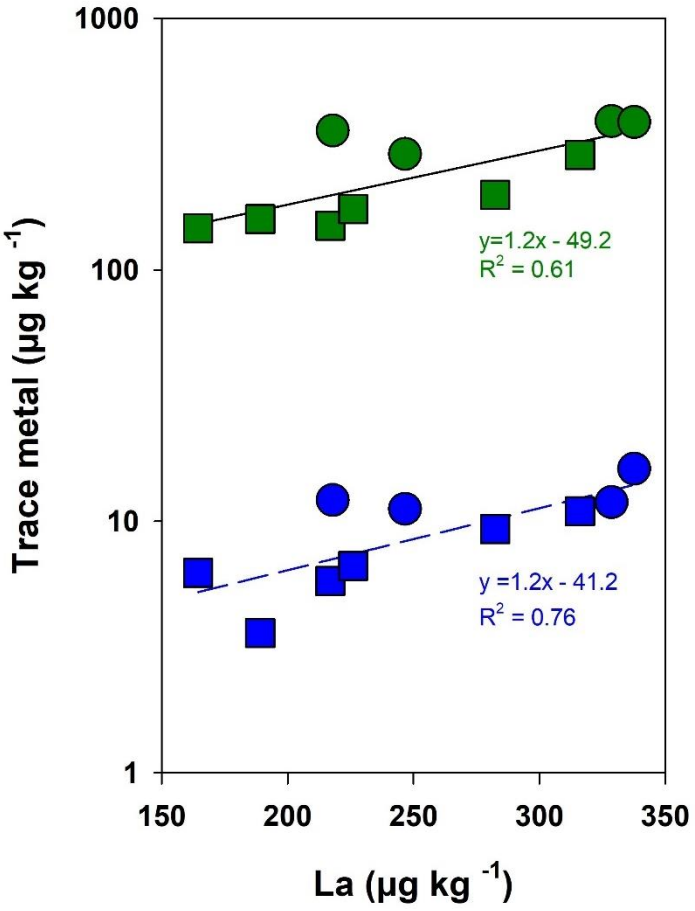

Figure A1.4 [La] (ug kg $^{-1}$) vs. [Cs] (blue), and [V] (green) concentrations in partitioned tissues of the soft tissue (circle) and hard tissue (square) of snails.

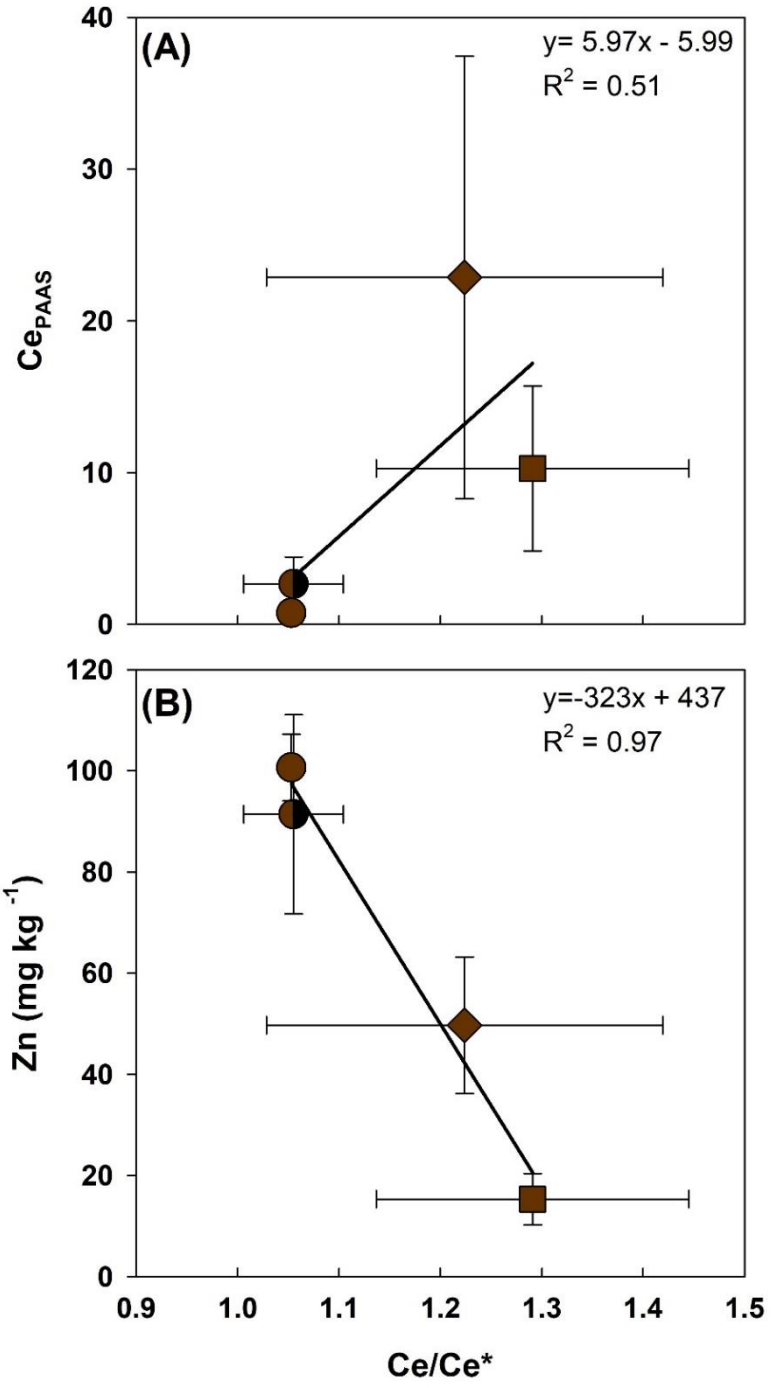

Figure A1.5 Correlation between (A) normalized values of Ce against Ce/Ce* in crayfish tissues and (B) standard error of [Zn] (mg kg $^{-1}$) against Ce/Ce*.

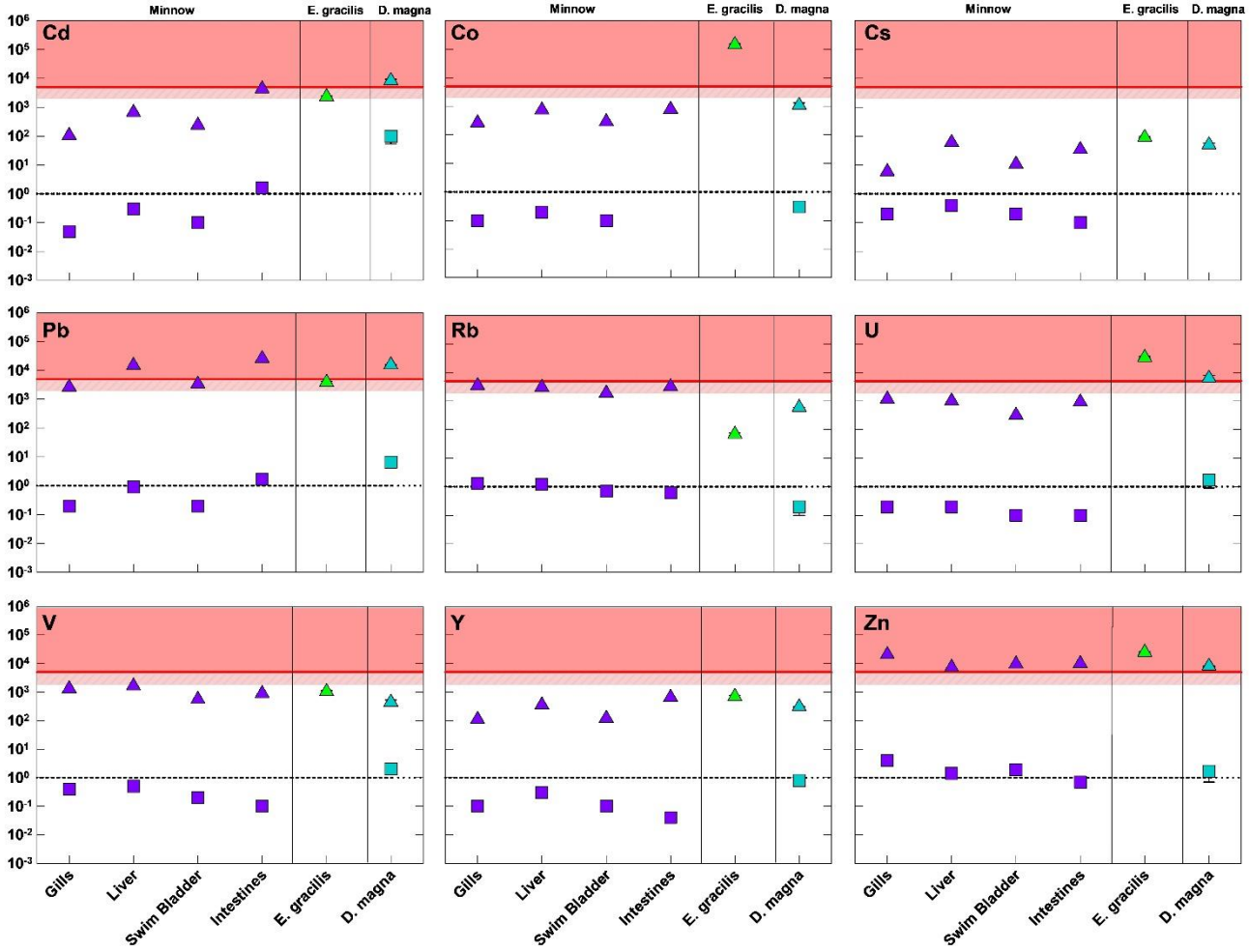

Figure A1.6 Diet bioaccumulation factors (square) and bioaccumulation concentration factors (triangle) ratios for trace elements in pelagic organisms. Organisms are represented by various colours: purple (minnow), green (*E. gracilis*), and blue (*D. magna*).

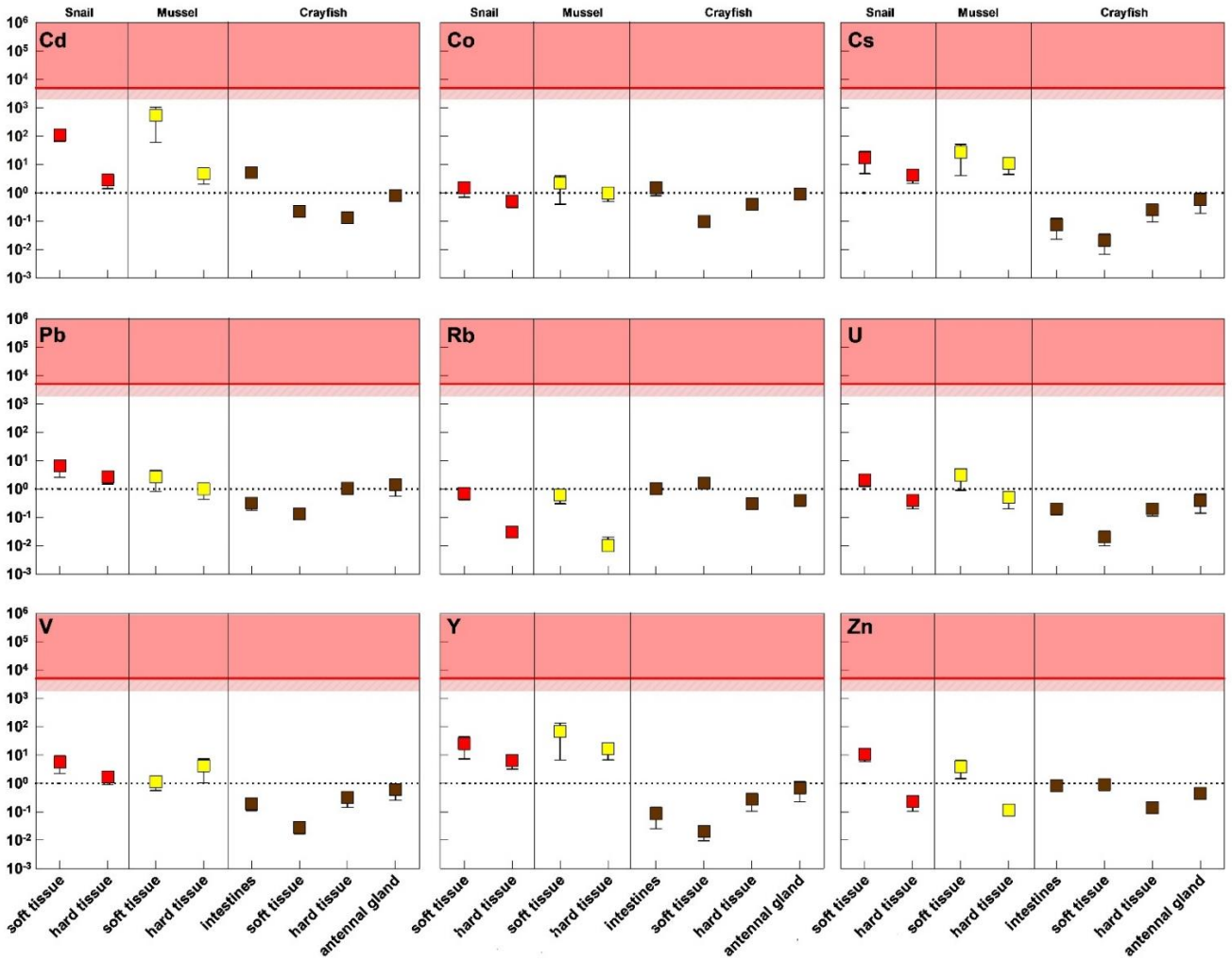

Figure A1.7 Diet bioaccumulation factors (square) for trace elements in benthic organisms. Organisms are represented by various colours: red (snail), yellow (mussel), and brown (crayfish).

Appendix A2: Chapter 3

Supplementary Text 1: Description of Swan Lake

Swan Lake was originally farmland that was converted into a gravel quarry pit in the 1850s. After operations, the sand and gravel pit were filled with soils from construction site (Gertrud Nürnberg and LaZerte, 2020) and was recharged with groundwater (Muir and Parhizgari, 2021; Parhizgari and Muir, 2021). Swan Lake was turned into a small (0.055 km^2) highly eutrophic, polymictic, and hardwater urban pond, which has had a history of cyanobacterial blooms since the 1980s (Nurnerg et al., 2016). The lake is in a restored park-like area, with a mean depth of 2.0 m and a maximum depth of 4.5 m (Parhizgari and Muir, 2021). The area of the lake at maximum water levels is 5.4 ha and the volume at maximum level is 112,000 m^3, with inflows of water including precipitation, stormwater runoff from surrounding subdivisions, two wet extended detention ponds, three oil and grit separators, flow bypass ponds, and groundwater (Parhizgari and Muir, 2021). The Swan Lake catchment is 45 ha large and includes 75% residential community, 15% open water, and 10% tree canopy or parks (Parhizgari and Muir, 2021). The phosphorus budget in Swan Lake showed that 63.4% of phosphorus was present due to internal load from sediment, 20.1% was due to external sources such as the addition of goose feces, and 7% was due to inflows from stormwater ponds (Parhizgari and Muir, 2021). The typical range of background chemistry for Swan Lake between 2013 and 2014 was a pH of 7 to 9, calcium concentrations were 42 mg L^{-1}, and DOC levels were 10 mg L^{-1} (Nürnberg and LaZerte, 2016).

Supplementary Text 2: Lithology of the region

The local lithology of the area consists of interbedded siltstone and minor limestone from the Georgian Bay formation (Ontario Ministry of Natural Resources, 1990). Siltstone comprises a mixture of broken pieces of micas, quartz, feldspars, and clay minerals that hold particle sizes smaller than sand, 1/16 of a millimeter (Aird, 2019; Bonewitz, 2012). Moreover, siltstone contains an average percentage of around 70% silicon dioxide, 14% aluminum oxide, 4% iron (III) oxide, and a small percentage of calcium oxide (2%) and magnesium oxide (2.4%) (Cullers, 1995; Haldar, 2020). Limestone is dominated by calcium-bearing carbonate minerals such as calcite and dolomite (Folk, 1959). While most siltstones are depleted in MnO, CaO, and Na_2O relative to geological standards PAAS and UCC (Cullers, 1995), the presence of weathered limestone could increase Ca concentrations in the sediment of both lakes to be five times more enriched than the UCC.

Supplementary References:

Aird, P., 2019. Deepwater Geology & Geoscience, in: Deepwater Drilling. Elsevier, pp. 17–68. https://doi.org/10.1016/b978-0-08-102282-5.00002-8

Bonewitz, R., 2012. Rocks and Minerals, 1st ed. DK Publishing, London.

Cullers, R., 1995. The controls on the major-and trace-element evolution of shales, siltstones and sandstones of Ordovician to Tertiary age in the Wet Mountains region, Colorado, U.S.A. Chem Geol 123, 107–131. https://doi.org/https://doi.org/10.1016/0009-2541(95)00050-V

Folk, R., 1959. Practical Petrographic Classification of Limestones. AAPG BULL 43, 1–38. https://doi.org/https://doi.org/10.1306/0BDA5C36-16BD-11D7-8645000102C1865D

Gertrud Nürnberg, P., LaZerte, B., 2020. Swan Lake Water Quality Management [WWW Document]. URL https://friendsofswanlakepark.ca/wp-content/uploads/2020/08/Freshwater-Research-Swan-Lake-Water-Quality_Final-Report_-2020-07-17-1.pdf (accessed 12.14.24).

Haldar, S.K., 2020. Sedimentary rocks, in: Introduction to Mineralogy and Petrology. Elsevier, pp. 187–268. https://doi.org/10.1016/B978-0-12-820585-3.00006-5

Muir, R., Parhizgari, Z., 2021. Swan Lake Long Term Management Plan [WWW Document]. URL https://pub-markham.escribemeetings.com/filestream.ashx?DocumentId=46635 (accessed 1.2.25).

Nürnberg, G.K., LaZerte, B.D., 2016. Trophic state decrease after lanthanum-modified bentonite (Phoslock) application to a hyper-eutrophic polymictic urban lake frequented by Canada geese (Branta canadensis). Lake Reserv Manag 32, 74–88. https://doi.org/10.1080/10402381.2015.1133739

Ontario Ministry of Natural Resources, 1990. Quaternary Geology Toronto and Surrounding Area Southern Ontario [WWW Document]. Ontario Geological Survey Preliminary Map. URL https://collections.library.utoronto.ca/view/mdl:G3501_C5_1891-P_2204 (accessed 12.14.24).

Parhizgari, Z., Muir, R., 2021. Swan Lake Long-Term Management Plan City of Markham [WWW Document]. URL https://pub-markham.escribemeetings.com/filestream.ashx?DocumentId=46635 (accessed 1.2.25).

Yeghicheyan, D., Aubert, D., Bouhnik-Le Coz, M., Chmeleff, J., Delpoux, S., Djouraev, I., Granier, G., Lacan, F., Piro, J.L., Rousseau, T., Cloquet, C., Marquet, A., Menniti, C., Pradoux, C., Freydier, R., Vieira da Silva-Filho, E., Suchorski, K., 2019. A New Interlaboratory Characterisation of Silicon, Rare Earth Elements and Twenty-Two Other Trace Element Concentrations in the Natural River Water Certified Reference Material SLRS-6 (NRC-CNRC). Geostand Geoanal Res 43, 475–496. https://doi.org/10.1111/ggr.12268

Table A2.1 Measured, certified, and informational (represented by *) concentration (mg kg^{-1}) of 34 elements in CRMs NIST 1515 and NIST 1566a.

	NIST 1515 (mg kg^{-1})			NIST 1566a (mg kg^{-1})		
Metals	**Measured Concentrations (n=1)**	**Certified Concentrations**	**S.D.**	**Measured Concentrations (n=1)**	**Certified Concentrations**	**S.D.**
Ag	0.005			0.85	0.68	0.1
As	0.04			13.2	14.0	1.2
Ba	48.7	48.8	2.3	1.3		
Cd	0.01	0.01	0.002	3.8	4.15	0.38
Ce	3.4	3.0*		0.2	0.4*	
Co	0.1	0.1*		0.4	0.57	0.11
Cu	5.8	5.7	0.1	60.1	66.3	4.3
Dy	1.8			0.04		
Er	0.6			0.03		
Eu	0.4	0.2*		0.01	0.01*	
Gd	3.1	3.0*		0.04		
Ho	0.3			0.01		
La	23.3	20.0*		0.2	0.3*	
Lu	0.02			0.004		
Mn	55.7	54.1	1.1	10.3	12.3	1.5
Mo	0.14	0.10	0.01	0.23		
Nd	17.9	17.0*		0.2		
Ni	0.8	0.9	0.1	2.2	2.3	0.4
Pb	0.37	0.47	0.02	0.34	0.37	0.01
Pr	4.8			0.04		
Rb	9.4	10.2	1.6	2.5	3.0*	
Sb	0.007	0.013*		0.008	0.01*	
Sc	0.01	0.03*		0.03	0.06*	
Sm	3.1	3.0*		0.04	0.06*	
Sr	26.3	25.1	1.1	9.3	11.1	1.0
Tb	0.4	0.4*		0.01	0.01*	
Th	0.01	0.03*		0.01	0.04*	
Ti	0.1			3.5		
Tm	0.06			0.003		
U	0.004	0.006*		0.1	0.13	0.01
V	0.1	0.3	0.03	4.5	4.68	0.15
Y	11.4			0.3		
Yb	0.5	0.3*		0.04		
Zn	11.8	12.5	0.4	762.0	830.0	57.0

Table A2.2 Measured, certified and literature concentrations (μg L^{-1}) of 42 trace elements in liquid CRM NIST 1640a and SLRS-6. Symbol (*) demarks concentrations reported by Yeghicheyan et al., (2019).

Metals	NIST 1640a (μg L^{-1})				SLRS – 6 (μg L^{-1})			
	Measured Concentrations	S.D. (n=20)	Certified Concentrations	S.D.	Measured Concentrations	S.D. (n=20)	Certified Concentrations	S.D.
Ag	7.8	0.2	8.1	0.1	0.004	0.006		
Al	51.6	3.2	53.0	1.8	30.4	1.7	33.8	2.2
As	8.2	0.2	8.1	0.1	0.55	0.04	0.57	0.08
Ba	151.7	2.1	151.8	0.8	14.2	0.3	14.3	0.5
Be	2.36	0.46	3.00	0.03			0.01	0.0
Cd	3.92	0.11	3.99	0.07			0.006	0.0001
Ce	0.003	0.003			0.31	0.01	0.29*	0.02
Co	18.07	0.78	20.24	0.24			0.05	0.01
Cr	36.40	4.51	40.50	0.30	0.09	0.05	0.25*	0.01
Cs	0.018	0.006			0.013	0.001	0.005*	0.001
Cu	77.6	3.6	85.8	0.5	22.7	0.9	24.0	1.8
Dy	0.005	0.003			0.020	0.003	0.02*	0.001
Er	0.010	0.002			0.012	0.002	0.012*	0.001
Eu	0.027	0.002			0.0092	0.0016	0.0073*	0.0004
Fe	33.5	1.3	36.8	1.8	80.0	2.6	84.5	3.6
Ga	0.014	0.001			0.014	0.009	0.011	0.007
Gd	0.003	0.003			0.031	0.004	0.032*	0.003
Ge	0.01	0.02			0.03	0.07	0.01*	0.01
Ho	0.001	0.002			0.0035	0.0021	0.0043*	0.0003
La	0.01	0.02			0.25	0.01	0.25*	0.01
Lu	0.0041	0.0025			0.0016	0.0024	0.0019*	0.0002
Mg	1002	47	1057	41	2023	95	2137	58
Mn	37.9	1.6	40.4	0.4	1.4	0.1	2.1	0.1
Mo	44.96	0.73	45.60	0.61	0.23	0.04	0.22	0.02
Nd	0.015	0.003			0.23	0.01	0.23*	0.01
Ni	23.48	1.05	25.32	0.14	0.31	0.03	0.62*	0.02
Pb	11.28	0.38	12.10	0.05	0.14	0.01	0.17	0.03
Pr	0.002	0.002			0.060	0.003	0.059*	0.002
Rb	1.15	0.06	1.20	0.01	1.38	0.06	1.41*	0.05
Re	0.0062	0.0005			0.0128	0.0006	0.0135*	0.0002
Rh	0.0047				0.0020		0.0007*	0.0002
Sm	0.008	0.002			0.037	0.003	0.040*	0.002
Sr	120.43	3.03	126.00	0.91	38.74	0.71	40.72	0.32
Tb	0.0049	0.0015			0.0080	0.0007	0.0041*	0.0003
Th	0.002	0.002			0.009	0.005	0.016*	0.007
Tm	0.0014	0.0021			0.0027	0.0030	0.0018*	0.0002
U	22.45	0.88	25.40	0.27			0.07	0.003
V	15.01	0.47	15.00	0.25	0.33	0.02	0.35	0.006
Yb	0.092	0.008			0.135	0.008	0.011*	0.001
Zn	54.6	2.0	55.6	0.4	1.4	0.2	1.8	0.1
Zr	0.01	0.01			0.05	0.01	0.06	0.01

Table A2.3 Measured and certified concentration (mg kg^{-1}) of 37 trace elements in the sediment certified reference materials of MESS-4 using the microwave digestion lab station in aqua regia analyzed by 8800 QQQ-ICP-MS.

Elements	Measured Concentrations	S.D. (n=4)	Certified Concentrations	S.D.
As	21.6	2.4	21.7	2
Be	1.9	0.3	2.1	0.3
Cd	0.2	0.1	0.3	0.1
Ce	71.3	12.1	72.0	
Co	13.3	2.3	13.0	0.8
Cr	105.0	18.0	94.3	1.8
Cs	8.0	1.5	10.0	
Cu	39.1	5.7	32.9	1.8
Dy	3.7	0.7		
Er	1.8	0.3		
Eu	1.2	0.2	1.3	
Ga	21.1	3.7	18.0	
Gd	5.3	0.9		
Ho	0.7	0.1		
La	39.3	6.8	35.0	
Li	56.8	9.0	65.3	6.8
Lu	0.21	0.04	0.11	
Mo	2.6	0.5	2.5	0.1
Nb	7.8	1.3	12.0	
Nd	32.5	5.6	42.0	
Ni	50.5	8.1	42.8	1.6
Pb	24.2	2.8	21.5	1.2
Pr	8.9	1.5		
Sb	1.4	0.7	1.1	0.2
Sc	16.9	3.1	13.4	
Se	2.1	1.3	1.5	
Sm	6.0	1.0	5.5	
Sn	2.7	0.1	2.4	0.1
Tb	0.7	0.2		
Th	15.8	3.2	12.0	
Tm	0.22	0.03		
U	2.3	0.4	3.4	0.4
V	210.8	32.7	216.0	8.0
W	1.1	0.5	1.3	
Y	17.2	3.6	20.0	
Yb	1.2	0.5	2.0	
Zn	163.9	16.4	147.0	6

Table A2.4 Measured and certified concentrations of 22 elements in the soil CRM TILL-2 Using EDXRF.

Elements	Units	Measured Concentrations	S.D. (n=3)	Certified Concentrations
Na_2O	%	2.17	0.04	2.19
MgO	%	2.12	0.01	1.83
Al_2O_3	%	17.56	0.02	16.0
SiO_2	%	60.36	0.04	60.8
P_2O_5	%	0.155	0.001	0.17
S	mg kg^{-1}	463.0	3.3	
Cl	mg kg^{-1}	97.8	6.5	
K_2O	%	2.712	0.003	3.07
CaO	%	1.037	0.002	1.27
TiO_2	%	0.776	0.003	0.88
Cr_2O_3	%	71.9	4.8	
MnO	mg kg^{-1}	855	6	1000
Fe_2O_3	%	4.74	0.01	5.4
As	mg kg^{-1}	25	1	26
Br	mg kg^{-1}	10	0.3	12
Cu	mg kg^{-1}	132	1	150
Mo	mg kg^{-1}	13	2	14
Nb	mg kg^{-1}	14	1	20
Rb	mg kg^{-1}	128	1	143
Sr	mg kg^{-1}	121	1	144
Zn	mg kg^{-1}	108	1	130
Zr	mg kg^{-1}	289	1	390

Table A2.5 Average and standard deviation (S.D.) of soil organic matter and inorganic carbon of sediment from Swan Lake and Toogood Pond.

Analysis	Sediment Sample	Organic Matter (%)	S.D. (n=3)	Inorganic C (%)	S.D.	Total SOM (%)	S.D. (n=3)	number
LOI	SL1	4.4	0.1	12.7	0.2	17.1	0.31	2
	SL2	10.7	0.4	12.6	0.1	23.3	0.27	3
	SL3	14.5	0.8	12.4	0.6	26.8	0.22	3
	SL4	11.6	0.5	12.5	0.4	24.2	0.07	2
	SL5	12.8		11.8		24.7		1
	SL6	12.9	0.7	11.6	0.4	24.5	0.47	4
	SL7	14.1	1.8	10.8	1.1	24.9	0.81	3
	SL8	15.7	1.2	9.5	0.7	25.4	0.60	4
	SL9	16.7	0.2	7.2	0.5	24.0	0.38	4
	SL10	17.4	0.4	3.9	0.3	21.3	0.17	3
	TG1	8.7		17.3		26.0		1
	TG2	6.5		9.6		16.0		1
	TG3	7.5		11.8		19.3		1
	TG4	8.5		12.4		21.0		1

Table A2.6 REE anomalies within sediment samples of Toogood Pond and Swan Lake.

	REE Anomalies (REE/REE*)												
Site #	**La/La***	**Ce/Ce***	**Pr/Pr***	**Nd/Nd***	**Sm/Sm***	**Eu/Eu***	**Gd/Gd***	**Tb/Tb***	**Dy/Dy***	**Ho/Ho***	**Er/Er***	**Tm/Tm***	**Yb/Yb***
TG1	1.04	1.21	0.80	0.92	1.04	1.11	1.12	0.91	1.05	0.98	1.03	0.94	1.03
TG2	0.94	1.29	0.76	0.90	1.04	1.11	1.15	0.91	1.01	1.01	0.97	0.94	1.27
TG3	1.02	1.29	0.80	0.90	1.07	1.12	1.12	0.97	0.97	1.03	1.02	0.99	0.98
TG4	0.98	1.13	0.98	0.94	0.96	1.09	1.20	0.96	1.01	0.97	1.10	0.76	1.30
AVG	1.00	1.23	0.84	0.91	1.03	1.11	1.15	0.94	1.01	1.00	1.03	0.91	1.15
SE	0.02	0.03	0.04	0.01	0.02	0.01	0.02	0.01	0.02	0.01	0.02	0.04	0.07
S1	13.83	1.26	0.78	0.90	1.06	1.10	1.12	0.95	1.02	0.95	0.98	0.90	1.37
S2	21.20	1.21	0.89	0.92	1.04	1.11	1.12	1.01	0.95	1.02	1.00	1.03	0.92
S3	28.27	1.21	0.81	0.92	1.02	1.06	1.13	0.95	1.00	1.02	0.94	1.29	0.66
S4	17.22	1.18	0.75	0.93	1.01	1.04	1.17	0.92	0.99	1.02	1.06	0.71	1.68
S5	20.82	1.11	0.85	0.95	1.01	1.06	1.15	0.95	1.00	1.00	1.06	0.73	1.51
S6	25.88	1.17	0.90	0.93	1.02	1.09	1.12	0.98	1.00	0.97	1.05	1.10	0.71
S7	41.94	1.26	0.81	0.91	1.08	1.12	1.08	0.96	1.01	0.99	0.99	1.08	0.88
S8	23.20	1.22	0.83	0.92	1.03	1.10	1.14	0.95	1.00	1.02	0.96	0.97	1.11
S9	28.14	1.33	0.67	0.90	1.09	1.07	1.11	0.94	1.02	0.95	1.04	1.13	0.76
S10	4.08	1.27	0.78	0.91	1.04	1.10	1.14	0.93	1.01	0.98	1.04	0.83	1.38
AVG	22.5	1.22	0.81	0.92	1.04	1.09	1.13	0.95	1.00	0.99	1.01	0.98	1.10
SE	3.00	0.02	0.02	0.00	0.01	0.01	0.01	0.01	0.01	0.01	0.01	0.06	0.11

Table A2.7 Elemental composition of sediment within sampling sites from Toogood Pond (n=4) and Swan Lake (n=10). An unpaired t-test was performed (p-value = 0.05) to determine significant differences between elemental concentrations within the sediment of Toogood Pond vs. Swan Lake. Values have been rounded to the most appropriate significant figures.

Analysis	Elements	Units	Location														Unpaired t-test
			Toogood Pond				Swan Lake										
			1	2	3	4	1	2	3	4	5	6	7	8	9	10	P-value (0.05)
Depth		m	0.63	0.43	0.74	0.84	2.6	1.4	1.8	1.7	1.6	1.9	3.0	1.8	1.9	0.64	
Total analysis - EDXRF	Na_2O	%	0.31	0.94	0.71	0.70	0.94	1.0	1.1	1.3	1.2	1.1	1.3	1.4	1.6	1.6	0.001*
	MgO	%	1.7	1.8	1.9	2.0	1.4	1.9	1.9	1.9	1.8	1.6	1.7	1.7	1.7	1.8	0.4
	Al_2O_3	%	7.8	9.2	9.0	9.1	7.2	8.7	8.3	8.5	8.2	7.9	8.5	8.5	9.7	11.0	0.8
	SiO_2	%	35	45	42	41	36	36	34	36	34	34	35	36	41	47	0.1
	P_2O_5	mg kg^{-1}	0.13	0.21	0.19	0.19	0.24	0.24	0.28	0.25	0.27	0.30	0.34	0.32	0.33	0.29	0.0003**
	S	mg kg^{-1}	2500	3100	2600	2200	4600	4100	6100	4400	5700	5600	5900	6700	7200	5900	0.0001**
	Cl	mg kg^{-1}	470	480	63	510	5000	4700	6900	5500	6300	6100	8000	7800	7400	6000	0.0001**
	K_2O	%	1.4	1.8	1.7	1.6	1.6	1.7	1.6	1.7	1.7	1.6	1.6	1.8	1.9	2.2	0.3
	CaO	%	24	20	20	20	29	22	20	21	21	23	21	19	13	9.0	0.7
	TiO_2	mg kg^{-1}	0.42	0.62	0.57	0.53	0.65	0.53	0.47	0.51	0.57	0.54	0.50	0.56	0.56	0.66	0.6
	Cre_2O_3	%	52	83	64	63	140	100	120	10	120	130	170	130	130	66	0.002*
	MnO	mg kg^{-1}	650	800	850	800	890	750	670	710	810	710	660	720	630	660	0.3
	Fe_2O_3	%	2.8	3.7	3.6	3.6	4.5	3.7	3.9	3.7	4.5	4.0	3.9	4.5	4.2	4.2	0.006*
	As	mg kg^{-1}	7.7	8.1	8.4	8.1	9.2	8.2	9.8	9.0	10.0	10.0	10.0	9.0	10.0	9.1	0.003*
	Br	mg kg^{-1}	9.4	11	12	11	12	15	17	13	17	16	18	19	19	7	0.0008**
	Cu	mg kg^{-1}	271	2	22	22	23	38	39	33	42	31	30	37	37	29	0.004*
	Nb	mg kg^{-1}	4.3	8.8	7.2	7.2	10.0	8.2	6.4	6.1	5.5	9.8	8.0	10.0	8.5	8.5	0.2
	Rb	mg kg^{-1}	52	62	59	56	80	68	66	64	75	69	65	75	73	83	0.002*
	Sr	mg kg^{-1}	320	450	370	310	770	41	360	390	440	470	380	420	320	310	0.4
	Zn	mg kg^{-1}	110	110	110	110	94	110	150	10	140	120	110	140	140	130	0.1
	Zr	mg kg^{-1}	140	300	240	220	370	260	220	25	270	300	260	300	280	300	0.1

Table A2.8 Contamination factors (C_f) of trace and major elements within the sediment of Swan Lake. When $C_f < 1$ (blue colour), contamination potential is low, C_f; $1 \leq C_f < 6$ (pink colour) is moderate, and $C_f \geq 6$ (red colour) is very high contamination potential. The C_f values have been rounded to the most appropriate significant figures.

Sampling Location	Sampling Site	Element													
		La	Ce	Pr	Nd	Sm	Eu	Gd	Tb	Dy	Ho	Er	Tm	Yb	Lu
Swan Lake	1	10	0.73	0.75	0.76	0.79	0.78	0.78	0.80	0.81	0.80	0.86	1.0	1.2	0.97
Swan Lake	2	24	1.1	1.1	1.1	1.1	1.1	1.0	1.1	1.0	1.1	1.0	1.1	0.85	1.1
Swan Lake	3	29	1.0	0.99	0.97	0.94	0.91	0.91	0.93	0.91	0.90	0.85	0.97	0.51	0.83
Swan Lake	4	17	0.99	0.97	0.97	0.95	0.89	0.95	0.92	0.92	0.96	0.97	0.92	1.4	0.96
Swan Lake	5	36	1.8	1.8	1.8	1.7	1.7	1.7	1.7	1.7	1.7	1.7	1.5	2.1	1.7
Swan Lake	6	41	1.6	1.5	1.5	1.4	1.4	1.5	1.4	1.5	1.3	1.5	1.3	0.80	1.3
Swan Lake	7	73	1.7	1.7	1.7	1.7	1.6	1.5	1.5	1.5	1.5	1.4	1.5	1.1	1.4
Swan Lake	8	32	1.4	1.4	1.4	1.3	1.3	1.3	1.3	1.3	1.3	1.3	1.4	1.3	1.4
Swan Lake	9	42	1.6	1.5	1.6	1.6	1.5	1.5	1.5	1.5	1.4	1.5	1.5	0.97	1.4
Swan Lake	10	8.0	2.0	2.0	1.9	1.9	1.8	1.8	1.8	1.8	1.8	1.8	1.8	2.1	1.7
Sampling Location	**Sampling Site**	**Ni**	**Cu**	**Zn**	**V**	**Co**	**Ag**	**Cd**	**Sn**	**As**	**Pb**	**Th**	**U**	**Cs**	**Y**
Swan Lake	1	1.3	0.99	0.86	0.82	0.52	0.32	0.04	0.54	1.1	1.3	0.57	0.77	0.42	1.6
Swan Lake	2	1.2	1.7	1.0	1.2	1.0	0.58	0.57	0.71	1.0	2.0	1.1	1.2	1.3	1.3
Swan Lake	3	1.4	1.7	1.4	1.0	0.96	0.60	0.61	0.80	1.2	1.6	1.0	1.1	1.2	1.1
Swan Lake	4	1.3	1.4	0.96	0.97	0.85	0.71	0.47	0.81	1.1	1.2	0.97	1.0	0.94	1.2
Swan Lake	5	1.7	1.8	1.3	1.7	1.6	2.0	1.1	0.61	1.3	2.1	1.6	1.8	1.9	1.3
Swan Lake	6	1.4	1.4	1.1	1.5	1.2	1.1	1.4	0.66	1.2	1.5	1.4	1.5	1.4	1.3
Swan Lake	7	1.3	1.3	1.0	1.7	1.4	1.3	0.78	0.56	1.3	1.4	1.7	1.6	1.8	1.2
Swan Lake	8	1.5	1.6	1.3	1.4	1.3	1.2	1.0	0.52	1.1	2.1	1.5	1.3	1.3	1.4
Swan Lake	9	1.2	1.6	1.3	1.5	1.4	1.1	0.35	0.49	1.3	1.8	1.6	1.7	1.7	1.3
Swan Lake	10	1.5	1.3	1.1	1.8	1.8	0.94	2.6	0.51	1.1	2.0	2.3	2.0	2.0	1.3
Sampling Location	**Sampling Site**	**Na_2O**	**MgO**	**Al_2O_3**	**SiO_2**	**P_2O_5**	**S**	**Cl**	**K_2O**	**CaO**	**TiO_2**	**V_2O_5**	**Cr_2O_3**	**MnO**	**Fe_2O_3**
Swan Lake	1	1.4	0.79	0.82	0.88	1.3	1.8	9.6	0.97	1.4	1.2	2.1	2.1	1.2	1.3
Swan Lake	2	1.5	1.03	0.99	0.88	1.3	1.6	9.0	1.0	1.0	1.0	1.6	1.6	0.97	1.1
Swan Lake	3	1.7	1.03	0.94	0.83	1.6	2.4	13	1.0	0.96	0.88	1.7	1.8	0.86	1.1
Swan Lake	4	1.9	1.01	0.97	0.89	1.4	1.7	11	1.0	0.98	0.96	1.3	1.6	0.91	1.1
Swan Lake	5	1.9	0.97	0.94	0.84	1.5	2.2	12	1.0	1.0	1.1	2.2	1.8	1.0	1.3
Swan Lake	6	1.6	0.89	0.90	0.83	1.7	2.2	12	0.98	1.1	1.0	1.5	2.0	0.91	1.2
Swan Lake	7	2.0	0.95	0.97	0.86	1.9	2.3	15	1.0	0.98	0.93	1.4	2.6	0.85	1.1
Swan Lake	8	2.1	0.91	0.97	0.87	1.8	2.6	15	1.1	0.90	1.1	2.4	2.0	0.93	1.3
Swan Lake	9	2.4	1.03	1.1	1.0	1.8	2.8	14	1.2	0.64	1.1	1.6	2.1	0.81	1.2
Swan Lake	10	2.4	1.00	1.3	1.1	1.6	2.3	12	1.4	0.43	1.2	1.9	1.0	0.85	1.2

Table A2.9 Enrichment factors (E_f) of REEs compared to Al and Ti values for Swan Lake sediment and normalized against Toogood Pond. The E_f values have been rounded to the most appropriate significant figures.

Sampling Location	Sampling Site	Element													
		La		Ce		Pr		Nd		Sm		Eu		Gd	
		/Al	/Ti	/Al	/Ti	/Al	/Ti	/Al	/Ti	/Al	/Ti	/Al	/Ti	/Al	/Ti
Swan Lake	1	12	8.1	0.88	0.58	0.91	0.60	0.92	0.6	0.96	0.63	0.95	0.63	0.94	0.62
Swan Lake	2	24	24	1.1	1.1	1.1	1.2	1.1	1.1	1.1	1.1	1.1	1.1	1.0	1.0
Swan Lake	3	31	32	1.1	1.1	1.0	1.1	1.0	1.1	1.0	1.1	0.96	1.0	0.97	1.0
Swan Lake	4	17	17	1.0	1.0	1.0	0.99	1.0	0.99	0.98	0.97	0.92	0.91	0.98	0.97
Swan Lake	5	39	33	1.9	1.7	1.9	1.6	1.9	1.6	1.8	1.6	1.8	1.5	1.8	1.5
Swan Lake	6	45	40	1.7	1.5	1.7	1.5	1.7	1.5	1.6	1.4	1.6	1.4	1.5	1.3
Swan Lake	7	76	77	1.8	1.8	1.7	1.8	1.7	1.8	1.7	1.8	1.7	1.7	1.5	1.6
Swan Lake	8	32	29	1.4	1.3	1.4	1.3	1.4	1.3	1.4	1.3	1.4	1.2	1.4	1.2
Swan Lake	9	38	39	1.4	1.5	1.4	1.4	1.4	1.5	1.5	1.5	1.3	1.4	1.4	1.4
Swan Lake	10	6.6	6.6	1.6	1.6	1.6	1.6	1.5	1.5	1.5	1.5	1.5	1.5	1.5	1.5
Sampling Location	**Sampling Site**	**Tb**		**Dy**		**Ho**		**Er**		**Tm**		**Yb**		**Lu**	
		/Al	/Ti	/Al	/Ti	/Al	/Ti	/Al	/Ti	/Al	/Ti	/Al	/Ti	/Al	/Ti
Swan Lake	1	0.97	0.64	0.98	0.65	0.97	0.64	1.0	0.69	1.24	0.83	1.2	0.96	1.2	0.78
Swan Lake	2	1.1	1.1	1.0	1.0	1.2	1.0	1.0	1.0	1.1	1.1	1.1	0.85	1.1	1.1
Swan Lake	3	0.98	1.0	0.97	1.0	0.96	1.0	0.90	0.95	1.0	1.1	0.88	0.58	0.88	0.93
Swan Lake	4	0.95	0.94	0.95	0.94	0.99	0.99	1.0	0.99	0.95	0.95	1.0	1.4	1.0	0.99
Swan Lake	5	1.8	1.6	1.8	1.5	1.8	1.5	1.8	1.5	1.6	1.4	1.8	1.9	1.8	1.5
Swan Lake	6	1.6	1.4	1.5	1.4	1.4	1.3	1.5	1.3	1.5	1.3	1.4	0.79	1.4	1.3
Swan Lake	7	1.6	1.6	1.6	1.6	1.5	1.6	1.5	1.5	1.6	1.6	1.4	1.2	1.4	1.5
Swan Lake	8	1.4	1.2	1.4	1.2	1.4	1.2	1.3	1.2	1.5	1.3	1.4	1.3	1.4	1.3
Swan Lake	9	1.4	1.4	1.3	1.4	1.3	1.3	1.4	1.4	1.4	1.5	1.3	0.92	1.3	1.3
Swan Lake	10	1.4	1.4	1.4	1.4	1.4	1.4	1.4	1.4	1.4	1.4	1.3	1.7	1.3	1.3

Table A2.10 Enrichment factors (E_f) of trace metals compared to Al and Ti values for Swan Lake sediment and normalized against Toogood Pond. The E_f values have been rounded to the most appropriate significant figures.

Sampling Location	Sampling Site	Element													
		Ni		Cu		Zn		Br		Co		Ag		Cd	
		/Al	/Ti	/Al	/Ti	/Al	/Ti	/Al	/Ti	/Al	/Ti	/Al	/Ti	/Al	/Ti
Swan Lake	1	1.5	1.0	1.2	0.78	1.0	0.69	1.4	0.91	0.62	0.41	0.38	0.25	0.05	0.03
Swan Lake	2	1.3	1.2	1.7	1.6	1.0	1.0	1.4	1.4	1.0	0.98	0.58	0.56	0.57	0.56
Swan Lake	3	1.5	1.5	1.8	1.9	1.5	1.5	1.7	1.8	1.0	1.0	0.63	0.66	0.64	0.67
Swan Lake	4	1.3	1.3	1.4	1.4	0.99	0.98	1.2	1.2	0.87	0.85	0.73	0.7	0.49	0.48
Swan Lake	5	1.8	1.5	1.9	1.6	1.4	1.2	1.7	1.5	1.6	1.4	2.1	1.8	1.2	0.99
Swan Lake	6	1.6	1.4	1.5	1.3	1.2	1.1	1.7	1.5	1.3	1.1	1.2	1.0	1.5	1.4
Swan Lake	7	1.4	1.4	1.3	1.4	1.1	1.1	1.7	1.8	1.5	1.5	1.4	1.4	0.80	0.82
Swan Lake	8	1.5	1.4	1.6	1.5	1.3	1.2	1.8	1.7	1.3	1.2	1.3	1.1	1.0	0.93
Swan Lake	9	1.1	1.2	1.5	1.5	1.1	1.2	1.6	1.7	1.2	1.3	0.98	1.0	0.31	0.33
Swan Lake	10	1.1	1.1	1.0	1.0	0.91	0.91	1.2	1.2	1.5	1.4	0.75	0.75	2.1	2.1
Sampling Location	**Sampling Site**	**Sn**		**As**		**Pb**		**Th**		**U**		**Cs**		**Y**	
		/Al	/Ti	/Al	/Ti	/Al	/Ti	/Al	/Ti	/Al	/Ti	/Al	/Ti	/Al	/Ti
Swan Lake	1	0.66	0.45	1.4	0.92	1.6	1.1	0.7	0.45	0.93	0.61	0.51	0.33	1.9	1.3
Swan Lake	2	0.72	0.73	1.0	1.0	2.0	2.0	1.1	1.1	1.2	1.2	1.3	1.2	1.3	1.3
Swan Lake	3	0.85	0.93	1.3	1.4	1.7	1.8	1.1	1.1	1.2	1.2	1.3	1.3	1.2	1.3
Swan Lake	4	0.84	0.87	1.2	1.1	1.2	1.2	0.99	0.98	1.0	1.0	0.96	0.94	1.2	1.2
Swan Lake	5	0.66	0.59	1.4	1.2	2.2	1.9	1.7	1.4	1.9	1.6	2.0	1.7	1.4	1.2
Swan Lake	6	0.74	0.68	1.4	1.2	1.7	1.5	1.6	1.4	1.7	1.5	1.5	1.3	1.4	1.3
Swan Lake	7	0.58	0.62	1.3	1.4	1.5	1.5	1.7	1.7	1.7	1.7	1.8	1.8	1.3	1.3
Swan Lake	8	0.54	0.50	1.2	1.0	2.2	1.9	1.5	1.4	1.4	1.2	1.4	1.2	1.4	1.3
Swan Lake	9	0.45	0.48	1.1	1.2	1.6	1.6	1.5	1.5	1.6	1.6	1.5	1.6	1.1	1.2
Swan Lake	10	0.42	0.43	0.90	0.91	1.5	1.6	1.8	1.8	1.6	1.6	1.6	1.6	1.1	1.1

Table A2.11 Enrichment factors (E_f) of metal oxides compared to Al and Ti values for Swan Lake sediment and normalized against Toogood Pond. The E_f values have been rounded to the most appropriate significant figures.

Sampling Location	Sampling Site	Element													
		Na_2O		MgO		Al_2O_3		SiO_2		P_2O_5		S		Cl	
		/Al	/Ti	/Al	/Ti	/Al	/Ti	/Al	/Ti	/Al	/Ti	/Al	/Ti	/Al	/Ti
Swan Lake	1	1.8	1.2	0.96	0.63	1.0	0.66	1.1	0.72	1.6	1.1	2.2	1.4	12	7.7
Swan Lake	2	1.6	1.6	1.0	1.0	1.0	0.98	0.89	0.88	1.4	1.3	1.6	1.6	9.1	8.9
Swan Lake	3	1.8	2.0	1.1	1.2	1.0	1.1	0.88	0.93	1.7	1.8	2.5	2.7	14	14
Swan Lake	4	2.0	2.0	1.0	1.0	1.0	1.0	0.92	0.92	1.4	1.4	1.8	1.8	11	11
Swan Lake	5	2.0	1.8	1.0	0.89	1.0	0.86	0.90	0.78	1.6	1.4	2.3	2.0	13	11
Swan Lake	6	1.8	1.7	0.99	0.88	1.0	0.89	0.93	0.83	1.8	1.7	2.4	2.1	13	12
Swan Lake	7	2.1	2.2	0.99	1.0	1.0	1.0	0.89	0.92	1.9	2.0	2.3	2.4	16	16
Swan Lake	8	2.2	2.1	0.94	0.85	1.0	0.91	0.90	0.81	1.8	1.7	2.7	2.4	15	14
Swan Lake	9	2.2	2.3	0.93	0.97	1.0	1.0	0.90	0.94	1.6	1.7	2.5	2.6	12	13
Swan Lake	10	1.9	2.0	0.80	0.81	1.0	1.0	0.91	0.92	1.3	1.3	1.8	1.9	9.3	9.3
Sampling Location	**Sampling Site**	**K_2O**		**CaO**		**TiO_2**		**V_2O_5**		**Cr_2O_3**		**MnO**		**Fe_2O_3**	
		/Al	/Ti	/Al	/Ti	/Al	/Ti	/Al	/Ti	/Al	/Ti	/Al	/Ti	/Al	/Ti
Swan Lake	1	1.2	0.79	1.7	1.1	1.5	1.0	2.6	1.7	2.6	1.7	1.4	0.93	1.6	1.1
Swan Lake	2	1.0	1.0	1.0	1.0	1.0	1.0	1.6	1.5	1.6	1.6	0.98	0.96	1.1	1.1
Swan Lake	3	1.1	1.1	1.0	1.1	0.94	1.0	1.8	1.9	1.9	2.1	0.91	0.97	1.2	1.3
Swan Lake	4	1.1	1.1	1.0	0.99	1.0	1.0	1.3	1.3	1.7	1.7	0.94	0.94	1.1	1.1
Swan Lake	5	1.1	0.94	1.1	0.91	1.2	1.0	2.3	2.0	1.9	1.7	1.1	0.96	1.4	1.2
Swan Lake	6	1.1	0.97	1.2	1.1	1.1	1.0	1.6	1.4	2.3	2.0	1.0	0.90	1.3	1.2
Swan Lake	7	1.0	1.1	1.0	1.0	0.96	1.0	1.4	1.5	2.7	2.9	0.88	0.91	1.2	1.2
Swan Lake	8	1.1	1.0	0.92	0.82	1.1	1.0	2.5	2.3	2.1	1.9	0.96	0.87	1.3	1.2
Swan Lake	9	1.1	1.1	0.57	0.59	0.95	1.0	1.5	1.5	1.9	2.0	0.73	0.76	1.1	1.2
Swan Lake	10	1.1	1.1	0.34	0.34	0.98	1.0	1.5	1.6	0.82	0.83	0.68	0.68	0.98	1.0

Table A2.12 Pairwise comparison using Friedman test for dependent samples and Conover Post Hoc for REE concentrations (μg L^{-1}) within acid-leachable particulate, colloidal, or dissolved Swan Lake water between the surface, intermediate, and deep levels.

		Surface			Intermediate			Deep			Friedman	Post Hoc Conover
AVG Depth (m)		**0.03m**			**0.68 ± 0.1 m**			**1.44 ± 0.2 m**				
Element	**Filter Level**	**AVG**	**SE**	**Count**	**AVG**	**SE**	**Count**	**AVG**	**SE**	**Count**	**P-value (<0.05)**	
	Particulate	0.15	0.02	8	1.7	1.1	8	59.5	20.7	8	0.002	Deep > Intermediate > Surface
La	Colloidal	0.03	0.01	7	0.4	0.3	7	0.8	0.7	7	0.03	Deep > Surface, Intermediate
	Dissolved	0.06	0.01	8	0.10	0.04	8	0.9	0.6	8	0.2	-
	Particulate	0.060	0.002	8	0.2	0.1	8	4.8	1.5	8	0.002	Deep > Intermediate > Surface
Ce	Colloidal	0.022	0.003	8	0.03	0.01	8	0.1	0.1	8	0.7	-
	Dissolved	0.03	0.01	8	0.03	0.01	8	0.08	0.03	8	0.9	-
	Particulate	0.007	0.001	8	0.02	0.01	8	0.5	0.2	8	0.002	Deep > Intermediate > Surface
Pr	Colloidal	0.0019	0.0003	7	0.004	0.002	7	0.02	0.01	7	1	-
	Dissolved	0.0042	0.0006	8	0.005	0.001	8	0.010	0.003	8	0.3	-
	Particulate	0.022	0.002	8	0.08	0.03	8	2.0	0.7	8	0.002	Deep > Intermediate > Surface
Nd	Colloidal	0.009	0.001	7	0.015	0.008	7	0.06	0.05	7	1	-
	Dissolved	0.024	0.002	8	0.028	0.003	8	0.05	0.01	8	0.6	-
	Particulate	0.0033	0.0005	8	0.012	0.004	8	0.3	0.1	8	0.004	Deep > Intermediate, Surface
Sm	Colloidal	0.0027	0.0007	5	0.004	0.002	5	0.01	0.01	5	0.8	-
	Dissolved	0.0053	0.0005	8	0.006	0.001	8	0.010	0.002	8	0.2	-
	Particulate	0.0009	0.0001	8	0.004	0.001	8	0.06	0.02	8	0.002	Deep > Intermediate > Surface
Eu	Colloidal	0.0005	0.0002	6	0.0013	0.0004	6	0.004	0.001	6	0.5	-
	Dissolved	0.0056	0.0002	8	0.0054	0.0002	8	0.0067	0.0007	8	0.2	-
	Particulate	0.002	0.001	8	0.008	0.003	8	0.4	0.1	8	0.0003	Deep > Intermediate > Surface
Gd	Colloidal	0.002	0.001	5	0.003	0.001	5	0.01	0.01	5	0.8	-
	Dissolved	0.006	0.0004	6	0.003	0.001	6	0.012	0.008	6	0.1	-
	Particulate	0.0011	0.0004	8	0.004	0.002	8	0.19	0.06	8	0.004	Deep > Intermediate, Surface
Dy	Colloidal	0.0016	0.0004	5	0.002	0.001	5	0.009	0.007	5	1.0	-
	Dissolved	0.0037	0.0003	8	0.0047	0.0004	8	0.007	0.001	8	0.1	-
	Particulate	0.0010	0.0002	7	0.0008	0.0005	7	0.10	0.04	7	0.01	Deep > Intermediate, Surface
Er	Colloidal	0.0007	0.0002	7	0.0009	0.0002	7	0.0007	0.0002	7	0.3	
	Dissolved	0.0023	0.0006	8	0.0031	0.0011	8	0.0046	0.0022	8	0.03	Deep > Surface
	Particulate	0.0013	0.0005	3	0.0017	0.0001	3	0.15	0.02	3	0.1	-
Yb	Colloidal	0.001	0.001	3	0.0022	0.0008	3	0.005	0.004	3	0.7	-
	Dissolved	0.0037	0.0001	8	0.0044	0.0003	8	0.0055	0.0007	8	0.06	-

Table A2.13 Pairwise comparison using Friedman test for dependent samples and Conover Post Hoc for REE concentrations (μg L^{-1}) within the acid-leachable particulate, colloidal, or dissolved Toogood Pond waters within the surface, intermediate, and deep levels.

AVG Depth (m)		0.03 m			0.3 ± 0.04 m			0.7 ± 0.08 m				
Element	**Filter Level**	**AVG**	**SE**	**Count**	**AVG**	**SE**	**Count**	**AVG**	**SE**	**Count**	**P-value (0.05)**	
La	Particulate	0.65	0.08	4	0.67	0.06	4	2.67	0.96	4	0.05	Deep > Intermediate, Surface
	Colloidal	0.04	0.01	2	0.02	0.01	2	0.03	0.01	2	1.0	-
	Dissolved	0.03	0.01	4	0.06	0.02	4	0.05	0.01	4	0.4	-
Ce	Particulate	1.00	0.13	4	1.07	0.10	4	4.50	1.71	4	0.04	Deep > Intermediate, Surface
	Colloidal	0.04	0.01	2	0.027	0.002	2	0.03	0.01	2	0.6	-
	Dissolved	0.22	0.17	4	0.07	0.03	4	0.07	0.02	4	0.4	-
Pr	Particulate	0.12	0.02	4	0.13	0.01	4	0.5	0.2	4	0.04	Deep > Intermediate, Surface
	Colloidal	0.005	0.002	2	0.002	0.001	2	0.004	0.001	2	1.0	-
	Dissolved	0.0035	0.0008	4	0.008	0.003	4	0.007	0.001	4	0.8	-
Nd	Particulate	0.47	0.06	4	0.50	0.06	4	2.1	0.8	4	0.04	Deep > Intermediate, Surface
	Colloidal	0.015	0.007	2	0.013	0.002	2	0.016	0.003	2	0.6	-
	Dissolved	0.11	0.08	4	0.04	0.01	4	0.04	0.01	4	0.4	-
Sm	Particulate	0.09	0.01	4	0.96	0.01	4	0.4	0.2	4	0.05	Deep > Intermediate, Surface
	Colloidal	0.004	0.002	2	0.0032	0.0003	2	0.005	0.002	2	1.0	-
	Dissolved	0.02	0.02	4	0.007	0.003	4	0.006	0.002	4	0.4	-
Eu	Particulate	0.019	0.002	4	0.020	0.002	4	0.09	0.03	4	0.04	Deep > Intermediate, Surface
	Colloidal	0.0006		2	0.0006	0.0003	2	0.002		2	0.2	-
	Dissolved	0.018	0.003	4	0.0149	0.0006	4	0.0143	0.0002	4	0.8	-
Gd	Particulate	0.09	0.02	4	0.09	0.01	4	0.4	0.2	4	0.04	Deep > Intermediate, Surface
	Colloidal	0.0020	0.0002	2	0.0023	0.0004	2	0.00175	0.00002	2	0.6	-
	Dissolved	0.02	0.01	4	0.007	0.003	4	0.008	0.003	4	0.5	-
Dy	Particulate	0.07	0.02	4	0.07	0.01	4	0.3	0.1	4	0.04	Deep > Intermediate, Surface
	Colloidal	0.003	0.001	2	0.0016	0.0003	2	0.0028	0.0004	2	1.0	-
	Dissolved	0.02	0.01	4	0.005	0.002	4	0.005	0.001	4	0.4	-
Er	Particulate	0.03	0.005	4	0.036	0.003	4	0.15	0.06	4	0.04	Deep > Intermediate, Surface
	Colloidal	0.0007	0.0004	2	0.0007	0.0005	2	0.0004	0.0001	2	1	-
	Dissolved	0.009	0.006	4	0.0038	0.0009	4	0.0040	0.0004	4	0.4	-
Yb	Particulate	0.029	0.005	4	0.029	0.003	4	0.12	0.05	4	0.04	Deep > Intermediate, Surface
	Colloidal	0.001	0.001	2	0.0012	0.0003	2	0.001		2	1.0	-
	Dissolved	0.009	0.004	4	0.0043	0.0005	4	0.0045	0.0007	4	0.4	-

Table A2.14 Average (AVG) La and anomalies and standard error (SE) in biological organisms, water, and sediment collected from Swan Lake, Ontario.

Location	Organisms	Number	Tissues	La/La*	
				AVG	SE
Swan Lake	English bullhead	3	internal organs	9.67	2.27
		3	brain	4.33	1.92
		3	soft tissue	3.72	1.47
		3	gills	5.83	1.14
	Fathead minnow	6 composite samples	Internal organs	8.17	0.25
		3 composite samples	brain	548.59	235.33
		5 composite samples	soft tissue	5.36	0.46
		4 composite samples	gills	12.72	3.74
		5 composite samples	intestines	7.86	0.94
	Zooplankton	4	whole	2.93	0.14
	Plankton	23	whole	8.64	0.47
	Macroalgae	9	whole	5.75	1.47
	Root of grass	1	whole	2.10	
	Bloodworms	1 composite sample	whole	2.97	
	Common pillbug	1 composite sample	whole	1.02	
	Endogeic earthworms	1 composite sample	whole	1.09	0.08
	Surface unfiltered	10	Water	5.47	0.42
	Surface < 1.2 µm	9	Water	6.62	0.33
	Surface < 0.2 µm	10	Water	7.62	1.01
	Intermediate unfiltered	9	Water	9.38	2.14
	Intermediate < 1.2 µm	9	Water	9.86	3.50
	Intermediate < 0.2 µm	8	Water	9.22	1.10
	Deep unfiltered	8	Water	19.93	5.66
	Deep < 1.2 µm	10	Water	9.33	1.50
	Deep < 0.2 µm	10	Water	15.33	3.77
	Sediment	10		22.5	3.0

Table A2.15 Average (AVG) La and anomalies and standard error (SE) in biological organisms, water, and sediment collected from Toogood Pond, Ontario.

Location	Organisms	Number	Tissues	La/La*	
				AVG	SE
Toogood Pond	English bullhead	2	soft tissue	0.82	0.2
		2	brain		
		2	gills	1.88	0.28
		2	liver	1.35	0.16
	Gobie	2	soft tissue	2.64	0.56
		2	brain		
		2	gills	6.73	3.02
	Plankton	5	whole	1.44	0.11
	Macroalgae	7	whole	1.03	0.02
	Root of grass	1	whole	1.79	
	Common pillbug	1 composite sample	whole	4.70	
	Anecic earthworms	2 composite samples	whole	0.95	0.02
	Endogenic earthworms	1 composite sample	whole	0.89	
	Surface unfiltered	4	Water	1.39	0.03
	Surface < 1.2 μm	4	Water	2.54	0.32
	Surface < 0.2 μm	4	Water	4.21	1.07
	Intermediate unfiltered	4	Water	1.40	0.04
	Intermediate < 1.2 μm	4	Water	2.46	0.24
	Intermediate < 0.2 μm	4	Water	3.50	0.68
	Deep unfiltered	4	Water	1.35	0.07
	Deep < 1.2 μm	4	Water	2.51	0.21
	Deep < 0.2 μm	4	Water	1.87	0.24
	Sediment	4		1.00	0.02

Table A2.16 Average concentrations (mg kg $^{-1}$, AVG) and standard error (SE) of La and Pr in biological organisms collected from Swan Lake and Toogood Pond.

Location	Organisms	Number	Tissues	La		Pr	
				AVG	SE	AVG	SE
Toogood Pond	English bullhead	2	soft tissue	0.003	0.002	0.0006	0.0003
		2	brain			0.0006	0.0003
		2	gills	0.17	0.03	0.024	0.006
		2	liver	0.008	0.003	0.001	0.001
	Gobie	2	soft tissue	0.012	0.001	0.0007	0.0001
		2	brain			0.0018	0.0001
		2	gills	0.08	0.05	0.002	0.001
	Plankton	5	whole	0.4	0.2	0.07	0.03
	Macroalgae	7	whole	1.1	0.3	0.3	0.1
	Root of grass	1	whole	0.68		0.08	
	Common pillbug	1 composite sample	whole	1.23		0.06	
	Anecic earthworms	2 composite samples	whole	1.10	0.06	0.27	0.01
	Endogeic earthworms	1 composite sample	whole	0.84		0.22	
Location	**Organisms**	**Number**	**Tissues**	**La**		**Pr**	
				AVG	**SE**	**AVG**	**SE**
Swan Lake	English bullhead	3	Internal organs	0.032	0.006	0.0009	0.0003
		3	brain	0.001	0.001	0.0001	0.0001
		3	soft tissue	0.0009	0.0002	0.00008	0.00003
		3	gills	0.2	0.1	0.007	0.004
	Fathead minnow	6 composite samples	liver	2.8	0.5	0.09	0.02
		3 composite samples	brain	0.73	0.40	0.0004	0.0002
		5 composite samples	soft tissue	0.055	0.009	0.0021	0.0002
		4 composite samples	gills	0.24	0.07	0.004	0.001
		5 composite samples	intestines	19.7	4.9	0.6	0.1
	Zooplankton	4	whole	0.056	0.009	0.004	0.001
	Plankton	23	whole	1.98	0.48	0.05	0.01
	Macroalgae	9	whole	1.41	0.40	0.12	0.05
	Root of grass	1	whole	1.36		0.13	
	Bloodworms	1 composite sample	whole	6.22		0.48	
	Common pillbug	1 composite sample	whole	2.41		0.58	
	Endogeic earthworms	1 composite sample	whole	1.79	0.23	0.35	0.03

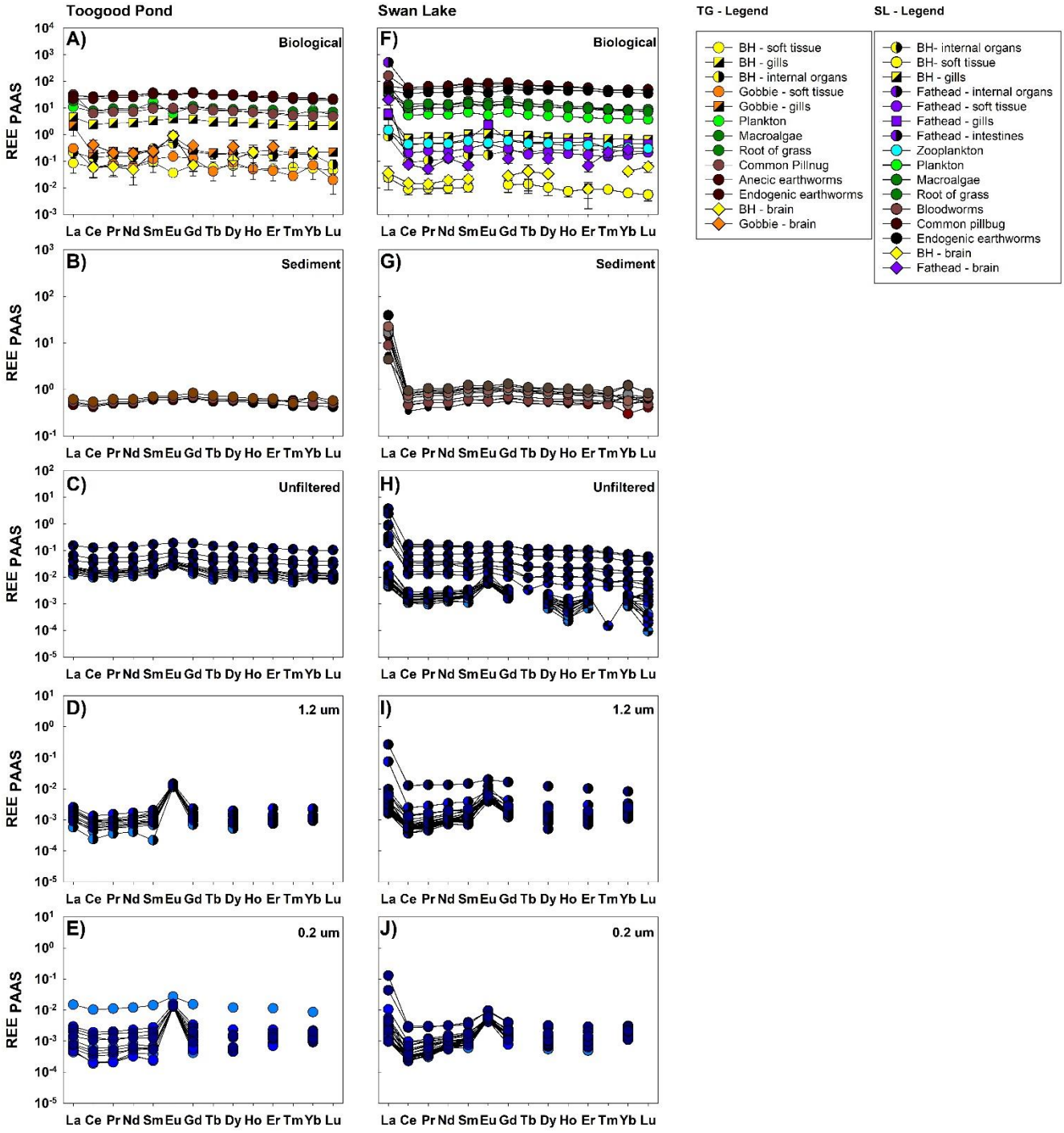

Figure A2.1 [REE] normalized against Post-Archean Australian shale (PAAS) to characterize REE patterns within partitioned tissues of organisms, sediment, and filtration water levels (0.2 µm, 1.2 µm, acid-leachable) collected from Toogood Pond and Swan Lake. Symbol shapes represent specific organism tissues: 1. whole filled circle (soft tissue or whole body), 2. half filled square (gills) 3. half filled circle (intestines), 4. diamond (brain).

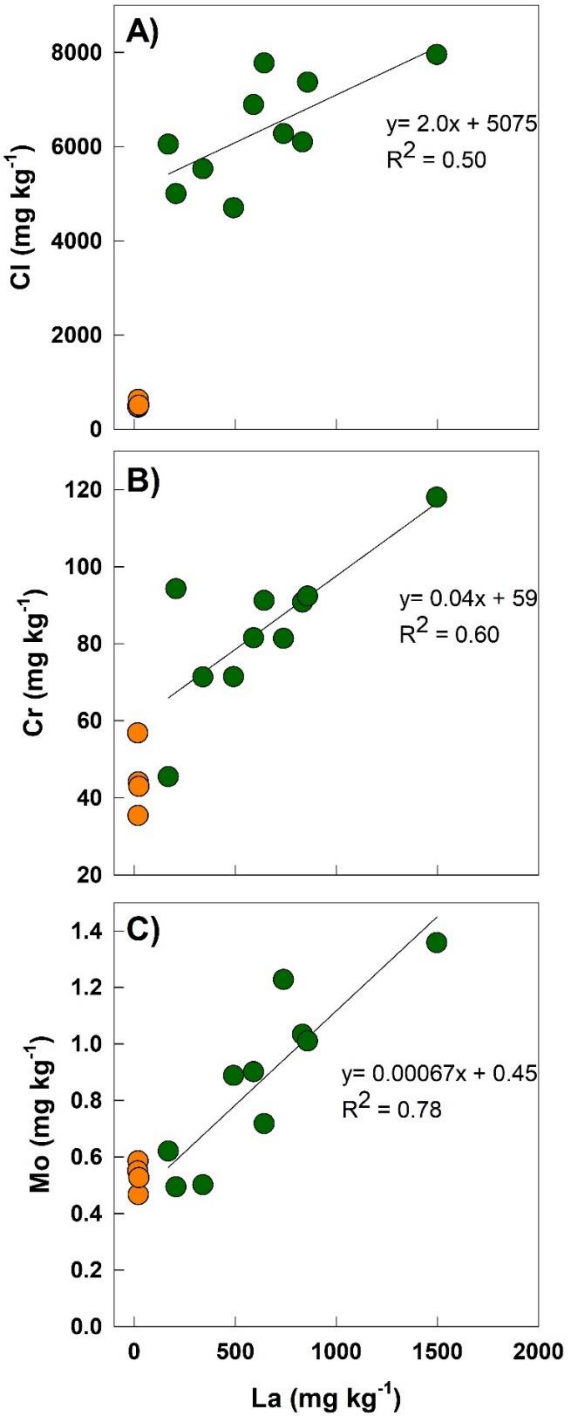

Figure A2.2 Biplots showing the relationship between the concentrations of La (**A-C**) vs. Cl, Cr, and Mo in the sediments of Toogood Pond (orange symbols) and Swan Lake (green symbols).

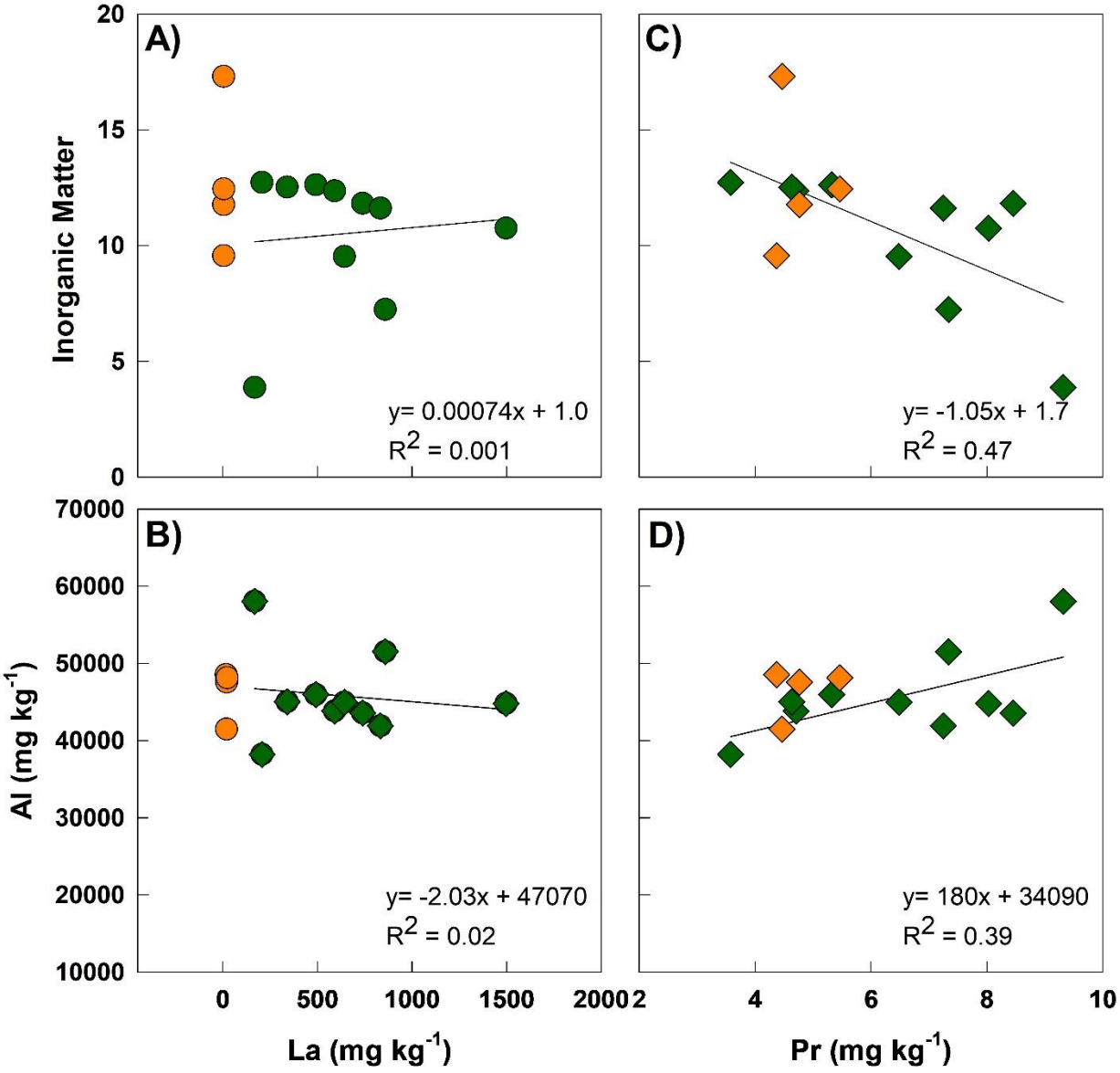

Figure A2.3 Biplots showing the relationship between the concentrations of La (**A-B**) and Pr (**C-D**) vs. inorganic matter and Al in the sediments of both Toogood Pond (orange symbols) and Swan Lake (green symbols).

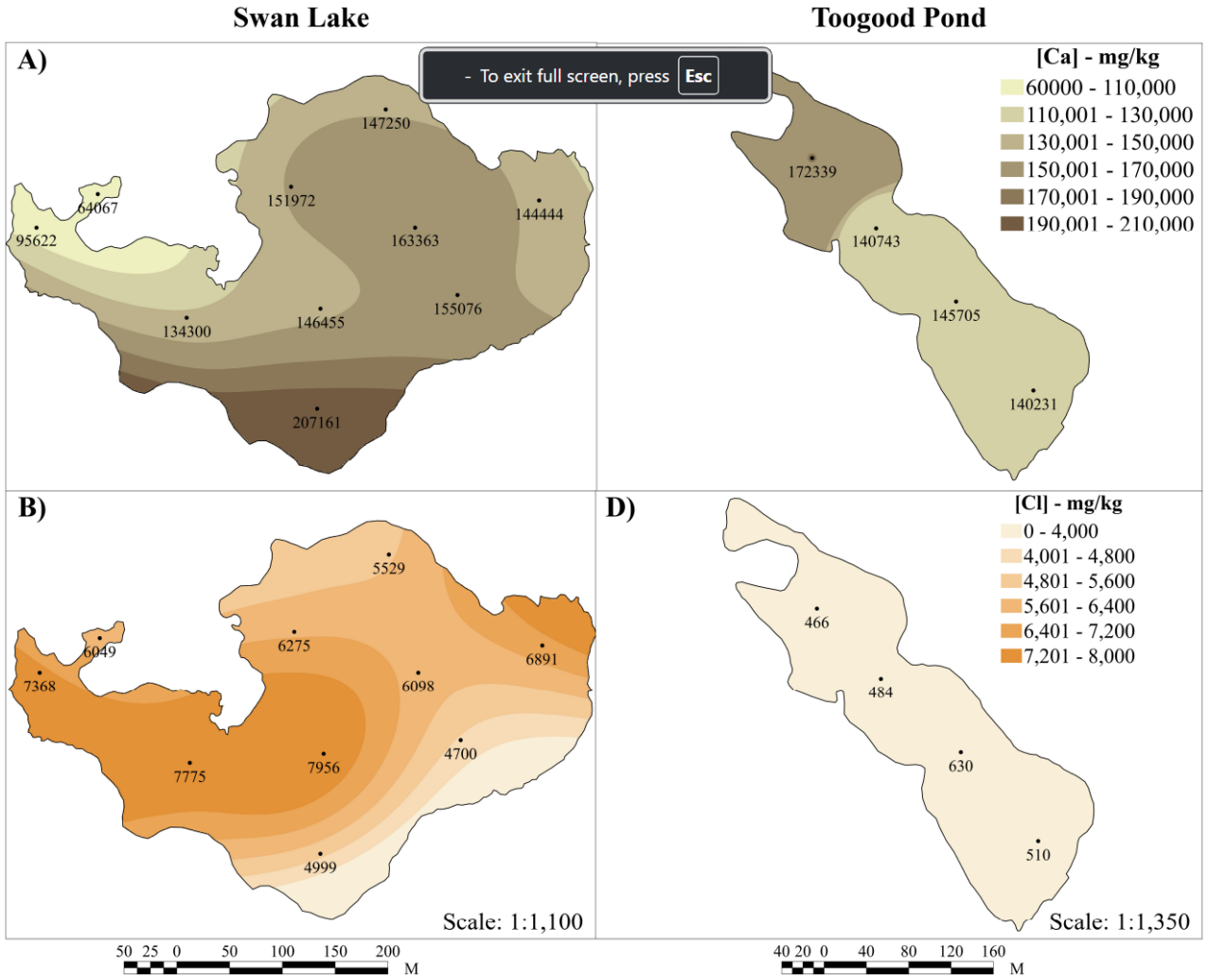

Figure A2.4 Horizontal spatial distribution and concentrations of Ca (beige - mg kg^{-1}, upper panels) and Cl (yellow - mg kg^{-1}, lower panels), in the sediment of Swan Lake (**A & B**) and Toogood Pond (**C & D**). Spatial interpolation of REEs in Swan Lake was completed using ArcGIS spline 3D analyst tool and Toogood Pond interpolation with inverse distance weighted analyst tool.

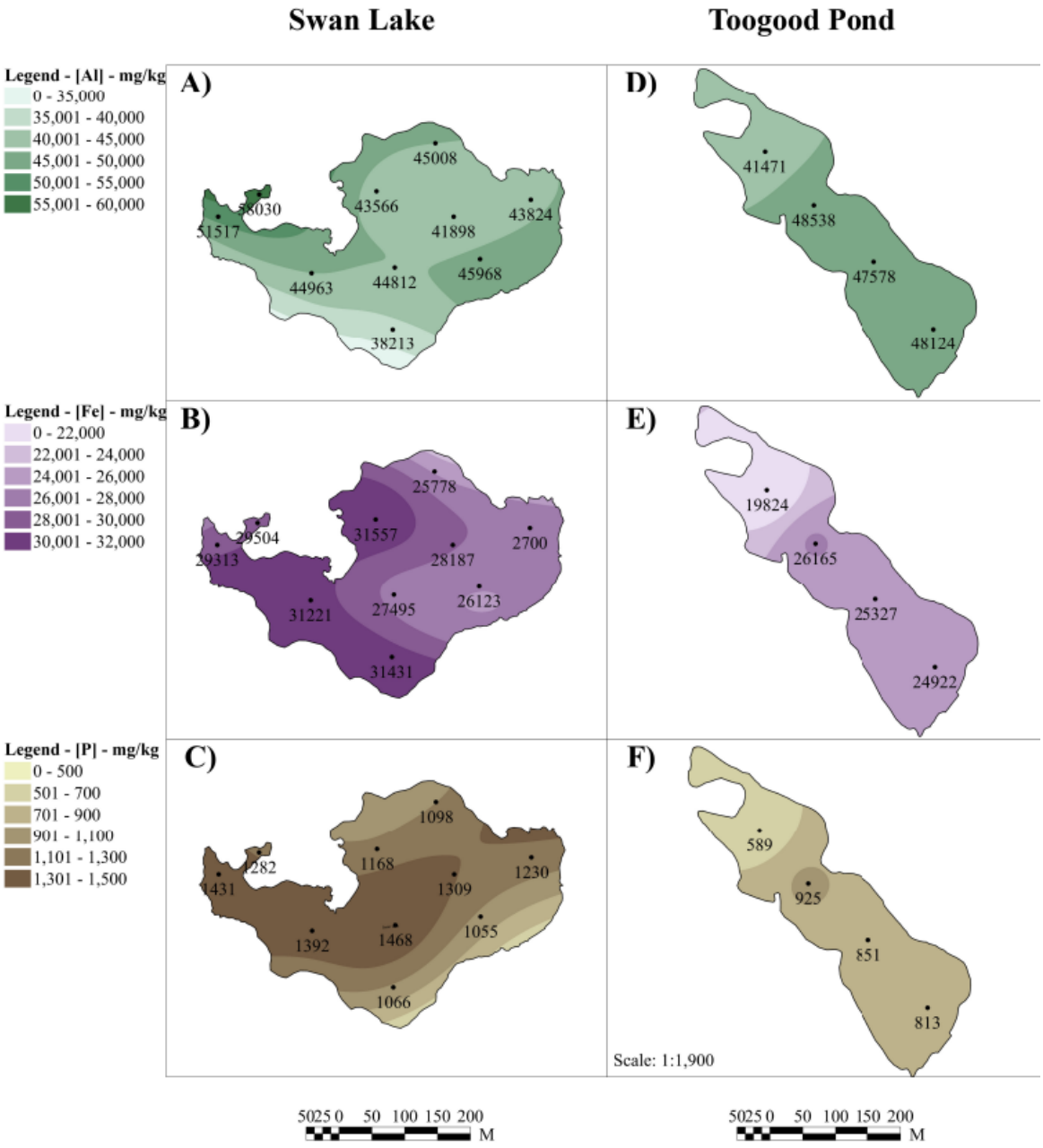

Figure A2.5 Horizontal spatial distribution and concentrations of Al (green - mg kg^{-1}, upper panels), Fe (purple - mg kg^{-1}, middle panels), and P (brown - mg kg^{-1}, lower panels) in the sediment of Swan Lake (**A-C**) and Toogood Pond (**D-F**). Spatial interpolation of REEs in Swan Lake was completed using ArcGIS spline 3D analyst tool and Toogood Pond interpolation with inverse distance weighted analyst tool.

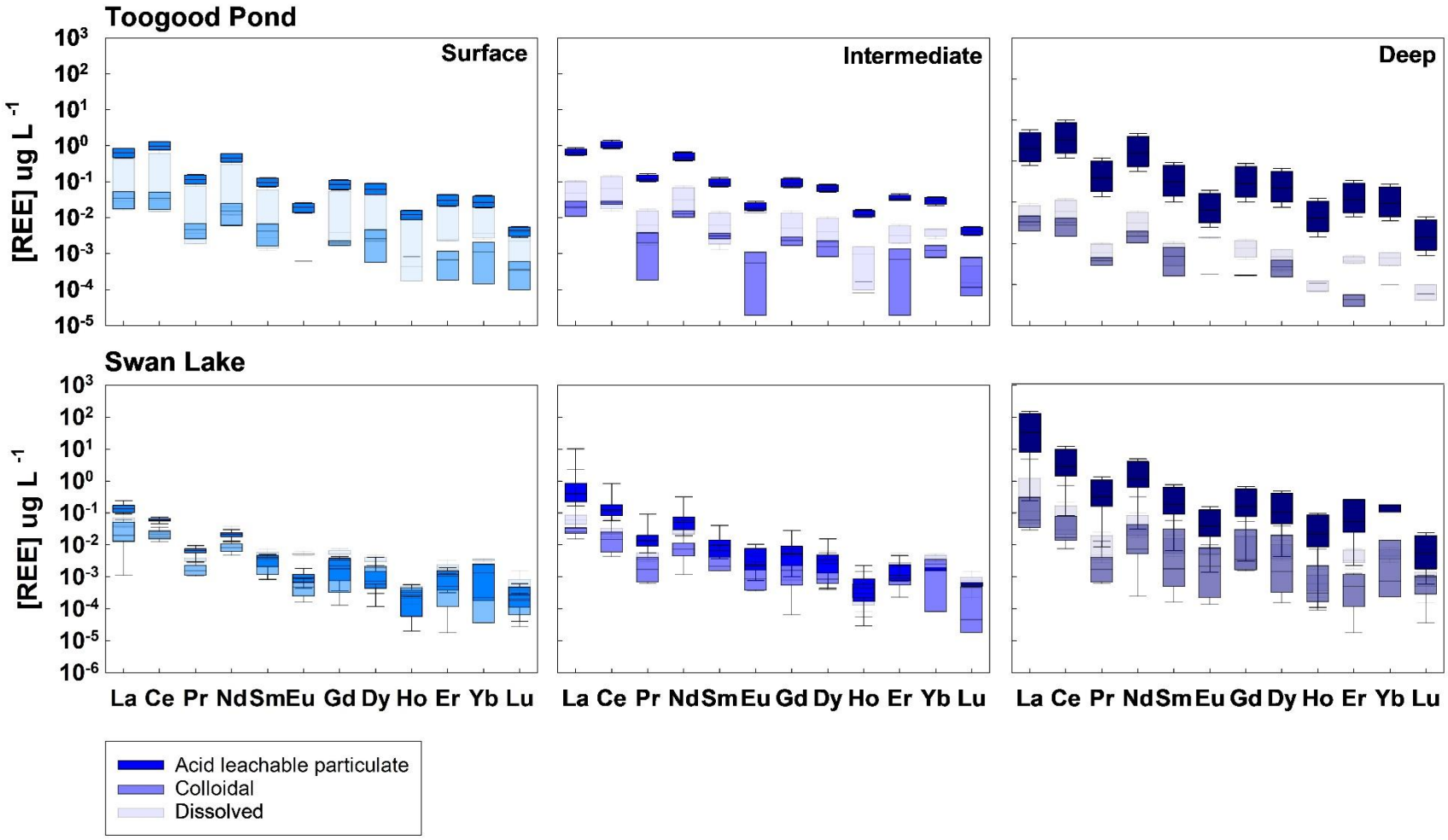

Figure A2.6 REE concentrations found in acid leachable particulate, colloidal, and dissolved fractions of surface, intermediate, and deep water of Toogood Pond and Swan Lake. Results from pairwise comparison using Friedman and Conover Post Hoc of REE concentrations between the surface, intermediate, and deep levels at three filtration levels can be found in **Table S12** & **S13.**

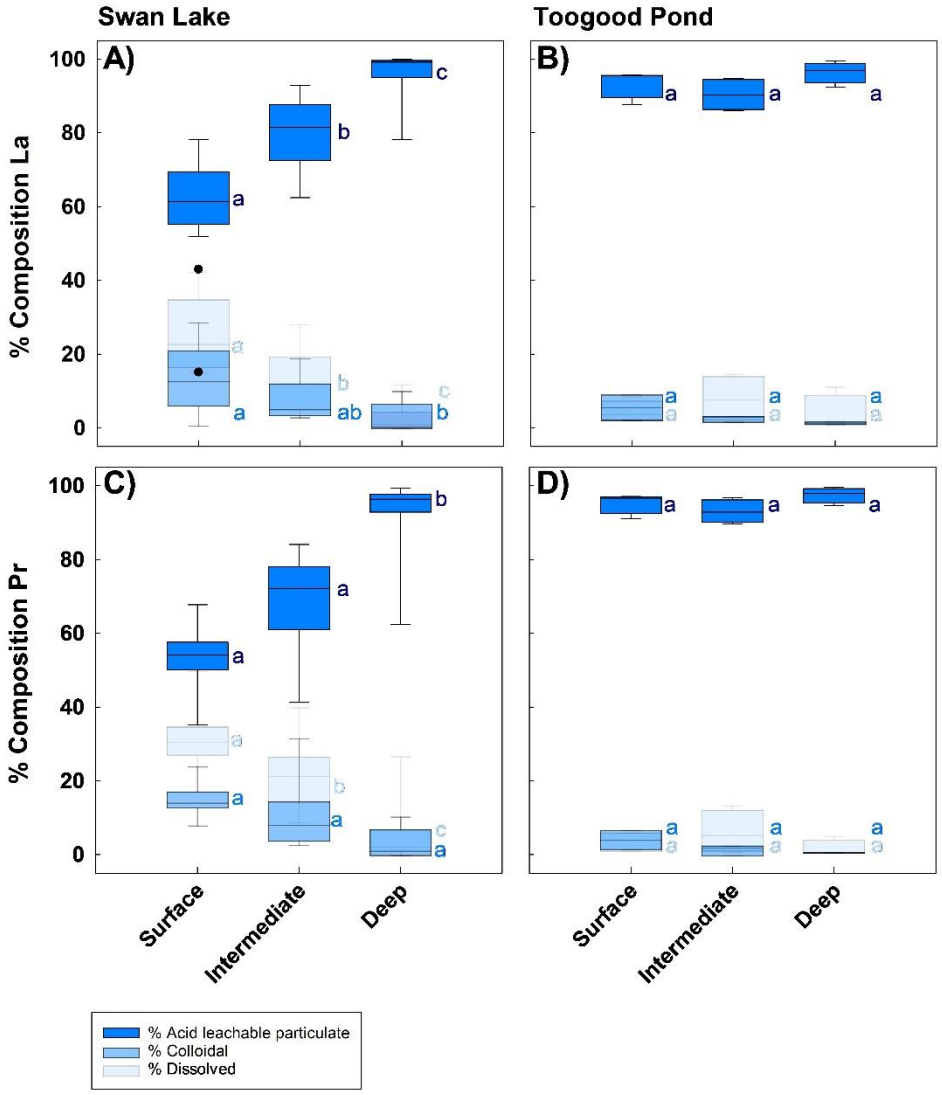

Figure A2.7 Percent composition of La and Pr found in the acid-leachable particulate, colloidal, and dissolved fractions of water within surface, intermediate, and deep locations of Swan Lake (**A & C**) and Toogood Pond (**B & D**). The compact letter displays Conover post hoc results for pairwise comparison among acid-leachable particulate REEs, dissolved REEs, and colloidal REEs between surface, intermediate, and deep levels. (Toogood Pond water samples, n = 4, Swan Lake water samples, n =8 to 10).

Figure A2.8 Dissected intestines of fathead minnows containing green algae from Swan Lake.